Expeditious Reactivity of Sulfoximines and *o*-Alkynylanilines Towards the Construction of C–C and C–Heteroatom Bonds

A dissertation submitted in partial fulfillment for the degree of

Doctor of Philosophy

Submitted By

Nikita Chakraborty

Roll No. 176122113

Department of Chemistry

Indian Institute of Technology Guwahati

Guwahati-781039, Assam, India

April, 2024

DEDICATED TO

MAA & PAPA

INDIAN INSTITUTE OF TECHNOLOGY GUWAHATI

Department of Chemistry

STATEMENT

I do hereby declare that the matter embodied in this thesis is the result of investigations carried out by me in the Department of Chemistry, Indian Institute of Technology Guwahati, India, under the guidance of Prof. Bhisma K. Patel. I have submitted this thesis to the Department of Chemistry, Indian Institute of Technology Guwahati for the award of the degree of Doctor of Philosophy.

In keeping with the general practice of reporting scientific observations, due acknowledgements have been made wherever the work described is based on the findings of other investigators. I further declare that this work has not been submitted anywhere else for any degree, diploma, associateship or membership, etc. of any Institute or University to the best of my knowledge.

Nikita Chakraborty

05 July, 2024

IIT Guwahati

Nikita Chakraborty

भारतीय प्रौद्योगिकी संस्थान गुवाहाटी
Indian Institute of Technology Guwahati

INDIAN INSTITUTE OF TECHNOLOGY GUWAHATI
Department of Chemistry

CERTIFICATE

This is to certify that Nikita Chakraborty has been working under my supervision since April 2018 as a regular registered Ph.D. student. Her thesis entitled "**Expeditious Reactivity of Sulfoximines and *o*-Alkynylanilines Towards the Construction of C–C and C–Heteroatom Bonds**" is an authentic record of the results obtained from the research work in the Department of Chemistry, Indian Institute of Technology Guwahati, Assam, India. I am forwarding her thesis to submit for the Ph.D. (Science) degree from this institute. I certify that she has fulfilled all the requirements according to the rules of this institute regarding the investigations embodied in her thesis, and this work has not been submitted elsewhere for a degree.

05 July 2024

Prof. Bhisma K. Patel
(Thesis Supervisor)
Department of Chemistry
IIT Guwahati

भारतीय प्रौद्योगिकी संस्थान गुवाहाटी
Indian Institute of Technology Guwahati

ACKNOWLEDGEMENT

Finding myself very close to completing the highest academic qualification, a Ph.D. degree, I feel indebted to many people who have encouraged, supported, guided, loved, and pushed me to walk the extra mile and achieve it.

First and foremost, I want to express my deepest respect and profound gratitude to my supervisor, Prof. Bhisma K. Patel, for allowing me to be his Ph.D. student. His continuous support, guidance, and motivation through creative and unique scientific ideas helped me explore the domain of my work assembled in this thesis. I feel blessed to have him as my mentor, who offered full freedom to explore unique ideas, supported me when things were not working as planned, and motivated me to achieve more.

I would also like to extend my heartiest gratitude to the doctoral committee members, Prof. A. S. Achalkumar, Prof. Shankar Prasad Kanaujia, and Dr. Dipankar Srimani, for timely evaluation of my Ph.D. work and all the precious suggestions, which helped me a lot in the betterment of my thesis.

I sincerely thank all the faculty and staff members of the Department of Chemistry, IIT Guwahati, for their cooperative nature. I would like to thank Babulal da for single-crystal XRD, Imdadul da for NMR, Basab da, Tapu, and Michel for various official work and support in the Department of Chemistry.

I wish to express sincere gratitude to UGC (University Grants Commission) for the financial support and to IIT Guwahati for all the facilities that were made available to me for learning several analytical instruments required during my research work. I am grateful to the Central Instruments Facility (CIF) for the 600 MHz NMR and single-crystal XRD facilities, MHRD for the 400 MHz NMR facility under the COE-FAST program, DST for the 500 MHz NMR facility under the DST-FIST program, NECBH, IIT Guwahati, and DBT, Govt. of India for the 400 MHz NMR and single-crystal XRD facilities.

I would like to thank all the operators inside and outside IIT Guwahati for successfully carrying out all the instrumental experiments required during my research. Further, I am extremely thankful to all the co-authors, editors, associate editors, and reviewers for their valuable comments and suggestions.

The credit for completing the most memorable journey of academia must go to all the BKP warriors. I would like to express my deepest gratitude to my Ph.D. senior, Dr.

Anju Modi, for her guidance during the initial phase of my journey. This journey would not have been possible without the utmost guidance from Dr. Anjali Dahiya and Dr. Amitava Rakshit, who helped a lot in the initial days by giving shape to my ideas and teaching me basic lab techniques. Anjali Di has not only been a senior but also a close ally and confidante.

Some other wonderful lab seniors, Dr. Ahalya Behera, Dr. Suresh Rajamanickam, Dr. Bilal Ahmed Mir, Dr. Prasenjit Sau, Subendhu Gosh, and Prakash bhaiya, have helped in times with their precious suggestions and support. I would like to thank postdoctoral lab seniors Dr.Gaurav Shukla, Dr. Ritush Kumar, Dr. Pakiza Begum, Dr. Bhaskar Deka, Dr. Binoyargha Dam, and Dr. Kamal Krishna Rajbongshi for their help, and support. A special mention to my senior cum friends Ashish and Tipu for all the healthy discussions and enjoyment during all the parties and picnics.

I want to heartily appreciate all my talented juniors Tamanna, Bubul, Hiru, Pritishree, Raju, Dinabandhu, Shalini, Deepjyoti, Supriyo, and Manjunath for their extreme enthusiasm for research and for maintaining a friendly environment in the lab. I will forever cherish all the lab trips, outings, and parties, those were some of the most memorable days of my life. Moreover, the journey would not have been easier if Bubul had not offered his ears to listen to all my outbursts and cries; this meant a lot. I also had the opportunity to work with some dedicated summer and M.Sc. trainees like Surya Pravo, Priyabrta, Prashant, Rani, Arihant, Kunika, Sreyashi, Pankaj, Abhishek, Akshar, Abhishek, Angshu, Sourasish, Kaustav, Pratip Amisha and Shalini.

A special mention to my friend Subhamoy who has been my go-to person during all the highs and lows of this rough journey. Thank you for being a constant support and listening to all my worries and rants regarding all my professional, personal, and technical problems and trying to solve them with utmost patience.

I would like to express millions of gratitude to my closest friends, Priyanka and Priya, for their help and support, for staying by my side, and for making good times better and the hard times a whole lot easier. From sharing jokes to watching late-night movies, making fun of each other, and partying on the smallest occasion, it was always great to have you two by my side. I would also like to thank my friends Manideepa, Sonbidya, Sudip, Monikha, Partha, Chandrakanta, Amit, Manmath, Himangshu, Angana, and Sourav for all their help and joyful moments here at IITG.

Some friends have had a big impact on my life and have helped me overcome some of the toughest phases; Dr. Bhupalee Kalita, Dr. Raktim Abha Saikia, Dr. Trishna Rajbongshi, Dr. Shahnaz Rohman, Dr. Suvodeep Sen, Pranjal, Juri, Wahida, Parmeeta, Shahnaz, Sanjoy, Rajiv, Jayashree, Anup, Subrata, you all mean a lot. Because of you all, I can proudly say that I have some of the best people in my life.

I would also like to thank some of my Ph.D. fellowmates, seniors, and juniors here at IITG; Archana Di, Nimisha Di, Upasana Di, Sandip Da, Bipin, Bikoshita, Pallav, Archana, Hirok, Suravi, Biman, Monuranjan, Neha, Subhashree for making the journey a lot better, easier, and entertaining.

No words would suffice to express my feelings toward my teachers to whom I owe my obligations for their great teachings and philosophy to be a good human. Dr. Ankur K. Guha, Dr. Pankaz Sharma, Dr. Pradosh P. Chakraborti, and Dr. Subhash Ghosh have been the initial push factors for my choosing the research career. Further, I owe a lot to the entire fraternity from my school, B. Borooah College (Gauhati University), and Cotton University.

Lastly, and most importantly, my Ph.D. endeavour could not have been completed without the endless love, unending support, tolerance, and blessings from my family. I would like to express my deepest gratitude to my parents, whose unconditional love in every stage of my life motivated me to overcome all the challenges, and I owe my entire life to them. Dedicating this thesis to them is a minor recognition of their love, support, and encouragement. I wish Papa was here to see his daughter hold this prestigious degree, but I know he is always watching and blessing me from above. Special thanks to my brother for being the toughest critic, showing me the hardest mirror, and being a push factor to achieve more than I can. Much love to my little brother Mithun for all the love and care. Moreover, my Masi and Mama have a deep role in shaping my journey.

Lastly, I am thankful to Almighty for continuous blessing throughout my life, especially during my research career, and for providing me the willpower and strength to accomplish this remarkable journey.

Nikita Chakraborty

SYNOPSIS

The contents embodied in this thesis is divided into five chapters including one introductory chapter based on experimental results obtained during the research period. The introductory chapter represents an overview of the utility of sulfoximines and *o*-alkynylanilines towards the construction of C–C and C–heteroatom bonds. This includes a brief discussion about all the possible reactive sites present in sulfoximines and their possibility of forming different functionalized molecular complexities. Similarly, the reactivity of *o*-alkynylanilines for the formation of diverse heterocyclic scaffolds has been discussed.

Chapter II demonstrates a visible-light-induced decarboxylative strategy between cinnamic acids and NH-sulfoximines for the synthesis of α-keto-*N*-acylsulfoximines. The reaction proceeds with a catalytic amount of *N*-iodosuccinimide without the requirement of any external photosensitizer, base, or transition metal.

Chapter III describes a visible-light-induced PIDA-I_2-mediated synthesis of *N*-acylsulfoximines from NH-sulfoximines and methylarenes. Here, methylarenes serve as the acyl source without the requirement of any transition metal or oxygenated peroxide sources.

Chapter IV describes an Et_3N-promoted synthesis of 1,4-diarylisothiazolones from α-keto-*N*-acylsulfoximines. The developed protocol explores the intrinsic reactivity of the α-C−H in *N*-substituted sulfoximines with a mild base.

Chapter V describes a route for the synthesis of tricyanovinylindoles from *o*-alkynylanilines utilizing DMSO as a carbon synthon and NH_4SCN as the cyano source. Further, selective hydrolysis of the synthesized tricyanovinylindoles leads to the formation of indolylmaleimides.

Each of these chapters comprises seven subsections which include an introduction, previous work, present work, experimental section, references, spectral data, and a few representative spectra.

CHAPTER I. An Overview of Sulfoximines and *o*-Alkynylanilines Towards C–C and C–Heteroatom Bond Formation

The introductory chapter is divided into two parts. Part A covers a brief understanding of sulfoximine chemistry, including its general properties, biological aspects, reactivity, and application. The second part of this chapter (Part B) includes a brief discussion on *o*-alkynylanilines and their utility for constructing different heterocyclic motifs.

Part A: Over the past few decades, sulfoximines have been used as reagents, chiral auxiliaries, ligands, organocatalysts, drugs, and agrichemicals. Since 1949, when sulfoximines were discovered as a new class of compounds, they have attracted wide attention. After the initial discovery of the irreversible glutamine synthetase inhibitor L-methionine-(*S*)-sulfoximine (MSO), there has been a substantial increase in the number of bioactive molecules incorporating the sulfoximine moiety into their structure (Figure IA.1).

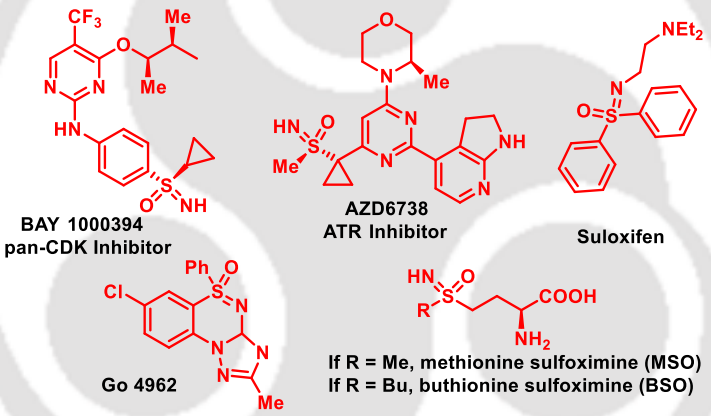

Figure IA.1. *Some biologically relevant sulfoximines.*

Structurally, sulfoximine is isoelectronic with sulfone having a tetrahedral sulfur atom and a basic nitrogen atom (pKa (NH_2^+) = 2.7 in water). The S atom bears a stereocenter (if not substituted symmetrically) and is chemically and configurationally stable. The basic nitrogen atom can form complexes with metal ions and form salts with mineral acids. Modifying the substitution pattern at the nitrogen atom makes it possible to modulate the acidic/basic properties of the compounds. Sulfoximines exhibit distinctive H–bond donor/acceptor capabilities. The sulfur-bound heteroatoms act as hydrogen-bond acceptors, whereas, N-unsubstituted sulfoximines have the potential to serve both as hydrogen-bond donors (via NH) and acceptors. Sulfoximines show good solubility in protic solvents (in water or alcohol) and

display a high level of metabolic stability. All these properties of sulfoximines make it a hydrophilic, and stable functional group in organic synthesis and drug discovery.

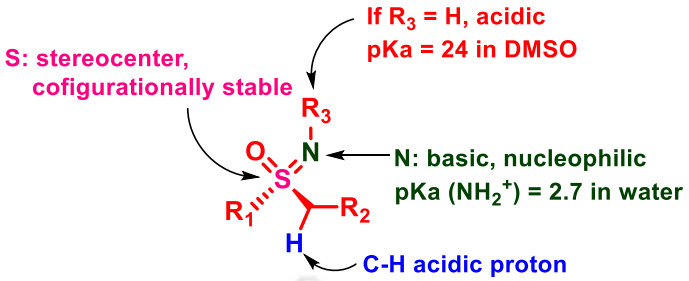

Figure IA.2. *General properties of sulfoximines.*

The physicochemical properties of sulfoximines can be further adjusted through their functionalization reactions.

I.A.1 Transformations of Sulfoximines

Depending on the structure and the reactive centres present, sulfoximines mainly undergo the following types of functionalization

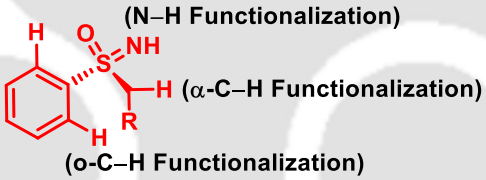

Figure IA.3. *Reactive sites of sulfoximines.*

–NH Functionalization

The high reactivity of the N-atom in NH-sulfoximines allows it to undergo various transformations, including arylations, alkylations, vinylations, alkynylations, acylation, halogenation, phosphorylation, and many more. This versatile N-reactivity facilitates the construction of various N-C and N-heteroatom bonds making it a valuable building block in synthetic organic chemistry.

–α-C–H Functionalization

Another interesting aspect of sulfoximine chemistry is the reactivity of the α-C–H attached to the S in N-substituted sulfoximines. This reactivity is mainly governed by the types of substituents attached to the N atom. The more electron-withdrawing the substituent, the

more the acidity of the α-C–H, and hence more easily it undergoes deprotonation. The reactions usually take place in the presence of a strong base.

–Ortho-C–H Functionalization

Ortho C–H functionalization is another aspect of sulfoximine chemistry. However, in most cases, the C–H activation is directed by the sulfoximidoyl group. The reactions typically proceed in the presence of transition metals such as Rh, Ru, Co, Ni, Au, Pd, etc.

Beyond their significance in typical functionalization reactions and drug discovery programs, the S(VI) functionality of sulfoximines is actively utilized in modern synthesis as chiral auxiliaries or ligands for asymmetric catalysis. The renewed interest in sulfoximine chemistry is evident through the ongoing development of new synthetic strategies for their preparation and functionalization, underscoring their evolving importance in contemporary chemical research.

Part B: The second part of this chapter gives a brief synopsis of exploring the chemistry of *o*-alkynylanilines towards the construction of C−C, and C−heteroatom bonds. The reactivity of *o*-alkynylanilines in the formation of different five, six, seven, and eight-membered heterocyclic motifs including fused systems will be discussed.

o-Alkynylanilines are useful synthetic intermediates as they possess two reactive sites, a nucleophile (–NH) and a triple bond. Derivatives of *o*-alkynylanilines have a long history, dating back to the early 19th century. The development of the Sonogashira cross-coupling reaction played a crucial role in providing a versatile preparative route to this building block, allowing the synthesis of diversely substituted *o*-alkynylanilines. The starting compounds for Sonogashira coupling, namely 2-iodo or bromo anilines, can be easily obtained through direct halogenation of aniline. Additionally, various methods for modifying amino groups offer extensive opportunities for synthesizing diverse derivatives of 2-(alkynyl)anilines.

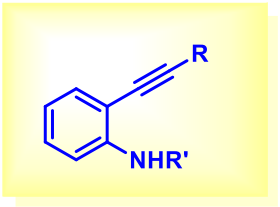

Figure IB.1. *Structure of o-alkynylaniline.*

It is well-known that alkynes possessing a nucleophile in proximity to the triple bond can participate in the construction of diverse heterocycles *via* transition metal- or Lewis acid-catalyzed intramolecular annulation. Depending on the catalysts, reaction conditions, and substituents on nitrogen, alkyne moiety, and the phenyl ring, there are several possibilities for the cyclization of *o*-alkynylaniline. Various heterocycles such as indole, quinoline, quinazolinone, benzoxazinone, oxindole, indazoles, thiazines, and many others originate from metal- or metal-free reactions of *o*-alkynylanilines (Figure IB.2). Therefore, as a useful synthetic intermediate, *o*-alkynylanilines have attracted considerable attention in the fields of organic and medicinal chemistry.

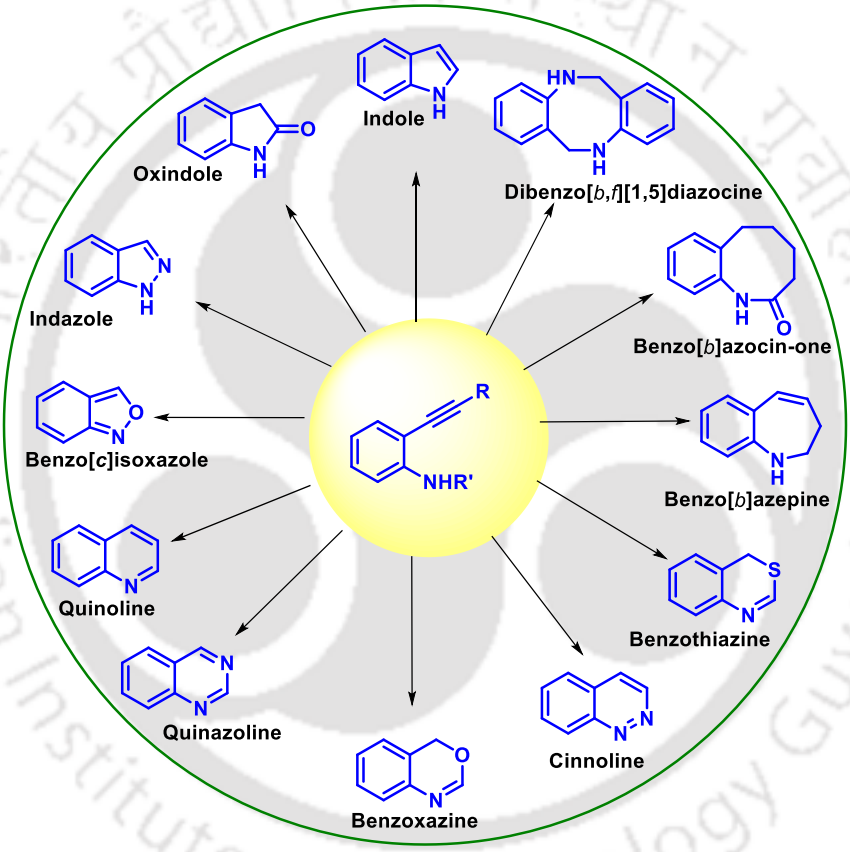

Figure IB.2. *Heterocycles originating from o-alkynylanilines.*

The synthesis of each of these heterocycles from *o*-alkynylanilines will be briefly discussed in the introductory section giving an insight into the reactivity of the alkynyl compounds.

CHAPTER II: NIS-Initiated Photo-Induced Oxidative Decarboxylative Sulfoximidation of Cinnamic Acids

This chapter demonstrates a visible-light-induced decarboxylative strategy between cinnamic acids and *NH*-sulfoximines for the synthesis of α-keto-*N*-acylsulfoximines. The reaction proceeds with a catalytic amount of *N*-iodosuccinimide without the requirement of any external photosensitizer, base, or transition metal. The two new oxygen in the product originates from moisture and dioxygen respectively.

Decarboxylative cross-coupling is a remarkable strategy for the construction of C–C and C–heteroatom bonds. This method is advantageous over conventional transition metal-catalyzed cross-coupling reactions. Decarboxylative cross-coupling involves the use of carboxylic acid and its derivatives and proceeds *via* the extrusion of CO_2. Visible-light-induced decarboxylative cross-coupling reactions have emerged as one of the powerful synthetic methodologies for various C−C and C−heteroatom bond formations. Cai *et al.* disclosed a decarboxylative cross-coupling reaction of cinnamic acids with sulfonyl hydrazides under visible-light irradiation in the presence of eosin Y, oxygen, and base (Scheme II.1a). In 2021, Singh and co-workers reported a concerted metallophotoredox catalysis for the decarboxylative arylation of α,β-unsaturated carboxylic acids using aryl iodides in the presence of Cu catalyst, a perylene bisimide dye (PC), TBHP, and Et_3N (Scheme II.1b). Recently, Ritter group disclosed the decarboxylative sulfoximination of benzoic acid which proceeds *via* photo-induced Cu-LMCT-enabled decarboxylative carbometallation (Scheme II.1c). Taking cues from the above-mentioned works, herein we designed a photoinduced decarboxylative sulfoximidation of cinnamic acid under metal and base-free conditions. (Scheme II.1d).

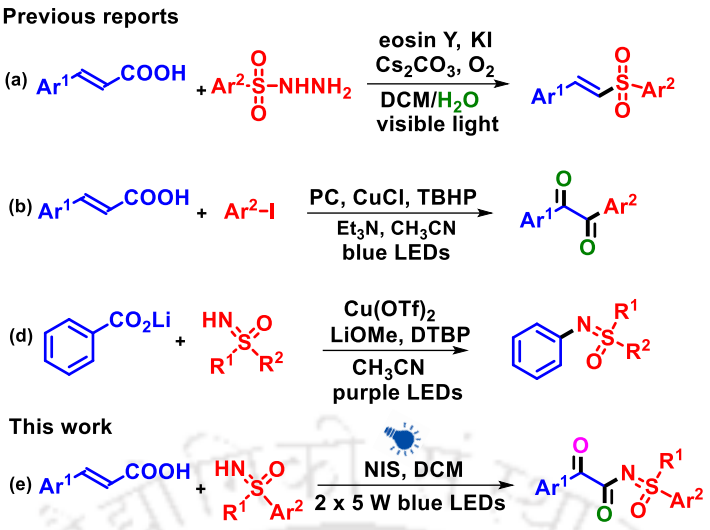

Scheme II.1. *Different approaches for visible-light-induced decarboxylative cross-coupling.*

For the desired transformation, the best condition was found to be the use of *S*-phenyl-*S*-methyl sulfoximine (**a**, 1 equiv), cinnamic acid (**1**, 1 equiv), and *N*-iodosuccinimide (20 mol%) in DCM under the irradiation of 2 x 5 W blue LEDs at room temperature. The anticipated α-keto-*N*-acylsulfoximine (**1a**) was obtained in 82% yield and characterized by spectroscopic techniques, including ^{1}H and $^{13}C\{^{1}H\}$ NMR and X-ray diffraction. With the optimized reaction condition in hand, the scope of this protocol was extended to a variety of cinnamic acids and *NH*-sulfoximines. It was observed that the reaction went smoothly for diverse types of substituents on both of the coupling partners. Further, a large-scale reaction was conducted which led to the product formation in an appreciable yield. Next, to ascertain the mechanistic path, various control experiments including radical trapping, H_2O^{18}-labelling, and reaction with presynthesized intermediates were performed. Further, UV-vis measurements concluded that *N*-iodosulfoximine serves as the light-absorbing species in this photochemical strategy.

Based on all the observations, a tentative mechanism was proposed. Initially, the N-iodination of NH-sulfoximine (**a**) with NIS generates the key intermediate *N*-iodosulfoximine (**A**). The photoinduced homolysis of the N−I bond in **A** results in a *N*-centered sulfoximidoyl radical (**B**), and an iodo radical. The vicinal addition of **B** and I$^{\bullet}$ radical to cinnamic acid (**1**) results in intermediate (**C**) (path-I). Decarboxylation and concurrent elimination of HI from **C** generate the alkene intermediate (**D**). Alternatively, the addition of radical **B** to cinnamic acid (**1**) produces a benzylic radical intermediate (**C'**) (path-II). The intermediate **C'** upon SET with

iodo radical generates an iodide ion and a carbocation intermediate (**C''**) which upon decarboxylation gives an alkene intermediate (**D**). The I• radical is regenerated by reducing molecular oxygen to a superoxide ion ($O^{2\bullet-}$). This process generates H_2O_2 in the medium which has been confirmed by a few H_2O_2 detection experiments. Next, the vicinal addition of I• radical and superoxide ion $O^{2\bullet-}$ across the double bond of alkene (**D**) produces intermediate **E**, which on elimination of H_2O gives intermediate **F**. The nucleophilic substitution of iodo group by H_2O in intermediate **F** (confirmed by H_2O^{18}) produces an acyloin intermediate (**G**). The final product **1a** is obtained by the oxidation of intermediate **G** (Scheme II.2).

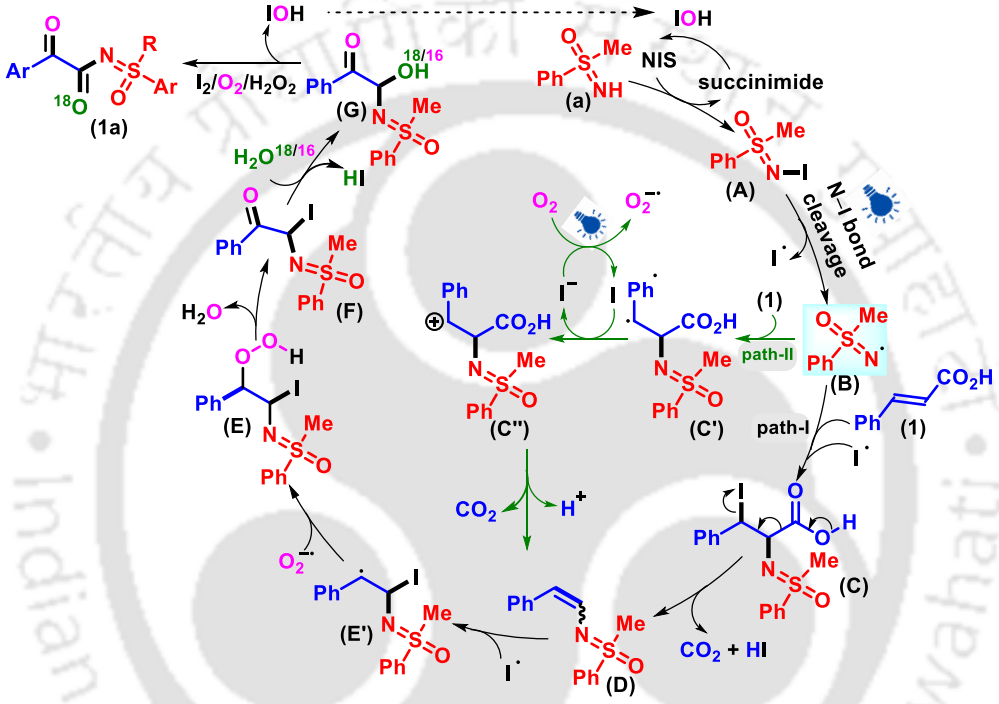

Scheme II.2. *Plausible mechanism for this decarboxylative sulfoximidation reaction.*

In summary, we have disclosed a visible-light-induced decarboxylative coupling between cinnamic acids and NH-sulfoximines which leads to a spectrum of α-keto-*N*-acyl sulfoximines. The reaction proceeds via sulfoximidation, followed by decarboxylation, with concomitant oxidation of the double bond of cinnamic acid, all in the presence of a catalytic amount of NIS. The intrinsic photochemical reactivity of *N*-iodosulfoximines as an excellent reacting partner in the absence of an external photosensitizer is explored.

CHAPTER III: PIDA/I_2-Mediated Photo-Induced Aerobic *N*-Acylation of Sulfoximines with Methylarenes

This chapter describes a visible-light-induced, PIDA/I_2-mediated acylation of NH-sulfoximines with methylarenes as an acyl source. This transition metal, photosensitizer-free approach provides easy access to *N*-acylsulfoximines *via* oxidative coupling of sulfoximines with easily available methylarenes without using any peroxide source.

The acylation of nitrogen atoms stands as one of the most extensively employed chemical transformations in organic synthesis. This reaction holds significant prominence as approximately 20% of all medicinal chemistry experiments rely on this reaction. In this context, the *N*-acylation of sulfoximines is also an area of interest, as to date, there are few biologically active *N*-acylated sulfoximines and the development of newer protocols will lead to their further expansion and utilization in related areas. In the realm of synthesis, methylarenes are particularly appealing for the construction of intricate molecules, including pharmaceuticals, polymers, agrochemicals, and commodity chemicals. Over time, a myriad of methodologies has been established to facilitate direct transformations of benzylic C−H bonds of methylarenes to C−C, C−heteroatom bonds. Further, they serve as a commonly available and inexpensive acyl surrogate. The conventional acylation of sulfoximines with methylarenes requires an appropriate peroxide source and high reaction temperatures, and proceeds in the presence of transition metals or additives (Scheme III.1a).

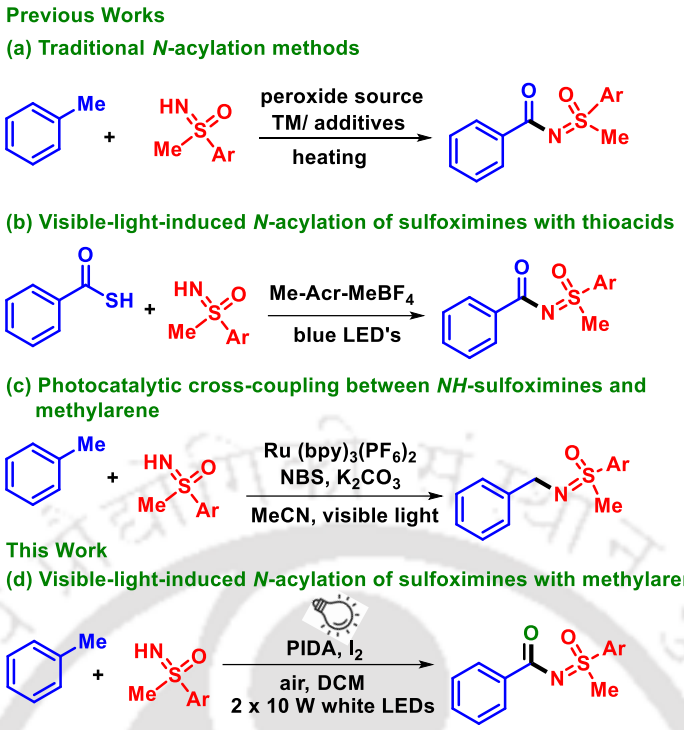

Scheme III.1. *Synthetic approaches for N-acylation and benzylation of sulfoximines.*

Recently, photochemical approaches have gained immense prominence, owing to their operational simplicity, sustainability, and safety. With the advancement of visible-light-mediated reactions, researchers have disclosed methodologies to access *N*-acylsulfoximines under photocatalytic conditions. In 2022, the Song group reported a strategy to access *N*-acylated sulfoximines utilizing thioacids and organic photoredox catalysts (Scheme III.1b). Another, visible light-induced cross-coupling reaction between methylarene and *NH*-sulfoximine was disclosed by Mo *et al.* in 2022, wherein under the presence of $Ru(bpy)_3(PF_6)_2$ photocatalyst and NBS, selective alkylation is obtained (Scheme III.1c).

To further explore this domain, we designed an oxidative cross-coupling strategy between methylarenes and *NH*-sulfoximines under the influence of visible light. In pursuit of accomplishing this idea, a reaction was carried out between *S*-phenyl-*S*-methylsulfoximine (**a**, 1 equiv), toluene (**1**, 5 equiv) in the presence of diacetoxyiodobenzene (PIDA) (3 equiv), and I_2 (1 equiv) in DCM (3 mL) under the irradiation of 2 x 10 W white LEDs at room temperature. After around 30 h, a new product was obtained which was isolated, characterized and found to be *N*-(methyl(oxo)(phenyl)-λ^6-sulfaneylidene)benzamide (**1a**). The formation of *N*-acylsulfoximines through oxidative cross-coupling of sulfoximines with methylarenes under photochemical and peroxide-free conditions appeared interesting from both a mechanistic and

synthetic point of view. After extensive optimization of different reaction parameters such as solvents, oxidants, and light sources, the initial condition was found to be the best for this desired transformation. Further, the scope of this protocol was investigated with different methylarenes and NH-sulfoximines having diverse functionalities. The reaction was found to be well-compatible for all cases except for sulfoximines having an active allylic or benzylic group. Reaction on a large (5 mmol) scale was also performed to check the synthetic utility of this protocol.

Further, a few control experiments, including radical trapping, H_2O^{18}-labelling, and reaction with presynthesized intermediates were performed to get insight into the mechanistic path. Based on all the observations, a plausible mechanism was proposed which is as follows. Initially, the *N*-iodination of *NH*-sulfoximine (**a**) takes place in the presence of IOAc which is generated *in situ* from PIDA and I_2 and gives the key intermediate *N*-iodo sulfoximine (**A**). The intermediate **A** serves as the energy-absorbing species (λ_{max} = 363 nm) under visible light irradiation and undergoes a homolytic N−I bond cleavage resulting in the *N*-centered sulfoximidoyl radical (**a′**), and iodine radical. The iodo radical abstracts a proton from the benzylic C(sp^3)–H bond of toluene and generates the benzylic radical intermediate (**B**) and HI. Intermediate **B** captures O_2 from the atmosphere, along with concurrent abstraction of a proton from HI, resulting in the peroxo intermediate **C** and regenerating iodo radical. The loss of H_2O from **C** gives the benzaldehyde intermediate **D**, which in the presence of iodo radical forms intermediate **E**. The final product **1a** is a result of the coupling between **E** and **a′** (Scheme III.2).

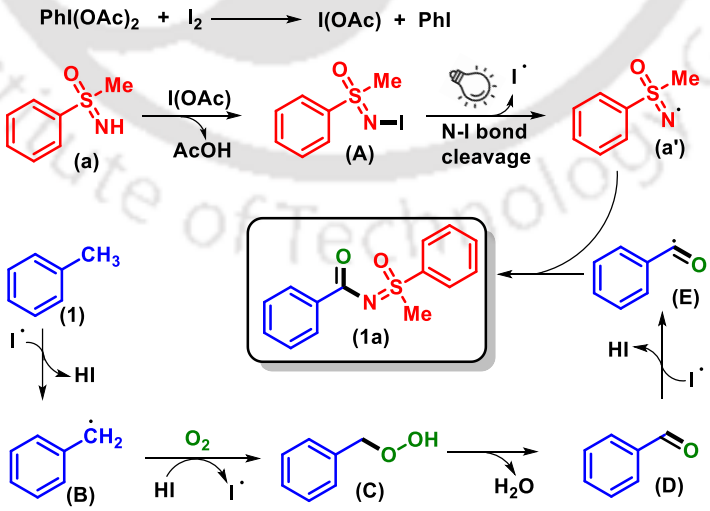

Scheme III.2. *Mechanism for the formation of N-acylsulfoximines.*

In summary, a visible-light-induced transition metal and photocatalyst-free approach for *N*-acylation of sulfoximines has been disclosed. This PIDA/I_2-mediated acylation approach utilizes methylarenes as the acyl donor without using highly oxygenated peroxide sources. The reaction involves *in situ* generated IOAc for the generation of the reactive intermediate *N*-iodosulfoximine which drives out the entire reaction without any external photocatalyst.

CHAPTER IV: Base-Promoted Synthesis of *S*-Arylisothiazolones *via* Intramolecular Dehydrative Cyclization of α-Keto-*N*-acylsulfoximines

This chapter describes a base-promoted synthesis of 1,4-diarylisothiazolones from α-keto-*N*-acylsulfoximines. The developed protocol explores the intrinsic reactivity of the α-C–H in *N*-substituted sulfoximines in the presence of triethylamine. The reaction is driven by the strongly electron-withdrawing dicarbonyl group in the starting material which enhances the acidity of the protons for easy deprotonation. The $\Delta E_{LUMO-HOMO}$ is calculated using Gaussian 16 at the B3LYP/6-31G(d,p) level of theory.

Isothiazolones are a significant class of *N*,*S*-containing heterocycle, which possesses remarkable biological activities, including antimicrobial, anti-inflammatory, antifouling, and antitumor. They are prevalent in various biocides, agrochemicals, preservatives, household cleaning products, and personal care products. For instance, substituted *N*-phenylisothiazolones act as inhibitors of histone acetyltransferase, telomerase, and cartilage destruction enzymes. Isothiazolone-*S*-oxides also exhibit a potential role in the inhibition of PCAF histone acetyltransferase and tumor-associated carbonic anhydrase (hCA IX and XII). The rich chemistry, biological properties, and profound application of these heterocycles have garnered enormous interest in developing more sustainable, efficient, and cost-effective methodologies for their synthesis. Over time, researchers have disclosed diverse multistep strategies to access *N*-substituted isothiazolones, from various prefunctionalized starting materials. Besset group, in 2019, presented a Pd-catalyzed synthesis of isothiazolones from simple acrylamides and an electrophilic SCN source (Scheme IV.1a). In 2021, Song *et al.* reported a Selectfluor-mediated intramolecular oxidative annulation of α-carbamoyl ketene dithioacetals leading to the synthesis of multifunctonalized isothiazolones (Scheme IV.1b).

Bolm group in 2021, reported base mediated synthesis of isothiazolones which proceeded *via* 5-*exo*-*dig* cyclization of *S*-Methyl-*N*-ynonylsulfoximines (Scheme IV.1c).

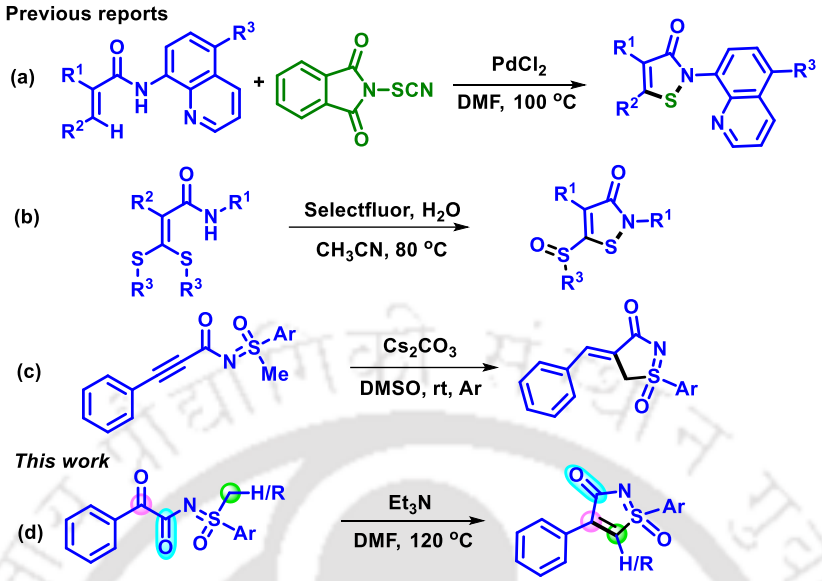

Scheme IV.1. *Different approaches for synthesis of isothiazolones*.

Continuing our quest in exploring sulfoximine chemistry, we emphasized on examining the same behaviour on α-keto-*N*-acylsulfoximines which has a similar acidic carbon and a keto carbonyl in close proximity. An initial reaction was carried out with α-keto-*N*-acylsulfoximines (**1**) in the presence of Et_3N (2equiv.) in DMF at 100 °C and a new product was obtained in 71% yield. The spectroscopic evidence (^1H and $^{13}C\{^1H\}$ NMR and X-ray diffraction) revealed the structure of the product to be 1,4-diphenyl-3H-1λ^6-isothiazol-3-one 1-oxide (**1a**). Intrigued by this outcome, further optimization of various reaction parameters such as base, solvent, and temperature were carried out and after detailed studies, it was concluded that the best condition for this base-promoted cyclization is the use of *α*-keto-*N*-acylsulfoximine (1 equiv) and Et_3N (7 equiv) in 1.5 mL of DMF at 120 °C. With the set conditions, the scope of this intramolecular dehydrative cyclization protocol was explored for a variety of α-keto-*N*-acylsulfoximines. Different substituents on both the phenyl rings (towards the sulfoximidoyl part and the carbonyl part) reacted efficiently to result in the products in good to excellent yields. Moreover, α-keto-*N*-acylsulfoximines having a secondary carbon center adjacent to the *S*-atom, that is, benzylic, also underwent smooth conversion to the isothiazolone products.

Further, a mechanistic path has been proposed based on control experiments and literature reports. In the presence of Et_3N, one of the protons on the *S*-methyl is deprotonated to form a carbanionic intermediate **A**. The C-nucleophile (carbanion) then attacks the more electrophilic keto-carbonyl group intramolecularly and forms the cyclic intermediate **B**. The formation of either intermediate **A** and/or **B** was confirmed by HRMS analysis of the reaction mixture. Protonation of the anionic counterpart with elimination of Et_3N gives the intermediate **C**. The formation of product **1a** from hydroxy intermediate **C** proceeds *via* an E1cB mechanism, wherein, the abstraction of another α-H results in the carbanion intermediate **D**, which is stabilized by the neighboring sulfoxide group. Finally, the leaving –OH group departs from **D** to give the isothiazolone (**1a**) (Scheme IV.2).

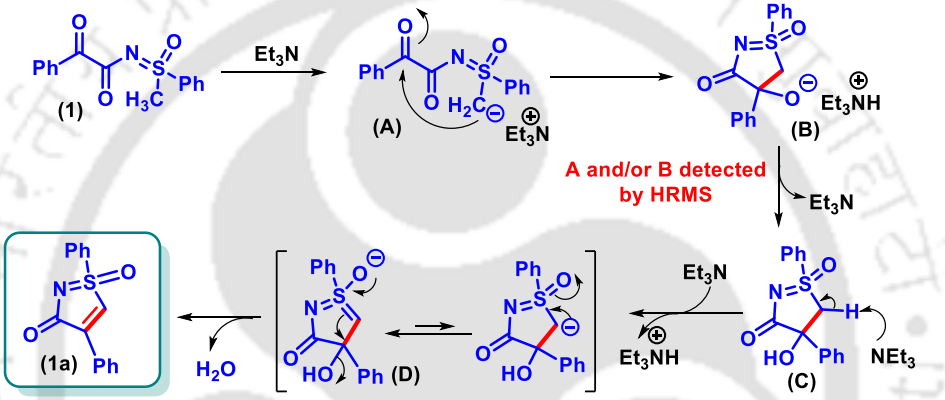

Scheme IV.2. *Mechanism for the formation of 1,4-diarylisothiazolones.*

To demonstrate the scalability of the reaction, a gram-scale reaction of **1** (3.5 mmol, 1.004 g) was conducted in an identical reaction setup which resulted in the product with 71% yield. To gain insight into the geometry and electronic structure of the isothiazolones, density functional theory (DFT) calculations were performed with a B3LYP/6-31G (d, p) level of theory in DMF solvent modelled by the polarizable continuum model (PCM) approach (the Gaussian 16 program). The calculated HOMO-LUMO energy gap was found in the range of 3.79–4.48 eV. Moreover, the UV–vis absorption spectra of some of the synthesized compounds were recorded and the UV absorption maximum (wavelength) was in close correlation with the computationally determined $\Delta E_{\text{LUMO–HOMO}}$ values.

In conclusion, an efficient method to synthesize *S*-substituted isothiazolones *via* a base-promoted intramolecular dehydrative cyclization of α-keto-*N*-acylsulfoximines is presented. The reaction proceeds *via* α-hydrogen abstraction from sulfoximine, followed by an intramolecular nucleophilic attack at the keto carbonyl to form a *tert*-hydroxy isothiazolone

intermediate. The 1,4-substituted isothiazolone is obtained after dehydration *via* an E1cB path. This one-pot synthesis of isothiazolinones has a broad substrate scope, high atom economy, and provides products with good to excellent yields.

CHAPTER V: An Expedient Route to Tricyanovinylindoles and Indolylmaleimides from *o*-Alkynylanilines Utilizing DMSO as a One-Carbon Synthon

This chapter describes a route for synthesizing tricyanovinylindoles from *o*-alkynylanilines utilizing DMSO as a carbon synthon and NH_4SCN as a cyano source. Further, selective hydrolysis of the synthesized tricyanovinylindoles leads to the formation of indolylmaleimides.

In the past decades, the intramolecular cyclization of *o*-alkynylaniline derivatives and their subsequent functionalization have garnered much attention as one of the key strategies to form substituted indoles. Indole is one of the most privileged nitrogenous heterocycles found in nature. The widespread application of indoles in pharmaceuticals, bioactive natural products, and functional materials makes them a hot molecule among medicinal and synthetic chemists. Indole is the fourth most predominant heterocycle having its core skeleton in 24 marketed drugs. Considering the demand and usefulness of functionalized indole scaffolds, much attention has been paid to their synthesis, through either construction or modification of the pre-existing indole rings.

Our group is actively involved in the domino synthesis of different *N*-heterocycles such as 3-aroylindole, benzofuran[3,2-*c*]quinolin-6[5*H*]ones, indolo[2,3-*b*]quinolones and quinoline-4(1*H*)-thiones utilizing *o*-alkynylanilines as the synthetic precursor. To further explore *o*-alkynylanilines, we treated 2-(phenylethynyl)aniline (**1**) (1 equiv.) with malononitrile (**a**) (2 equiv.) in the presence of KSCN (2 equiv.), CuBr (15 mol%), and NBS (1 equiv.) in DMSO at 110 ^{o}C in open air. After 6 hours, complete consumption of **1** with the appearance of a sharp orange colour spot in the TLC marked the completion of the reaction. The spectroscopic analysis of the isolated product (43%) and single-crystal X-ray diffraction studies of one of its derivatives, confirmed the structure to be 2-(2-phenyl-1*H*-indol-3-yl)ethene-1,1,2-tricarbonitrile (**1a**). Intrigued by this outcome, a series of reactions were conducted to find out the optimized condition for this transformation. The best condition for this transformation is found as the use of malononitrile (**a**) (4 equiv), $PdCl_2$ (7 mol%),

$Cu(OAc)_2$ (7 mol%), NH_4SCN (2 equiv), and NBS (1 equiv) in DMSO at 110 ^oC. Having the optimized reaction conditions in hand, the scope of this novel cyclization-functionalization protocol was extended to various *o*-alkynylanilines diverse functionalities in the phenyl ring towards the amine and alkynyl side of *o*-alkynylaniline. The reaction was successful in most cases including aliphatic and heteroaromatic substrates. However, the reaction failed when there was a strongly withdrawing $-NO_2$ or –CN group in the para position of the amine group.

After the successful demonstration of the substrate scope, further investigations were carried out to understand the mechanism of this unprecedented reaction. Reaction with presynthesized intermediates, HRMS, and NMR analysis of the reaction aliquots, and radical trapping experiments suggested a radical pathway and involvement of DMSO as the carbon source and NH_4SCN as the cyano source. The mechanism was proposed as follows (Scheme V.1). Initially, 2-(phenylethynyl)aniline (**1**) undergoes 5-*endo-dig* cyclization *via* aminopalladation to give 2-phenyl indole (**B**). This heterocycle **B** is oxidized to aminyl intermediate **C**. On the other hand, the heterolytic cleavage of DMSO to the CH_3 radical occurs in the presence of Cu^{II} and O_2. The radical coupling of intermediate **C** and the CH_3 radical gives 3-methyl-2-phenyl indole (**D**). Next, the CH_3SO species abstracts an H radical from intermediate **D** to give intermediate **E** and methanesulfonic acid in the presence of oxygen. Further oxidation of intermediate **E** in the presence of Cu^{II}/O_2 generates a peroxy species (**F**) *via* intermediate **F'**. The peroxy intermediate **F** generates a formyl intermediate (**G**), which subsequently undergoes Knoevenagel type condensation with malononitrile to give intermediate **H**. Next, the conjugate addition of the CN^- ion (obtained from NH_4SCN) to intermediate **H** occurs with concurrent bromination utilizing NBS. The formation of the desired tricyanovinylindole (**1a**) is achieved *via* the elimination of HBr which is facilitated by a succinimide anion.

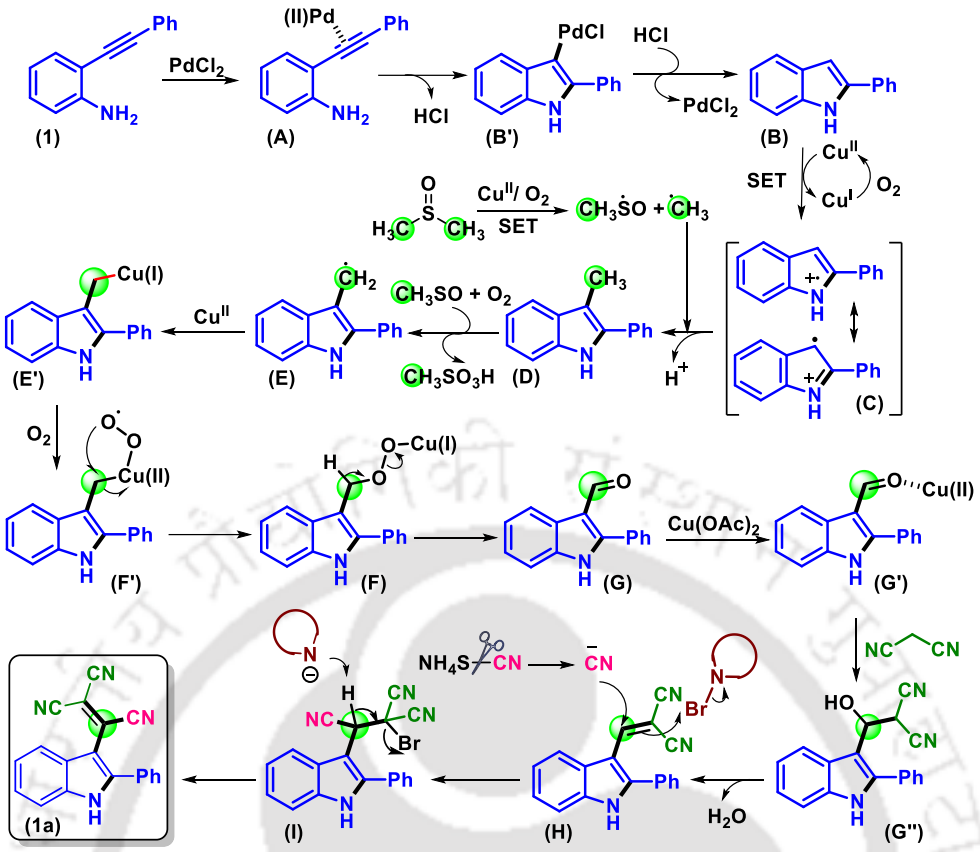

Scheme V.1. *Mechanism for the formation of tricyanovinylindoles.*

To account for the relative stability of 3-methylindole (intermediate **D**) and its further oxidation even in the presence of methyl groups in other positions in the substrate, DFT calculations were carried out using a Gaussian-16 program package.

In an attempt to carry out further synthetic transformations of the product, selective hydrolysis was attempted to convert the nitrile functionality to an amide functionality. Treatment of tricyanovinylindoles with $Cu(OAc)_2.H_2O$ in AcOH at 80 ^oC resulted in selective hydrolysis of one of the nitrile functionalities and its concomitant cyclization to form 3-cyanoindolylmaleimides (**1ab**) (Scheme V.2). The *cis*-cyano groups originating from malononitrile is selectively hydrolyzed due to the higher electron density owing to conjugation with the nitrogen atom of the pyrrole ring.

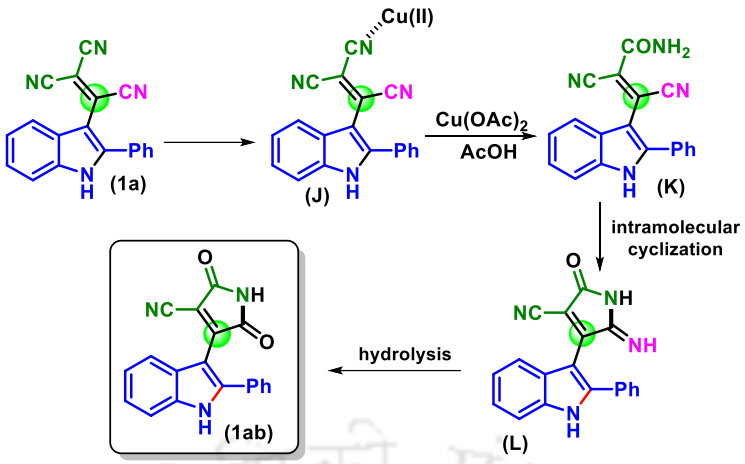

Scheme V.2. *Mechanism for the formation of 3-cyanoindolylmaleimides.*

Next, photophysical studies such as UV-vis and photoluminescence were conducted on a few selected compounds. As evident from the UV-vis spectra, most compounds exhibited three distinct absorption maxima. The fluorescence emission spectra infer that few compounds show good fluorescence intensity, and thus they may find potential application in various fields of research.

In conclusion, an efficient one-pot strategy for the synthesis of tricyanovinylindoles utilizing DMSO as a one-carbon surrogate is developed. This operationally simple reaction leads to the formation of one C–N, one C–C, and two C– C bonds. This cascade reaction undergoes sequential cyclization, formylation followed by cyanation to generate functionalized indoles. The post-synthetic modification resulted in the unprecedented formation of 4-cyano-3-indolylmaleimides.

CONTENTS

Chapter I. An Overview of Sulfoximines and *o*-Alkynylanilines Towards C–C and C–Heteroatom Bond Formation

Chapter III. PIDA/I_2-Mediated Photo-Induced Aerobic *N*-Acylation of Sulfoximines with Methylarenes

LIST OF ABBREVIATIONS

CCDC	*cambridge crystallographic data centre*
ORTEP	*oak ridge thermal ellipsoid plot*
NMR	*nuclear magnetic resonance*
MHz	*megahertz*
HRMS	*high resolution mass spectrometry*
ESI-MS	*electrospray ionization mass spectrometry*
IR	*infrared*
XRD	*X-ray diffraction*
LED	*light emitting diode*
M.p.	*melting point*
DMSO	*dimethyl sulfoxide*
DMF	*dimethylformamide*
DCM	*dichloromethane*
DCE	*1,2-dichloroethane*
THF	*tetrahydrofuran*
NIS	*N-iodosuccinimide*
NBS	*N-bromosuccinimide*
NCS	*N-chlorosuccinimide*
PIDA	*phenyliodonium diacetate*
PC	*photocatalyst*
DFT	*density functional theory*
MO	*molecular orbital*
HOMO	*highest occupied molecular orbital*
LUMO	*lowest occupied molecular orbital*

भारतीय प्रौद्योगिकी संस्थान गुवाहाटी
Indian Institute of Technology Guwahati

Chapter I

An Overview of Sulfoximines and o-Alkynylanilines Towards C–C and C–Heteroatom Bond Formation

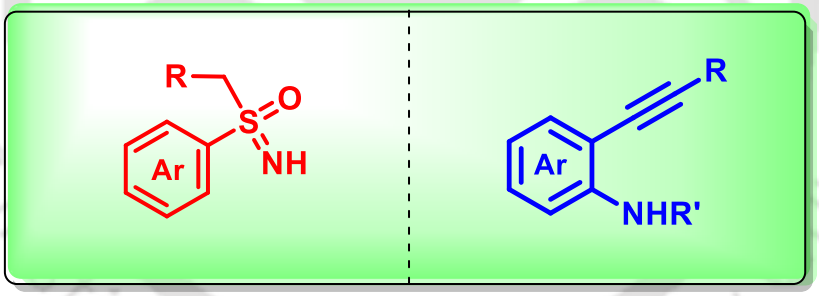

भारतीय प्रौद्योगिकी संस्थान गुवाहाटी
Indian Institute of Technology Guwahati

CHAPTER IA

An Overview on the Chemistry and Reactivity of Sulfoximines

IA.1. Introduction:

Sulfoximines, which are mono-aza analogue of sulfones have witnessed continuous attention over the past decades owing to their unique structural architecture. Over time, sulfoximines have been used as reagents, chiral auxiliaries, ligands, organocatalysts, pharmaceuticals, and agrichemicals.[1] Since 1949, when sulfoximines were discovered as a new class of compounds, they attracted wide attention. Since the initial discovery of the irreversible glutamine synthetase inhibitor L-methionine-(*S*)-sulfoximine (MSO), there has been a substantial increase in the number of bioactive molecules incorporating the sulfoximine moiety into their structure. Following this breakthrough, buthionine sulfoximine (BSO), identified as a gamma-glutamyl-cysteine synthetase inhibitor, proved effective in treating tumours with overexpressed glutathione (GSH) and was utilized as an adjuvant in chemotherapy. Various sulfoximines have been evaluated as bioactive agents, with some progressing to clinical trials including the kinase inhibitors roniciclib, BAY 1143572, and AZD 6738 (Figure IA.1).[1,2]

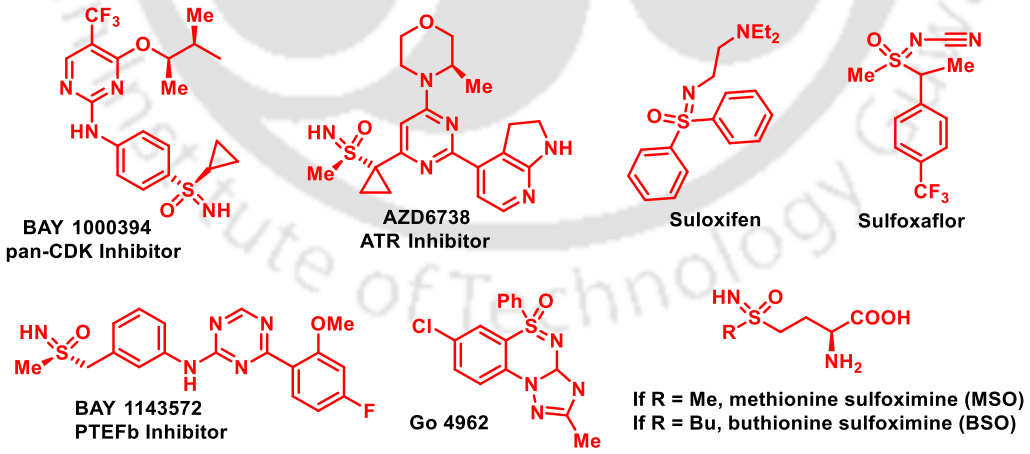

Figure IA.1. *Some biologically relevant sulfoximines.*

Structurally, sulfoximines are isoelectronic with sulfones having a tetrahedral sulfur atom and a basic nitrogen atom (pKa (NH_2^+) = 2.7 in water). The S atom bears a stereocenter (if not substituted symmetrically) and is chemically and configurationally stable. The basic

nitrogen atom can form complexes with metal ions and form salts with mineral acids. Modifying the substitution pattern at the nitrogen atom makes it possible to modulate the acidic/basic properties of the compounds. Sulfoximines exhibit distinctive H–bond donor/acceptor capabilities. The sulfur-bound heteroatoms act as hydrogen-bond acceptors, whereas, N-unsubstituted sulfoximines have the potential to serve both as hydrogen-bond donors (*via* NH) and acceptors. Sulfoximines show good solubility in protic solvents (in water or alcohol) and display high metabolic stability levels. All these properties of sulfoximines make it a hydrophilic, and stable functional group in organic synthesis and drug discovery.[1]

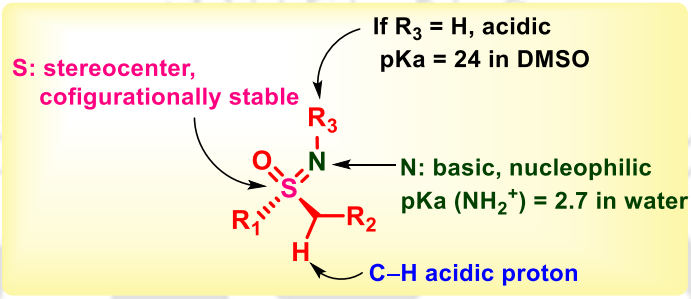

Figure IA.2. *General properties of sulfoximines.*

Various synthetic methods are available for the synthesis of sulfoximine (Scheme IA.1). One approach involves the imination of sulfides to produce sulfilimines, which are then oxidized to obtain sulfoximines (path I). Alternatively, the synthesis of sulfoximines may start from the oxidation of sulfides to first obtain sulfoxides, which are then imidized (path II). The deprotection of *N*-protected sulfoximines can result in NH-sulfoximines. The most commonly employed method involves simultaneously introducing oxygen and nitrogen groups into sulfides to prepare NH-sulfoximines (path III). These diverse pathways provide flexibility in synthesizing sulfoximines depending on the specific requirements of the desired compounds.[1]

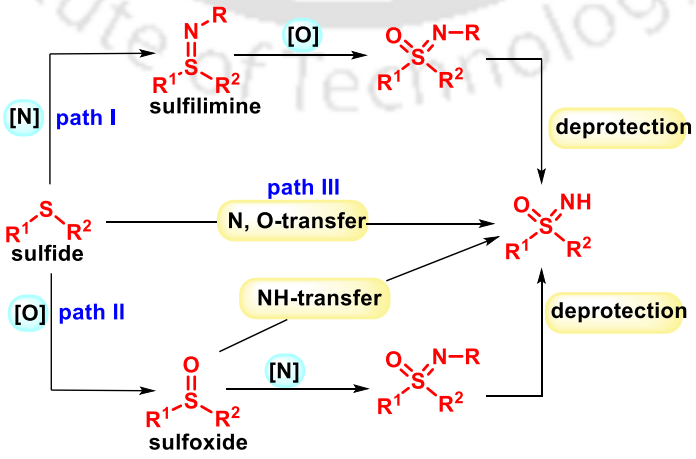

Scheme IA.1. *General strategies for the synthesis of sulfoximines.*

The S(VI) functionality of sulfoximines is actively utilized in modern synthesis as an excellent reacting partner and as chiral auxiliaries or ligands for asymmetric catalysis. The renewed interest in sulfoximine chemistry is evident through the ongoing development of new synthetic strategies for their preparation and functionalization, underscoring their evolving importance in contemporary chemical research.

IA.2. Transformations of Sulfoximines:

The functionalization of sulfoximines is an area of considerable interest due to the diverse applications of these compounds in different fields of research. Figure IA.3 illustrates the various active positions in *S*-aryl-*S*-alkyl-NH-sulfoximines that are amenable to further functionalization.

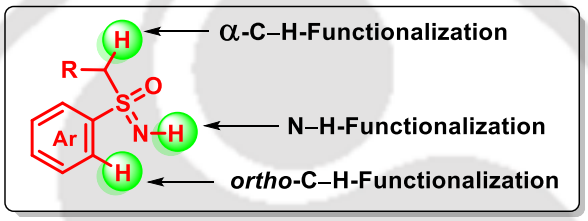

Figure IA.3. *Reactive sites in sulfoximines.*

Depending on the structure, the reactive site present in sulfoximines can undergo the following types of transformation:

- N–H Functionalization
- α-C–H Functionalization
- *Ortho*-C–H Functionalization

IA.2.1. NH Functionalization of Sulfoximines:

The high reactivity of the N-atom in NH-sulfoximines allows it to undergo various transformations, including arylations, alkylations, vinylations, alkynylations, acylation, halogenation, phosphorylation, and many more. This N-reactivity is mainly governed by the nucleophilicity of the N-atom and the stability of the N-centered radical. This facilitates the construction of various N–C and N–heteroatom bonds making it a valuable building block in synthetic chemistry.

IA.2.1.1. *N*-Halogenation:

The N-atom of NH-sulfoximines has a nucleophilic and basic character and can be halogenated in the presence of an appropriate alkylating source. Treatment of NH-sulfoximines with halogenating reagents such as Cl_2, NaOCl, ^{t}BuOCl, NCS, Br_2, or NBS, and NIS or I_2 can efficiently generate a series of the *N*-halo sulfoximines in good yields (Scheme IA.2.1.1.1).[3]

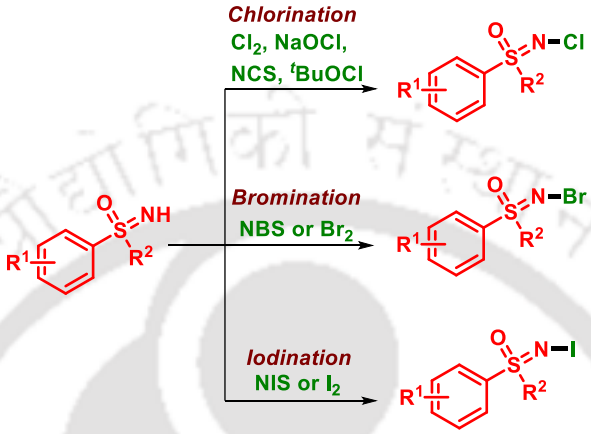

Scheme IA.2.1.1.1. *Synthesis of N-halo sulfoximines.*

In 2021, Bolm group reported a visible light-promoted NH-chlorination and bromination of sulfoximines *via* an *in situ* formed sulfoximidoyl-containing hypervalent iodine reagent. The reaction utilizes dichloromethane and dibromomethane as the halogen source and proceeds under air in a catalyst and additive-free condition delivering the products in good yields (Scheme IA.2.1.1.2).[4]

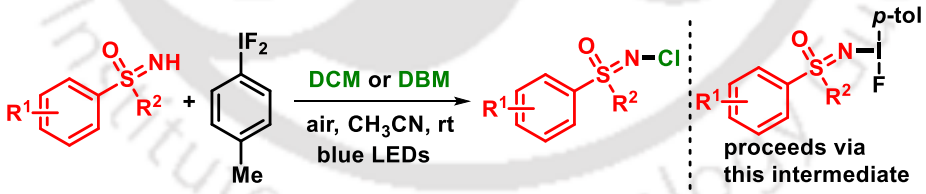

Scheme IA.2.1.1.2. *Visible-light-promoted synthesis of halogenated sulfoximines.*

IA.2.1.2. *N*-Nitration:

The exclusive method for synthesizing *N*-nitro sulfoximines was first reported by Mutti and Winternitz in 1986 which involved a two-step process. NH-sulfoximines were first treated with concentrated HNO_3 at 0 to 10 °C, followed by subsequent addition of Ac_2O and H_2SO_4 at temperatures ranging from 20 and 50 °C. The resulting nitro compounds were obtained in good to excellent yields of up to 100% (Scheme IA.2.1.2).[5]

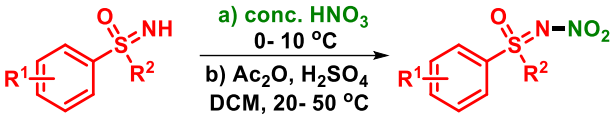

Scheme IA.2.1.2. *Synthesis of N-nitro sulfoximines.*

IA.2.1.3. *N*-Arylation:

A Pd-catalyzed *N*-arylation of sulfoximines was first reported by Bolm and Hildebrand in 1998 which was inspired by Buchwald-Hartwig Pd-catalyzed C–N cross-coupling between amines and aryl halides. Herein, under the presence of a catalytic amount of Pd and biphosphine ligand, various NH-sulfoximines were coupled with aryl bromides generating a series of N-arylated products. (Scheme IA.2.1.3.1, condition A).[6a] In 2004, the Bolm group disclosed a Cu-mediated cross-coupling reaction between sulfoximines with aryl iodides and bromides to provide *N*-arylated sulfoximines in high yields (Scheme IA.2.1.3.1, condition B).[6b] In 2008, they again disclosed a Fe(III)-catalyzed cross-coupling between sulfoximines and aryl iodides which features the combination of environmentally friendly $FeCl_3$ and N,N′-dimethylethylenediamine (DMEDA) as a catalytic system (Scheme IA.2.1.3.1, condition C).[6c]

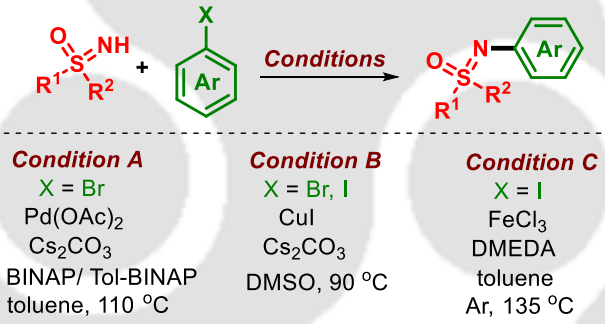

Scheme IA.2.1.3.1. *TM-catalyzed N-arylation of sulfoximines with aryl halides.*

In 2005, Moessner and Bolm presented a $Cu(OAc)_2$ catalyzed *N*-arylation of NH-sulfoximines using aryl boronic acids as arylating agents. This Cu-activated C–N bond formation was inspired by Chan-Lam type couplings and could prepare some special N-arylsulfoximines that were previously difficult to access (Scheme IA.2.1.3.2, top).[7a] In 2012, Varma and coworkers presented an ultrasound-expedited route for the preparation of *N*-aryl sulfoximines utilizing aryl iodonium salts as arylating agents. This C–N cross-coupling reaction proceeds using $CuBr_2$ as the catalyst in aqueous polyethylene glycol-400 solvent under mild reaction conditions (Scheme IA.2.1.3.2, down).[7b]

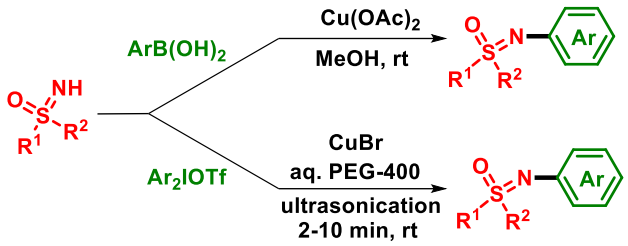

Scheme IA.2.1.3.2. *N-arylation of sulfoximines.*

Arynes present an appealing alternative in organic chemistry, primarily due to their unique electronic properties, making them excellent substrates in metal-free organic transformations. In 2015, Pal and co-workers reported a transition metal-free, operationally simple approach for *N*-arylation of sulfoximines using aryne precursors. This methodology is compatible with a broad range of substrates including enantiopure substrates, making it a more versatile and practical approach for the arylation of sulfoximines (Scheme IA.2.1.3.3).[8]

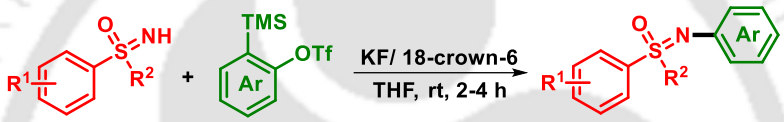

Scheme IA.2.1.3.3. *N-arylation of sulfoximines.*

In the following year, the same group developed a strategy for the preparation of N-azine sulfoximines from NH-sulfoximines and (quinoline, isoquinoline, and pyridine) azine-*N*-oxides. This metal-free, phosphonium-salt mediated, DIPEA-promoted reaction proceeds at room temperature, is operationally simple, and has broad functional group compatibility. Further, this method finds application in the sulfoximination of azine-based functional molecules such as 1,10-phenanthroline, 2,2′-bipyridine, and quinine (Scheme IA.2.1.3.4).[9]

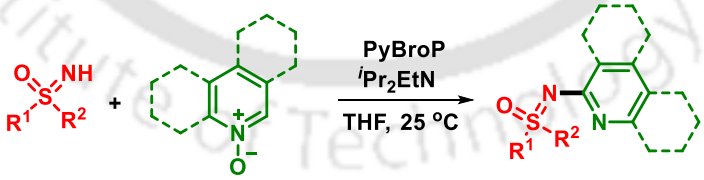

Scheme IA.2.1.3.4. *Reaction between azine-N-oxide and sulfoximines.*

In 2018, Yotphan *et al.* devised a mild and efficient methodology for the direct incorporation of the sulfoximine group into the C3 position of quinoxalinones. This $K_2S_2O_8$-promoted oxidative C–N bond coupling strategy proceeds smoothly without the requirement of a metal catalyst. The protocol demonstrates its versatility for a broad spectrum of quinoxalinone and NH-sulfoximines to yield the coupling products in moderate to excellent yields (Scheme IA.2.1.3.5).[10]

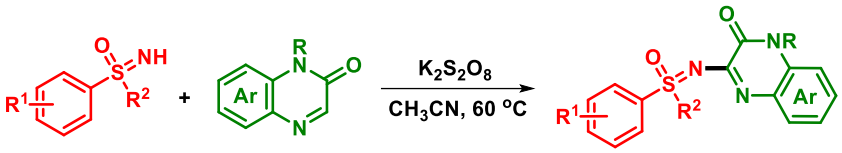

Scheme IA.2.1.3.5. *Oxidative C-N coupling between quinoxalinone and sulfoximines.*

Wimmer and König applied a dual nickel photocatalytic method for *N*-arylation of sulfoximines with brominated (het)arenes as coupling partners. This approach involves the combination of nickel and photoredox catalysis, providing a powerful and flexible strategy for the synthesis of *N*-arylated sulfoximines (Scheme IA.2.1.3.6).[11]

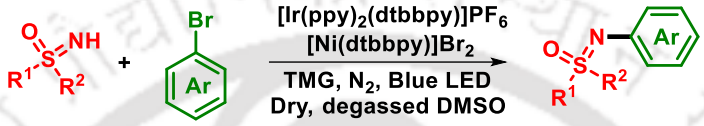

Scheme IA.2.1.3.6. *[Ir]/[Ni]-photocatalyzed N-arylation of sulfoximines.*

A novel strategy for the *N*-arylation of NH-sulfoximines was developed by Mei and co-workers in 2021 by combining nickel catalysis and electrochemistry in an undivided cell. The protocol utilizes paired electrolysis, eliminating the need for a sacrificial anode. Mechanistic investigation suggests that the anodic oxidation of a Ni^{II} species is crucial for promoting the reductive elimination of a C–N bond from the resulting Ni^{III} species at room temperature (Scheme IA.2.1.3.7).[12]

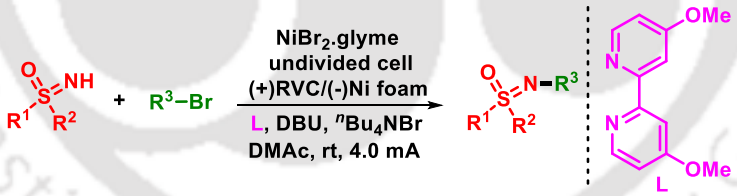

Scheme IA.2.1.3.7. *Electrochemical N-arylation of sulfoximines.*

IA.2.1.4. *N*–Alkylation:

Some of the pioneer studies include the reaction of *S*-phenyl-*S*-methyl sulfoximine with formaldehyde and formic acid to give *N*-methylsulfoximine and the use of methyl fluorosulfate.[13] Along the same line of study, Johnson *et al.* in 1993, revealed an alkylation strategy with alkyl bromides in dimethoxyethane (DME), utilizing potassium hydride (KH) as the base, and tetrabutylammonium bromide as the phase transfer catalyst (Scheme IA.2.1.4.1).[14]

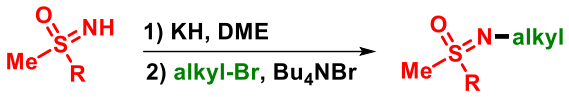

Scheme IA.2.1.4.1. *Alkylation of NH-sulfoximines.*

Another report by the Bolm group presented a room-temperature alkylation of NH-sulfoximines wherein they subjected alkyl bromide to NH-sulfoximine in the presence of KOH in DMSO. A variety of *N*-alkylated sulfoximines were prepared in good to excellent yields including the biologically active Suloxifen (Scheme IA.2.1.4.2).[15]

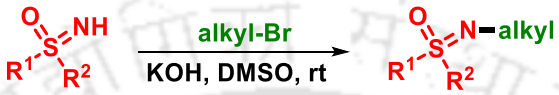

Scheme IA.2.1.4.2. *Bolm's alkylation of NH-sulfoximines.*

In 2014, the same group developed a method for synthesizing *N*-alkylated sulfoximines *via* an Fe-catalyzed hetero-cross-dehydrogenative coupling reaction of NH-sulfoximines with diarylmethanes. The transformation exhibited good functional group tolerance, producing the respective alkylation products in moderate to good yields (Scheme IA.2.1.4.3).[16] In the following year, Yu and Cheng disclosed a Cu(II)-catalyzed C(sp^3)–H/N–H coupling of sulfoximines with alkanes in the presence of DTBP as an oxidant (Scheme IA.2.1.4.4).[17]

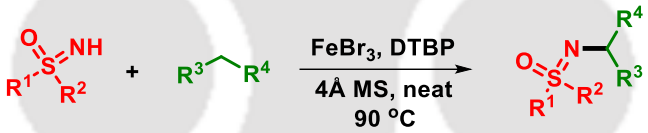

Scheme IA.2.1.4.3. *Fe(II)-catalyzed alkylation of NH-sulfoximines.*

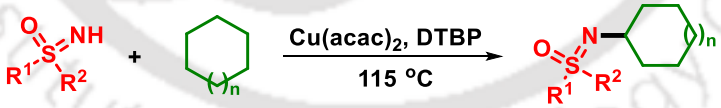

Scheme IA.2.1.4.4. *Cu(II)-catalyzed NH-alkylation of sulfoximines*

Bolm and coworkers developed a strategy for enantio- and regioselective allylic alkylation of sulfoximines with Morita-Baylis-Hillman carbonates. This asymmetric reaction is guided by a quinidine-derived organocatalyst, yielding a variety of optically active α-methylene β-sulfoximidoyl esters in high yields, of up to 93% and enantiomeric excess of up to 95% (Scheme IA.2.1.4.5).[18]

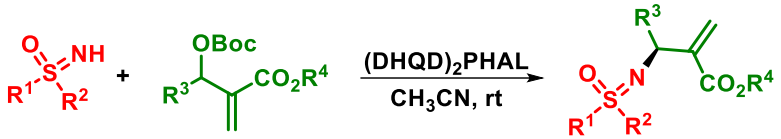

Scheme IA.2.1.4.5. *Organocatalytic asymmetric allylic alkylation of sulfoximines.*

Very recently, Jia *et al*. synthesized *N*-alkylated sulfoximines from NH-sulfoximines and alkenes through a photocatalytic anti-Markovnikov hydroamination strategy. This approach exhibits broad substrate tolerance, accommodating primary, secondary, and tertiary alkyl substituents, as well as a diverse range of sulfoximines. Mechanistic studies support the involvement of a photocatalytic pathway, indicating that the alkene radical cation, rather than the iminium radical, serves as the intermediate in the transformation (Scheme IA.2.1.4.6).[19]

Scheme IA.2.1.4.6. *Photocatalytic N-Alkylation of NH-sulfoximines via anti–Markovnikov hydroamination of alkene.*

IA.2.1.5. *N*-Acylation:

The acidic imine nitrogen can be deprotonated with an organic base, generating a weakly nucleophilic anion which could then react with a suitable electrophile to yield *N*-acylated products. Generally, *N*-acylations of NH sulfoximines can be achieved using acyl halides, anhydrides, aldehydes, and carboxylic acid as the common acylating source.[1] One of the earlier examples of *N*-acylation involves the DMAP catalyzed reaction between acyl halides and NH-sulfoximines in the presence of a base such as Et_3N or pyridine, resulting in the high-yield of *N*-acylated products (Scheme IA.2.1.5.1).[20]

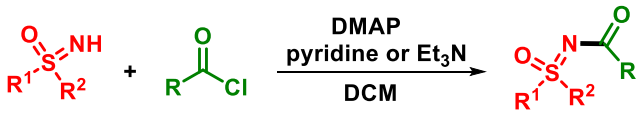

Scheme IA.2.1.5.1. *N-Acylation of sulfoximines with acyl halides.*

In 2004, Bolm and coworkers reported a carbodiimide-mediated coupling reaction involving NH-sulfoximines and acyl halides, resulting in the synthesis of *N*-acylated products. Despite the inherent weak nucleophilicity of sulfoximines, NH-sulfoximines were effectively coupled with carboxylic acids using DCC (dicyclohexylcarbodiimide) or EDC [1-ethyl-3-(3-

dimethylaminopropyl)carbodiimide] (Scheme IA.2.1.5.2).[21] Garimallaprabhakaran and Harmata contributed to this area by developing a boric acid-mediated *N*-acylation of sulfoximines with carboxylic acids (Scheme IA.2.1.5.2).[22]

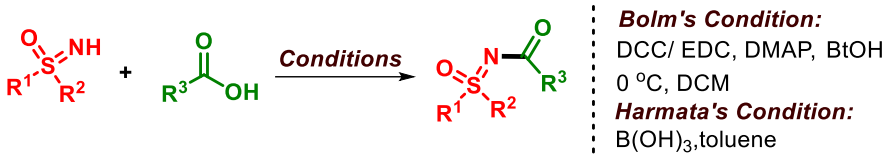

Scheme IA.2.1.5.2. *N-Acylation of sulfoximines with carboxylic acids.*

Deng *et al*. reported the first C−H/N−H cross-coupling reaction targeting *N*-aroylated sulfoximines utilizing TBAI/TBHP catalytic system and n-hexane as the solvent (Scheme IA.2.1.5.3).[23a] In the subsequent year, Guin and coworkers disclosed a NHC-catalyzed acylation of NH-sulfoximines with aldehydes, utilizing DBU as the base and bisquinone as the oxidant. This approach allowed the amidation of numerous unactivated aliphatic and heteroaromatic aldehydes, achieving high yields (Scheme IA.2.1.5.3).[23b] Zeng group developed the first visible light-mediated synthesis of *N*-aroylsulfoximines, utilizing a combination of TBHP and $K_2S_2O_8$ as oxidants, without the need for any photosensitizer, metal catalyst, or base (Scheme IA.2.1.5.3).[23c]

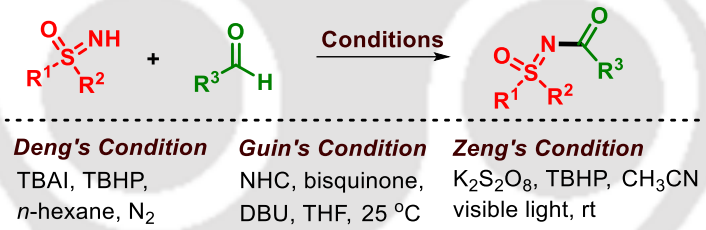

Scheme IA.2.1.5.3. *N-Acylation of sulfoximines with aldehyde.*

Kumar and Yuan in 2017 disclosed a Pd-catalyzed aroylation of NH-sulfoximines with aryl halides utilizing chloroform as the CO source. Under the optimized reaction conditions, a diverse array of aryl halides and sulfoximines exhibited smooth reactivity, leading to the formation of the corresponding products in moderate to good yields (Scheme IA.2.1.5.4).[24]

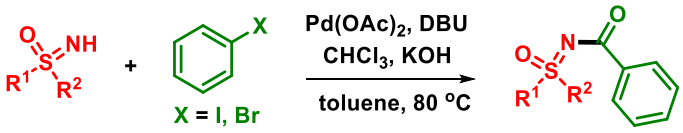

Scheme IA.2.1.5.4. *N-Acylation of sulfoximines with arylhalides.*

Another interesting approach for the formation of *N*-acyl sulfoximines involves oxidative C–C bond cleavage of ketones under blue light irradiation. Here, NH-sulfoximines are subjected to ketones in the presence of NBS using blue LED light at room temperature in the presence of air. The photoinduced process relies on radicals generated through a Norrish Type 1 bond cleavage mechanism. The methodology is successful for a broad range of NH-sulfoximines and ketones providing the products in good to excellent yields (Scheme IA.2.1.5.5).[25]

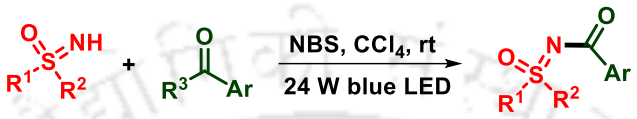

Scheme IA.2.1.5.5. *Visible-light-induced acylation of sulfoximines with ketones.*

An electrochemical strategy for *N*-acylation of sulfoximines using hydroxamic acid as the acyl source has been recently disclosed by Jiang and Ji. The importance of the methodology is evident through its mild conditions, eliminating the need for an external oxidant or catalyst. Through mechanistic studies, key by-products N_2O and H_2 were identified, and a plausible mechanistic rationale was proposed. Further, the reaction has a broad substrate scope with good functional group tolerance and is easily scalable (Scheme IA.2.1.5.6).[26]

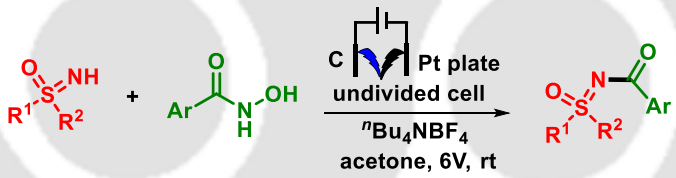

Scheme IA.2.1.5.6. *Electrochemical acylation of sulfoximines with hydroxamic acid.*

IA.2.1.6. α-keto-*N*-Acylation:

Dong and An reported a CuI-mediated α-ketoacylation of sulfoximines in 2015 which proceeds utilizing DTBP as an oxidant under a solvent-free condition. The plausible mechanistic rationale of this C(sp^3)–N coupling involves a double catalytic cycle comprising elemental iodine and copper. The *in situ* generated aryl-α-iodo-ethanone and a sulfoximine-liganded-Cu^{II} intermediate plays crucial roles in the overall strategy (Scheme IA.2.1.6.1).[27]

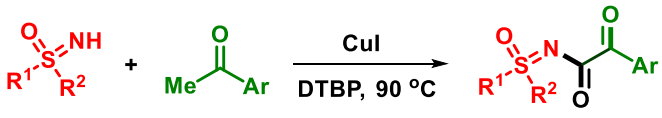

Scheme IA.2.1.6.1. *CuI-mediated α-ketoacylation of sulfoximines.*

In 2021, Kandasamy *et al.* disclosed a metal-free approach of α-keto-*N*-acylation of sulfoximines by a SeO_2-promoted reaction between NH-sulfoximines and acetophenones. The reaction occurs in DCE at 60 °C and has a good functional group tolerance resulting in the desired products in good yield (Scheme IA.2.1.6.2).[28]

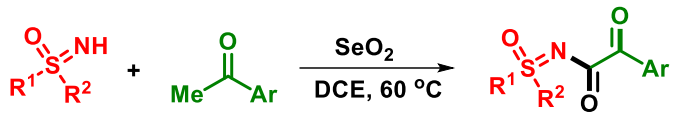

Scheme IA.2.1.6.2. *SeO_2-promoted α-ketoacylation of sulfoximines.*

Another recent work disclosed a photochemical way for the synthesis of α-keto-*N*-acyl sulfoximines from NH sulfoximines and gem-difluoroalkenes. The reaction occurs in air under the irradiation of blue light without the requirement for a photocatalyst or additional oxidant. Mechanistic studies indicate that the two oxygens in the products originate from water and dioxygen, respectively (Scheme IA.2.1.6.3).[29]

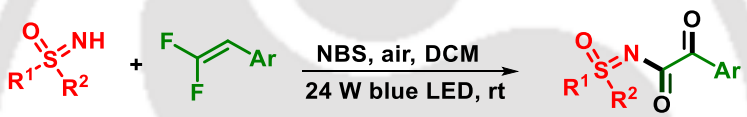

Scheme IA.2.1.6.3. *α-Keto-N-Acylation of sulfoximines.*

IA.2.1.7. *N*-Alkenylation:

The first instance of NH-vinylation of sulfoximines was reported by Dehli and Bolm in 2004 wherein *N*-vinyl sulfoximines were obtained in high yields through the reaction of NH-sulfoximines with vinyl bromides. The reaction employed a Pd catalyst, BINAP, and ^{t}BuONa for the reduction of the vinyl moiety and the successful formation of the product (Scheme IA.2.1.7.1).[30]

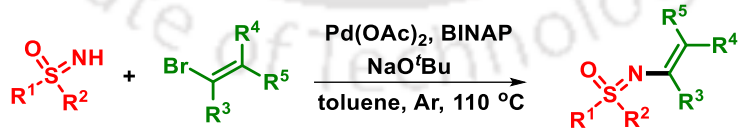

Scheme IA.2.1.7.1. *Pd(II)-catalyzed NH-vinylations of sulfoximines.*

Bolm group reported a Pd/Cu-cocatalyzed oxidative amidobromination reaction of acrylates with NH-sulfoximines. Control experiments suggest that the reaction proceeds through a dual N–H/C–H coupling, followed by oxidative enamide bromination (Scheme IA.2.1.7.2).[31]

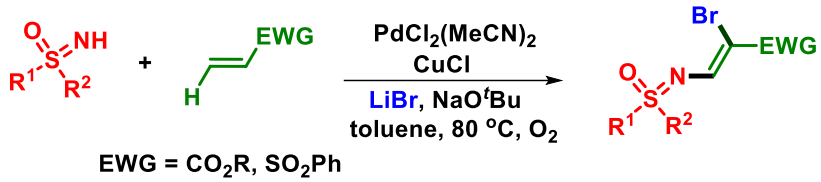

Scheme IA.2.1.7.2. *Pd/Cu-cocatalyzed amidobromination of NH-sulfoximines with acrylates.*

IA.2.1.8. *N*-Alkynylation:

Alkynylation of sulfoximines has remained an interesting aspect of *N*-functionalization, and it mostly takes place in the presence of transition metals. In 2013, a synthetically useful protocol for alkynylation of sulfoximines, involving Cu(II)-catalyzed oxidative coupling of sulfoximines and terminal alkynes was developed (Scheme IA.2.1.8.1). The method allows the generation of various yne sulfoximines from the corresponding sulfoximines, and demonstrates good tolerance to both electron-rich and electron-deficient terminal alkynes.[32]

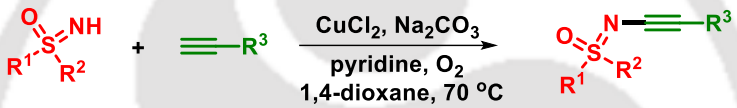

Scheme IA.2.1.8.1. *Cu(II)-catalyzed oxidative coupling of sulfoximines and terminal alkynes.*

Another Cu(II)-catalyzed *N*-alkynylation of sulfoximines *via* oxidative decarboxylative coupling of sulfoximines with aryl propiolic acids was disclosed by the Bolm group. This protocol utilizes an economical copper catalytic system and air as the oxidant and the only by-products generated are water and carbon dioxide, thus contributing to the environmental friendliness of the method (Scheme IA.2.1.8.2).[33]

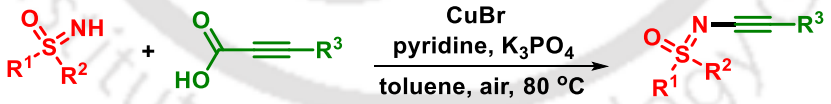

Scheme IA.2.1.8.2. *Cu(II)-catalyzed N-alkynylation of sulfoximines.*

In 2016, alkynylation of sulfoximine was reported to proceed *via* a new kind of sulfoximine hypervalent iodine (III) compound. This iodine(III) reagent featuring a transferable sulfoximidoyl group was obtained through a ligand exchange reaction of methoxy(tosyloxy)iodobenzene (MTIB) with NH sulfoximine. Subsequently, they reacted with terminal alkynes to obtain the desired alkynylated product (Scheme IA.2.1.8.3).[34]

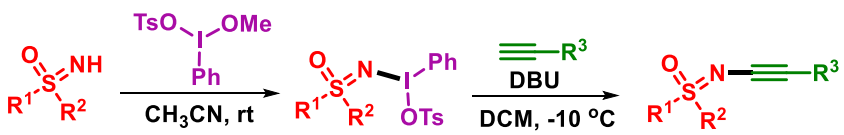

Scheme IA.2.1.8.3. *NH-Alkynylation of sulfoximines proceeding via hypervalent iodine (III) compound.*

IA.2.1.9. *N*-Sulphenylation:

In 2016, Yu and Cheng demonstrated a Cu-catalyzed *N*-sulfenylation of sulfoximines with disulfides, enabling the direct access to *N*-sulfenylsulfoximines. The transformation utilized a combination of CuI, NaOAc, and disulfides to result in a series of useful *N*-arylthiosulfoximines with various functional groups in moderate to good yields (Scheme IA.2.1.9.1).[35]

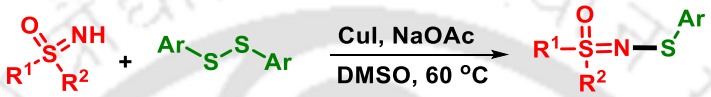

Scheme IA.2.1.9.1. *Cu-catalyzed N-sulfenylation of sulfoximines.*

A recent advancement in sulfoximine chemistry presents a metal-free cross-coupling reaction between sulfoximines and *N*-(phenylthio)-succinimides in an aqueous medium. The transformation exhibits good functional group tolerance and delivers products in moderate to excellent yields. The utilization of an environmentally benign medium, coupled with metal-free conditions and good scalability, establishes this reaction as a green and practical approach for the synthesis of *N*-sulfenyl sulfoximines (Scheme IA.2.1.9.2).[36]

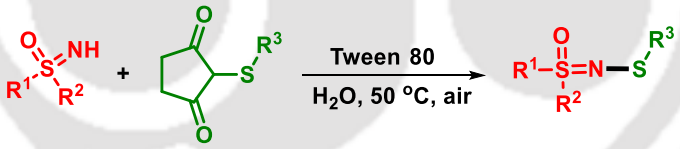

Scheme IA.2.1.9.2. *Synthesis of N-sulfenyl sulfoximines in water.*

In the same year, Zeng group disclosed another *N*-sulfenylation strategy which presented an N–H/S–H dehydrocoupling between sulfoximines and thiols. This reaction was conducted under mild conditions using hydrogen peroxide in polyethylene glycol 400 (PEG400). The *N*-sulfenyl sulfoximines, spanning a range of structural variations, were successfully synthesized with yields up to 97% (Scheme IA.2.1.9.3).[37]

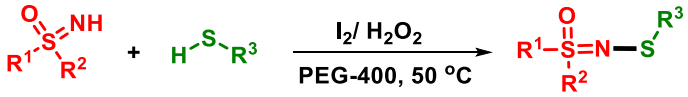

Scheme IA.2.1.9.3. *N-Sulfenylation of sulfoximines.*

Very recently, the same group disclosed another sulfenylation strategy wherein they employed thiosulfonates as the sulfenyl source under NaH promoted conditions (Scheme IA.2.1.9.4).[38]

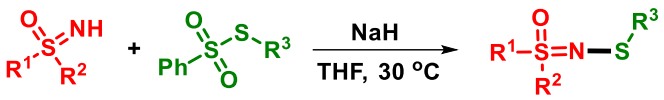

Scheme IA.2.1.9.4. *N-Sulfenylation of sulfoximines.*

IA.2.1.10. *N*-Sulphonylation:

In 2020, the Zeng group reported an oxidative coupling between NH-sulfoximines and aryl sulfinates catalyzed by I_2 and H_2O_2 in water. A wide range of *N*-sulfonyl sulfoximines were prepared in good to excellent yields by this methodology which proceeds at room-temperature (Scheme IA.2.1.10).[39]

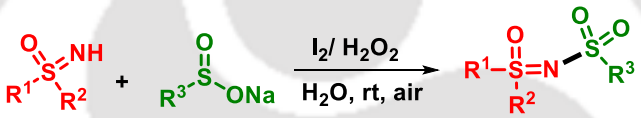

Scheme IA.2.1.10. *N-Sulfonylation of sulfoximines.*

IA.2.1.11. *N*-Phosphinylation:

A novel approach for synthesizing *N*-phosphinyl sulfoximines *via* I_2-catalyzed oxidative N−P cross-coupling reaction between sulfoximines and diarylphosphine oxides was reported by Zeng and coworkers in 2019. The method utilizes H_2O_2 as a green oxidant, and PEG400 as a greener solvent. Importantly, the chirality of *S*-methyl-*S*-phenylsulfoximine is maintained in the coupling products, exhibiting a remarkable enantiomeric excess of 100%. This advancement presents an environmentally conscious and efficient route for synthesizing *N*-phosphinyl sulfoximines (Scheme IA.2.1.11.1).[40]

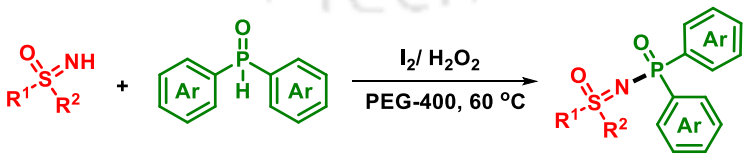

Scheme IA.2.1.11.1. *Synthesis of N-phosphinyl sulfoximines.*

A recent report by Liu and Wei described an electrochemical oxidative method for the synthesis of N-phosphinyl sulfoximines using readily available NH-sulfoximines and diarylphosphine oxides. This approach is based on the synergistic effect of halide salt and

electrochemical oxidation, enabling the product formation at room temperature. Notably, this process occurs in the absence of any acidic, basic, or metallic additives, underscoring the simplicity and efficiency of the electrochemical approach for the synthesis of N-phosphinyl sulfoximines (Scheme IA.2.1.11.2).[41]

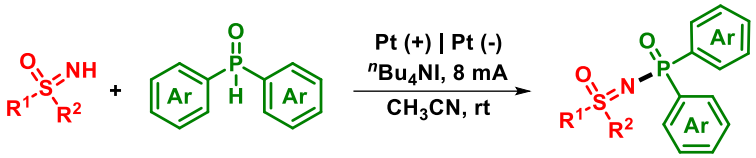

Scheme IA.2.1.11.2. *Electrochemical N-phosphinylation of sulfoximines.*

IA.2.1.12. *N*-Amidation:

In 2017, Chen and coworkers disclosed an amidation strategy of NH-sulfoximines by employing acyl azides without the requirement of any external catalyst or additive. The reaction involves a formal Curtius rearrangement between NH-sulfoximines and acyl azides as the key step. A wide range of substituents on sulfoximines such vinylic, alkylic and heterocyclic were well compatible under this reaction condition. This reaction omits the generation of hazardous by-products and is easily scalable (Scheme IA.2.1.12).[42]

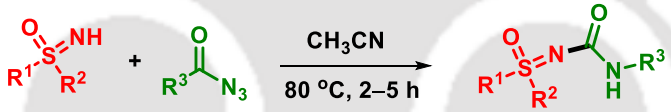

Scheme IA.2.1.12. *NH-Amidation of sulfoximines.*

IA.2.1.13. *N*-Carboxylation:

An organocatalytic synthesis of sulfoximidoyl-containing carbamates was reported by Bolm *et al.* in 2019. This method involves a highly chemoselective reaction between Morita-Baylis-Hillman carbonates and sulfoximines in the presence of triethylamine as the base, and ortho-hydroxybenzoic acid as the oxidant. The reaction proceeds *via* a dual-reagent organocatalysis mechanism and involves ion-pair formations (Scheme IA.2.1.13).[43]

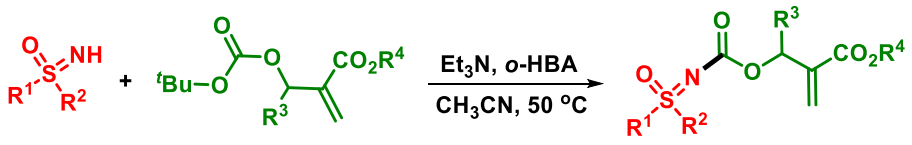

Scheme IA.2.1.13. *NH-Carboxylation of sulfoximines.*

IA.2.1.14. *N*-Ketoesterification:

In 2020, the Bolm group developed a one-pot room temperature protocol for the preparation of sulfoximines with α-ketoester functionalities at nitrogen by a multicomponent reaction between NH-sulfoximines, methoxy(mesyloxy)iodobenzene and cyanoacetates. Here, the NH-sulfoximines reacts with methoxy(mesyloxy)iodobenzene to produce hypervalent iodine reagents which are capable of transferring sulfoximidoyl units to deprotonate the cyanoacetates. Subsequent aerobic oxidation then leads to the desired products in good yields (Scheme IA.2.1.14).[44]

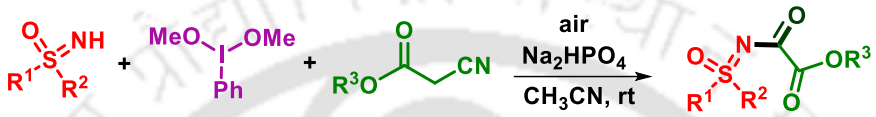

Scheme IA.2.1.14. *Preparation of sulfoximines with α-ketoester functionalities at nitrogen.*

IA.2.1.15. *N*-Trifluoromethylation:

The incorporation of $-CF_3$ groups into organic molecules has been an area of utmost importance as it significantly influences the chemical and physical properties of the molecules. This method holds high value in the pharmaceutical and agrochemical industries.[45] In 2015, Cheng and Bolm group reported a methodology for trifluoromethylation of NH-sulfoximines using commercially available trifluoromethyltrimethylsilane as a CF_3 source and Ag_2CO_3 as a catalyst. The presence of oxygen and 1,10-phenanthroline played a crucial role in the formation of the products. This method successfully *N*-trifluoromethylated various sulfoximines, yielding previously unreported products with good functional group tolerance in modest yields (Scheme IA.2.1.15).[46]

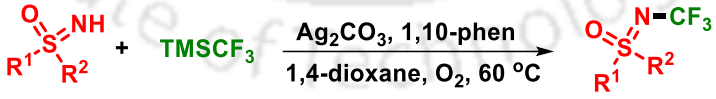

Scheme IA.2.1.15. *Synthesis of N-trifluoromethylated sulfoximine.*

IA.2.1.16. *N*-Cyanation:

One of the first examples of *N*-cyanation of sulfoximines was developed by Cheng and co-workers which employed CuCN as the cyanation source, $CuBr_2$ as the catalyst, O_2 as the oxidant, and Na_2SO_4 as the base in MeCN (Scheme 1A.2.1.16, condition A). Controlled experiments indicated that CuCN acts as the cyanating source and MeCN had no role in the

cyanation.[47] Another report by the same group disclosed this transformation, using environmental-friendly azobisisobutyronitrile (AIBN) as the cyano radical source (Scheme IA.2.1.16, condition B).[48]

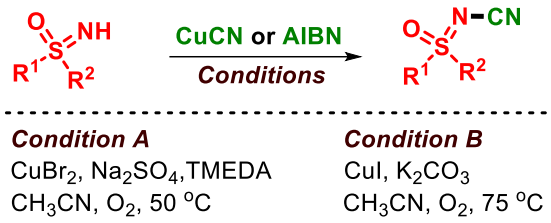

Scheme IA.2.1.16. *NH-Cyanation of sulfoximines.*

IA.2.1.17. Cyclization Involving the NH functionality:

Three-dimensional heterocycles containing sulfur and nitrogen as core elements can be synthesized from inter and intramolecular reactions of NH-sulfoximines, which may lead to new N−C/ C−C bond functionalizations.

An interesting method for halocyclizations of *S*-alkenylsulfoximines was reported by the Bolm group in 2016. Here, unsaturated NH-sulfoximines were treated with iodobenzene diacetate and potassium iodide at room temperature to obtain the corresponding five- and six-membered cyclic products. Specifically, *S*-oxides of dihydroisothiazoles and tetrahydro-1,2-thiazines are obtained in moderate to high yields, excellent regioselectivities and good diastereoselectivities (Scheme IA.2.1.17.1).[49]

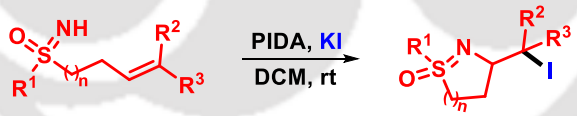

Scheme IA.2.1.17.1. *Halocyclization of unsaturated NH-sulfoximines.*

In 2017, the same group developed an iodine mediated Hofmann-Löffler-Freytag type cyclization of *S*-aryl-*S*-phenylpropyl sulfoximine derivatives. In this process, *S*-aryl-*S*-phenylpropyl sulfoximines were reacted with I_2 and PIDA in DCM under visible light which led to the formation of five-membered cyclic products in good yields. This protocol is not limited to five-membered rings and can also be employed in the synthesis of dihydroisothiazole oxides and benzo[*d*]isothiazoles-1-oxides (Scheme IA.2.1.17.2).[50]

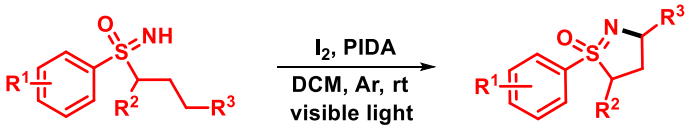

Scheme IA.2.1.17.2. *Hofmann-Loffler-Freytag reaction of NH-sulfoximines.*

In the same year, Li group disclosed a method for synthesizing five membered endocyclic sulfoximines *via* addition/cyclization of chloromethyl aryl sulfoximines with aryl isothiocyanates. The reaction sequence involves a nucleophilic attack by sulfoximine on the isothiocyanate forming the thiourea intermediate, which after tautomerization and intramolecular nucleophilic substitution results in the cyclic product (Scheme IA.2.1.17.3).[51]

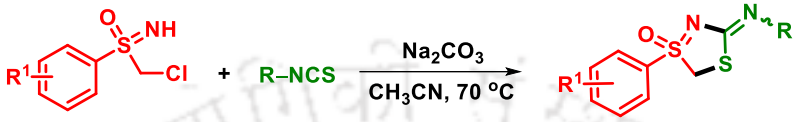

Scheme IA.2.1.17.3. *Synthesis of 5-membered endocylic sulfoximine.*

In 2020, Lücking *et al*. have developed a protocol for accessing five-, six-, and seven-membered cyclic sulfoximines from chloroalkyl sulfoximines using an aqueous solution of ammonia. This method is compatible for a variety of substituents at the ortho, meta, and para positions, providing a versatile approach to access cyclic sulfoximines with different ring sizes and substitution patterns (Scheme IA.2.1.17.4).[52]

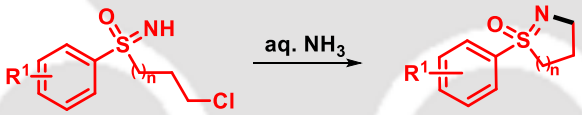

Scheme IA.2.1.17.4. *Synthesis of endocyclic sulfoximines with aqueous solution of ammonia.*

IA.2.2. α-C–H Functionalization:

IA.2.2.1. Intermolecular Reactions:

The α-H functionalization is a comparatively lesser explored domain within sulfoximine chemistry. The reactivity of the α-carbon attached to the sulfur in N-substituted sulfoximines is driven by the acidity of the hydrogen at the α-carbon, which in turn depends on the nature of the substituents on the nitrogen atom. In most cases, the reaction proceeds in presence of a strong base.[53]

In 1978, Johnson and co-workers reported an α-halogenation of N-protected sulfoximines using ^{t}BuOCl, K_2CO_3 at 0 °C. This approach yielded various α-halo sulfoximines in moderate to good yields, regardless of the electronic nature of the substitutents on the aryl ring of sulfoximine. Further, *N*-chloro-*S*-(chloroalkyl)-*S*-phenyl sulfoximines were obtained using NH sulfoximines as reactants (Scheme IA.2.2.1.1).[54]

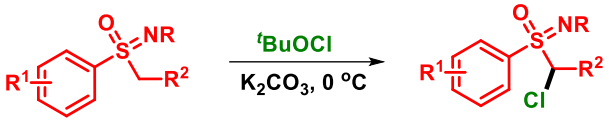

Scheme IA.2.2.1.1. *α-Halogenation of sulfoximine.*

In 2004, Raabe *et al*. developed a strategy for an asymmetric synthesis of sulfoximine substituted acyclic homoallylic alcohols. One of the interesting steps in this protocol involves the α-H abstraction from *N*-methyl sulfoximine by ^{n}BuLi with concomitant attack on ketone and subsequent dehydration to form the *S*-alkenic sulfoximine (Scheme IA.2.2.1.2).[55]

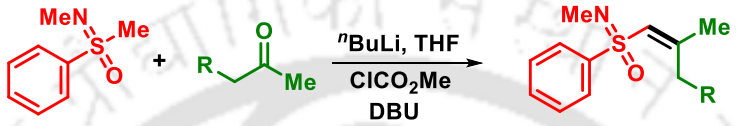

Scheme IA.2.2.1.2. *α-H abstraction of N-methylsulfoximine.*

A Pd-catalyzed α-arylation of *N*-benzoyl sulfoximine ethyl ester with various aryl bromides was developed by the Bolm group in 2005. Further hydrolysis and deprotection of the α-arylated products gave the NH-benzylphenyl sulfoximines (Scheme IA.2.2.1.3).[56]

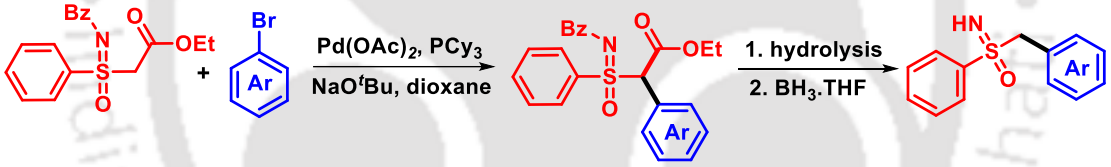

Scheme IA.2.2.1.3. *Pd-catalyzed α-arylation of N-benzoyl sulfoximine ethyl ester.*

Rodriguez *et al*. in 2009, reported a chemo- and regio-selective synthesis of 2-sulfonimidoylylidene tetrahydrofurans through a consecutive reaction involving sulfoximines and α,ω- haloesters. The dianion generated from Johnson's sulfoximine readily reacts with α,ω-haloesters in the presence of ^{n}BuLi at –20 °C *via* an acylation/ heterocyclization reaction to produce the respective product (Scheme IA.2.2.1.4).[57]

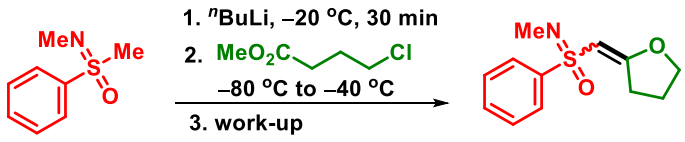

Scheme IA.2.2.1.4. *α-H abstraction of N-methylsulfoximine.*

IA.2.2.2. Intramolecular Cyclization:

In 1998, Gais *et al*. reported that the treatment of *N*-tosylated sulfoximine with an appropriate base in THF afforded its cyclic sulfoximine which on subsequent treatment with ^{n}BuLi and an alkyl halide leads to stereochemically enriched sulfoximine (Scheme IA.2.2.2.1).[58]

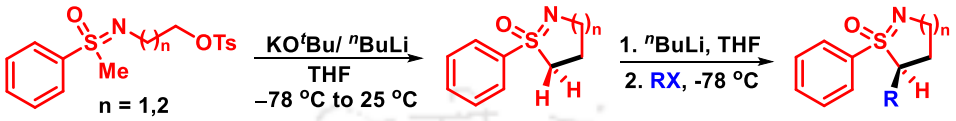

Scheme IA.2.2.2.1. *Synthesis and alkylation of cyclic α-sulfonimidoyl carbanions.*

In the subsequent year, Harmata and coworkers reported multiple base-promoted reactions to access benzothiazines originating from *N*-aryl substituted sulfoximines *via* one-pot, one-operation [3 + 3] annulation. Treatment of *N*-aryl sulfoximine having an ortho acetate group with KH in THF resulted in the cyclized product (Scheme IA.2.2.2.2).[59] In another set of reaction, the cinnamate derivative of *N*-aryl sulfoximine was reacted with lithium diisopropylamide (LDA) in THF, which successfully yielded the respective benzothiazine in 78% yield (Scheme IA.2.2.2.3).[59]

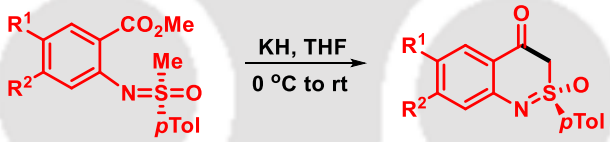

Scheme IA.2.2.2.2. *Access to benzothiazines promoted by α-H abstraction.*

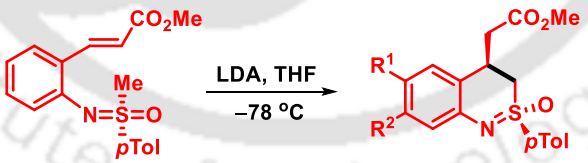

Scheme IA.2.2.2.3. *Access to benzothiazines promoted by α-H abstraction.*

One of the recent reports of α-H abstraction followed by intramolecular cyclization of *S*-methyl-*N*-ynonylsulfoximines was disclosed by Bolm group. Here, treatment of the sulfoximine with Cs_2CO_3 in DMSO in an atmosphere of Ar, results in the formation of 4,5-dihydro-3H-1λ^6-isothiazol-3-one-1-oxides. This protocol is compatible for a wide range of substrates, leading to the formation of the corresponding products in good to excellent yields (Scheme IA.2.2.2.4).[60]

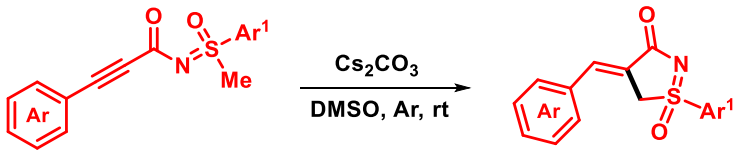

Scheme IA.2.2.2.4. *5-Exo-dig cyclization of S-Methyl-N-ynonylsulfoximines.*

IA.2.3. Ortho C–H Functionalization:

Ortho functionalization reactions are an interesting aspect of sulfoximine chemistry. The C–H activation mostly proceeds in the presence of transition metals such as Rh, Co, Ru, Au, Ni and Pd. Though the functionalization of the *ortho*–C–H of aryl bound to the S of *S*-phenyl sulfoximine is comparatively limited, most ongoing investigations focus on the use of the sulfonimidoyl group as a directing group for ortho-functionalizations.

Transition metal-free ortho metalation reaction of *S*-trifluoromethyl sulfoximine was disclosed by Thanh and Magnier in 2016. The NH *S*-trifluoromethyl sulfoximine was employed as an *ortho* directing group for the functionalization of the aryl ring bonded to the sulfur atom. Various electrophiles, including halogens, hydroxyl, azido, thiol, and functional groups containing boron, Sn, Si, etc, were introduced onto the aromatic ring (Scheme IA.2.3.1).[61]

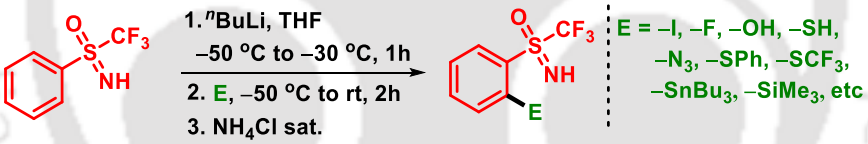

Scheme IA.2.3.1. *Ortho-functionalization of S-trifluoromethyl sulfoximine.*

Further, the synthesis of cyclic *S*-trifluoromethyl sulfoximine which proceeds *via* ortho lithiation and *N*-alkylation was achieved under similar reaction condition by employing different electrophiles. This method allows for the controlled introduction of diverse functional groups onto the aryl moiety of NH *S*-trifluoromethyl sulfoximines, showcasing their versatility in synthetic transformations (Scheme IA.2.3.2).[61]

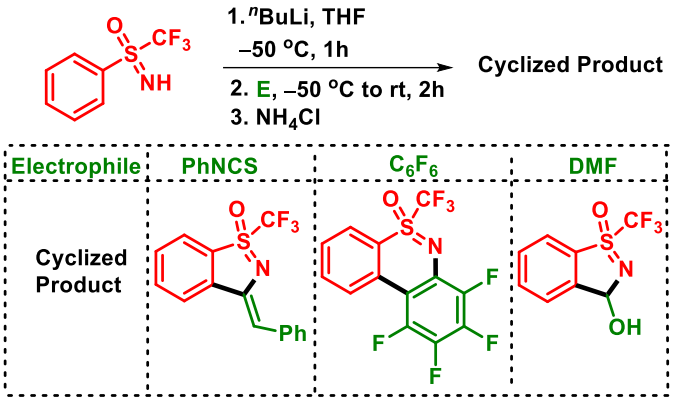

Scheme IA.2.3.2. *Ortho-functionalization and cyclization.*

A Rhodium(III)-catalyzed N-directed ortho C–H activation reactions for the synthesis of heterocyclic benzoisothiazoles was developed by Dong group. This novel tandem annulation approach efficiently constructs benzoisothiazoles from free NH-sulfoximines and alkenes *via* C–H activation, olefination, and subsequent intramolecular aza-Michael cyclization (Scheme IA.2.3.3).[62]

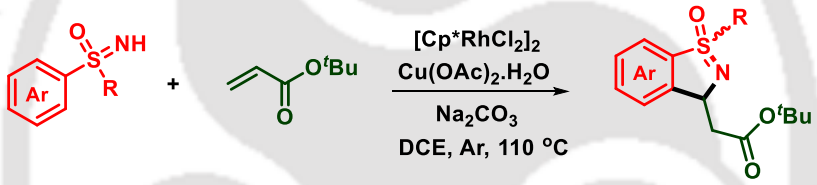

Scheme IA.2.3.3. *Rh(III)-catalyzed N-directed ortho C–H activation of sulfoximines.*

In 2018, Li group disclosed a Rh-catalyzed annulative coupling between sulfoximines and sulfoxonium ylides for synthesizing diverse N-heterocycles. Here, sulfoxonium ylides serve as bifunctional carbene reagents, offering a versatile alternative to diazo compounds in C–H activation chemistry (Scheme IA.2.3.4).[63]

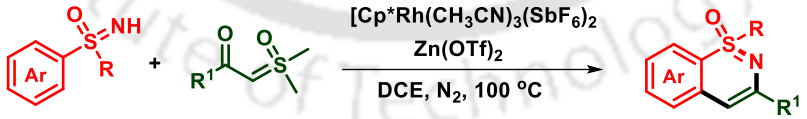

Scheme IA.2.3.4. *Rh-catalyzed annulative coupling between sulfoximines and sulfoxinium ylides.*

A Rh-catalyzed C−H amidation and cyclization strategy was established to synthesize benzothiadiazine-1-oxides. This method efficiently utilizes sulfoximines and 1,4,2-dioxazol-5-ones to afford the desired products in good yields (Scheme IA.2.3.5).[64]

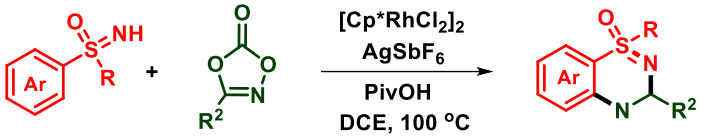

Scheme IA.2.3.5. *Rh-catalyzed C−H amidation and cyclization strategy.*

IA.2.3.1 Sulfoximidoyl Group Directed C–H Functionalization:

The Sahoo group demonstrated a Ru(II)-catalyzed intermolecular ortho-C–H amidation of arenes in *N*-benzoylated sulfoximines with sulfonyl azides in 2013. This reaction exhibited a broad substrate scope and was successfully utilized for synthesizing HMR 1766, also known as Ataciguat, which is a nitric oxide-independent soluble guanylate cyclase (sGC) activator (Scheme IA.2.3.1.1).[65]

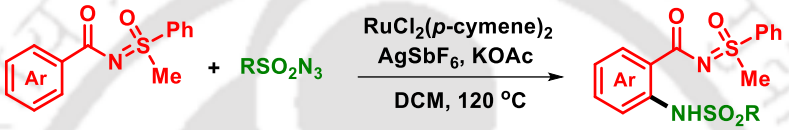

Scheme IA.2.3.1.1 *Sulfoximine directed ortho C−H amidation of arenes.*

A versatile Ru catalysis regime enabled C−H oxygenations of sulfoximine benzamides was developed by Ackermann group in 2017. The strategy exhibited exceptional mono- and chemoselectivity, along with positional selectivity facilitated by facile base-assisted intramolecular electrophilic substitution-type C−H activation. This approach demonstrated high functional group tolerance and allowed for the removal of sulfoximine in a traceless manner, underscoring its synthetic versatility and potential impact in organic synthesis (Scheme IA.2.3.1.2).[66]

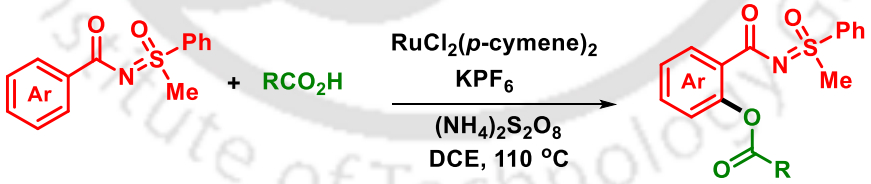

Scheme IA.2.3.1.2. *Ru(III)-catalyzed C−H oxygenations of sulfoximines.*

1A.2.4. Miscellaneous Reactions of Sulfoximines:

While sulfoximine chemistry is mainly dominated by the above three types of reactions, there is still room for further exploration of newer functionalization methodologies to broaden the library of existing compounds.

Bolm group in 2013 accessed the reactivity of *N*-alkynylated sulfoximines towards [2 + 2]-cycloaddition reaction with ketenes. This approach led to the formation of a series of

valuable sulfoximidoyl-functionalized cyclobutenones in moderate to high yields. Further, it was found that the attached sulfoximidoyl group makes the alkyne moiety sufficiently electron-rich to behave as a nucleophile in the presence of a suitable electrophile (Scheme 2A.2.4.1).[67]

Scheme IA.2.4.1. *[2 + 2]-Cycloaddition of N-alkynylated sulfoximines with ketenes.*

The same group in the subsequent year explored the reactivity of N-alkynylated sulfoximines towards hydroacyloxylations and hydroamination. The transformations take place without the need of any catalysts or additional reagents within short reaction times and generates the products in excellent yields of up to 99% and very high stereoselectivities (Scheme 1A.2.4.2).[68]

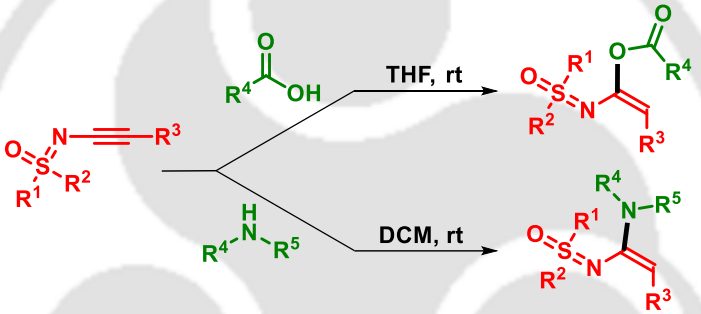

Scheme IA.2.4.2. *Hydroacyloxylations and hydroaminations of N-alkynylated sulfoximines.*

IA.3. Conclusion:

Over the years, there has been a notable surge in sulfoximine chemistry, with the emergence of safer and efficient methodologies for their synthesis, along with significant ongoing clinical trials of several sulfoximine containing drugs such as BAY 1143572, BAY 1000394, and AZD 6738. Sulfoximines display excellent chemical reactivity and their physicochemical properties can also be adjusted through functionalization reactions. Sulfoximines offer potential as isosteres for various functional groups in drug design, boasting favorable characteristics compared to other more established functional groups in pharmaceutical chemistry. The versatility and promising attributes make them valuable additions to the toolkit of medicinal chemists, with the potential to enhance small molecule drug discovery efforts. Therefore, continued innovations in sulfoximine synthesis are crucial for advancing their utility as pharmacophores, ultimately driving further progress in the field of sulfoximine-based therapeutics.

IA.4. References:

(1) (a) M. Andresini, A. Tota, L. Degennaro, J. A. Bull and R. Luisi, *Chem. Eur. J*., 2021, **27**, 17293–17321; (b) W. Zheng, X. Chen, F. Chen, Z. He and Q. Zeng, *Chem. Rec*., 2021, **21**, 396–416; (c) R. Luisi and J. A. Bull, *Molecules*, 2023, **28**, 1120; (d) P. Ghosh, B. Ganguly and S. Das, *Asian J. Org. Chem*., 2020, **9**, 2035–2082.

(2) (a) M. Frings, C. Bolm, A. Blum and C. Gnamm, *Eur. J. Med. Chem.*, 2017, **126**, 225–245; (b) Y. Han, K. Xing, J. Zhang, T. Tong, Y. Shi, H. Cao, H. Yu, Y. Zhang, D. Liu and L. Zhao, *Eur. J. Med. Chem.*, 2021, **209**, 112885; (c) P. Mäder and L. Kattner, *J. Med. Chem*., 2020, **63**, 14243–14275.

(3) (a) T. Abe, J. M. Shreeve, *J. Chem. Soc. Chem. Commun*., 1981, 242–243; (b) D. R. Rayner, D. M. Von Schriltz, J. Day, D. J. Cram, *J. Am. Chem. Soc*., 1968, **90**, 2721–2723; (c) C. R. Johnson, H. G. Corkins, *J. Org. Chem*., 1980, **43**, 4136; (d) T. Yoshida, S. Naruto, H. Uno, H. Nishimura, *Chem. Pharm. Bull*., 1982, **30**, 4346–4351; (e) T. Yoshida, S. Naruto, H. Uno, H. Nishimura, *Chem. Pharm. Bull*., 1982, **30**, 1175–1182; (f) A. Zupanc and M. Jereb, *J. Org. Chem*., 2021, **86**, 5991–6000.

(4) C. Wang, P. Shi and C. Bolm, *Org. Chem. Front.*, 2021, **8**, 2919–2923.

(5) R. Mutti, P. Winternitz, *Synthesis*, 1986, 426–427.

(6) (a) C. Bolm and J. P. Hildebrand, *Tetrahedron Lett.*, 1998, **39**, 5731–5734; (b) G. Y. Cho, P. Rémy, J. Jansson, C. Moessner and C. Bolm, *Org. Lett.*, 2004, **6**, 3293–3296; (c) A. Correa and C. Bolm, *Adv. Synth. Catal.*, 2008, **350**, 391–394.

(7) (a) C. Moessner and C. Bolm, *Org. Lett.*, 2005, **7**, 2667–2669; (b) B. Vaddula, J. Leazer and R. S. Varma, *Adv. Synth. Catal.*, 2012, **354**, 986–990.

(8) S. K. Aithagani, S. Dara, G. Munagala, H. Aruri, M. Yadav, S. Sharma, R. A. Vishwakarma and P. P. Singh, *Org. Lett.*, 2015, **17**, 5547–5549.

(9) S. K. Aithagani, M. Kumar, M. Yadav, R. A. Vishwakarma and P. P. Singh, *J. Org. Chem.*, 2016, **81**, 5886–5894.

(10) L. Sumunnee, C. Pimpasri, M. Noikham and S. Yotphan, *Org. Biomol. Chem.*, 2018, **16**, 2697–2704.

(11) A. Wimmer and B. König, *Org. Lett.*, 2019, **21**, 2740–2744.

(12) D. Liu, Z.-R. Liu, C. Ma, K.-J. Jiao, B. Sun, L. Wei, J. Lefranc, S. Herbert and T.-S. Mei, *Angew. Chem. Int. Ed.*, 2021, **60**, 9444–9449.

(13) (a) C. R. Johnson, C. W. Schroeck, J. R. Shanklin, *J. Am. Chem. Soc*., 1973, **95**, 7424–7431; (b) R. B. Greenwald, D. H. Evans, *Synthesis*, 1977, 650.

(14) C. R. Johnson and O. M. Lavergne, *J. Org. Chem.*, 1993, **58**, 1922–1923.

(15) C. M. M. Hendriks, R. A. Bohmann, M. Bohlem and C. Bolm, *Adv. Synth. Catal.*, 2014, **356**, 1847–1852.

(16) Y. Cheng, W. Dong, L. Wang, K. Parthasarathy and C. Bolm, *Org. Lett.*, 2014, **16**, 2000–2002.

(17) F. Teng, S. Sun, Y. Jiang, J.-T. Yu and J. Cheng, *Chem. Commun.)*, 2015, **51**, 5902–5905.

(18) Z. Li, M. Frings, H. Yu, G. Raabe and C. Bolm, *Org. Lett.*, 2018, **20**, 7367–7370.

(19) C. Wang and T. Jia, *Adv. Synth. Catal.*, 2023, **365**, 3666–3673.

(20) C. Bolm, C. P. R. Hackenberger, O. Simić, M. Verrucci, D. Müller, F. Bienewald, *Synthesis*, 2002, 879.

(21) C. P. R. Hackenberger, G. Raabe and C. Bolm, *Chem. Eur. J.*, 2004, **10**, 2942–2952.

(22) A. Garimallaprabhakaran and M. Harmata, *Synlett*, 2011, **2011**, 361–364.

(23) (a) W.-J. Qin, Y. Li, X. Yu and W.-P. Deng, *Tetrahedron*, 2015, **71**, 1182–1186; (b) A. Porey, S. Santra and J. Guin, *Asian J. Org. Chem.*, 2016, **5**, 870–873; (c) W. Jiang, Y. Huang, L. Zhou and Q. Zeng, *Sci. China Chem.*, 2019, **62**, 1213–1220.

(24) S.-R. Guo, P. Santhosh Kumar, Y.-Q. Yuan and M.-H. Yang, *Tetrahedron Lett.*, 2017, **58**, 2681–2684.

(25) Y. Tu, D. Zhang, P. Shi, C. Wang, D. Ma and C. Bolm, *Org. Biomol. Chem.*, 2021, **19**, 8096–8101.

(26) W. Huang, S. Wang, M. Li, L. Zhao, M. Peng, C. Kang, G. Jiang and F. Ji, *J. Org. Chem.*, 2023, **88**, 17511–17520.

(27) Y. Zou, Z. Peng, W. Dong and D. An, *Eur. J. Org. Chem.*, 2015, **2015**, 4913–4921.

(28) S. Baranwal, S. Gupta and J. Kandasamy, *Asian J. Org. Chem.*, 2021, **10**, 1835–1845.

(29) Y. Tu, P. Shi and C. Bolm, *Org. Lett.*, 2022, **24**, 907–911.

(30) J. R. Dehli and C. Bolm, *J. Org. Chem.*, 2004, **69**, 8518–8520.

(31) X. Y. Chen, R. A. Bohmann, L. Wang, S. Dong, C. Räuber and C. Bolm, *Chem. Eur. J.*, 2015, **21**, 10330–10333.

(32) L. Wang, H. Huang, D. L. Priebbenow, F.-F. Pan and C. Bolm, *Angew. Chem. Int. Ed.*, 2013, **52**, 3478–3480.

(33) D. L. Priebbenow, P. Becker and C. Bolm, *Org. Lett.*, 2013, **15**, 6155–6157.

(34) H. Wang, Y. Cheng, P. Becker, G. Raabe and C. Bolm, *Angew. Chem. Int. Ed.*, 2016, **55**, 12655–12658.

(35) H. Zhu, J.-T. Yu and J. Cheng, *Chem. Commun.*, 2016, **52**, 11908–11911.

(36) Y. Lin, Y. Liu, Y. Zheng, R. Nie, L. Guo and Y. Wu, *ACS Sustain. Chem. Eng.*, 2018, **6**, 13644–13649.

(37) L. Yang, J. Feng, M. Qiao and Q. Zeng, *Org. Chem. Front.*, 2018, **5**, 24–28.

(38) X. Kang, H. Wang and Q. Zeng, *Eur. J. Org. Chem.*, 2022, DOI:10.1002/ejoc.202201229

(39) W. Zheng, M. Tan, L. Yang, L. Zhou and Q. Zeng, *Eur. J. Org. Chem.*, 2020, **2020**, 1764–1768.

(40) M. Tan, W. Zheng, L. Yang, L. Zhou and Q. Zeng, *Asian J. Org. Chem.*, 2019, **8**, 2027–2031.

(41) X. Li, J. Huang, L. Xu, J. Liu and Y. Wei, *Adv. Synth. Catal.*, 2023, **365**, 4647–4653.

(42) H. Zhou, J. Hong, J. Huang and Z. Chen, *Asian J. Org. Chem.*, 2017, **6**, 817–820.

(43) Z. Li, M. Frings, H. Yu and C. Bolm, *Org. Lett.*, 2019, **21**, 3119–3122.

(44) C. Wang, H. Wang and C. Bolm, *Adv. Synth. Catal.*, 2021, **363**, 747–750.

(45) C. Ni and J. Hu, *Chem. Soc. Rev.*, 2016, **45**, 5441–5454.

(46) F. Teng, J. Cheng and C. Bolm, *Org. Lett.*, 2015, **17**, 3166–3169.

(47) F. Teng, J.-T. Yu, Y. Jiang, H. Yang and J. Cheng, *Chem. Commun.*, 2014, **50**, 8412–8415.

(48) F. Teng, J.-T. Yu, Z. Zhou, H. Chu and J. Cheng, *J. Org. Chem.*, 2015, **80**, 2822–2826.

(49) H. Wang, M. Frings and C. Bolm, *Org. Lett.*, 2016, **18**, 2431–2434.

(50) D. Zhang, H. Wang, H. Cheng, J. G. Hernández and C. Bolm, *Adv. Synth. Catal.*, 2017, **359**, 4274–4277.

(51) Y. Hua, W. Zhang, X. Wang, Z. Ge and R. Li, *Tetrahedron*, 2017, **73**, 4387–4391.

(52) E. Boulard, V. Zibulski, L. Oertel, P. Lienau, M. Schäfer, U. Ganzer and U. Lücking, *Chem. Eur. J.*, 2020, **26**, 4378–4388.

(53) (a) F. G. Bordwell, J. C. Branca, C. R. Johnson and N. R. Vanier, *J. Org. Chem.*, 1980, **45**, 3884–3889; (b) H.-J. Gais, H. Mueller, J. Bund, M. Scommoda, J. Brandt and G. Raabe, *J. Am. Chem. Soc.*, 1995, **117**, 2453–2466; (c) L. R. Reddy, H.-J. Gais, C.-W. Woo and G. Raabe, *J. Am. Chem. Soc.*, 2002, **124**, 10427–10434.

(54) C. R. Johnson and H. G. Corkins, *J. Org. Chem.*, 1978, **43**, 4136-4140.

(55) H.-J. Ais, L. R. Reddy, G. S. Babu and G. Raabe, *J. Am. Chem. Soc.*, 2004, **126**, 4859–4864.

(56) G. Y. Cho and C. Bolm, *Org. Lett.*, 2005, **7**, 1351–1354.

(57) M.-A. Virolleaud, V. Sridharan, D. Mailhol, D. Bonne, C. Bressy, G. Chouraqui, L. Commeiras, Y. Coquerel and J. Rodriguez, *Tetrahedron*, 2009, **65**, 9756–9764.

(58) S. Boßhammer and H.-J. Gais, *Synthesis.*, 1998, **1998**, 919–927.

(59) M. Harmata and L. Pavri, *Angew. Chem. Int. Ed.*, 1999, **38**, 2419–2421.

(60) D. Ma, D. Kong, C. Wang, K.-N. Truong, K. Rissanen and C. Bolm, *Org. Lett.*, 2021, **23**, 8287–8290.

(61) T.-N. Le, P. Diter, B. Pégot, C. Bournaud, M. Toffano, R. Guillot, G. Vo-Thanh and E. Magnier, *Org. Lett.*, 2016, **18**, 5102–5105.

(62) Y. Li and L. Dong, *Org. Biomol. Chem.*, 2017, **15**, 9983–9986.

(63) G. Zheng, M. Tian, Y. Xu, X. Chen and X. Li, *Org. Chem. Front.*, 2018, **5**, 998–1002.

(64) P. Shi, Y. Tu, C. Wang, D. Kong, D. Ma and C. Bolm, *Org. Lett.*, 2020, **22**, 8842–8845.

(65) M. R. Yadav, R. K. Rit and A. K. Sahoo, *Org. Lett.*, 2013, **15**, 1638–1641.

(66) K. Raghuvanshi, D. Zell and L. Ackermann, *Org. Lett.*, 2017, **19**, 1278–1281.

(67) R. Pirwerdjan, D. L. Priebbenow, P. Becker, P. Lamers and C. Bolm, *Org. Lett.*, 2013, **15**, 5397–5399.

(68) R. Pirwerdjan, P. Becker and C. Bolm, *Org. Lett.*, 2015, **17**, 5008–5011.

CHAPTER IB

A Brief Account on the Reactivity of *o*-Alkynylanilines Towards Formation of Diverse Heterocycles

IB.1. Introduction:

Heterocycles are recurring building blocks in natural products, biologically active compounds, and functional materials.[1] They are prevalent in approximately 90% of newly developed drugs, thus bridging the gap between biology and chemistry. Over the years, the research interest in heterocyclic compounds has rapidly grown due to extensive studies on their synthesis and functional utility. In this context, the development of new heterocyclic skeletons represents a formidable challenge for organic chemists, given the broad applicability of these novel compounds in pharmaceutical and agrochemical industries. In recent decades, there has been a growing focus on developing environmentally benign, cost-effective, and more convergent methodologies for constructing heterocyclic skeletons. In the realm of organic synthesis, the annulation reaction of alkynyl-containing compounds has emerged as an intriguing method for synthesizing various heterocyclic backbones.[2] In this regard, *o*-alkynylanilines have been extensively employed for the construction of a variety of molecular frameworks under different reaction conditions.

o-Alkynylanilines are useful synthetic precursors in organic chemistry as they possess two reactive sites, a nucleophile (–NHR) and a triple bond. Derivatives of 2-(alkynyl)anilines have been recognized since the 19th century, but the advent of the Sonogashira cross-coupling reaction revolutionized their synthesis, offering a practical route to this versatile building block. The starting compounds for Sonogashira coupling are 2-iodo or bromo-anilines, which are readily accessible and can be prepared by directly halogenating aniline. Furthermore, numerous methods for modifying amino groups present formidable opportunities for synthesizing various derivatives of 2-(alkynyl)anilines.[3]

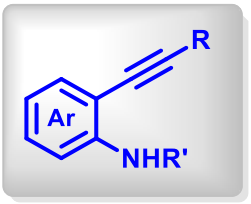

Figure IB.1. *Structure of o-alkynylaniline.*

It is well-known that alkynes possessing a nucleophile in proximity to the triple bond can construct diverse heterocycles *via* transition metal- or Lewis acid-catalyzed or base-mediated intramolecular annulation in an efficient way. Further, the outcomes of 2-(alkynyl)aniline cyclization can vary depending on the catalysts, reaction conditions, and substituents on the nitrogen, alkyne moiety, and aryl ring. *o*-Alkynylanilines have been remarkably successful as substrates in furnishing highly demanded and fused heterocyclic structures. Hence, it is not surprising to find that nearly every organic structure can be synthesized from these versatile alkynyl motifs. Thus, over time, *o*-alkynylanilines have attracted considerable attention as a useful synthetic intermediate, in the fields of organic and medicinal chemistry. The different heterocyclic motifs that can be synthesized from *o*-alkynylanilines can be classed as follows:

- Five-membered heterocycles- indoles, oxindoles, indazoles, benzoisoxazole;
- Six-membered heterocycle- quinoline, cinnoline, benzothiazine, quinazoline, benzoxazine;
- Seven- and eight-membered heterocycle- benzoazepine, azocin, diazocines,

The following section gives a brief account of the different heterocyclic scaffolds originating from *o*-alkynylanilines-

IB.2. Five-Membered Heterocycles:

IB.2.1. Indoles:

The indole ring is one of the most widely distributed heterocycles in nature. Although indole was first isolated by Baeyer from the treatment of indigo with oleum, its importance in chemistry grew impressively from the year 1950s, when several structurally diverse indole derivatives were found to have significant biological activities. The indole moiety appears as a substructure of numerous pharmaceuticals, with its core skeleton present in 24 pharmaceutically marketed drugs.[1e] Moreover, indole has become a privileged structure in other research areas relevant to life, such as agrochemistry and materials science.[4] The great attention in organic chemistry that indole preparation has attracted, has turned into a large number of different synthetic approaches. Thus, while traditional approaches are based on condensation and cyclization sequences,[5,4b] transition metal-catalyzed C–C and C–N bond formation reactions have recently enabled the development of alternative methodologies toward modular indole syntheses.[6] Despite the plentiful collection of available protocols to

prepare indoles, the enormous interest in the indole structure results in this research area being continuously active.

o-Alkynylaniline derivatives are usually employed as versatile building blocks to assemble indole scaffolds through their transition metal-catalyzed activation, non-metal mediated reactions, and photochemical and microwave-assisted cyclizations.[3] The differential reactivity of *o*-alkynylaniline towards various electrophiles promoted many organic chemists to explore different routes for the construction of functionalized indoles. One of the pioneer reports of Pd-catalyzed intramolecular cyclization of *o*-alkynylaniline was disclosed by Taylor *et al*. in 1985.[7] Since then, numerous reports have described the use of different metal catalysts including, Pd, Rh, Cu, Ag, and Au for the synthesis of poly-substituted indoles. Moreover, this research area has expanded to metal-free, photochemical, and electrochemical pathways as well. Herein, a few schemes showcasing the utility of *o*-alkynylaniline as a potential starting material for a variety of functionalized indole scaffolds has been discussed.

A highly efficient Au(III)-catalyzed double-hydroamination reaction of *o*-alkynylanilines with terminal alkynes leading to *N*-alkenylindoles was developed by the Li group in 2007. The reaction proceeds through intermolecular hydroamination, forming an imine intermediate, with concomitant intramolecular cyclization to yield the desired product (Scheme IB.2.1.1).[8]

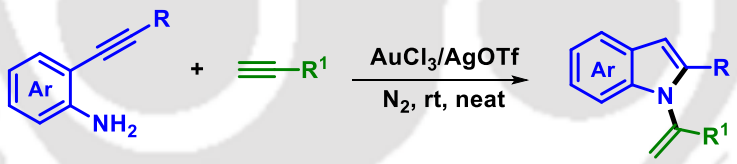

Scheme IB.2.1.1. *Synthesis of N-alkenylindoles.*

A Pd-catalyzed synthesis of free N–H 2,3-disubstituted indoles from 2-alkynyltrifluoroacetanilides and arenediazonium tetrafluoroborates was reported by Cacchi *et al.* in 2010. The reaction proceeds by domino cyclization to form the 2-arylindole moiety with further functionalization at the 3-position resulting in the desired product (Scheme IB.2.1.2).[9]

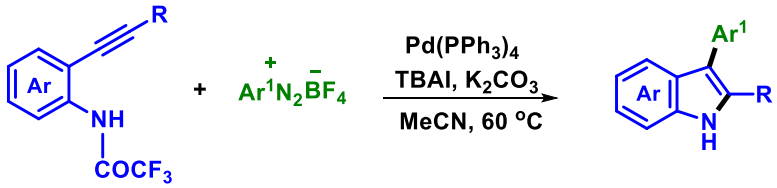

Scheme IB.2.1.2. *Synthesis of 2,3-disubstituted indoles.*

Catalytic synthesis of indole-3-carboxamides from *o*-alkynylanilines and isocyanates using a Rh catalyst was achieved by Inamoto group in 2016. The tandem cyclization−C3

carboxamidation sequence occurs under mild reaction conditions affording 2,3-substituted indoles in moderate to excellent yields (IB.2.1.3).[10]

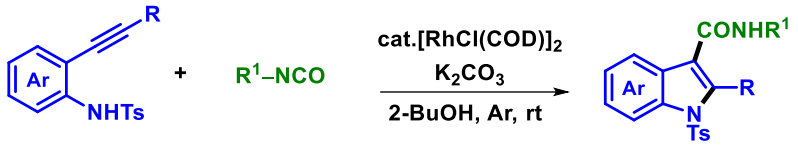

Scheme IB.2.1.3. *Synthesis of indole-3-carboxamides.*

An $AgSbF_6$-catalyzed cascade protocol involving the ring opening of donor–acceptor cyclopropanes (DACs) followed by the cyclization of *N*-protected-2-ethynylaniline was described by Singh and co-workers (Scheme IB.2.1.4). This method discloses a step-economic route to 2,3-disubstituted indoles, where the Ag catalyst is found to trigger the cascade process by activating both alkyne and DACs.[11]

Scheme IB.2.1.4. *Synthesis of 2,3-disubstituted indole involving ring opening of DAC.*

Very recently, Satyanarayana group disclosed an electrochemical approach to access 3-selenylindoles through oxidative cyclization of *o*-alkynylanilines with diselenides. This metal, oxidant, and base-free approach is well compatible with a broad range of *o*-alkynylanilines and diselenides resulting in the products in good to excellent yields of up to 95% (Scheme 1B.2.1.5).[12]

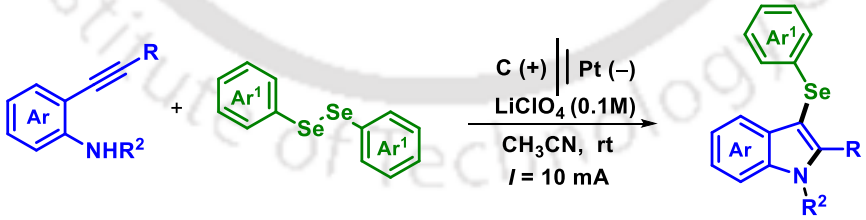

Scheme IB.2.1.5. *Electrochemical approach to access 3-selenylindoles.*

Our group has had a continuous interest in exploring *o*-alkynylaniline chemistry. Continuing this zeal, we employed *o*-alkynylated *N*,*N*-dimethylamines to synthesize 3-aroylindoles *via* an sp^3 C–H bond activation followed by C–C and C–O bond formation using *tert*-butyl hydroperoxide (TBHP) as the oxidant. One method uses an inexpensive Cu catalyst without the requirement of any cocatalyst and additives and proceeds at a relatively lower

temperature (Scheme IB.2.1.6).[13a] The other method is a metal-free approach for the synthesis of 3-aroylindole through a TBAI-catalyzed intramolecular oxidative coupling (Scheme IB.2.1.6).[13b]

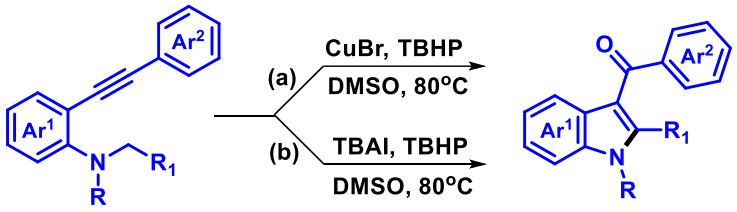

Scheme IB.2.1.6. *Synthesis of 3-aroylindole.*

IB.2.2. Oxindoles:

In 1995, Hirao *et al.* reported a Rh-catalyzed carbonylation cyclization of *o*-alkynylanilines to give 3-alkyl-2-oxindoles under conditions of water-gas shift reaction.[14] In 2001, Gabriele and Salerno disclosed a method for the direct synthesis of (*E*)-3-(methoxycarbonyl)methylene-1,3-dihydroindol-2-ones by Pd-catalyzed oxidative carbonylation of 2-ethynylanilines (IB.2.2.1).[15]

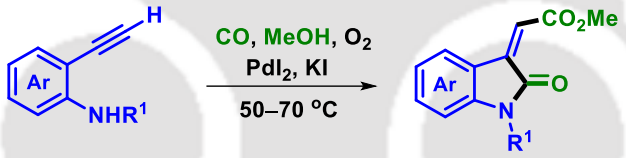

Scheme IB.2.2.1. *Synthesis of 3-substituted oxindole.*

A novel and selective carbonylative annulation method for the synthesis of 3-(halomethylene)-indolin-2-ones has been developed by Tang *et al*. In the presence of PdX_2 and CuX_2, a variety of 2-(1-alkynyl)anilines underwent the carbonylative annulation reaction with CO to afford the target products in good yields (Scheme IB.2.2.2).[16]

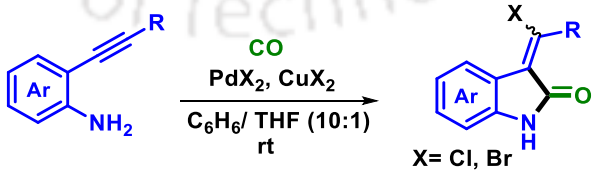

Scheme IB.2.2.2. *Synthesis of 3-(halomethylene)indolin-2-ones.*

IB.2.3. Indazoles:

o-Alkynylanilines can be transformed into alkynylbenzene diazonium salts by treatment with nitrite under acidic conditions. These diazonium intermediates can be further treated under different reaction conditions to synthesize various heterocyclic compounds.[17] In

2003, Fedenok *et al.* synthesized 3-acyl indazole *via* ring closure of the alkynyl diazonium intermediate (Scheme IB.2.3.1).[17a]

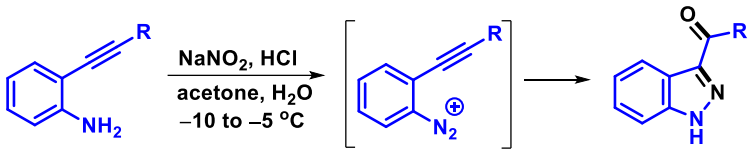

Scheme IB.2.3.1. *Synthesis of indazoles.*

Wang *et al.* in 2017 reported a $Pd(dba)_2$/TBN-catalyzed approach for synthesizing 1-benzylindazole 2-oxides, with the formation of three new bonds *viz,* N–NO, C–N, and C–O. Notably, this method stands out for the dual role played by TBN, functioning both as a NO source and a redox co-catalyst (Scheme IB.2.3.2).[18]

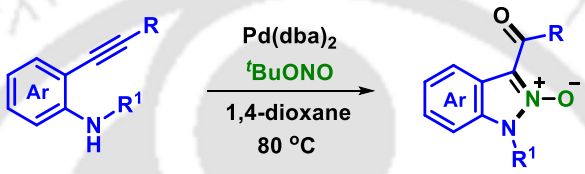

Scheme IB.2.3.2. *Synthesis of indazole-2-oxides.*

I.B.2.4. Benzisoxazole (Anthranil):

In 2017, Michelet and co-workers reported the formation of anthranils by silver catalyzed oxidative cyclization reaction of *o*-alkynylanilines using oxone. Control experiments suggest the involvement of an Ag^{I}/Ag^{III} catalytic cycle in the unusual oxidative cyclization of the alkynyl compounds (Scheme IB.2.4).[19]

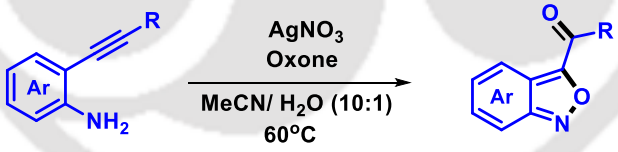

Scheme IB.2.4. *Synthesis of anthranils.*

IB.3. Six-Membered Heterocycles:

IB.3.1. Quinolines:

Quinolines represent a vital class of heterocyclic compounds found in numerous biologically active natural products, particularly alkaloids. They exhibit diverse pharmacological activities, including anti-cancer, anti-bacterial, anti-inflammatory, and anti-malarial properties. Over time, various synthetic methodologies, such as Skraup, Doebner–von Miller, Combes syntheses, Friedländer, modified Friedländer, and hetero-Diels-Alder reactions have been developed for the synthesis of functionalized quinolines.[20] Despite this, new

methodologies continue to emerge regularly. Tsushima *et al*. in 1985 synthesized 2,2-dimethyl-1,2-dihydroquinolines, which is found to have anti-juvenile hormone activity, by cyclization of *N*-alkynylanilines.[21] Over time, *o*-alkynylaniline has emerged as a valuable synthetic precursor for the construction of diverse functionalized quinoline frameworks.[3]

In 2010, Zhu group reported *p*-toluenesulphonic acid promoted annulation of *o*-alkynylanilines with activated ketones forming the corresponding 4-alkylquinolines (Scheme IB.3.1.1). The broad tolerance exhibited by a wide range of functional groups on both substrates provides complimentary access to the Friedländer reaction.[22]

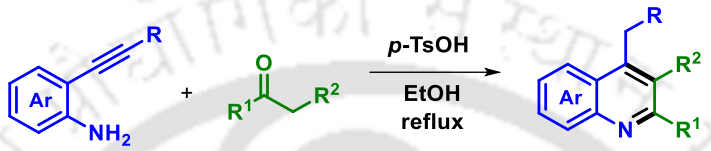

Scheme IB.3.1.1. *Synthesis of 4-alkyl-2,3-disubstituted quinoline.*

Yamada *et al*. developed a method for the synthesis of 4-hydroxyquinolin-2-one derivatives, from *o*-alkynylanilines, DBU, silver catalyst, and an atmospheric pressure of carbon dioxide (Scheme IB.3.1.2). The key step in the proposed reaction mechanism is the generation of the isocyanate and the enolate through C–O bond cleavage and new C–C bond formation induced by deprotonation of the amide after the formation of the benzoxazin-2-one.[23]

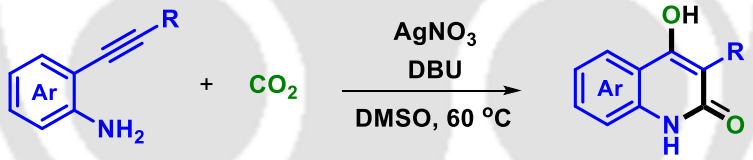

Scheme IB.3.1.2. *Synthesis of 4-hydroxyquinolin-2(1H)-one.*

An efficient, and mild synthetic route for the preparation of 2-aminoquinolines *via* a gold-catalyzed cascade reaction between β-(2-aminophenyl)-α,β-ynones and ynamides was developed by Arcadi and co-workers. Notably, this process tolerates a wide range of aryl/alkyl substituents linked at the C3-position of the quinoline scaffold and of the −CH_2COR moiety linked at their C4-position (Scheme IB.3.1.3).[24]

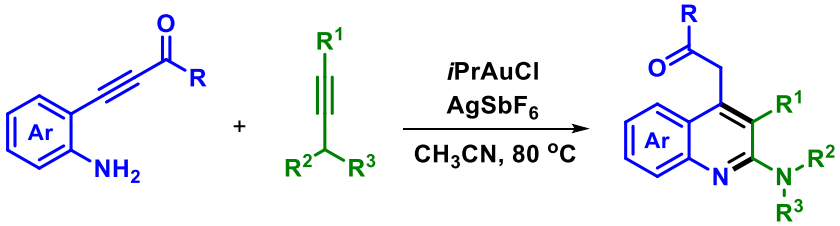

Scheme IB.3.1.3. *Synthesis of 2-aminoquinolines.*

In 2017, our group developed a metal-free, base-promoted synthesis of quinoline-4(1*H*)-thiones which proceeds *via in situ* generated *o*-alkynylthiourea, obtained by reacting 2-(phenylethynyl)aniline with aroyl isothiocyanates. A 6-*exo*-dig *S*-cyclization of the *in situ* generated thiourea is followed by a rearrangement to give the corresponding quinoline-thiones (Scheme IB.3.1.4).[25]

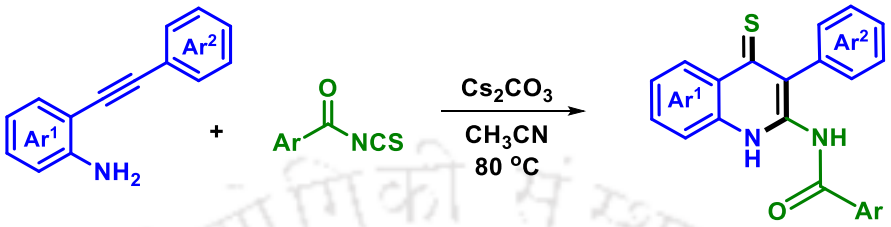

Scheme IB.3.1.4. *Synthesis of quinoline-4(1H)-thiones.*

In the same year, our group reported another methodology for the synthesis of fused indoloquinolines *via* a microwave assisted strategy between *o*-alkynylanilines and phenylisocyanoacetates. This methodology offers good functional group tolerance under mild microwave conditions within a shorter reaction time (Scheme IB.3.1.5).[26]

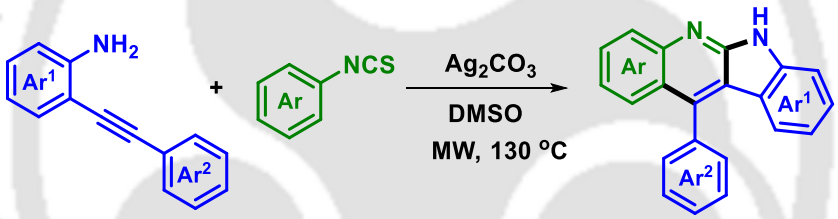

Scheme IB.3.1.5. *Synthesis of quinoline-4(1H)-thiones.*

IB.3.2. Benzoxazines:

Saito and co-workers in 2011 reported a highly regio- and stereoselective Pd(II)-catalyzed 6-exo-dig-cyclization of *N*-acyl-*o*-alkynylanlines producing 4-alkylidene-3,1-benzoxazine (Scheme IB.3.2.1).[27] Another work by Yamashita and Iida described the synthesis of 2-arylbenzoxazine *via* Cu-catalyzed intramolecular cyclization of 2-alkynylacetamide (Scheme IB.3.2.2).[28]

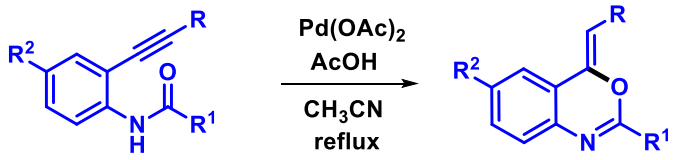

Scheme IB.3.2.1. *Synthesis of 4-alkylidene-3,1-benzoxazine.*

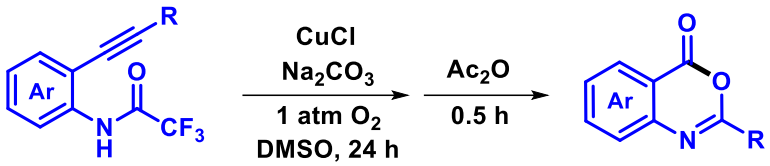

Scheme IB.3.2.2. *Synthesis of 2-arylbenzoxazine.*

IB.3.3. Benzothiazines:

$AgNO_3$-catalyzed tandem addition-cyclization reactions of *o*-alkynylanilies with CS_2 was carried out by Ding and Peng in 2012. Six-membered 2-mercapto-4-benzylidene-4H-benzo[*d*][1,3]thiazines were generated in good to moderate yields *via* 6-exo-dig *S*-cyclization of the alkynyl compounds under mild reaction conditions (Scheme IB.3.3.1).[29]

Scheme IB.3.3.1. *Synthesis of 2-mercapto-4-benzylidene-4H-benzo[d][1,3]thiazines.*

The 6-*exo*-dig ring closure of *ortho*-alkynylanilines with readily available aroyl isothiocyanate was reported by Verma group in 2019. This iodine-promoted, metal- and base-free approach, facilitates the cascade synthesis of highly functionalized benzothiazines. The methodology utilizes *in situ* generated *ortho*-alkynylthiourea and is one of the first examples of iodine-mediated alkyne activation without using any base on water. Further, the protocol holds significant prominence in the late-stage synthesis of pharmaceutically active molecules containing 1,3-benzothiazine motifs (Scheme IB.3.3.2).[30]

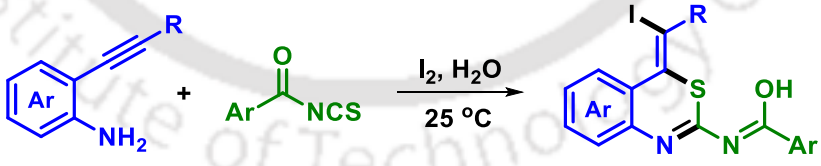

Scheme IB.3.3.2. *I_2-promoted synthesis of benzothiazines.*

IB.3.4. Quinazolines:

Wu and Jiang in 2018 disclosed a Cu(II)-catalyzed synthesis of quinazolines by the reaction between *o*-alkynylanilines and benzonitriles utilizing O_2 as the sole oxidant. The reaction involves the cleavage of the C–C triple bond of the alkyne moiety with the construction of a new C–C and C–N bonds (Scheme IB.3.4).[31]

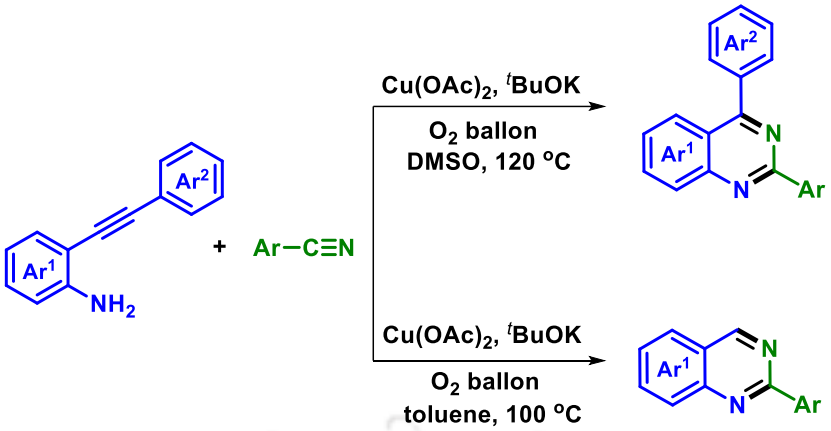

Scheme IB.3.4. *Synthesis of quinazolines from benzonitriles and 2-ethynylanilines.*

IB.3.5. Cinnolines:

In 2011, B. C. Ranu group disclosed an efficient methodology for the synthesis of 4-(1*H*)-cinnolones from 2-phenylethynylaniline derivatives (Scheme IB.3.5.1). The reaction proceeds through the formation of a diazonium intermediate and has been used very often employed for the detection of nitrite ions in water at ppm concentration.[17b]

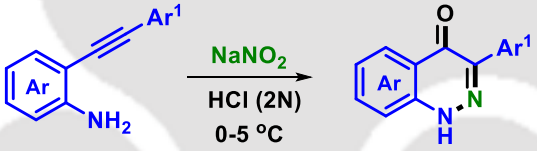

Scheme IB.3.5.1. *Synthesis of 4(1H)-cinnolones.*

A BF_3-etherate-promoted cascade reaction of nitriles with 2-alkynylanilines leading to 4-amido-cinnolines was reported by Wang *et al.* in 2016 (Scheme IB.3.5.2).[32] The reaction sequence involves diazotization with ^{t}BuONO, nucleophilic addition of the alkyne to the BF_3-coordinated diazonium ion, followed by nitrile addition to the vinyl cation intermediate and hydrolysis.

Scheme IB.3.5.2. *Synthesis of 4-amido-cinnolines.*

IB.4. Seven- and Eight-Membered Heterocycles:

A one-pot, three-component reaction between *o*-alkynylanilines, cyclic ketones, and trimethylsilyl cyanide (TMSCN) for the synthesis of 1-benzoazepine carbonitrile was reported

by Wang *et al*. This method involves an imination/annulation/cyanation sequence which is achieved by combining Pd(II) and Cu(II)-catalytic system in dimethyl sulfoxide utilizing trimethylsilyl cyanide as the cyanating agent. The seven-membered heterocycle with a carbonitrile substituent is achieved *via* 7-*endo*-dig cyclization/cyanation with an *in situ*-formed *N*-aryl enamine intermediate (Scheme IB.4.1).[33]

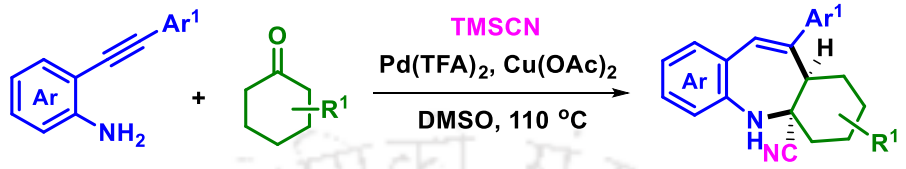

Scheme IB.4.1. *Synthesis of 1-benzoazepine carbonitrile*.

In 2016, Yao and Wu reported an interesting strategy for the synthesis of an eight membered fused heterocycle by Pd(II)-catalyzed tandem reaction of 2-alkynylanilines with 2-(2-bromobenzylidene)cyclobutanones. The resulting 7,8-dihydrobenzo[b]naphtho[2,3-d]azocin-6(*5H*)-ones was conveniently constructed with excellent selectivity and good functional group compatibility with respectable yields (Scheme IB.4.2).[34]

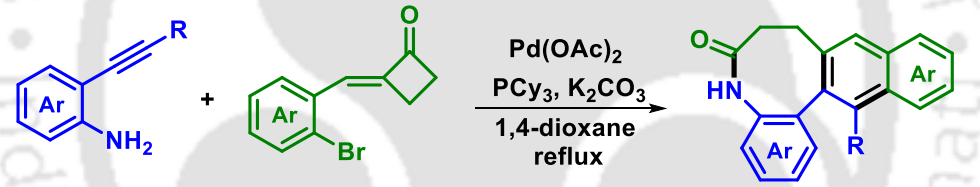

Scheme IB.4.2. *Synthesis of benzo[b]naphtho[2,3-d]azocin-6(5H)-ones.*

Merinelli and co-workers described an Au(I)-catalyzed formation of eight-membered ring, through a cascade intermolecular/intramolecular hydroamination of β-(2-aminophenyl)-α,β-ynones. enabling an innovative approach towards the construction of dibenzo[1,5]diazocine skeleton. The mild reaction conditions and high atomic efficiency make this methodology suitable for the synthesis of a library of products that could be of interest in different fields of research (Scheme IB.4.3).[35]

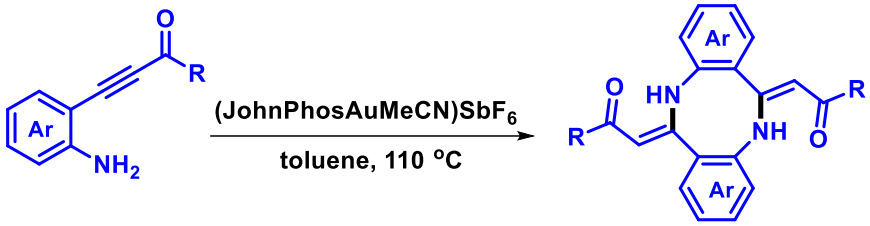

Scheme IB.4.3. *Synthesis of dibenzo[1,5]diazocines.*

IB.5. Conclusion:

o-Alkynylanilines represent highly valuable compounds for synthesizing a wide range of heterocycles. These alkynes are readily accessible, and the Sonogashira reaction offers mild conditions and excellent selectivity, enabling a broad scope of substituents both at the triple bond and in the aromatic ring of the aniline. While many reactions yield substituted indoles, the variation of substituents, reaction partners, and catalytic systems allows for complex cascade processes with diverse outcomes. It is worth noting that while 2-alkynylanilines have proven to be valuable building blocks for constructing diverse heterocyclic frameworks, particularly in the synthesis of complex bioactive molecules, there is still room for further development of newer synthetic routes which will open doors for compounds having a broad array of useful properties.

IB.6. References:

(1) (a) E. Kabir and M. Uzzaman, *Results Chem.*, 2022, **4**, 100606; (b) N. Kerru, L. Gummidi, S. Maddila, K. K. Gangu and S. B. Jonnalagadda, *Molecules*, 2020, **25**, 1909; (c) M. H. A. Al-Jumaili, A. A. Hamad, H. E. Hashem, A. D. Hussein, M. J. Muhaidi, M. A. Ahmed, A. H. A. Albanaa, F. Siddique and E. A. Bakr, *J. Mol. Struct.*, 2023, **1271**, 133970; (d) P. N. Kalaria, S. C. Karad and D. K. Raval, *Eur. J. Med. Chem.*, 2018, **158**, 917–936; (e) R. D. Taylor, M. MacCoss and A. D. G. Lawson, *J. Med. Chem.*, 2014, **57**, 5845–5859.

(2) (a) L. Li, D. Huang, C. Shi and G. Yan, *Adv. Synth. Catal.*, 2019, **361**, 1958–1984; (b) L. He, H. Nie, G. Qiu, Y. Gao and J. Wu, *Org. Biomol. Chem.*, 2014, **12**, 9045–9053; (c) H. Qian, W. Zhao and J. Sun, *Chem. Rec.*, 2014, **14**, 1070–1085; (d) K. Sun, J. Lei, Y. Liu, B. Liu and N. Chen, *Adv. Synth. Catal.*, 2020, **362**, 3709–3726; (e) J. Wu, C. Wei, F. Zhao, W. Du, Z. Geng and Z. Xia, *J. Org. Chem.*, 2022, **87**, 14374–14383.

(3) (a) A. A. Festa, P. V. Raspertov and L. G. Voskressensky, *Adv. Synth. Catal.*, 2022, **364**, 466–486; (b) O. S. Kamble, M. Khatravath and R. Dandela, *ChemistrySelect*, 2021, **6**, 7408–7427; (c) V. Fathi Vavsari, A. Nikbakht and S. Balalaie, *Asian J. Org. Chem.*, 2022, **11**, e202100772.

(4) (a) R. J. Sundberg, in *The Chemistry of Indoles*, Academic Press, New York, **1970**; (b) M. Bandini and A. Eichholzer, *Angew. Chem. Int. Ed Engl.*, 2009, **48**, 9608–9644; (c) S. Kumar and Ritika, *Futur. J. Pharm. Sci.*, 2020, DOI:10.1186/s43094-020-00141-y.

(5) (a) G. W. Gribble, *Contemp Org Synth*, 1994, **1**, 145–172; (b) G. W. Gribble, *J. Chem. Soc., Perkin Trans. 1*, 2000, 1045–1075; (c) G. R. Humphrey and J. T. Kuethe, *Chem. Rev.*, 2006, **106**, 2875–2911.

(6) (a) D. F. Taber and P. K. Tirunahari, *Tetrahedron*, 2011, **67**, 7195–7210; (b) J. Ma, R. Feng and Z.-B. Dong, *Asian J. Org. Chem.*, 2023, **12**, e202300092.

(7) E. C. Taylor, A. H. Katz, H. Salgado-Zamora and A. McKillop, *Tetrahedron Lett.*, 1985, **26**, 5963–5966.

(8) Y. Zhang, J. P. Donahue and C.-J. Li, *Org. Lett.*, 2007, **9**, 627–630.

(9) S. Cacchi, G. Fabrizi, A. Goggiamani, A. Perboni, A. Sferrazza and P. Stabile, *Org. Lett.*, 2010, **12**, 3279–3281.

(10) A. Mizukami, Y. Ise, T. Kimachi and K. Inamoto, *Org. Lett.*, 2016, **18**, 748–751.

(11) R. Karmakar, A. Suneja and V. K. Singh, *Org. Lett.*, 2016, **18**, 2636–2639.

(12) A. B. Dapkekar and G. Satyanarayana, *Chem. Commun.*, 2023, **59**, 8719–8722.

(13) (a) A. Gogoi, S. Guin, S. K. Rout and B. K. Patel, *Org. Lett.*, 2013, **15**, 1802–1805; (b) A. Gogoi, A. Modi, S. Guin, S. K. Rout, D. Das and B. K. Patel, *Chem. Commun.*, 2014, **50**, 10445–10447.

(14) K. Hirao, N. Morii, T. Joh and S. Takahashi, *Tetrahedron Lett.*, 1995, **36**, 6243–6246.

(15) B. Gabriele, G. Salerno, L. Veltri, M. Costa and C. Massera, *Eur. J. Org. Chem.*, 2001, **2001**, 4607–4613.

(16) S. Tang, Q.-F. Yu, Peng, J.-H. Li, P. Zhong and R.-Y. Tang, *Org. Lett.*, 2007, **9**, 3413–3416.

(17) (a) L. G. Fedenok and N. A. Zolnikova, *Tetrahedron Lett.*, 2003, **44**, 5453–5455; (b) R. Dey, T. Chatterjee and B. C. Ranu, *Tetrahedron Lett.*, 2011, **52**, 461–464.

(18) G. C. Senadi, J.-Q. Wang, B. S. Gore and J.-J. Wang, *Adv. Synth. Catal.*, 2017, **359**, 2747–2753.

(19) A. Arcadi, M. Chiarini, L. Del Vecchio, F. Marinelli and V. Michelet, *Eur. J. Org. Chem.*, 2017, **2017**, 2214–2222.

(20) (a) B. S. Matada, R. Pattanashettar and N. G. Yernale, *Bioorg. Med. Chem.*, 2021, **32**, 115973; (b) V. Kouznetsov, L. Mendez and C. Gomez, *Curr. Org. Chem.*, 2005, **9**, 141–161; (c) S. M. Prajapati, K. D. Patel, R. H. Vekariya, S. N. Panchal and H. D. Patel, *RSC Adv.*, 2014, **4**, 24463–24476; (d) O. F. Elebiju, O. O. Ajani, G. O. Oduselu, T. A. Ogunnupebi and E. Adebiyi, *Front. Chem.*, 2022, **10**

DOI:10.3389/fchem.2022.1074331; (e) O. O. Ajani, K. T. Iyaye and O. T. Ademosun, *RSC Adv.*, 2022, **12**, 18594–18614.

(21) K. Tsushima, M. Hatakoshi, N. Matsuo, N. Ohno and I. Nakayama, *Agric. Biol. Chem.*, 1985, **49**, 2421–2423.

(22) C. Peng, Y. Wang, L. Liu, H. Wang, J. Zhao and Q. Zhu, *Eur. J. Org. Chem.*, 2010, **2010**, 818–822.

(23) T. Ishida, S. Kikuchi and T. Yamada, *Org. Lett.*, 2013, **15**, 3710–3713.

(24) N. D. Rode, A. Arcadi, A. Di Nicola, F. Marinelli and V. Michelet, *Org. Lett.*, 2018, **20**, 5103–5106.

(25) A. Modi, P. Sau and B. K. Patel, *Org. Lett.*, 2017, **19**, 6128–6131.

(26) W. Ali, A. Dahiya, R. Pandey, T. Alam and B. K. Patel, *J. Org. Chem.*, 2017, **82**, 2089–2096.

(27) T. Saito, S. Ogawa, N. Takei, N. Kutsumura and T. Otani, *Org. Lett.*, 2011, **13**, 1098–1101.

(28) M. Yamashita and A. Iida, *Tetrahedron*, 2014, **70**, 5746–5751.

(29) Q. Ding, X. Liu, J. Yu, Q. Zhang, D. Wang, B. Cao and Y. Peng, *Tetrahedron*, 2012, **68**, 3937–3941.

(30) K. M. Saini, R. K. Saunthwal, S. Kumar and A. K. Verma, *Org. Biomol. Chem.*, 2019, **17**, 2657–2662.

(31) X. Wang, D. He, Y. Huang, Q. Fan, W. Wu and H. Jiang, *J. Org. Chem.*, 2018, **83**, 5458–5466.

(32) G. C. Senadi, B. S. Gore, W.-P. Hu and J.-J. Wang, *Org. Lett.*, 2016, **18**, 2890–2893.

(33) G. K. Dhandabani, M. R. Mutra and J.-J. Wang, *Adv. Synth. Catal.*, 2018, **360**, 4754–4763.

(34) X. Gong, M. Chen, L. Yao and J. Wu, *Chem. Asian J.*, 2016, **11**, 1613–1617.

(35) N. D. Rode, A. Arcadi, M. Chiarini, F. Marinelli and G. Portalone, *Adv. Synth. Catal.*, 2017, **359**, 3371–3377.

Chapter II

NIS-Initiated Photo-Induced Oxidative Decarboxylative Sulfoximidation of Cinnamic Acids

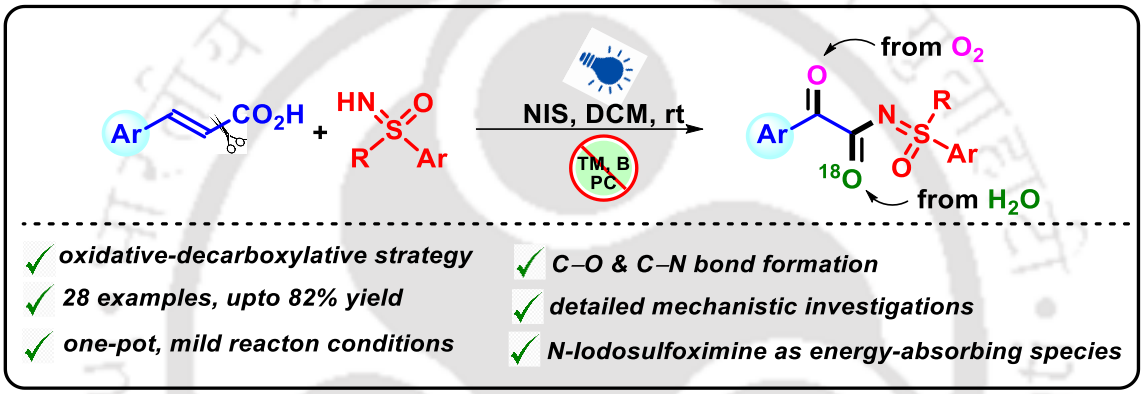

ChemComm
ROYAL SOCIETY OF CHEMISTRY
COMMUNICATION
View Article Online
View Journal | View Issue
Chem. Commun. 2023, **59**, 2779–2782

Abstract: *N-Iodosuccinimide catalyzed, visible-light-induced oxidative decarboxylative cross-coupling between cinnamic acids and NH-sulfoximines is presented. This strategy results in the formation of α-keto-N-acyl sulfoximines via the construction of two new C=O and one C–N bond. The in situ-generated N-iodosulfoximine serves as the light-absorbing species in the absence of any external photosensitizer. The keto carbonyl and amidic carbonyl oxygen in the resulting product originate from water and dioxygen respectively.*

भारतीय प्रौद्योगिकी संस्थान गुवाहाटी
Indian Institute of Technology Guwahati

CHAPTER II

NIS-Initiated Photo-Induced Oxidative Decarboxylative Sulfoximidation of Cinnamic Acids

II.1. Introduction:

Decarboxylative cross-coupling is a remarkable strategy for the formation of C–C and C–heteroatom bonds.[1] This method is advantageous over the conventional transition metal-catalyzed cross-coupling reactions considering the regioselectivity, atom and step economy, and environmental friendliness of the process. Decarboxylative cross-coupling involves carboxylic acid and its derivatives which are readily available, non-toxic, stable, and less air and moisture-sensitive than other cross-coupling organometallic reagents.[1] Moreover, there is only the extrusion of CO_2 as a byproduct, making the process environmentally benign.

The history of decarboxylation dates back to the 1930s when Hunsdiecker *et al.* found that α,β-unsaturated acids and certain carboxylic acids could undergo halogenative decarboxylation in the presence of Ag salts. Another classic method, the Barton decarboxylation, emerged in 1962 and has found widespread use in chemical synthesis.[2] Since then numerous different strategies have surfaced that involve transition metals or high reaction temperature. Further, radical decarboxylative functionalizations involving high-energy UV-light induction and electrochemical processes have been developed as efficient alternatives. Over the years, there has been a significant demand for the development of novel and efficient decarboxylative protocols for converting carboxylic acids into valuable fine chemicals.[1,2]

Based on the reaction conditions, carboxylic acids can be employed as electrophilic, nucleophilic, or radical synthetic equivalents in cross-coupling reactions.[1a,c] The generalized mechanistic pathways by which carboxylic acid and its derivatives can undergo decarboxylative functionalization is presented in Scheme II.1.[1c] Abstraction of a proton from carboxylic acid may generate the carboxylate anion, which, after extrusion of CO_2 results in the carbanion *via* path I. This carbanion is usually stabilized by coordination with a metal center and may react with heteroatom electrophiles or with nucleophiles in the presence of an appropriate oxidant. The CO_2 extrusion may also take place through a single electron transfer from carboxylate anion (path II) or direct hydrogen atom transfer from the acid (path III) and generate the carbon radical. Consequently, photochemical cleavage or single electron reduction may also generate the carboxylate anion (path III) which will produce the carbon radical. The

carbon radical may combine with an appropriate heteroatom counterpart or can be oxidized to carbocation intermediates which will eventually react with heteroatom nucleophiles.

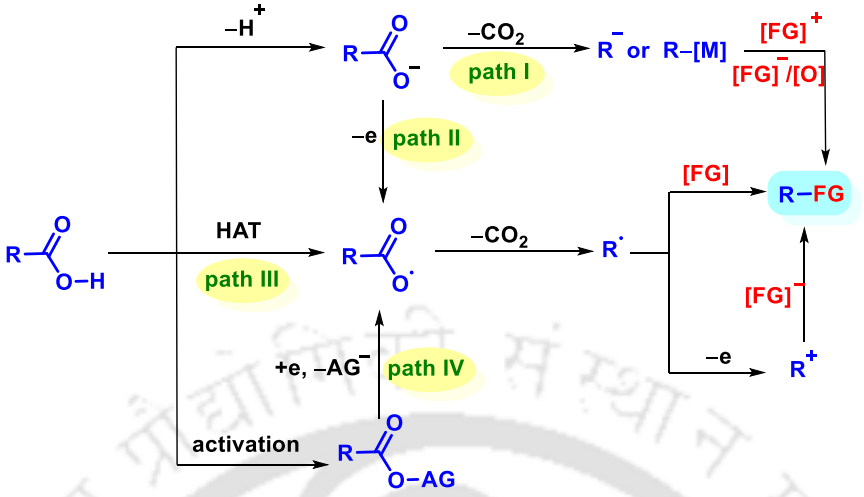

Scheme II.1. *Potential mechanistic pathways for decarboxylative functionalization.*

II.1.1. Visible-Light-Induced Decarboxylative Cross-Coupling Reactions:

Recently, there has been a rapid rise in visible-light-induced reactions due to their operational simplicity and sustainability.[3] This has influenced numerous cross-coupling reactions to be feasible that would otherwise require a high energy influx to overcome the activation barrier. Visible-light-induced decarboxylative cross-coupling reactions have become powerful synthetic methodologies, bringing about a range of organic transformations involving various C–C and C–heteroatom bond formations.[4]

Photo-induced decarboxylative C–N bond formation remains an interesting area of research, and several developments have been reported from time to time.[5] One of the earlier reports on visible light-induced decarboxylation/ oxidative amination of α-ketoacids was disclosed by Lei and coworkers in 2014 (Scheme II.1.1.1).[6] The reaction proceeds with O_2 as the terminal oxidant utilizing the $[Ru(phen)_3]Cl_2$ as the photocatalyst. Preliminary mechanistic studies indicate that the process involves an important single electron transfer (SET) between $[Ru(phen)_3]^{2+}$* and aniline, with the activation of O_2 potentially serving as the rate-determining step.

Scheme II.1.1.1 *Decarboxylative amination of α-ketoacids.*

In 2020, the Larionov group reported a decarboxylative N-alkylation reaction that facilitates the direct formation of $C(sp^3)$–N bonds from carboxylic acids. The reaction is

enabled by visible-light-driven, acridine-catalyzed decarboxylation, providing access to N-alkylated secondary and tertiary anilines and N-heterocycles. The success of the reaction can be attributed to the precise coordination between acridine photocatalysis and copper-catalyzed C(sp^3)–N bond formation, which was thoroughly examined through both experimental and computational studies (Scheme II.1.1.2).[5a]

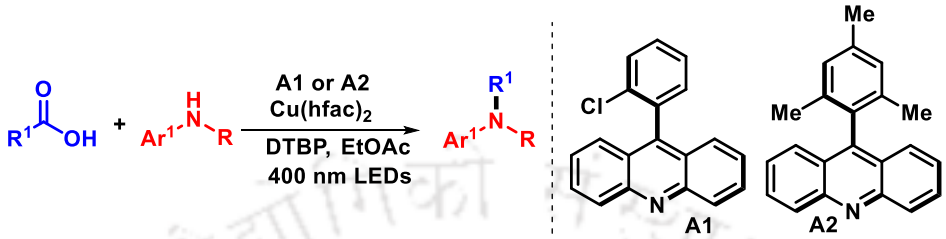

Scheme II.1.1.2. *Decarboxylative N-alkylation of carboxylic acids.*

Yoon *et al*. reported a Cu(II) mediated oxidative decarboxylative strategy between carboxylic acids and sulfonamides (Scheme II.1.1.3). The oxidative cross-coupling occurs as a result of visible-light excitation to the ligand-to-metal charge transfer state. The methodology shows good functional group tolerance and applies to complex drug molecules thus facilitating the discovery of new pharmaceutical agents.[7]

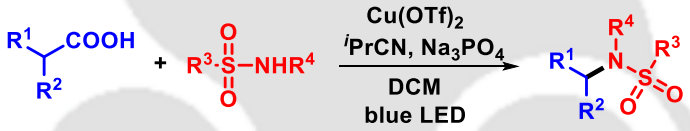

Scheme II.1.1.3. *Cu(II)-mediated oxidative decarboxylation of carboxylic acids.*

Recently, the Ritter group disclosed the first decarboxylative sulfoximination of benzoic acid which proceeds *via* photo-induced Cu-LMCT-enabled decarboxylative carbometallation (Scheme II.1.1.4).[8]

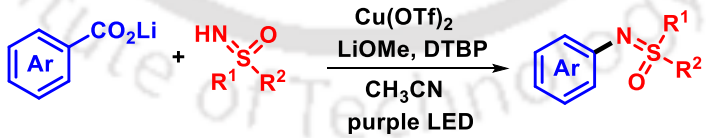

Scheme II.1.1.4. *Cu-LMCT-enabled decarboxylative sulfoximination.*

II.2. Previous Approaches on Visible-Light-Induced Decarboxylation of Cinnamic Acids:

The last few years have witnessed an upsurge in the use of cinnamic acids as a potential cross-coupling partner to access various synthetically valuable compounds after decarboxylation.[9] These α,β–unsaturated acid derivatives are available in great structural diversity and can be readily prepared in the laboratory. They also ensure good regio- and stereoselectivity in the resulting products.

In 2017, Noel *et al.* developed a visible-light mediated decarboxylation strategy for the stereoselective synthesis of difluoromethylated styrenes using fac-Ir(ppy)$_3$ as the photocatalyst. The stereoselectivity is based on the substitution pattern of cinnamic acids, where, *meta*- and *para*-substituted cinnamic acids yield the expected *E*-isomer, on the other hand, *ortho*-substituted cinnamic acids selectively produce the less stable *Z*-product (Scheme II.2.1).[10]

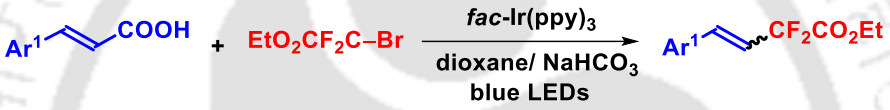

Scheme II.2.1. *Decarboxylative difluoromethylation of cinnamic acids.*

Visible light-mediated photocatalytic decarboxylative phosphorylation of cinnamic acids was disclosed by Zou group in 2018. The reaction proceeds in the presence of rose Bengal as a photocatalyst under air to result in *β*-ketophosphine oxides without the requirement of any oxidant or additive (Scheme II.2.2).[11]

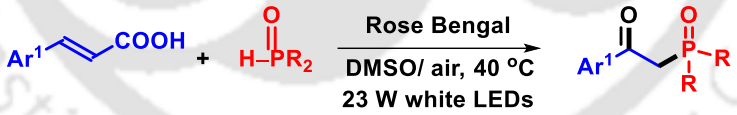

Scheme II.2.2. *Decarboxylative phosphorylation of cinnamic acids.*

Cai *et al*. disclosed a decarboxylative cross-coupling reaction of cinnamic acids with sulfonylhydrazides under visible-light irradiation in the presence of eosin Y, oxygen, and base. A range of vinyl sulfones with diverse functionalities were smoothly produced with oxygen as the terminal oxidant under this mild reaction condition (Scheme II.2.3).[12]

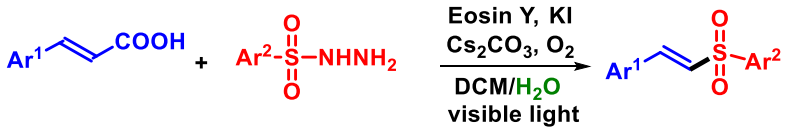

Scheme II.2.3. *Decarboxylative sulfonylation of cinnamic acids.*

In 2021, Singh and co-workers reported a concerted metallophotoredox catalysis for the decarboxylative functionalizations of α,β–unsaturated carboxylic acids with aryl iodides in the presence of a Cu catalyst, a perylene bisimide dye, TBHP, and Et_3N (Scheme II.2.4).[13] Unlike most decarboxylative coupling reactions, this methodology resulted in concomitant oxidation of the α,β–unsaturated counterpart to form 1,2-diketones.

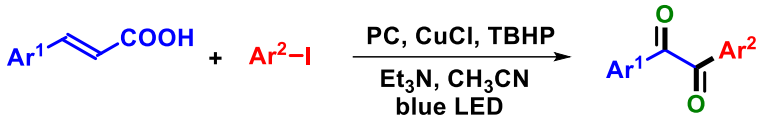

Scheme II.2.4. *Decarboxylative cross-coupling between cinnamic acids and aryl iodides.*

II.3. Present Work:

Conventional metal-catalyzed thermal decarboxylative cross-coupling reactions usually require high reaction temperatures and excessive additives and occur at ease for ortho-substituted derivatives. Photo-induced decarboxylation provides an eco-safe and effective pathway; however, they mostly depend on transition metals or organic dye-based catalysts. Consequently, many C−C and C−heteroatom bond-forming decarboxylative reactions are still out of reach in conventional chemistry. Considering all these aspects, we aimed to design a unique and mild approach for photoinduced decarboxylative sulfoximidation of cinnamic acid under metal and base-free conditions.

Several reports have demonstrated the unique reactivity of NH-sulfoximines under blue light irradiation in the presence of halogenated succinimides.[14] Leveraging all the remarkable previous reports, we envisioned designing a decarboxylation strategy between cinnamic acids and NH-sulfoximines. To synchronize our assumption, a preliminary reaction was carried out between cinnamic acid (**1**, 1 equiv) and *S*-aryl-*S*-methylsulfoximine (**a**, 1 equiv) in the presence of *N*-iodosuccinimide (NIS) (20 mol %), in DCM (2 mL) under the irradiation of 2 x 5 W blue LEDs at room temperature. Gratifyingly, a new product was isolated with a satisfactory yield of 82%. The spectroscopic evidence (^1H and $^{13}C\{^1H\}$ NMR and X-ray diffraction) revealed the structure of the product to be *N*-(methyl(oxo)(phenyl)-λ^6-sulfaneylidene)-2-oxo-2-phenylacetamide (**1a**). The formation of α-keto-*N*-acylsulfoximines from cinnamic acid appeared interesting in light of the mechanistic aspect of the reaction and the utility of α-ketoamides[15] as an important motif in medicinal chemistry.

Scheme II.3.1. *Our Approach.*

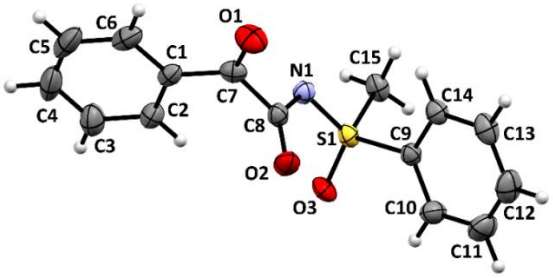

Figure.II.3.1. *ORTEP structure of **1a** with 30% ellipsoid probability (CCDC 2227206).*

II.3.1. Optimization of Reaction Conditions:

Inspired by this oxidative decarboxylative approach, extensive optimization studies involving the selection of different reaction conditions were carried out. Initially, different catalysts such as *N*-bromosuccinimide (NBS), *N*-chlorosuccinimide (NCS), and molecular iodine (I_2) were screened. Though NCS and I_2 failed to result in the anticipated product, NBS resulted in **1a** with 47% yield (Table II.3.1, entry 2). Moreover, the desired product was not formed at all in the absence of NIS (Table II.3.1, entry 3). Further, to improve the yield, the reaction was carried out with different concentrations of NIS (Table II.3.1, entries 4-5). However, there were no substantial changes in the yield, so all further reactions were carried out with 20 mol % of NIS. Next, different solvents such as DCE, CH_3CN, DMSO, DMF, EtOH, and 1,2-dioxane were screened instead of DCM. Except for DCE (34%) and CH_3CN (12%), the reaction did not proceed at all for other solvents (Table II.3.1, entries 6-8). To check the effect of wavelength and intensity of light, the standard reaction was carried out in 2 x 5 W white (46 mW/cm^2) and green (534 nm) LEDs. Both the lights failed to improve the reaction yield (Table II.3.1, entries 9 and 10). Hence, the optimized conditions for this reaction are the use of cinnamic acid (1 equiv), NH-sulfoximine (1 equiv), NIS (20 mol %) in DCM (2 mL) under 2 x 5 W blue LEDs (448 nm). For all the reactions, proper aeration was maintained using a fan.

Table II.3.1. *Optimization of the reaction conditions.*[a,b]

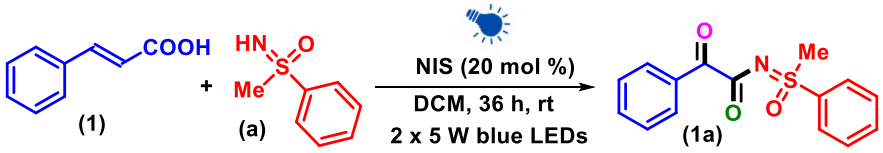

entry	variation from optimal conditions[a]	yield (%)[b]
1.	None	82
2.	NCS, NBS, I_2 (1 equiv) instead of NIS	Trace, 57, Trace
3.	Without NIS	N.D.
4.	50 mol % NIS	85
5.	1 equiv NIS	80
6.	DCE instead of DCM	34
7.	CH_3CN instead of DCM	12
8.	DMSO, DMF, EtOH, 1,2-dioxane instead of DCM	N.D.
9.	2 x 5 W white LEDs	78
10.	2 x 5 W green LEDs	25

[a]Reaction condition: **1** (0.4 mmol), **a** (0.4 mmol), NIS (0.08 mmol), DCM (2 mL) for 36 h in blue LED's (448 nm). [b]Isolated pure product. N.D. = not detected.

II.3.2. Substrate Scope:

With the optimized reaction condition in hand, the scope of this novel protocol was extended to a variety of cinnamic acids and NH-sulfoximines, and the results are summarized in Schemes II.3.2.1 and II.3.2.2. We began our investigation with varying different substituents on the phenyl containing ring of cinnamic acid (**1–17**) keeping the *S*-aryl-*S*-methyl sulfoximine (**a**) counterpart fixed. Cinnamic acids with electron-neutral as well as electron-donating substituents on the *para* and *meta* position successfully underwent the reaction to yield the products **1a**, **2a**, **3a**, **4a** in 82%, 74%, 72%, and 67% yields, respectively. Similarly, the presence of moderate electron-withdrawing groups in the *para* and *meta* position as in **5a–10a**, successfully yielded the products in good yields (63–75%). The present protocol was successful for strongly electron-withdrawing groups such as $–CF_3$ (**11a** and **12a**) and $–NO_2$ (**13a** and **14a**), resulting in products in appreciable yields of up to 63%. Moreover, bi-substituted cinnamic acid **15** was converted to product **15a** with 64% yield. Nevertheless, the protocol was unsuccessful for ferulic acid (**16**) and trans-3-(3-pyridyl)acrylic acid (**17**).

Scheme II.3.2.1. *Scope for formation of α-keto-N-acyl sulfoximines with different cinnamic acids.*[a–b]

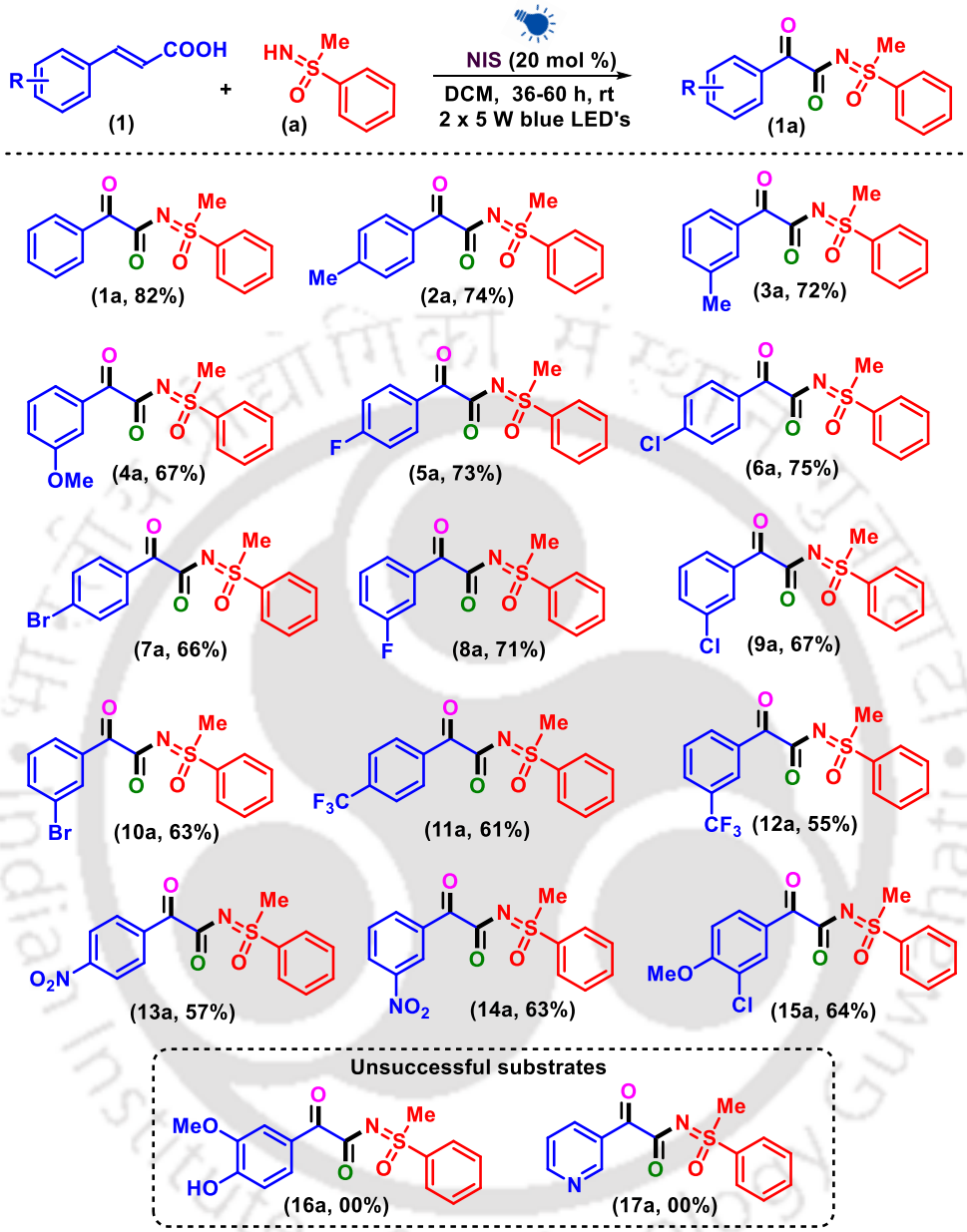

[a]Reaction conditions: (**1–17**) (0.4 mmol), (**a**) (0.4 mmol), NIS (0.08 mmol), DCM (2 mL) in 2 x 5 W blue LEDs (448 nm). [b]Yield of the isolated product.

Next, the scope of different NH-sulfoximines (**b–p**) bearing electron-donating (EDGs), as well as electron-withdrawing groups (EWGs), with simple cinnamic acid (**1**), are investigated, and the results as presented in Scheme II.3.2.2. All the products arising from *S*-aryl-*S*-methyl sulfoximines gave moderate to good yields of products irrespective of the electronic and steric nature of the substituents. The presence of electron-donating groups in the *para* position and *meta* position of the phenyl ring in *S*-aryl-*S*-methyl sulfoximines such as *p*-

Me, *p*-Et, *p*-OMe, and *m*-OMe successfully yielded the products (**1b–1e**) in good yields of 77%, 75%, 67%, and 64%, respectively. Similarly, the protocol was successful for diverse electron-withdrawing groups such as -F, -Cl, -Br, and -CF_3 in the *p* and *m*- and *o*-position with yields of the resulting products (**1f**–**1k**) being up to 81%. Moreover, the reaction was favorable for *S*-aryl-*S*-ethyl and *S*-aryl-*S*-propyl sulfoximines resulting in products **3l** and **3m** in appreciable yield. Finally, *S*-aryl-*S*-pyridinyl sulfoximines, when applied to the present protocol underwent successful conversion to product **1n**. However, the present protocol was unsuccessful for NH-sulfoximines having an active allylic or benzylic position (**o** and **p**).

Scheme II.3.2.2. *Scope for the formation of α-keto-N-acyl sulfoximines with different NH-sulfoximines.*[a–b]

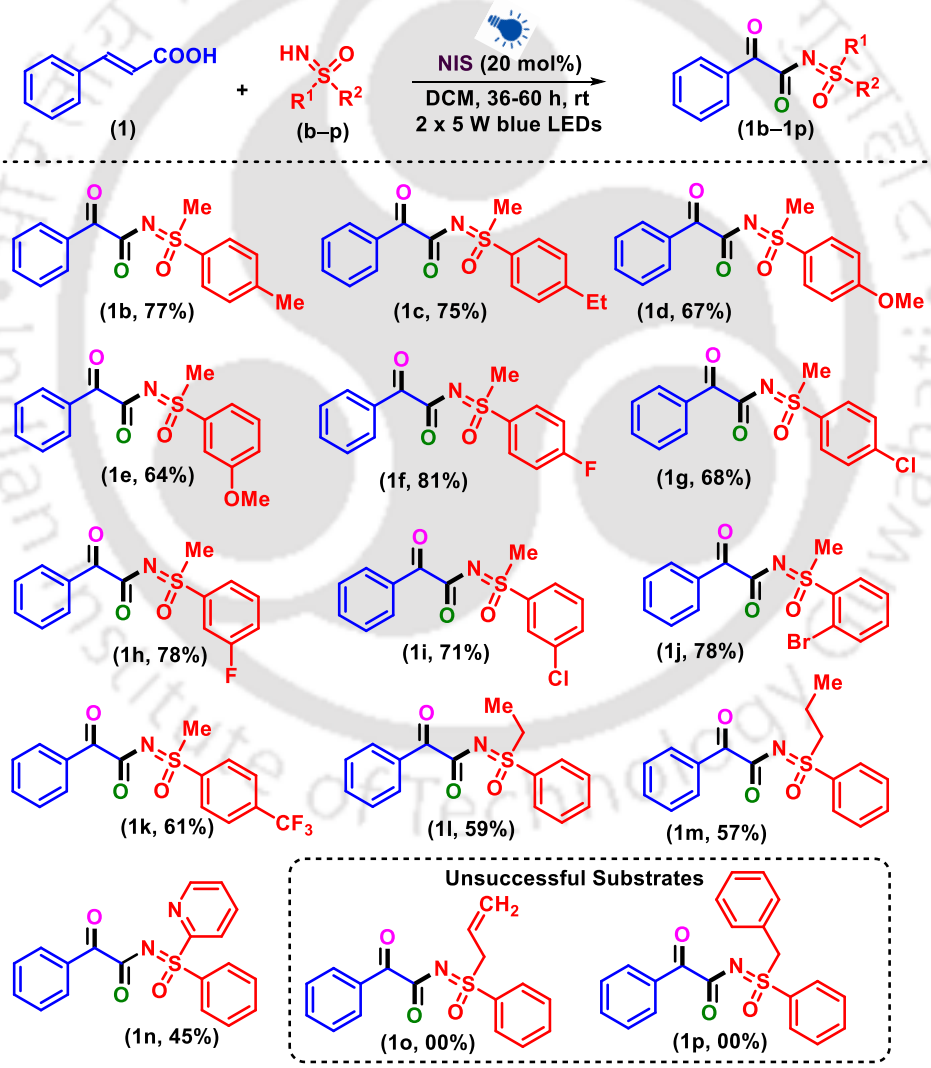

[a]Reaction conditions: (**1**) (0.4 mmol), (**b**–**p**) (0.4 mmol), NIS (0.08 mmol), DCM (2 mL) in 2 x 5 W blue LEDs (448 nm). [b]Yield of the isolated product.

II.3.3. Mechanistic Investigations:

To understand the relevant mechanistic steps involved in this process, various control experiments were conducted taking cinnamic acid (**1**) and *S*-aryl-*S*-methyl sulfoximine (**a**) as model substrates. Though the standard reaction results in 82% of the desired product (**1a**), however, the reaction, when conducted without light irradiation failed to form **1a** (Scheme II.3.3.1.b), suggesting the indispensable involvement of light in this photochemical approach. When the reaction was carried out in a nitrogen atmosphere instead of air, a trace amount of the product was obtained (Scheme II.3.3.1.c). Moreover, a slightly higher yield of 84% was obtained when conducted under an atmosphere of oxygen (Scheme II.3.3.1.d). Also, the reaction did not proceed at all for anhydrous and degassed DCM under an N_2 atmosphere (Scheme II.3.3.1.e). All these observations suggest the involvement of atmospheric oxygen and solvent moisture in the formation of the desired product **1a**.

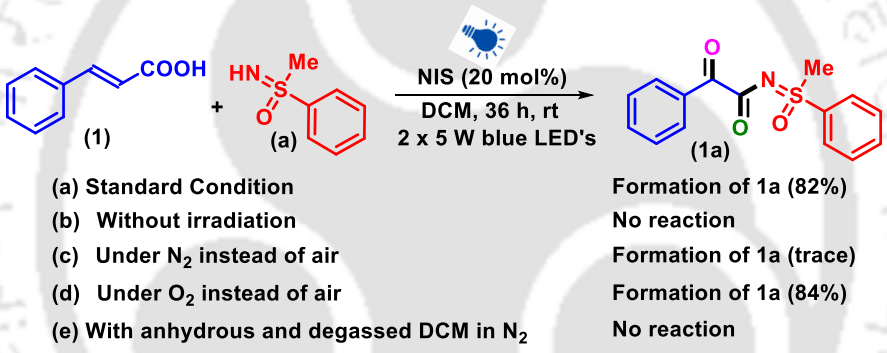

Scheme II.3.3.1. *Preliminary investigations.*

To ascertain the radical nature of the reaction, identical reactions were conducted in the presence of radical scavengers, 2,2,6,6-tetramethylpiperidine-1-oxyl (TEMPO, 1 equiv) and 1,1-diphenylethylene (1 equiv) (Scheme II.3.3.2). Failure of the reaction under the standard reaction conditions suggests the radical nature of the reaction.

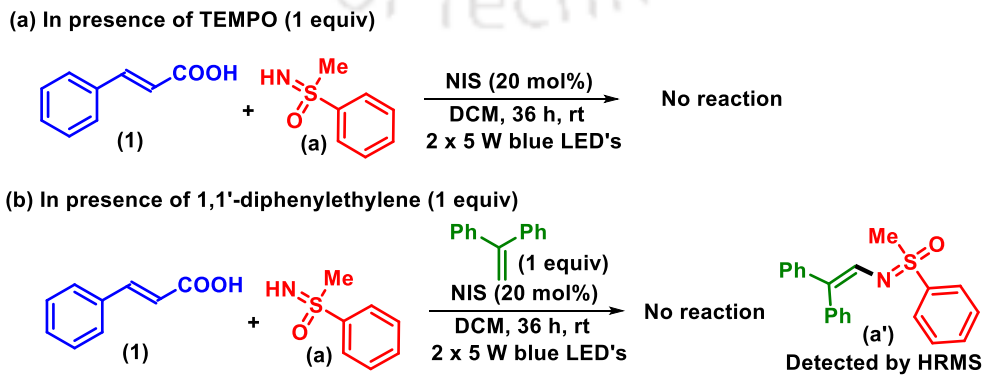

Scheme II.3.3.2. *Radical trapping experiments.*

Further, 1,1-diphenylethylene and sulfoximine adduct (**a'**) was detected in HRMS, which confirms the presence of N-centered sulfoximine radical in the reactive cycle (Figure II.3.3.1).

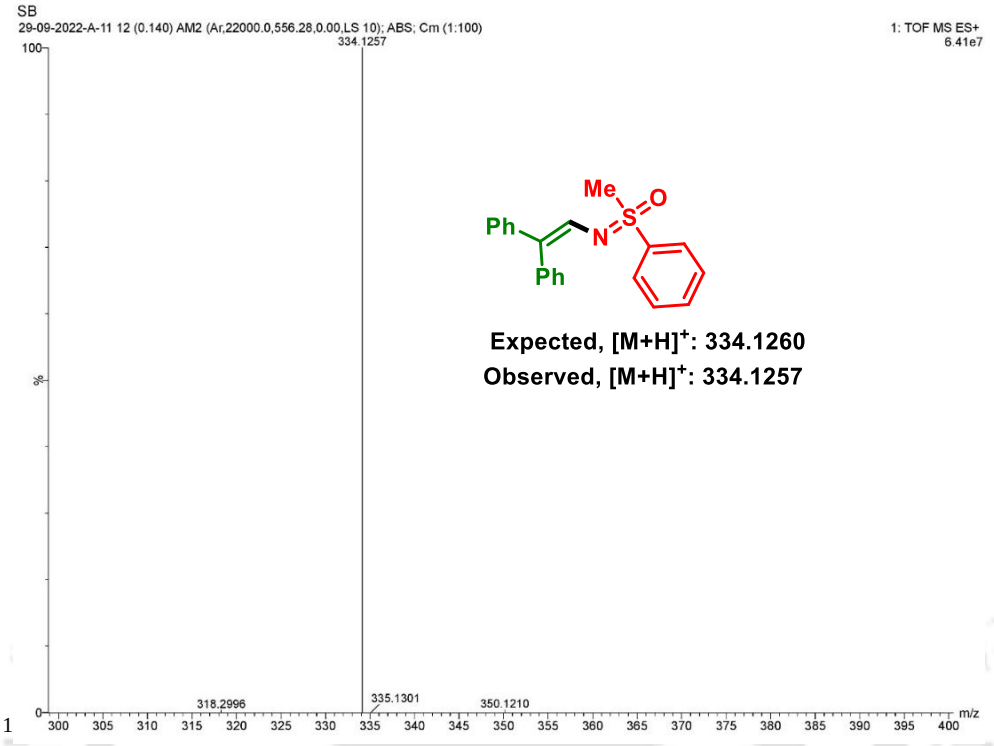

Figure II.3.3.1. *HRMS analysis of diphenylethylene-sulfoximine adduct* (**a'**).

To ascertain the possible source of the two-carbonyl oxygen in the product, a reaction was carried out in presence of H_2O^{18} (2 equiv) keeping the other reaction conditions fixed (Scheme II.3.3.3). The isolated product was subjected to HRMS and ^{13}C NMR analysis. The HRMS analysis confirms the formation of ^{18}O-labelled α-keto-*N*-acyl sulfoximines (**1a'**) with only one ^{18}O-labelled oxygen (Figure II.3.3.3). To confirm which oxygen originates from H_2O^{18}, a ^{13}C NMR of **1a'** was recorded. The ^{13}C NMR spectrum clearly shows two signals for the amidic carbonyl (δ 173.488 and 173.450 ppm) due to both labelled and unlabelled carbonyl groups of α-keto-*N*-acyl sulfoximines (Figure.II.3.3.2). This observation confirms that out of the two oxygen in the product, one originates from water and hence the other oxygen might be originating from atmospheric oxygen.

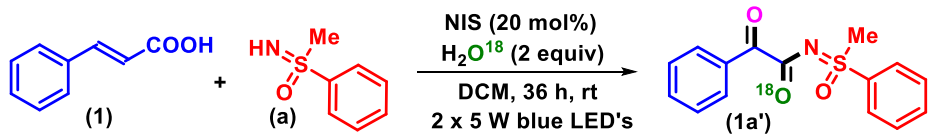

Scheme II.3.3.3. *H_2O^{18}-labelling experiments.*

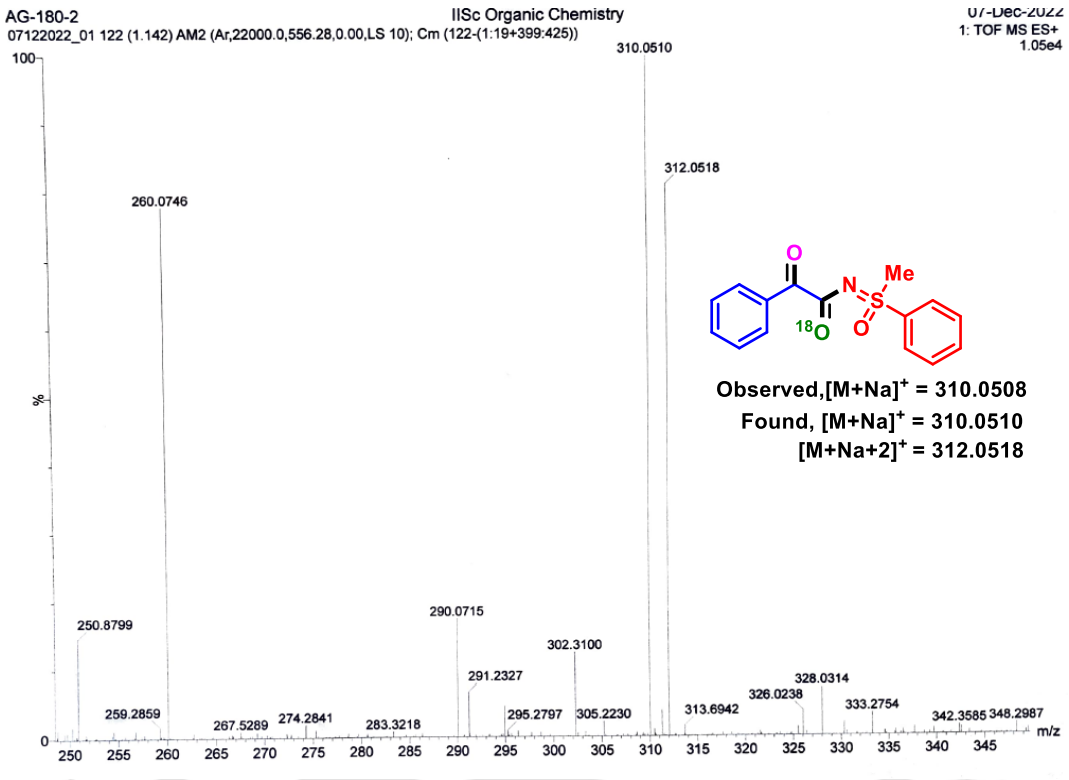

Figure II.3.3.2. *HRMS of ^{18}O labelled α-keto-N-acylsulfoximines* (**1a'**).

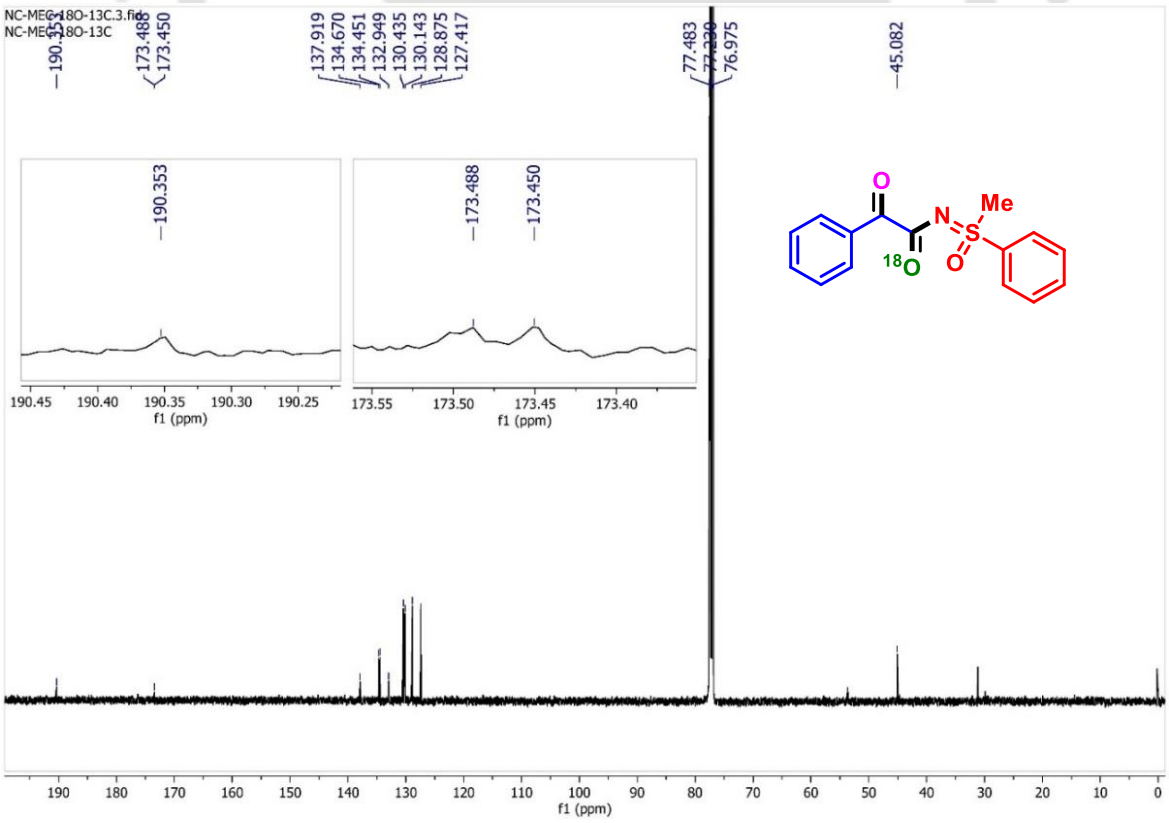

Figure II.3.3.3. *$^{13}C\{^{1}H\}$ spectrum of ^{18}O labelled α-keto-N-acylsulfoximines* (**1a'**).

To ascertain the formation of *N*-iodosulfoximine **A** as the possible intermediate, a reaction was carried out between preformed intermediate **A**[16] and cinnamic acid (**1**) without NIS (Scheme II.3.3.4). The successful formation of **1a** infers that the reaction must be proceeding through the formation of *N*-iodo-*S*-phenyl-*S*-methyl sulfoximine intermediate (**A**).

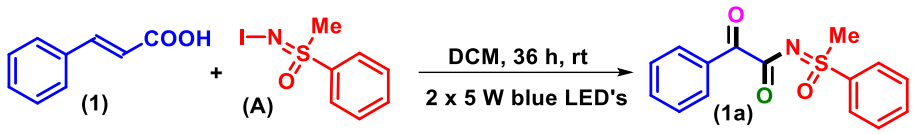

Scheme II.3.3.4. *Intermediacy of N-iodosulfoximine (**A**)*

In another case, the presynthesized *S*-alkenic intermediate **D**[17] was dissolved in 2 mL DCM and subjected to blue light irradiation standard condition (Scheme II.3.3.5). The formation of **1a** in 79% yield infers that the reaction must be proceeding through the alkene intermediate **D**.

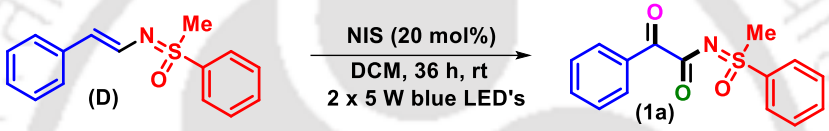

Scheme II.3.3.5. *Intermediacy of N-alkenicsulfoximine (**D**)*

For H_2O_2 Detection in the reaction mixture, a few experiments were conducted.[18] In one method, a reaction was set in identical conditions. After around 16 hours, a 100 μL solution of Mohr's Salt (10 mg in 100 μL H_2O + 1 mL CH_3CN) was added to the reaction mixture. After some time, a rapid setting of $Fe(OH)_3$ floc was observed. The floc observed was because of the rapid oxidation of Fe(II) to Fe(III) due to the presence of hydrogen peroxide, H_2O_2 in the medium (Figure II.3.3.4).

(a) **(b)**

Figure II.3.3.4. (a) *Reaction mixture before addition of Fe(II) solution; (b) Reaction mixture after addition of Fe(II) solution*

The above reaction mixture (5 μL) was withdrawn at approximately 16 h and was dissolved in 1 mL of DCM and subjected to UV-vis spectroscopy. An absorption maximum of 507 nm was recorded. Another portion of the same reaction mixture was admixed with 5 μL of $TiCl_4$ solution and was dissolved in 1 mL of DCM, and their UV absorption was recorded. Now, there was a shift from 507 nm to 495 nm upon the addition of $TiCl_4$. This shift was due to the formation of the peroxo complex of titanium (IV) (Figure II.3.3.5).

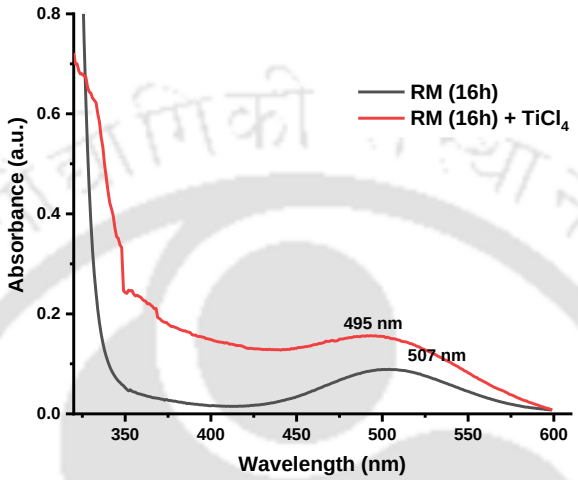

Figure II.3.3.5. *UV-absorption spectra for H_2O_2 detection in the medium.*

Moreover, since this is a photocatalyst-free photochemical approach, we were curious to find out the reactive species present in the reaction mixture which is responsible for absorbing light corresponding to the wavelength of blue light (448 nm).[19] Thus, we aimed at recording absorption spectra for the reaction components, **1**, **a**, and a combination of NIS and *NH*-sulfoximine (**A**). As expected, the spectra for the substrates **1** and **a** did not reveal any notable absorption pattern at either visible or near-UV light (λ>300 nm). However, the absorption spectra of **A**, recorded under the same condition exhibited a remarkable progressive increase of absorbance from around 480 nm, with a maximum in the near-UV region at 363 nm. This implied that intermediate **A** is serving as an energy-absorbing species in blue light and facilitates the entire reaction in the absence of any external photocatalyst (Figure II.3.3.6).

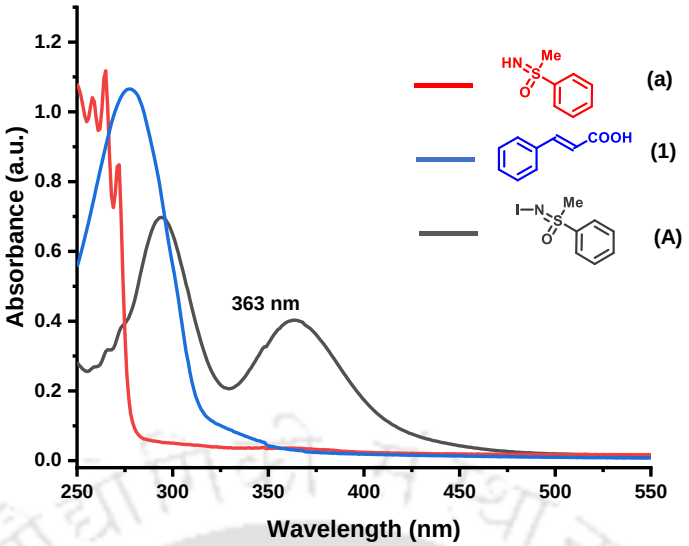

Figure II.3.3.6. *UV-vis spectra of **1**, **a**, and **A** in DCM.*

II.3.4. Plausible Mechanism:

Based on the control experiments and literature precedents, we suggest the reaction path as in Scheme 5.[12,20,21] Initially, the N-iodination of NH-sulfoximine (**a**) with NIS generates the key intermediate N-iodo sulfoximine (**A**).[16] The photoinduced homolysis of the N–I bond in **A** results in a N-centered sulfoximidoyl radical (**B**), and an iodo radical.[20] The vicinal addition of B and I• radical to cinnamic acid (1) results in intermediate (**C**) (path-I).[12] Decarboxylation and concurrent elimination of HI from C generate the alkene intermediate (**D**). Alternatively, the addition of radical **B** to cinnamic acid (**1**) produces a benzylic radical intermediate (**C'**) (path-II).[21a] The intermediate **C'** upon SET with iodo radical generates an iodide ion and a carbocation intermediate (**C''**) which upon decarboxylation gives alkene intermediate (**D**). The I• radical is regenerated by reducing molecular oxygen to a superoxide ion ($O_2^{\bullet-}$).[21b] This process generates H_2O_2 in the medium which has been confirmed. Next, the vicinal addition of I• radical and superoxide ion $O_2^{\bullet-}$ across the double bond of alkene (**D**) produces intermediate **E**, which on elimination of H_2O gives intermediate **F**. The nucleophilic substitution of iodo group by H_2O in intermediate **F** (confirmed by H_2O^{18}) produces an acyloin intermediate (**G**). The final product **1a** is resulted by the oxidation of intermediate **G** (Scheme II.3.4).[21c]

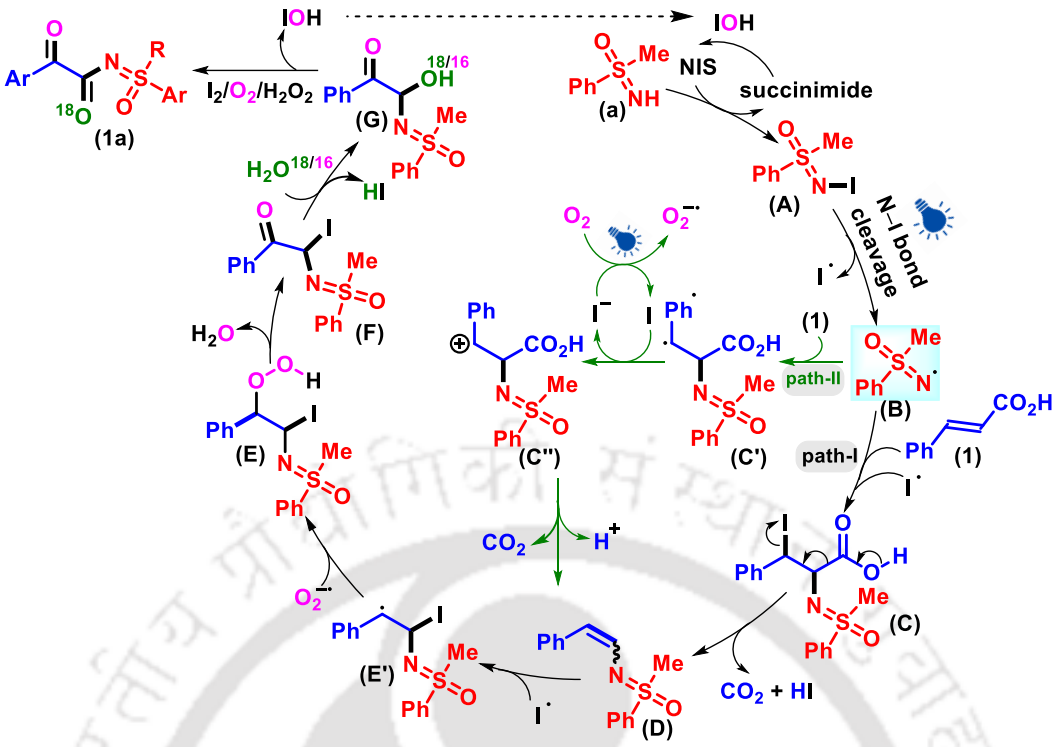

II.3.4. *Plausible mechanism.*

II.3.5. Scale-up Reaction:

To check the scalability of the reaction, a large-scale reaction between **1** and **a** was conducted on a 5 mmol scale. To our delight, the product **1a** was obtained in a good yield of 61%.

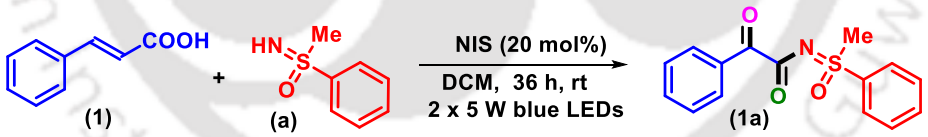

Scheme II.3.5. *Scale-up reaction for the synthesis of α-keto-N-acyl sulfoximines (**1a**).*

II.3.6. Conclusion:

In conclusion, we have disclosed a visible-light-induced decarboxylative coupling between cinnamic acids and NH-sulfoximines which leads to a spectrum of α-keto-*N*-acyl sulfoximines. The reaction proceeds *via* sulfoximidation, followed by decarboxylation, with concomitant oxidation of the double bond of cinnamic acid, all in the presence of a catalytic amount of NIS. This decarboxylative protocol offers an eco-safe and effective pathway for C–heteroatom bond formation compared to conventional decarboxylative reactions which require metal catalysts, excessive reagents, and high temperatures. The intrinsic photochemical

reactivity of *N*-iodo sulfoximines as an excellent reacting partner in the absence of an external photosensitizer is explored.

II.4. Experimental Section:

II.4.1. General Information:

All the reagents were commercial grade and purified according to the established procedures. All the reactions were carried out in oven-dried glassware. The highest commercial quality reagents were purchased and were used without further purification unless otherwise stated. All the cinnamic acids used in this protocol were commercially purchased from Sigma Aldrich and BLD Pharma. Reactions were monitored by thin layer chromatography (TLC) on 0.25 mm silica gel plates ($60F_{254}$) visualized under UV illumination at 254 nm. Organic extracts were dried over anhydrous sodium sulfate (Na_2SO_4). Solvents were removed using a rotary evaporator under reduced pressure. Column chromatography was performed to purify the crude product on silica gel 60–120 mesh using a mixture of hexane and ethyl acetate as eluent. The isolated compounds were characterized by spectroscopic [^{1}H, ^{13}C{1H} NMR, and IR] techniques and HRMS analysis. NMR spectra were recorded in deuterochloroform ($CDCl_3$). ^{1}H, ^{13}C{^{1}H} were recorded in 400 (100), 500 (125) or 600 (150) MHz spectrometers and were calibrated using tetramethylsilane or residual undeuterated solvent for ^{1}H NMR, deuterochloroform for ^{13}C NMR as an internal reference {$Si(CH_3)_4$: 0.00 ppm or $CHCl_3$: 7.260 ppm for ^{1}H NMR and 77.230 ppm for ^{13}C{1H}. ^{19}F NMR was calibrated without any internal standard in $CDCl_3$ in a 370 or 471 MHz spectrometer. The chemical shifts are quoted in δ units, parts per million (ppm). ^{1}H NMR data is represented as follows: Chemical shift, multiplicity (s = singlet, d = doublet, t = triplet, q = quartet, dd = doublet of doublets, m = multiplet), integration and coupling constant(s) *J* in hertz (Hz). High-resolution mass spectra (HRMS) were recorded on a mass spectrometer using electrospray ionization-time of flight (ESI-TOF) reflection experiments. FT-IR spectra were recorded in neat and reported in the frequency of absorption (cm^{-1}). All UV experiments were performed in 1 mL quartz cuvettes of path length 1 cm at 25 ^{o}C in UV/Vis spectrometer in HPLC grade solvent.

II.4.2. Light Information and Reaction Setup:

Philips 2 x 5 W blue LED (448 nm) bulb was used as the light source for this light-induced reaction, and no filter was used. Borosilicate round bottom glass was used as the reaction vessel. The distance from the light source to the irradiation vessel was ~3-5 cm. A regular fan was used to ventilate the area to maintain the room temperature (27–30 ^{o}C). The

reaction setup for this photochemical reaction and the corresponding images of the reaction mixture before the start of the reaction and after the completion of the reaction are shown below (Figure II.4.2.1).

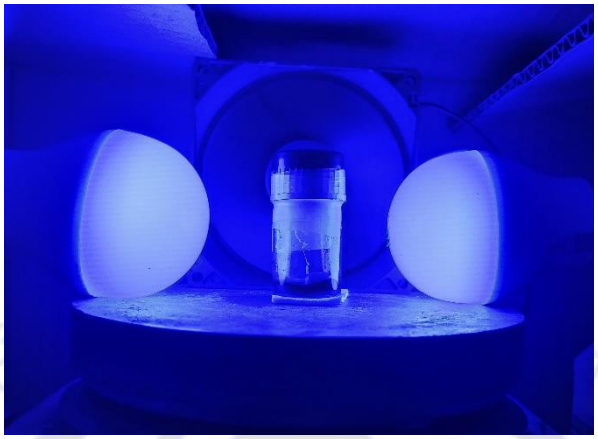

(a)

(b)

(c)

Figure II.4.2.1 (a) Photochemical Reaction Set-up (b) Before reaction (c) After reaction

II.4.3. Crystallographic Information:

Crystallographic Information of *N*-[Methyl(oxo)(phenyl)-λ^6-sulfaneylidene]-2-oxo-2-phenylacetamide (1a):

(i) Sample Preparation: The single crystal of compound **1a** was prepared by the slow evaporation method for which 10 mg of the compound (**1a**) was dissolved in 1 mL of DCM in a clean and dry 10 mL glass vial. MeOH (0.5 mL) was added to this solution slowly with a dropper. The mouth of the glass vial was covered with a cap having a small hole and kept for slow evaporation at room temperature. Crystals of **1a** were obtained after approximately 3-4 days as a transparent block-shaped crystal.

(ii) Data Collection: Diffraction data were collected at 292 K with MoKα radiation (λ = 0.71073 Ǻ) using a Bruker Nonius SMART APEX CCD diffractometer equipped with graphite monochromator and Apex CD camera. The SMART software was used for data collection and for indexing the reflections and determining the unit cell parameters. Data reduction and cell refinement were performed using SAINT software and the space groups of these crystals were determined from systematic absences by XPREP and further justified by the refinement results. The structures were solved by direct methods and refined by full-matrix least-squares calculations using SHELXTL-973 software. All the non-H atoms were refined in the anisotropic approximation against F2 of all reflections.

(iii) Crystallographic description of *N*-[methyl(oxo)(phenyl)-λ^6-sulfaneylidene]-2-oxo-2-phenylacetamide (1a):

$C_{15}H_{13}NO_3S$, colourless block shaped crystal; crystal dimensions 0.06 x 0.05 x 0.05 mm, M_r = 287.32, Orthorhombicic, space group F d d 2; a = 13.0303(7), b = 43.234 (3), c = 10.2922 (7) Å, α = 90°, β = 90°, γ = 90°, V = 5798.1 (6) Å^3, Z = 16, ρ_{calcd} = 1.317 g/cm^3, μ = 0.229 mm^{-1}, F(000)= 2400.0, reflection collected / unique = 2880 / 2269, refinement method = full-matrix least-squares on F^2, final R indices [I> 2\s(I)]: R_1 = 0.0532, wR_2 = 0.0856, R indices (all data): R_1 = 0.0758, wR_2 = 0.0947, goodness of fit = 1.065. **CCDC**-2227206 for *N*-[methyl(oxo)(phenyl)-λ^6-sulfaneylidene]-2-oxo-2-phenylacetamide (**1a**) contains the supplementary crystallographic data for this paper. These data can be obtained free of charge from The Cambridge Crystallographic Data Centre via www.ccdc.cam.ac.uk/data_request/cif.

II.4.4. General Procedure:

II.4.4.1. Procedure for the Synthesis of NH-Sulfoximines (a):

In an oven-dried 50 mL round bottom flask, methylphenylsulfide **S** (5 mmol, 1 equiv, 620 mg), ammonium carbamate (7.5 mmol, 1.5 equiv, 585 mg) and phenyliodo diacetate (PIDA) (11.5 mmol, 2.3 equiv, 3.7 g) in 15 mL methanol are taken and stirred at room temperature for 3 hours. After the disappearance of the sulfides, as indicated by TLC, the reaction was stopped and the solvent was evaporated under reduced pressure. The compound was purified by column chromatography and separated in 1:2 ratio of EtOAc:hexane to result in the product *S*-phenyl-*S*-methyl-sulfoximine (**a**) in 690 mg, 89% yield (Scheme II.4.4.1).

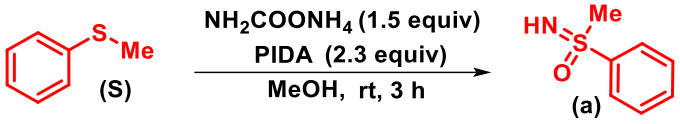

Scheme II.4.4.1. *Preparation of NH-sulfoximines (**a**).*

II.4.4.2. Procedure for the Synthesis of α-Keto-*N*-acyl sulfoximines (1a):

Cinnamic acid (**1**) (0.4 mmol, 1 equiv, 59 mg), *NH*-sulfoximine (**a**) (0.4 mmol, 1 equiv, 62 mg), and *N*-iodosuccinimide (NIS) (0.08 mmol, 20 mol%, 18 mg) in 2 mL of DCM were added to an oven-dried 10 mL borosilicate vial and stirred at room temperature, approximately at a distance of ~3−5 cm from two 448 nm 5 W blue LED bulbs. After completion of the reaction (monitored by TLC analysis), the reaction mixture was added ethyl acetate (25 mL) and washed with saturated $NaHCO_3$ solution (1 x 10 mL), 5% aqueous $Na_2S_2O_3$ (1 x 10 mL) solution followed by saturated brine solution (1 x 10 mL). The organic layer was dried over anhydrous Na_2SO_4, and then the solvent was evaporated under reduced pressure. The crude product obtained was purified over a column of silica gel using (3:1) of ethyl acetate in hexane to afford the *α*-keto-*N*-acyl sulfoximine (**1a**) in 82% yield. The identity and purity of the product was confirmed by spectroscopic analysis (Scheme II.4.4.2).

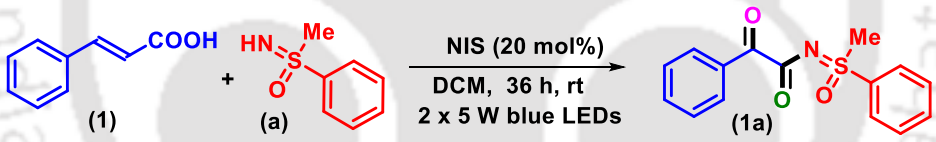

Scheme II.4.4.2. *Preparation of α-keto-N-acyl sulfoximines (**1a**).*

II.4.4.3. Procedure for the Synthesis of *N*-Iodosulfoximine (A):[16]

Intermediate **A** was prepared according to the previously reported literature procedure. In an oven-dried 10 mL round bottom flask, methylphenylsulfide **S** (1 mmol, 1equiv, 124 mg), ammonium carbonate (1.5 mmol, 1.5 equiv, 117 mg) and phenyliodo diacetate (PIDA) (2.3 mmol, 2.3 equiv, 741 mg) in 5 mL methanol were taken and stirred at room temperature for 1 hour. Then, 1.1 equiv of NIS (1.1 mmol, 248 mg) was added, and the stirring was continued for another 1 hour. After the completion of the reaction as indicated by TLC, the reaction was stopped and the precipitate was collected by vacuum filtration using a Büchner funnel, washed with a small amount of MeOH, and dried under reduced pressure (vacuum pump) to obtain pure product *N*-iodo-*S*-phenyl-*S*-methyl sulfoximine **A** in 83% yield (233 mg). The identity and purity of the product was confirmed by spectroscopic analysis and literature reports (Scheme II.4.4.3).

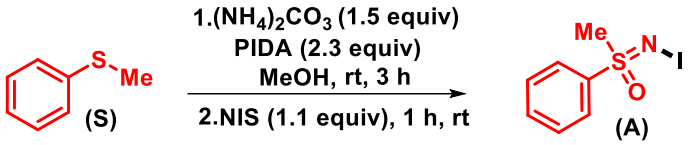

Scheme II.4.4.3. *Preparation of N-iodo-S-phenyl-S-methyl sulfoximine (**A**).*

II.4.4.4. Procedure for the Synthesis of Intermediate D.[17]

A Schlenk flask equipped with a magnetic stir bar was charged with CuI (190 mg, 1.0 mmol), K_2CO_3 (276 mg, 2.0 mmol) and the *S*-aryl-*S*-methyl sulfoximine (**a**, 1.0 mmol) and purged with argon. Then, 5 mL dry toluene was added through a glass syringe, followed by *N*,*N*'-dimethylethylenediamine (213 mL, 2.0 mmol) and the (*E*)-(2-bromovinyl)benzene (1.5 mmol, 271 mg). After heating the mixture at 110 °C under stirring for 24 h, it was allowed to cool to room temperature, diluted with diethyl ether, and filtered through a thin pad of celite. The solvents were then removed under vacuum. The crude product obtained was purified over a column of silica gel using (5:2) of ethyl acetate in hexane to afford the yielding the essentially pure *N*-vinylsulfoximine (**D**) in 71% yield (182 mg) (Scheme II.4.4.4).

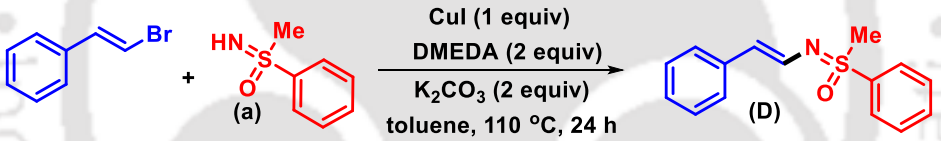

Scheme II.4.4.4. *Preparation of intermediate **D**.*

II.4.5. Mechanistic Investigations:

II.4.5.1. Radical-Trapping Experiment:

In an oven-dried 10 mL borosilicate vial, cinnamic acid (**1**) (0.2 mmol, 1 equiv, 30 mg), *NH*-sulfoximine (**a**) (0.2 mmol, 1 equiv, 31mg), *N*-iodosuccinimide (0.04 mmol, 20 mol%. 9mg), and 1,1'-diphenylethylene (2 equiv, 36 mg), were taken in DCM (1 mL) and was stirred at room temperature, approximately at a distance of ~3-5 cm from two 448 nm 5 W blue LED bulbs. A small aliquot of the reaction mixture was withdrawn at approximately 12 h and diluted with 60:40 acetonitrile:water mixture (1 mL) and subjected to HRMS. The HRMS analysis of this reaction aliquot shows HRMS values corresponding to diphenylethylene-sulfoximine adduct (**a'**).

II.4.5.2. H_2O^{18}-Labelling Experiment:

In an oven-dried 10 mL borosilicate vial, cinnamic acid (**1**) (1 mmol, 1 equiv, 148 mg), *NH*-sulfoximine (**a**) (1 mmol, 1 equiv, 155 mg), *N*-iodosuccinimide (0.2 mmol, 20 mol%. 45

mg), and H_2O^{18} (1 mmol, 1 equiv, 20 mg) were taken in DCM (3 mL) and was stirred at room temperature, approximately at a distance of ~3-5 cm from two 448 nm 5 W blue LED bulbs. After completion of the reaction (monitored by TLC analysis), the mixture was admixed with 20 mL ethyl acetate and sequentially washed with aqueous $NaHCO_3$ (1 x 10 mL), 5% aqueous $Na_2S_2O_3$ (1 x 10 mL) and brine solution (1 x 10 mL). The organic layer was dried over anhydrous Na_2SO_4, and the solvent was evaporated under reduced pressure. The crude residue thus obtained was purified by column chromatography over silica gel (60-120 mesh) using hexane and ethyl acetate (3:1) as eluent to afford *N*-[methyl(oxo)(phenyl)-λ^6-sulfaneylidene]-2-oxo-2-phenylacetamide (**1a'**) in 81% yield. To confirm the origin of the two carbonyl oxygens present in the product, the isolated product was subjected to ^{13}C NMR and HRMS analysis.

II.4.5.3 H_2O_2 Detection in the Reaction Mixture[18]

Method-1: H_2O_2 Detection by Mohr's Salt

In an oven-dried 10 mL borosilicate vial, cinnamic acid (**1**) (1 mmol, 1 equiv, 148 mg), *NH*-sulfoximines (**a**) (1 mmol, 1 equiv, 155 mg), *N*-iodosuccinimide (0.2 mmol, 20 mol%. 45 mg), and were taken in DCM (3 mL) and was stirred at room temperature, approximately at a distance of ~3-5 cm from two 448 nm 5 W blue LED bulbs. After around 16 hours, a 100 μL solution of Mohr's Salt (10 mg in 100 μL H_2O + 1 mL CH_3CN) was added to the reaction mixture. After some time, a rapid setting of $Fe(OH)_3$ floc was observed.

Method-2: H_2O_2 Detection by UV-Vis Experiment

The above reaction mixture (5 μL) was withdrawn at approximately 16 h and was dissolved in 1 mL of DCM and subjected to UV-vis spectroscopy. An absorption maximum of 507 nm was recorded. Another portion of the same reaction mixture was admixed with 5 μL of $TiCl_4$ solution and was dissolved in 1 mL of DCM, and their UV absorption was recorded.

II.4.6. UV-Vis Experiments:

A 0.1 mM 10 mL stock solution of cinnamic acid (**1**), *S*-aryl-*S*-methyl sulfoximine (**a**) and *N*-iodo-*S*-phenyl-*S*-methyl sulfoximine (**A**) were prepared separately in DCM. The UV absorption of cinnamic acid (**1**) (5 μM in 1mL DCM) and *S*-aryl-*S*-methyl sulfoximine (**a**) (5 μM in 1 mL DCM) and *N*-iodo-*S*-phenyl-*S*-methyl sulfoximine (**A**) were independently recorded. The absorption spectra for the substrates **1** and **a** did not show any notable absorption pattern at either blue or visible region (λ>350 nm). However, the absorption spectra of **A**, recorded under the same condition, exhibited a remarkable progressive increase of absorbance around 480 nm, with a maximum in the region at 363 nm.

II.5. Spectral Data

N-[Methyl(oxo)(phenyl)-λ⁶-sulfaneylidene]-2-oxo-2-phenylacetamide (1a):

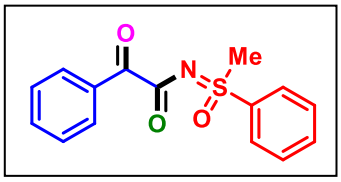

White solid (94 mg, 82%); purified over a column of silica gel (30% ethyl acetate in hexane); ^{1}H NMR (500 MHz, $CDCl_3$): δ (ppm) 8.09–8.04 (m, 4H), 7.73 (t, 1H, J = 9.5 Hz), 7.67–7.58 (m, 3H), 7.47 (t, 2H, J = 9.5 Hz), 3.48 (s, 3H); ^{13}C{^{1}H} NMR (125 MHz, $CDCl_3$): δ (ppm) 190.3, 173.5, 137.9, 134.7, 134.4, 133.0, 130.4, 130.1, 128.9, 127.4, 45.1; IR (neat, cm^{-1}): 3019, 2924, 2853, 1682, 1631, 1597, 1448, 1405, 1208; HRMS (ESI): calculated for $C_{15}H_{13}NO_3SNa$ [M + Na]$^{+}$: 310.0508, found 310.0503.

N-[Methyl(oxo)(phenyl)-λ⁶-sulfaneylidene]-2-oxo-2-(p-tolyl)acetamide (2a):

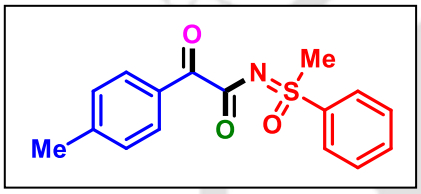

White solid (89 mg, 74%); purified over a column of silica gel (28% ethyl acetate in hexane); ^{1}H NMR (400 MHz, $CDCl_3$): δ (ppm) 8.08–8.06 (m, 2H), 7.94 (d, 2H, J = 8.4 Hz), 7.74–7.69 (m, 1H), 7.66–7.62 (m, 2H), 7.27 (s, 1H), 7.25 (s, 1H), 3.47 (s, 3H), 2.41 (s, 3H); ^{13}C{^{1}H} NMR (100 MHz, $CDCl_3$): δ (ppm) 190.1, 173.7, 145.6, 137.9, 134.6, 130.5, 130.4, 130.1, 129.6, 127.4, 45.0, 22.1; IR (neat, cm^{-1}): 3017, 2925, 2854, 1677, 1629, 1605, 1447, 1331, 1211; HRMS (ESI): calculated for $C_{16}H_{16}NO_3S$ [M + H]$^{+}$: 302.0845, found 302.0842.

N-(Methyl(oxo)(phenyl)-λ⁶-sulfaneylidene)-2-oxo-2-(m-tolyl)acetamide (3a):

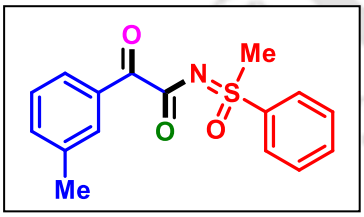

Off white solid (87 mg, 72%), purified over a column of silica gel (28% ethyl acetate in hexane); ^{1}H NMR (500 MHz, $CDCl_3$): δ (ppm) 8.08 (d, 2H, J = 7.5 Hz), 7.84 (s, 2H), 7.72 (t, 1H, J = 9.0 Hz), 7.64 (t, 2H, J = 7.5 Hz), 7.41 (d, 1H, J = 7.5 Hz), 7.35 (t, 1H, J = 7.5 Hz), 3.48 (s, 3H), 2.39 (s, 3H); ^{13}C{^{1}H} NMR (125 MHz, $CDCl_3$): δ (ppm) 190.6, 173.6, 138.7, 138.0, 135.3, 134.6, 132.9, 130.7, 130.1, 128.8, 127.7, 127.4, 45.0, 21.5; IR (neat, cm^{-1}): 3018, 2921, 2854, 1677, 1634, 1581, 1449, 1324, 1222; HRMS (ESI): calculated for $C_{16}H_{15}NO_3SNa$ [M + Na]$^{+}$: 324.0665, found 324.0670.

2-(3-Methoxyphenyl)-N-(methyl(oxo)(phenyl)-λ⁶-sulfaneylidene)-2-oxoacetamide (4a):

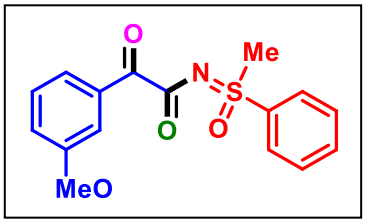

Yellow solid (85 mg, 67%), purified over a column of silica gel (25% ethyl acetate in hexane); ^{1}H NMR (500 MHz, $CDCl_3$): δ (ppm) 8.08 (d, 2H, J = 7.5 Hz), 7.73 (t, 1H, J = 7.5 Hz), 7.66–7.62 (m, 3H), 7.56 (s, 1H), 7.37 (t, 1H, J = 7.5 Hz), 7.15 (d, 1H, J = 8.5 Hz), 3.84 (s, 3H), 3.48 (s, 3H); ^{13}C{^{1}H} NMR (125 MHz, $CDCl_3$): δ (ppm) 190.2, 173.4, 160.0, 138.0, 134.6, 134.3, 130.1, 129.9, 127.4, 123.6, 121.6, 113.5, 55.7, 45.1; IR (neat, cm^{-1}): 3009, 2928, 2841, 1683, 1632, 1596, 1449, 1324, 1249; HRMS (ESI): calculated for $C_{16}H_{16}NO_4S$ [M + H]$^{+}$: 318.0795 found 318.0797.

2-(4-Fluorophenyl)-N-(methyl(oxo)(phenyl)-λ⁶-sulfaneylidene)-2-oxoacetamide (5a):

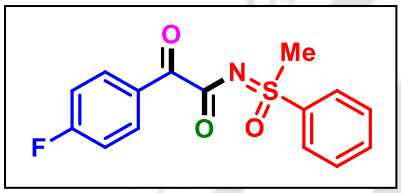

Light yellow solid (89 mg, 73%); purified over a column of silica gel (25% ethyl acetate in hexane); ^{1}H NMR (500 MHz, $CDCl_3$): δ (ppm) 8.08 (dd, 3H, J_1 = 9.0 Hz, J_2 = 6.0 Hz), 8.05 (s, 1H), 7.73 (t, 1H, J = 7.5 Hz), 7.64 (t, 2H, J = 7.5 Hz), 7.13 (t, 2H, J = 9.0 Hz), 3.47 (s, 3H); ^{13}C{^{1}H} NMR (125 MHz, $CDCl_3$): δ (ppm) 188.6, 173.1, 166.6 (d, J = 255.2 Hz), 137.7, 134.7, 133.2 (d, J = 9.5 Hz), 130.1, 129.4 (d, J = 3.0 Hz), 127.3, 116.1 (d, J = 21.9 Hz), 45.0; ^{19}F NMR ($CDCl_3$, 370 MHz): δ (ppm) –102.7; IR (neat, cm^{-1}): 3020, 2928, 1683, 1631, 1596, 1505, 1448, 1331, 1206; HRMS (ESI): calculated for $C_{15}H_{12}FNO_3SNa$ [M + Na]$^{+}$: 328.0414, found 328.0423.

2-(4-Chlorophenyl)-N-(methyl(oxo)(phenyl)-λ⁶-sulfaneylidene)-2-oxoacetamide (6a):

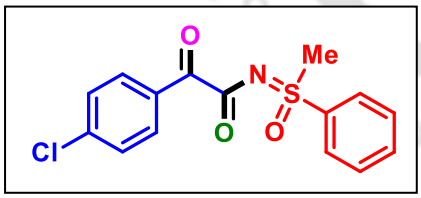

Pale yellow solid, (96 mg, 75% yield), purified over a column of silica gel (25% ethyl acetate in hexane); ^{1}H NMR (400 MHZ, $CDCl_3$): δ8.08–8.05 (m, 2H), 8.01–7.98 (m, 2H), 7.73 (t, 1H, J = 7.6 Hz), 7.65 (t, 2H, J = 8.0 Hz), 7.44 (d, 2H, J = 8.4 Hz), 3.48 (s, 3H); ^{13}C{^{1}H} NMR (100 MHZ, $CDCl_3$): δ188.9, 172.8, 141.0, 137.7, 134.7, 131.8, 131.4, 130.2, 129.2, 127.3, 45.0; IR (neat, cm^{-1}): 3016, 2925, 2851, 1681, 1630, 1586, 1447, 1329, 1205; HRMS (ESI): calculated for $C_{15}H_{12}ClNO_3SNa$ [M + Na]$^{+}$: 344.0119, found 344.0122.

2-(4-Bromophenyl)-N-(methyl(oxo)(phenyl)-λ⁶-sulfaneylidene)-2-oxoacetamide (7a):

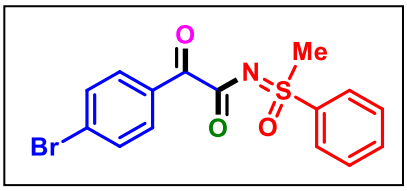

White solid (96 mg, 66%), purified over a column of silica gel (25% ethyl acetate in hexane); ^{1}H NMR (500 MHz, $CDCl_3$): δ (ppm) 8.07 (d, 2H, J = 8.0 Hz), 7.92 (d, 2H, J = 8.5 Hz), 7.73 (t, 1H, J = 7.5 Hz), 7.65 (t, 2H, J = 7.5 Hz), 7.61 (d, 2H, J = 8.5 Hz), 3.48 (s, 3H); ^{13}C{^{1}H} NMR (125 MHz, $CDCl_3$): 189.2, 172.8, 137.9, 134.7, 132.5, 132.3, 131.9, 130.2, 129.9, 127.4, 45.1; IR (neat, cm^{-1}): 3016, 2924, 2851, 1685, 1631, 1583, 1447, 1329, 1207; HRMS (ESI): calculated for $C_{15}H_{13}BrNO_3S$ [M + H]$^{+}$: 365.9794, found 365.9799.

2-(3-Fluorophenyl)-N-(methyl(oxo)(phenyl)-λ⁶-sulfaneylidene)-2-oxoacetamide (8a):

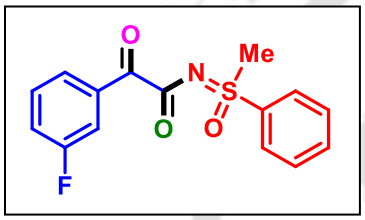

Yellow solid (87 mg, 71%), purified over a column of silica gel (25% ethyl acetate in hexane); ^{1}H NMR (500 MHz, $CDCl_3$): δ (ppm) 8.06 (d, 2H, J = 8.5 Hz), 7.84 (d, 1H, J = 7.5 Hz), 7.73 (t, 2H, J = 7.0 Hz), 7.65 (t, 2H, J = 7.5 Hz), 7.44 (dd, 1H, J_1 = 13.5 Hz, J_2 = 8.0 Hz), 7.29 (t, 1H, J = 8.5 Hz), 3.48 (s, 3H); ^{13}C{^{1}H} NMR (125 MHz, $CDCl_3$): δ188.9 (d, J = 2.3 Hz), 172.7, 162.8 (d, J = 247.0 Hz), 137.8, 135.1 (d, J = 6.5 Hz), 134.7, 130.6 (d, J = 7.5 Hz), 130.2, 127.4, 126.4 (d, J = 3.0 Hz), 121.5 (d, J = 21.5 Hz), 116.6 (d, J = 22.5 Hz), 45.0; ^{19}F NMR ($CDCl_3$, 471 MHz): δ (ppm) –111.5; IR (neat, cm^{-1}): 2955, 2926, 2872, 1687, 1632, 1587, 1447, 1329, 1235; HRMS (ESI): calculated for $C_{15}H_{12}FNO_3SNa$ [M + Na]$^{+}$: 328.0414, found 328.0424.

2-(3-Chlorophenyl)-N-(methyl(oxo)(phenyl)-λ⁶-sulfaneylidene)-2-oxoacetamide (9a):

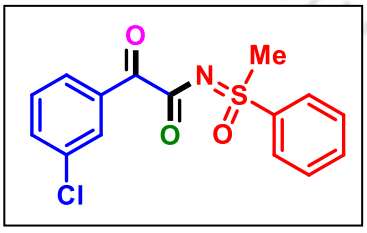

Yellow solid (86 mg, 67%), purified over a column of silica gel (25% ethyl acetate in hexane); ^{1}H NMR (500 MHz, $CDCl_3$): δ (ppm) 8.07 (d, 2H, J = 7.0 Hz), 8.02 (s, 1H), 7.94 (d, 1H, J = 8.0 Hz), 7.74 (t, 1H, J = 7.5 Hz), 7.66 (t, 2H, J = 7.5 Hz), 7.56 (d, 1H, J = 8.0 Hz), 7.41 (t, 1H, J = 8.0 Hz), 3.48 (s, 3H); ^{13}C{^{1}H} NMR (125 MHz, $CDCl_3$): δ 187.8, 171.6, 136.8, 134.2, 133.8, 133.6, 133.5, 133.3, 129.2, 129.1, 127.7, 126.4, 44.0; IR (neat, cm^{-1}): 2958, 2925, 2851, 1687, 1632, 1571, 1447, 1326, 1196; HRMS (ESI): calculated for $C_{15}H_{12}ClNO_3SNa$ [M + Na]$^{+}$: 344.0119, found: 344.0105.

2-(3-Bromophenyl)-N-(methyl(oxo)(phenyl)-λ⁶-sulfaneylidene)-2-oxoacetamide (10a):

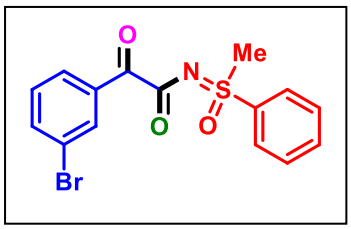

Yellow solid (92 mg, 63%), purified over a column of silica gel (25% ethyl acetate in hexane); purified over a column of silica gel (25% ethyl acetate in hexane); ^{1}H NMR (500 MHz, $CDCl_3$): δ (ppm) 8.17 (t, 1H, J = 2.0 Hz), 8.08–8.06 (m, 2H), 7.99–7.97 (m, 1H), 7.76–7.71 (m, 2H), 7.66 (t, 2H, J = 7.0 Hz), 7.35 (t, 1H, J = 7.5 Hz), 3.48 (s, 3H); ^{13}C{^{1}H} NMR (125 MHz, $CDCl_3$): δ (ppm) 188.7, 172.5, 137.8, 137.2, 134.9, 134.8, 133.1, 130.4, 130.2, 129.1, 127.4, 123.1, 45.1; IR (neat, cm^{-1}): 2955, 2921, 2849, 1688, 1635, 1563, 1456, 1328, 1198; HRMS (ESI): calculated for $C_{15}H_{13}BrNO_3S$ [M + H]$^{+}$: 365.9794, found: 365.9779.

N-(Methyl(oxo)(phenyl)-λ⁶-sulfaneylidene)-2-oxo-2-(4-(trifluoromethyl)phenyl) acetamide (11a):

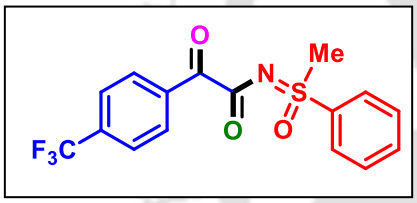

Yellow solid (87 mg, 61%), purified over a column of silica gel (30% ethyl acetate in hexane); ^{1}H NMR (500 MHz, $CDCl_3$): δ (ppm) 8.17 (d, 2H, J = 8.0 Hz), 8.07 (d, 2H, J = 7.0 Hz), 7.76–7.72 (m, 3H), 7.67 (d, 2H, J = 8.0 Hz), 3.49 (s, 3H); ^{13}C{^{1}H} NMR (125 MHz, $CDCl_3$): δ (ppm) 189.0, 172.4, 137.7, 135.9, 135.6, 135.3, 134.8, 130.8, 130.2, 127.4, 125.9 (q, J = 14.5 Hz), 45.1; ^{19}F NMR ($CDCl_3$, 471 MHz): δ (ppm) –63.3; IR (neat, cm^{-1}): 2953, 2925, 2854, 1693, 1637, 1581, 1449, 1325, 1210; HRMS (ESI): calculated for $C_{16}H_{13}F_3NO_3S$ [M + H]$^{+}$: 356.0563, found 356.0565.

N-(Methyl(oxo)(phenyl)-λ⁶-sulfaneylidene)-2-oxo-2-(3-(trifluoromethyl)phenyl) acetamide (12a):

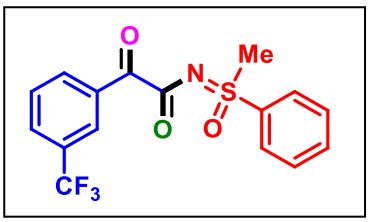

Yellow solid (78 mg, 55%), purified over a column of silica gel (30% ethyl acetate in hexane); ^{1}H NMR (500 MHz, $CDCl_3$): δ (ppm) 8.29 (s, 1H), 8.23 (d, 1H, J = 8.0 Hz), 8.06 (d, 2H, J = 7.5 Hz), 7.84 (d, 1H, J = 8.0 Hz), 7.73 (t, 1H, J = 7.5 Hz), 7.65 (t, 2H, J = 8.0 Hz), 7.61 (t, 1H, J = 7.5 Hz), 3.48 (s, 3H); ^{13}C{^{1}H} NMR (125 MHz, $CDCl_3$): δ (ppm) 188.6, 172.3, 137.7, 134.8, 133.8, 133.7, 131.5 (q, J = 131.5 Hz), 130.6 (q, J = 14.0 Hz), 130.2, 129.5, 127.3, 127.1 (q, J = 15.5 Hz), 122.7, 45.0; ^{19}F NMR

($CDCl_3$, 471 MHz): δ (ppm) –62.9; IR (neat, cm^{-1}): 3075, 3020, 2928, 1691, 1631, 1446, 1326, 1225; HRMS (ESI): calculated for $C_{16}H_{13}F_3NO_3S$ $[M + H]^+$: 356.0563, found 356.0565.

N-(Methyl(oxo)(phenyl)-λ⁶-sulfaneylidene)-2-(4-nitrophenyl)-2-oxoacetamide (13a):

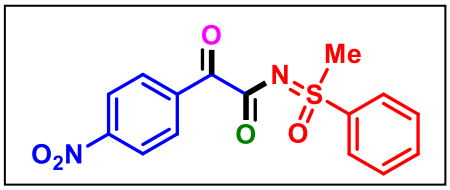

Yellow solid (76 mg, 57%), purified over a column of silica gel (30% ethyl acetate in hexane); ^1H NMR (500 MHz, $CDCl_3$): δ (ppm) 8.29 (d, 2H, J = 8.5 Hz), 8.22 (d, 2H, J = 8.5 Hz), 8.06 (d, 2H, J = 8.0 Hz), 7.75 (t, 1H, J = 7.0 Hz), 7.66 (t, 2H, J = 8.0 Hz), 3.50 (s, 3H); $^{13}C\{^1H\}$ NMR (125 MHz, $CDCl_3$): δ (ppm) 188.2, 171.8, 151.0, 137.8, 137.6, 134.9, 131.4, 130.2, 127.3, 123.9, 45.0; IR (neat, cm^{-1}): 3110, 3021, 2928, 1693, 1631, 1604, 1526, 1447, 1345, 1201; HRMS (ESI): calculated for $C_{15}H_{13}N_2O_5S$ $[M + H]^+$: 333.0540, found 333.0547.

N-(Methyl(oxo)(phenyl)-λ⁶-sulfaneylidene)-2-(3-nitrophenyl)-2-oxoacetamide (14a):

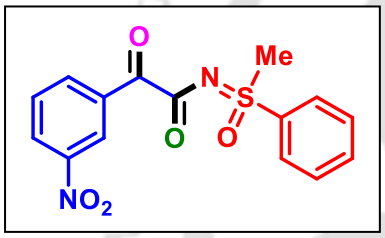

Yellow solid (84 mg, 63%), purified over a column of silica gel (30% ethyl acetate in hexane); ^1H NMR (500 MHz, $CDCl_3$): δ (ppm) 8.87 (s, 1H), 8.44 (d, 1H, J = 8.0 Hz), 8.40 (d, 1H, J = 7.5 Hz), 8.08 (d, 2H, J = 8.0 Hz), 7.76 (t, 1H, J = 7.5 Hz), 7.69 (d, 3H, J = 7.5 Hz), 3.51 (s, 3H); $^{13}C\{^1H\}$ NMR (125 MHz, $CDCl_3$): δ (ppm) 187.6, 171.6, 148.6, 137.6, 135.9, 134.9, 134.7, 130.3, 130.1, 128.4, 127.3, 125.2, 45.0; IR (neat, cm^{-1}): 3056, 2986, 2925, 1696, 1638, 1534, 1446, 1351, 1264; HRMS (ESI): calculated for $C_{15}H_{13}N_2O_5S$ $[M + H]^+$: 333.0540, found: 333.0536.

2-(3-Chloro-4-methoxyphenyl)-N-(methyl(oxo)(phenyl)-λ⁶-sulfaneylidene)-2-oxoacetamide (15a):

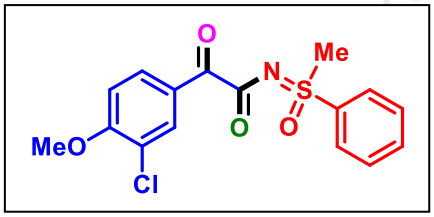

Yellow solid (90 mg, 64%), purified over a column of silica gel (28% ethyl acetate in hexane); ^1H NMR (400 MHz, $CDCl_3$): δ (ppm) 8.08 (dd, 3H, J_1 = 11.6 Hz, J_2 = 7.6 Hz), 7.99 (dd, 1H, J_1 = 8.8 Hz, J_2 = 2.0 Hz), 7.73 (t, 1H, J = 7.6 Hz), 7.65 (t, 2H, J = 7.6 Hz), 6.96 (d, 1H, J = 8.8 Hz), 3.97 (s, 3H), 3.47 (s, 3H); $^{13}C\{^1H\}$ NMR (100 MHz, $CDCl_3$): δ (ppm) 187.9, 173.0, 159.9, 137.9, 134.7, 132.3, 131.4, 130.2, 127.4, 126.7, 123.4, 111.6, 56.7, 45.1; IR (neat, cm^{-1}): 3014, 2926, 2849, 1676, 1631, 1590, 1500, 1445, 1308, 1191; HRMS (ESI): calculated for $C_{16}H_{14}ClNO_4SNa$ $[M + Na]^+$: 374.0224, found 374.0233.

N-(Methyl(oxo)(p-tolyl)- λ⁶-sulfaneylidene)-2-oxo-2-phenylacetamide (1b):

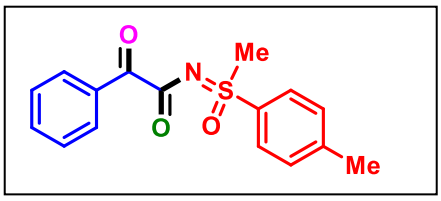

White solid (93 mg, 77%), purified over a column of silica gel (25% ethyl acetate in hexane); ^{1}H NMR (500 MHz, $CDCl_3$): δ (ppm) 8.05 (d, 2H, J = 7.5 Hz), 7.94 (d, 2H, J = 8.5 Hz), 7.59 (t, 1H, J = 7.0 Hz), 7.46 (t, 2H, J = 8.0 Hz), 7.43 (d, 2H, J = 8.5 Hz), 3.46 (s, 3H), 2.47 (s, 3H); ^{13}C{^{1}H} NMR (125 MHz, $CDCl_3$): δ (ppm) 190.4, 173.5, 145.9, 134.9, 134.3, 133.1, 130.7, 130.4, 128.8, 127.4, 45.2, 21.9; IR (neat, cm^{-1}): 2961, 2926, 2851, 1685, 1636, 1597, 1450, 1330, 1208; HRMS (ESI): calculated for $C_{16}H_{15}NO_3SNa$ $[M + Na]^+$: 324.0665, found 324.0662.

N-((4-Ethylphenyl)(methyl)(oxo)- λ⁶-sulfaneylidene)-2-oxo-2-phenylacetamide (1c):

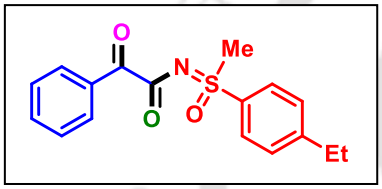

Yellow solid (94 mg, 75%), purified over a column of silica gel (25% ethyl acetate in hexane); ^{1}H NMR (500 MHz, $CDCl_3$): δ (ppm) 8.05 (d, 2H, J = 7.0 Hz), 7.97 (d, 2H, J = 8.5 Hz), 7.60 (t, 1H, J = 7.5 Hz), 7.48–7.44 (m, 4H), 3.47 (s, 3H), 2.77 (q, 2H, J = 7.5 Hz), 1.28 (t, 3H, J = 7.5 Hz); ^{13}C{^{1}H} NMR (125 MHz, $CDCl_3$): δ (ppm) 190.4, 173.5, 152.0, 134.9, 134.4, 133.0, 130.4, 129.6, 128.8, 127.5, 45.2, 29.1, 15.2; IR (neat, cm^{-1}): 3024, 2966, 1682, 1630, 1595, 1451, 1330, 1206; HRMS (ESI): calculated for $C_{17}H_{17}NO_3SNa$ $[M + Na]^+$: 338.0821, found 338.0824.

N-((4-Methoxyphenyl)(methyl)(oxo)-λ⁶-sulfaneylidene)-2-oxo-2-phenylacetamide (1d):

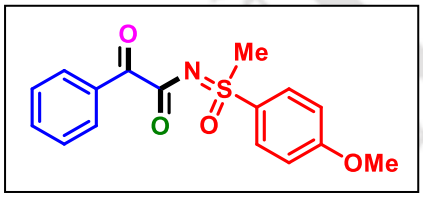

Yellow solid (85 mg, 67%), purified over a column of silica gel (25% ethyl acetate in hexane); ^{1}H NMR (500 MHz, $CDCl_3$): δ (ppm) 8.05 (d, 2H, J = 7.5 Hz), 7.99 (d, 2H, J = 9.0 Hz), 7.59 (t, 1H, J = 7.0 Hz), 7.46 (t, 2H, J = 7.5 Hz), 7.08 (d, 2H, J = 9.0 Hz), 3.90 (s, 3H), 3.46 (s, 3H); ^{13}C{^{1}H} NMR (125 MHz, $CDCl_3$): δ (ppm) 190.5, 173.5, 164.6, 134.4, 133.1, 130.4, 129.7, 129.0, 128.8, 115.4, 56.1, 45.5; IR (neat, cm^{-1}): 3014, 2927, 2846, 1682, 1631, 1592, 1496, 1449, 1310, 1207; HRMS (ESI): calculated for $C_{16}H_{15}NO_4SNa$ $[M + Na]^+$: 340.0614, found 340.0613.

N-((3-Methoxyphenyl)(methyl)(oxo)- λ⁶-sulfaneylidene)-2-oxo-2-phenylacetamide (1e):

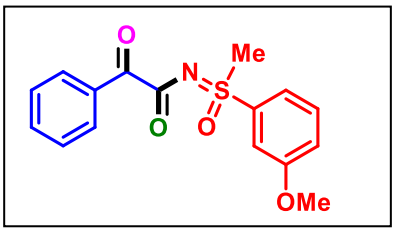

Yellow solid (81 mg, 64%), purified over a column of silica gel (25% ethyl acetate in hexane); ^{1}H NMR (400 MHz, $CDCl_3$): δ (ppm) 8.05 (d, 2H, J = 7.6 Hz), 7.64–7.58 (m, 2H), 7.56 (t, 1H, J = 3.2 Hz), 7.52 (d, 1H, J = 7.6 Hz), 7.47 (t, 2H, J = 7.6 Hz), 7.22 (dd, 1H, J_1 = 8.4 Hz, J_2 = 2.4 Hz), 3.89 (s, 3H), 3.46 (s, 3H); ^{13}C{^{1}H} NMR (100 MHz, $CDCl_3$): δ (ppm) 190.4, 173.5, 160.8, 139.1, 134.4, 133.0, 131.2, 130.4, 128.9, 121.2, 119.4, 111.9, 56.1, 45.1; IR (neat, cm^{-1}): 3015, 2927, 2839, 1682, 1631, 1596, 1482, 1429, 1206; HRMS (ESI): calculated for $C_{16}H_{15}NO_4SK$ [M + K]$^{+}$: 356.0353, found 356.0352.

N-((4-Fluorophenyl)(methyl)(oxo)- λ⁶-sulfaneylidene)-2-oxo-2-phenylacetamide (1f):

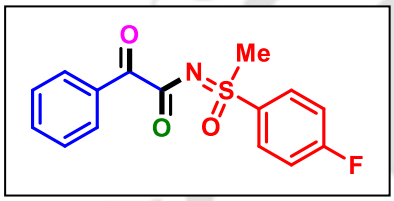

Light yellow solid (99 mg, 81%), purified over a column of silica gel (25% ethyl acetate in hexane); ^{1}H NMR (400 MHz, $CDCl_3$): δ (ppm) 8.10 (dd, 2H, J_1 = 8.8 Hz, J_2 = 4.8 Hz), 8.05 (d, 2H, J = 7.2 Hz), 7.61 (t, 1H, J = 7.6 Hz), 7.48 (t, 2H, J = 7.6 Hz), 7.33 (t, 2H, J = 9.2 Hz), 3.49 (s, 3H); ^{13}C{^{1}H} NMR (125 MHz, $CDCl_3$): δ (ppm) 190.2, 173.4, 166.5 (d, J = 256.8 Hz), 134.5, 133.92, 133.90, 133.0, 130.5, 130.4, 128.9, 117.5 (d, J = 23.0 Hz), 45.3; ^{19}F NMR ($CDCl_3$, 370 MHz): δ (ppm) –101.9; IR (neat, cm^{-1}): 3057, 2955, 2924, 2854, 1683, 1636, 1592, 1493, 1375, 1263; HRMS (ESI): calculated for $C_{15}H_{12}FNO_3SNa$ [M + Na]$^{+}$: 328.0414; found 328.0421.

N-((4-Chlorophenyl)(methyl)(oxo)-λ⁶-sulfaneylidene)-2-oxo-2-phenylacetamide (1g):

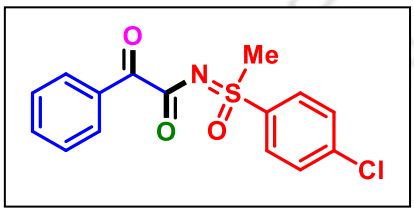

White solid (87 mg, 68%), purified over a column of silica gel (25% ethyl acetate in hexane); ^{1}H NMR (400 MHz, $CDCl_3$): δ (ppm) 8.05–8.01 (m, 4H), 7.63–7.59 (m, 3H), 7.48 (t, 2H, J = 8.0 Hz), 3.47 (s, 3H); ^{13}C{^{1}H} NMR (100 MHz, $CDCl_3$): δ (ppm) 190.2, 173.4, 141.7, 136.4, 134.5, 132.8, 130.5, 130.4, 128.93, 128.91, 45.1; IR (neat, cm^{-1}): 3055, 2960, 2921, 2860, 1680, 1635, 1590, 1495, 1372, 1260; HRMS (ESI): calculated for $C_{15}H_{16}ClN_2O_3S$ [M + NH_4]$^{+}$: 959.9858, found: 359.9648.

N-((3-Fluorophenyl)(methyl)(oxo)-λ⁶-sulfaneylidene)-2-oxo-2-phenylacetamide (1h):

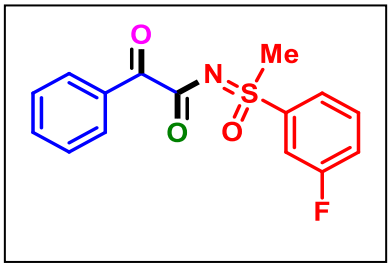

Light yellow solid (95 mg, 78%), purified over a column of silica gel (25% ethyl acetate in hexane); ^{1}H NMR (500 MHz, $CDCl_3$): δ (ppm) 8.04 (d, 2H, J = 7.0 Hz), 7.87 (d, 1H, J = 8.0 Hz), 7.80 (d, 1H, J = 8.0 Hz), 7.65 (t, 1H, J = 5.5 Hz), 7.60 (t, 1H, J = 7.0 Hz), 7.47 (t, 2H, J = 7.5 Hz), 7.42 (t, 1H, J = 8.0 Hz), 3.48 (s, 3H); ^{13}C{^{1}H} NMR (125 MHz, $CDCl_3$): δ (ppm) 190.1, 173.3, 162.9 (d, J = 252.8 Hz), 140.1 (d, J = 6.9 Hz), 134.5, 132.9, 132.0 (d, J = 7.8 Hz), 130.4, 128.9, 123.2, (d, J = 3.1 Hz), 122.0 (d, J = 21.4 Hz), 115.1 (d, J = 25.0 Hz), 45.0; ^{19}F NMR ($CDCl_3$, 471 MHz): δ (ppm) –107.5; IR (neat, cm^{-1}): 3070, 3021, 2927, 1682, 1633, 1594, 1478, 1331, 1206; HRMS (ESI): calculated for $C_{15}H_{12}FNO_3SNa$ $[M + Na]^+$: 328.0414, found 328.0424.

N-((3-Chlorophenyl)(methyl)(oxo)-λ⁶-sulfaneylidene)-2-oxo-2-phenylacetamide (1i):

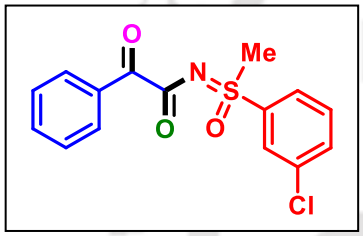

Light yellow solid (91 mg, 71%), purified over a column of silica gel (25% ethyl acetate in hexane); ^{1}H NMR (500 MHz, $CDCl_3$): δ (ppm) 8.05 (t, 3H, J = 7.0 Hz), 7.96 (d, 1H, J = 8.0 Hz), 7.69 (d, 1H, J = 8.0 Hz), 7.60 (q, 2H, J = 8.0 Hz), 7.48 (t, 2H, J = 7.5 Hz), 3.48 (s, 3H); ^{13}C{^{1}H} NMR (125 MHz, $CDCl_3$): δ (ppm) 190.0, 173.3, 139.8, 136.5, 134.9, 134.5, 132.9, 131.4, 130.4, 128.9, 127.6, 125.5, 45.0; IR (neat, cm^{-1}): 3055, 2928, 2851, 1686, 1639, 1576, 1374, 1264, 1240, 1207; HRMS (ESI): calculated for $C_{15}H_{12}ClNO_3SNa$ $[M + Na]^+$: 344.0119, found 344.0122.

N-((2-Bromophenyl)(methyl)(oxo)-λ⁶-sulfaneylidene)-2-oxo-2-phenylacetamide (1j):

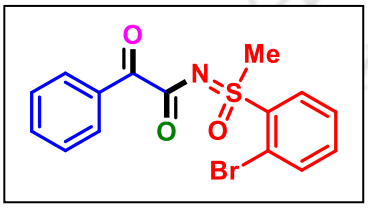

Light yellow solid (114 mg, 78%), purified over a column of silica gel (25% ethyl acetate in hexane); ^{1}H NMR (600 MHz, $CDCl_3$): δ (ppm) 8.36 (d, 1H, J = 7.8 Hz), 8.04 (d, 2H, J = 6.6 Hz), 7.82 (d, 1H, J = 7.8 Hz), 7.63 (t, 1H, J = 7.8 Hz), 7.59 (t, 1H, J = 7.2 Hz), 7.55 (t, 1H, J = 7.8 Hz), 7.45 (t, 2H, J = 7.8 Hz), 3.64 (s, 3H); ^{13}C{^{1}H} NMR (150 MHz, $CDCl_3$): δ (ppm) 189.8, 172.4, 137.1, 136.2, 135.5, 134.4, 133.0, 132.1, 130.4, 128.9, 128.8, 119.7, 42.6; IR (neat, cm^{-1}): 3011, 2927, 2854, 1682, 1632, 1596, 1449, 1329, 1206; HRMS (ESI): calculated for $C_{15}H_{12}BrNO_3SNa$ $[M + Na]^+$: 387.9613, found 387.9623.

N-(Methyl(oxo)(4-(trifluoromethyl)phenyl)-λ⁶-sulfaneylidene)-2-oxo-2-phenylacetamide (1k):

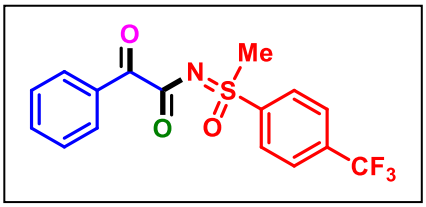

Light yellow solid (87 mg, 61%), purified over a column of silica gel (28% ethyl acetate in hexane); ^{1}H NMR (500 MHz, $CDCl_3$): δ (ppm) 8.22 (d, 2H, J = 8.5 Hz), 8.04 (d, 2H, J = 7.0 Hz), 7.92 (d, 2H, J = 8.5 Hz), 7.61 (t, 1H, J = 7.0 Hz), 7.48 (t, 2H, J = 7.5 Hz), 3.49 (s, 3H); ^{13}C{^{1}H} NMR (125 MHz, $CDCl_3$): δ (ppm) 190.0, 173.3, 141.7, 136.5, 136.3, 134.6, 132.8, 130.4, 128.9, 128.2, 127.3 (q, J = 14.5 Hz), 44.9; ^{19}F NMR ($CDCl_3$, 471 MHz): δ (ppm) –63.3; IR (neat, cm^{-1}): 3019, 2926, 2855, 1684, 1636, 1576, 1402, 1321, 1206; HRMS (ESI): calculated for $C_{16}H_{13}F_3NO_3S$ $[M + H]^+$: 356.0563, found 356.0567.

N-(Ethyl(oxo)(phenyl)-λ⁶-sulfaneylidene)-2-oxo-2-phenylacetamide (1l):

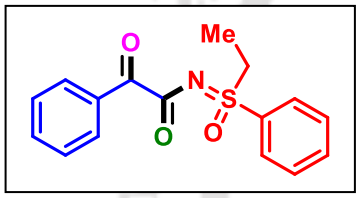

Light yellow solid (71 mg, 59%), purified over a column of silica gel (25% ethyl acetate in hexane); ^{1}H NMR (500 MHz, $CDCl_3$): δ (ppm) 8.04 (t, 3H, J = 8.5 Hz), 7.73 (t, 1H, J = 7.0 Hz), 7.64 (t, 2H, J = 7.5 Hz), 7.59 (t, 1H, J = 7.0 Hz), 7.54–7.41 (m, 3H), 3.66–3.54 (m, 2H), 1.33 (t, 3H, J = 7.5 Hz); ^{13}C{^{1}H} NMR (125 MHz, $CDCl_3$): δ (ppm) 190.5, 173.6, 135.6, 134.6, 134.4, 133.1, 130.4, 130.0, 128.8, 128.2, 51.5, 7.2; IR (neat, cm^{-1}): 3062, 2924, 2853, 1686, 1636, 1596, 1461, 1309, 1206; HRMS (ESI): calculated for $C_{16}H_{15}NO_3SNa$ $[M + Na]^+$: 324.0665, found 324.0666.

2-Oxo-N-(oxo(phenyl)(propyl)-λ⁶-sulfaneylidene)-2-phenylacetamide (1m):

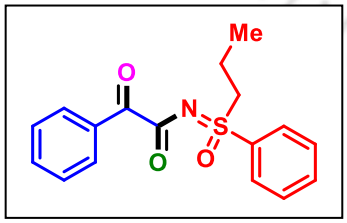

Light yellow solid (72 mg, 57%), purified over a column of silica gel (25% ethyl acetate in hexane); ^{1}H NMR (500 MHz, $CDCl_3$): δ (ppm) 8.04 (t, 3H, J = 8.5 Hz), 7.72 (t, 1H, J = 7.5 Hz), 7.64 (t, 2H, J = 7.5 Hz), 7.60–7.50 (m, 2H), 7.46 (t, 2H, J = 7.5 Hz), 3.62–3.44 (m, 2H), 1.87–1.79 (m, 2H), 1.00 (t, 3H, J = 7.5 Hz); ^{13}C{^{1}H} NMR (125 MHz, $CDCl_3$): δ (ppm) 190.5, 173.5, 136.3, 134.5, 134.3, 133.1, 130.4, 130.0, 128.8, 128.1, 58.4, 16.3, 12.9; IR (neat, cm^{-1}): 3065, 2921, 2854, 1685, 1634, 1449, 1327, 1276, 1207; HRMS (ESI): calculated for $C_{17}H_{17}NO_3SNa$ $[M + Na]^+$: 338.0821, found 338.0825.

2-Oxo-N-(oxo(phenyl)(pyridin-2-yl)-λ⁶-sulfaneylidene)-2-phenylacetamide (1n):

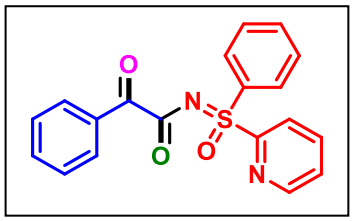

Light yellow solid (63 mg, 45%), purified over a column of silica gel (35% ethyl acetate in hexane); ^{1}H NMR (500 MHz, $CDCl_3$): δ (ppm) 8.69 (d, 1H, J = 5.5 Hz), 8.45 (d, 1H, J = 10.0 Hz), 8.19 (d, 2H, J = 11.5 Hz), 8.08 (d, 2H, J = 10.5 Hz), 8.02–7.98 (m, 1H), 7.66 (t, 1H, J = 9.0 Hz), 7.59–7.55 (m, 3H), 7.51–7.45 (m, 3H); ^{13}C{^{1}H} NMR (125 MHz, $CDCl_3$): δ (ppm) 190.1, 173.6, 157.4, 150.8, 138.7, 135.9, 134.6, 134.3, 133.2, 130.5, 129.6, 129.2, 128.8, 127.4, 123.9; IR (neat, cm^{-1}): 2955, 2918, 2869, 1690, 1642, 1578, 1459, 1377, 1190; HRMS (ESI): calculated for $C_{19}H_{14}N_2O_3SNa$ $[M + Na]^+$: 373.0617, found 373.0621.

***(Iodoimino)(methyl)(phenyl)-λ⁶-sulfanone* (A):**

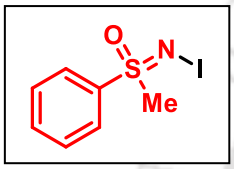

White solid (233 mg, 83%) ^{1}H NMR (400 MHz, $CDCl_3$): δ (ppm) 7.86–7.84 (m, 2H), 7.70–7.65 (m, 1H), 7.62–7.58 (m, 2H), 3.32 (s, 3H); ^{13}C{^{1}H} NMR (125 MHz, $CDCl_3$): δ (ppm) 140.1, 133.9, 129.8, 128.5, 42.9; IR (neat, cm^{-1}): 3020, 2917, 1445, 1405, 1312, 1199, 1088.

(E)-Methyl(phenyl)(styrylimino)-λ⁶-sulfanone (D):

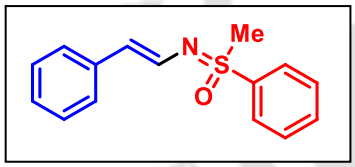

Brown gummy solid (182 mg, 71%), purified over a column of silica gel (20% ethyl acetate in hexane); ^{1}H NMR (500 MHz, $CDCl_3$): δ (ppm) 7.96 (d, 2H, J = 7.5 Hz), 7.64 (d, 1H, J = 7.0 Hz), 7.59 (t, 2H, J = 7.0 Hz), 7.18 (d, 4H, J = 4.5 Hz), 7.08–7.05 (m, 1H), 6.91 (d, 1H, J = 13.5 Hz), 6.20 (d, 1H, J = 13.5 Hz), 3.22 (s, 3H); ^{13}C{^{1}H} NMR (125 MHz, $CDCl_3$): δ (ppm) 139.5, 138.1, 133.7, 130.0, 129.9, 128.8, 128.6, 125.7, 125.2, 118.4, 45.5; IR (neat, cm^{-1}): 3274, 3061, 2925, 2854, 1685, 1639, 1446, 1221; HRMS (ESI) calculated for $C_{15}H_{15}NOS$ $[M + H]^+$: 258.0947, found 258.0953.

II.6. Representative NMR Spectra:

N-[Methyl(oxo)(phenyl)-λ⁶-sulfaneylidene]-2-oxo-2-phenylacetamide (1a): **^{1}H NMR (500 MHz, $CDCl_3$)**

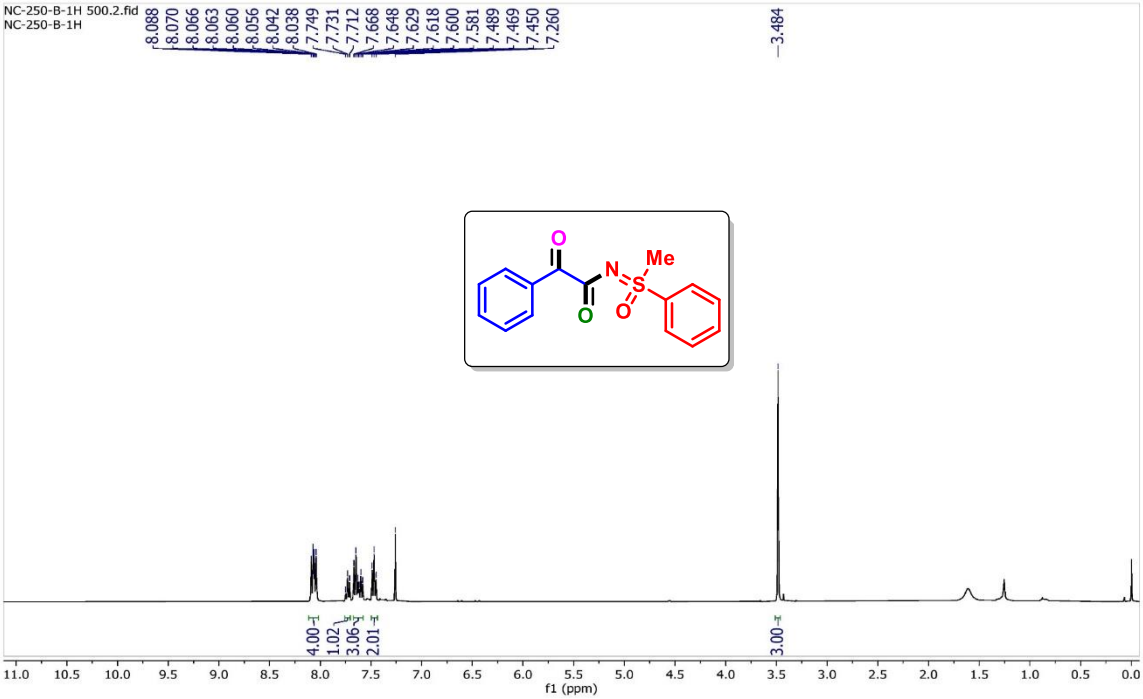

N-[Methyl(oxo)(phenyl)-λ⁶-sulfaneylidene]-2-oxo-2-phenylacetamide (1a): **^{13}C NMR (125 MHz, $CDCl_3$)**

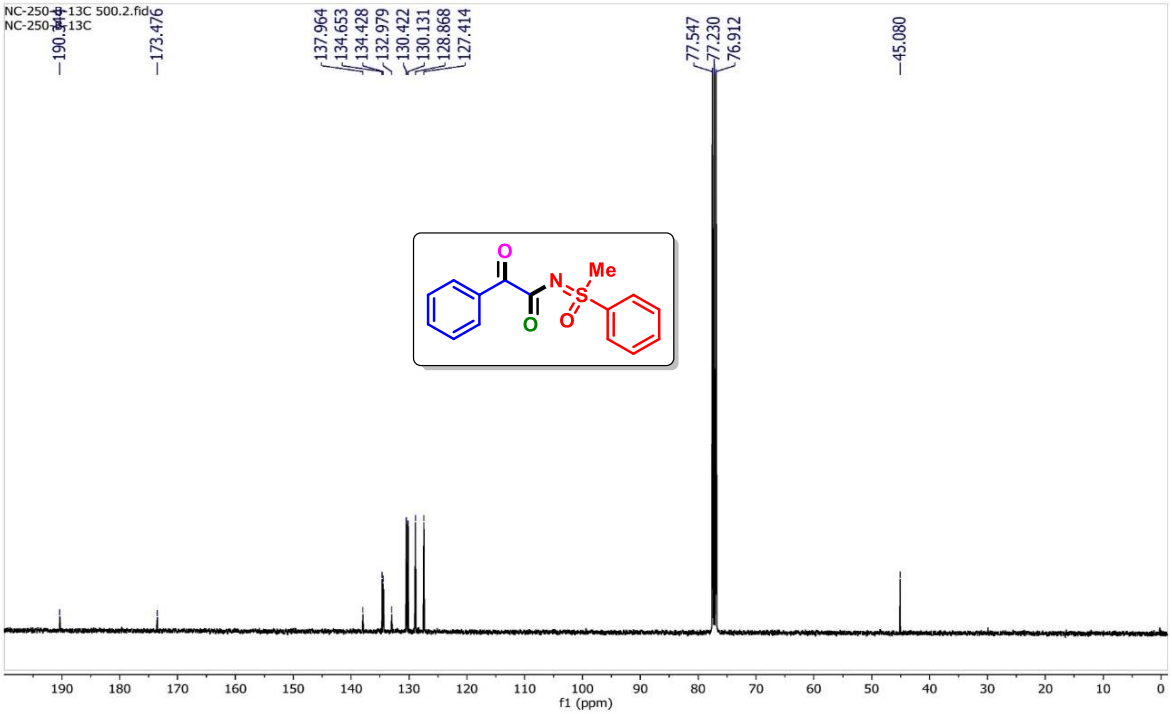

***N-[Methyl(oxo)(phenyl)-λ⁶-sulfaneylidene]-2-oxo-2-(p-tolyl)acetamide (2a):* ^{1}H NMR (400 MHz, $CDCl_3$)**

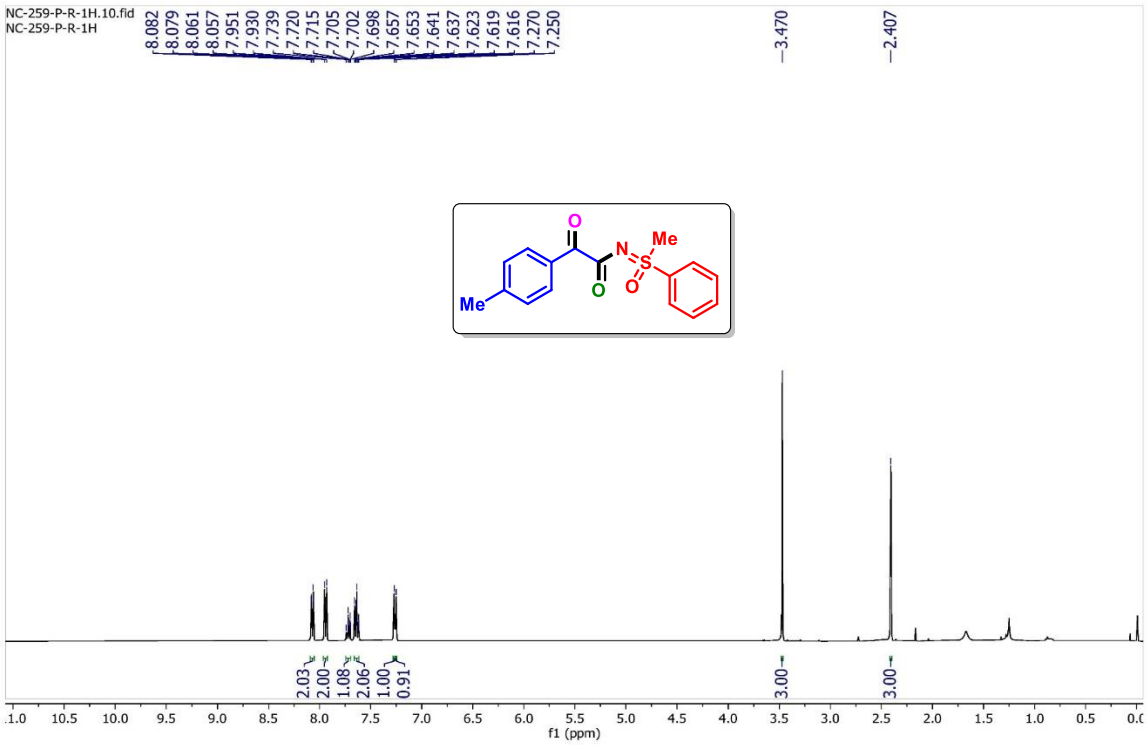

***N-[Methyl(oxo)(phenyl)-λ⁶-sulfaneylidene]-2-oxo-2-(p-tolyl)acetamide (2a):* ^{13}C NMR (100 MHz, $CDCl_3$)**

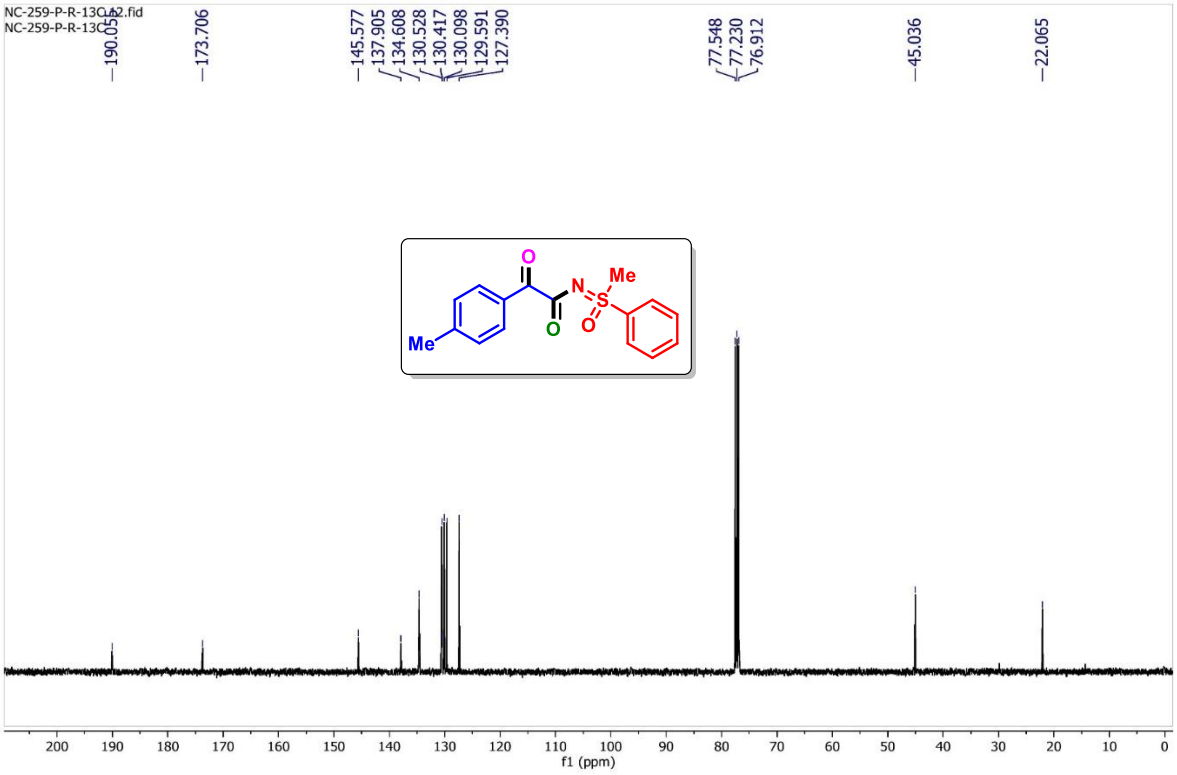

N-(Methyl(oxo)(phenyl)-λ⁶-sulfaneylidene)-2-(4-nitrophenyl)-2-oxoacetamide (13a): **^{1}H NMR (500 MHz, $CDCl_3$)**

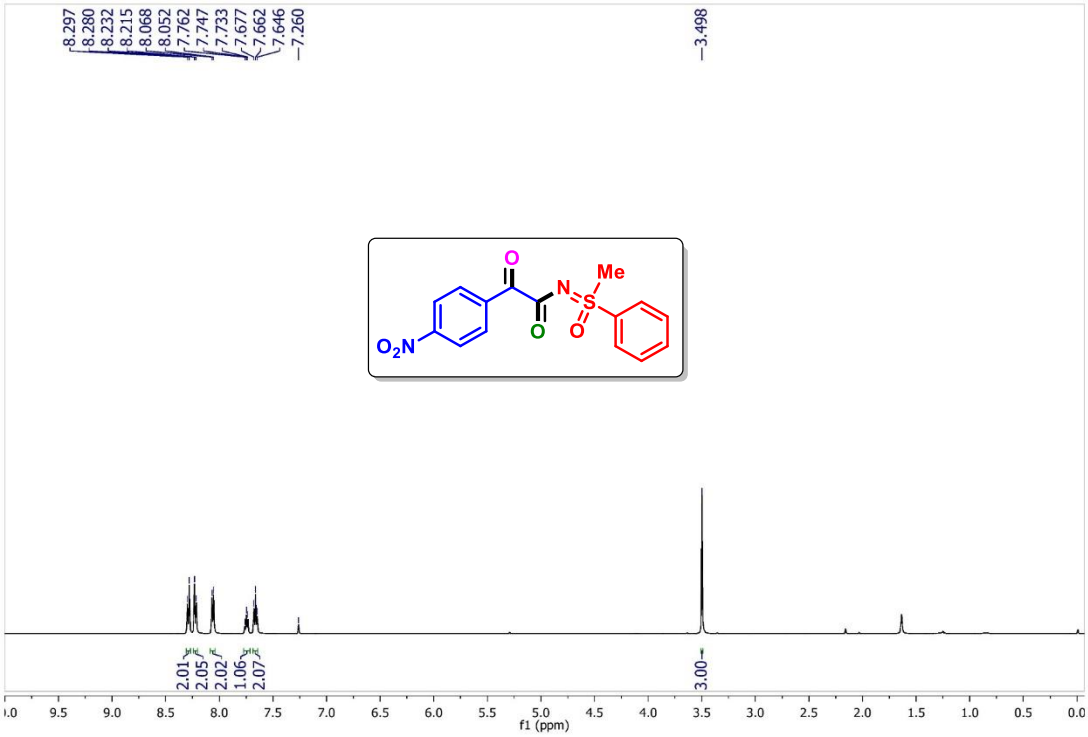

N-(Methyl(oxo)(phenyl)-λ⁶-sulfaneylidene)-2-(4-nitrophenyl)-2-oxoacetamide (13a): **^{13}C NMR (125 MHz, $CDCl_3$)**

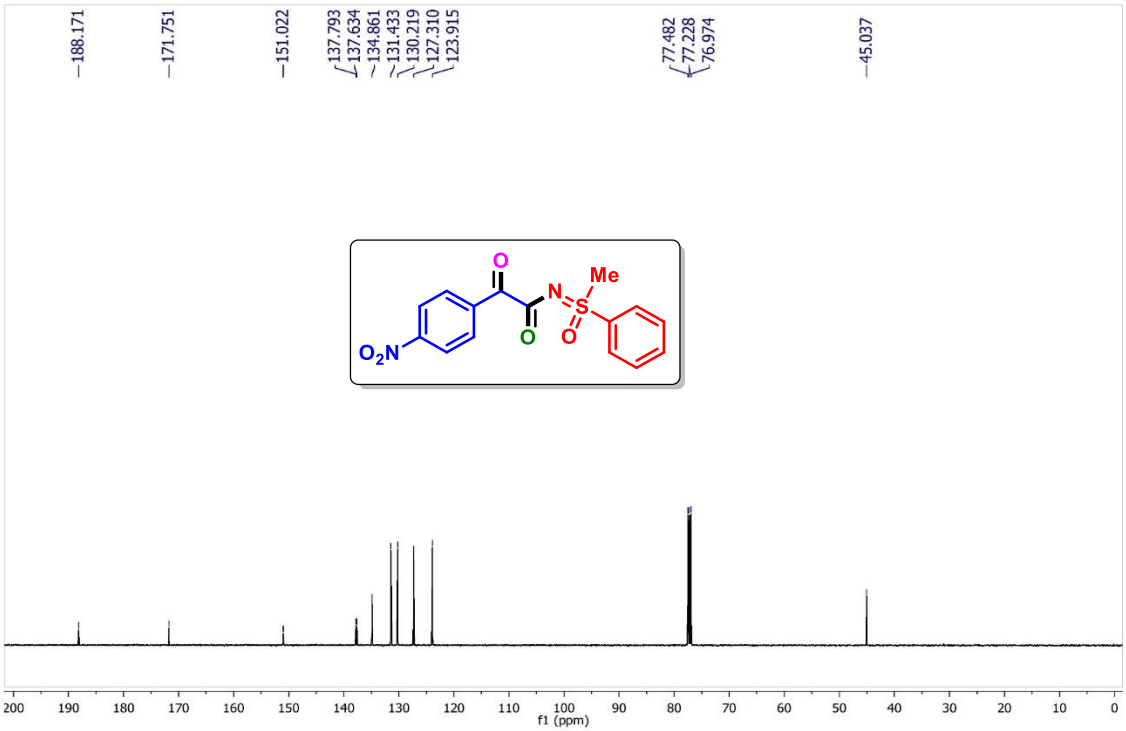

N-((4-Methoxyphenyl)(methyl)(oxo)-λ⁶-sulfaneylidene)-2-oxo-2-phenylacetamide (1d): **^{1}H NMR (500 MHz, $CDCl_3$)**

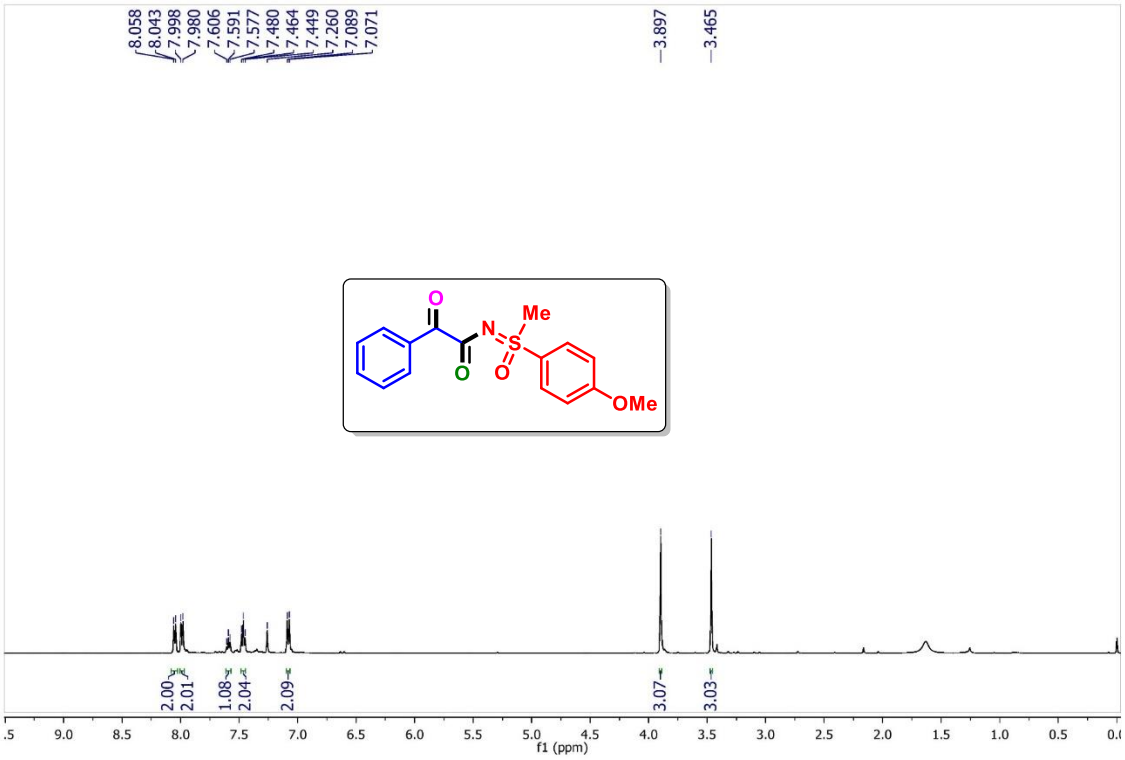

N-((4-Methoxyphenyl)(methyl)(oxo)-λ⁶-sulfaneylidene)-2-oxo-2-phenylacetamide (1d): **^{13}C NMR (125 MHz, $CDCl_3$)**

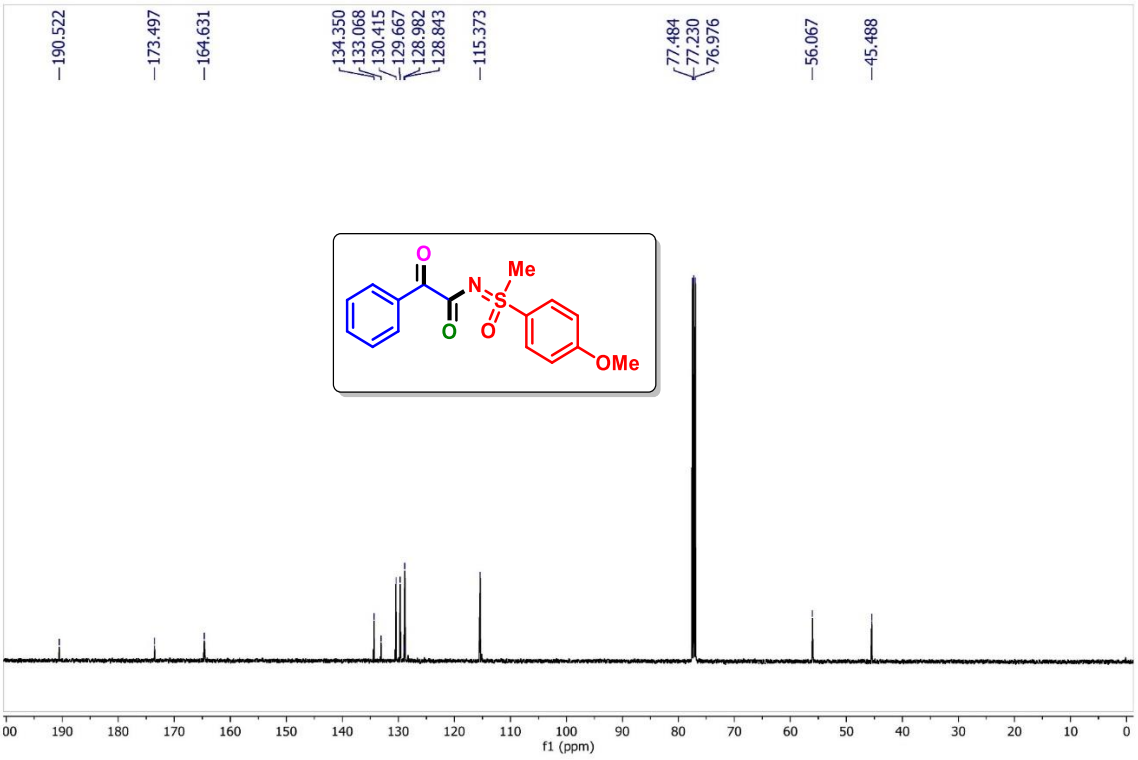

N-((3-Chlorophenyl)(methyl)(oxo)-λ⁶-sulfaneylidene)-2-oxo-2-phenylacetamide (1i): **^{1}H NMR (500 MHz, $CDCl_3$)**

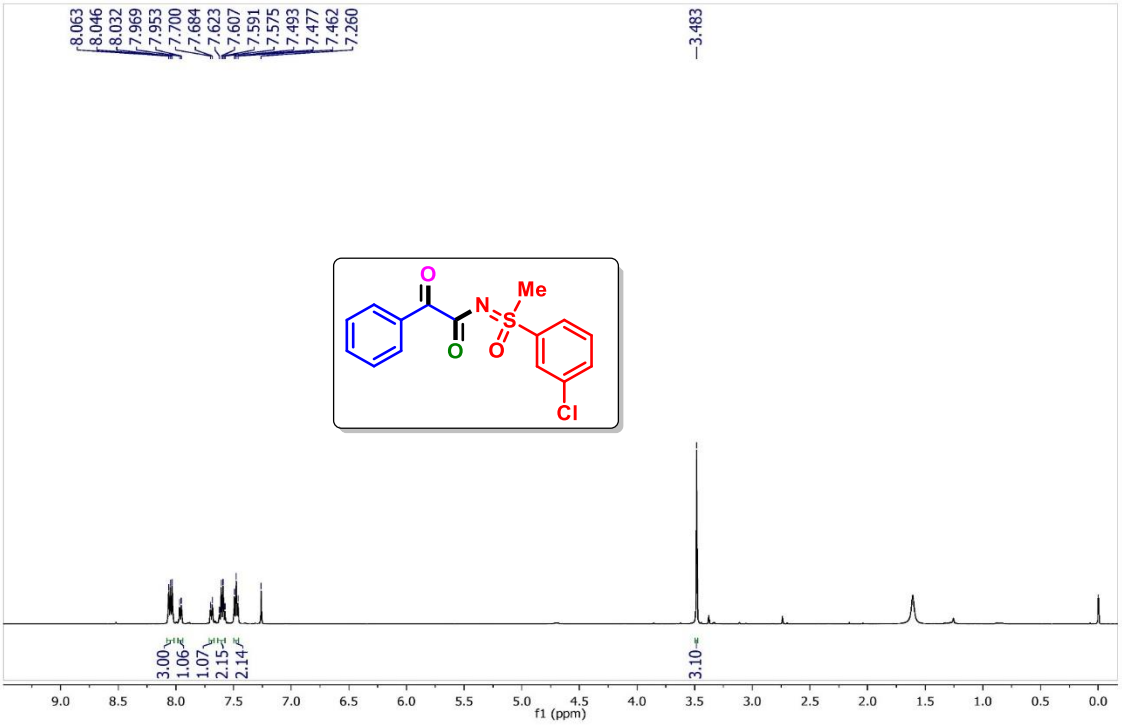

N-((3-Chlorophenyl)(methyl)(oxo)-λ⁶-sulfaneylidene)-2-oxo-2-phenylacetamide (1i): **^{13}C NMR (125 MHz, $CDCl_3$)**

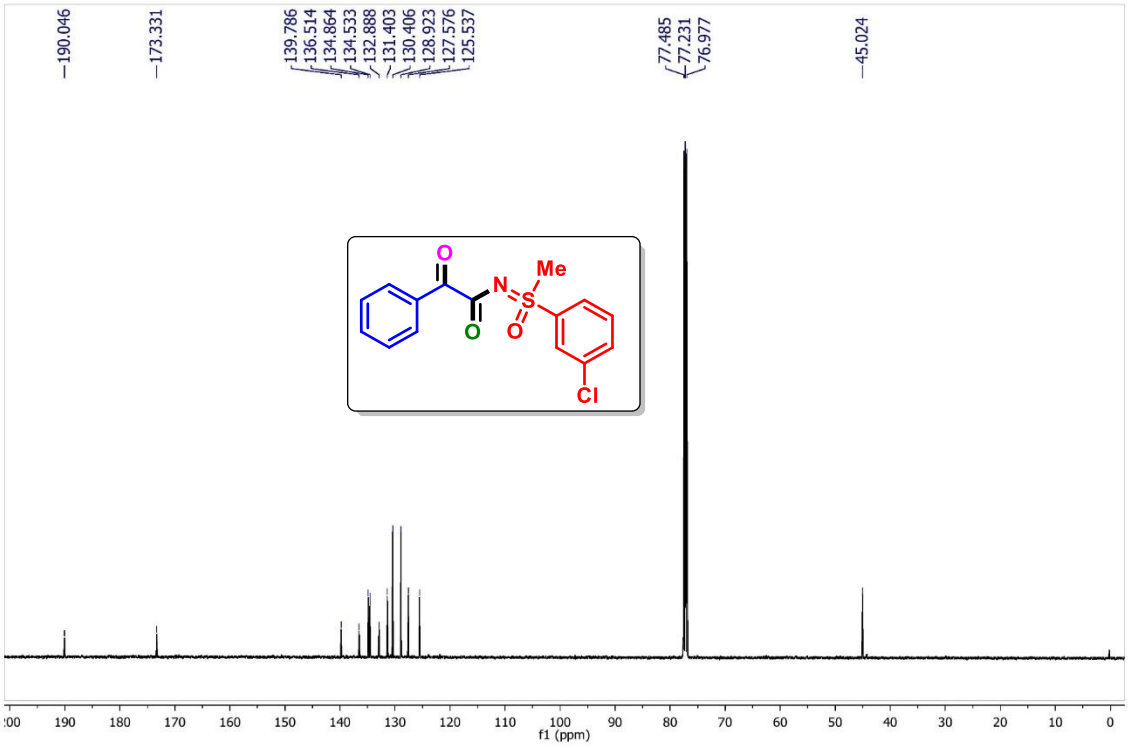

II.7. References:

(1) (a) T. Patra and D. Maiti, *Chem. Eur. J*., 2017, **23**, 7382–7401; (b) T. Zhang, N.-X. Wang and Y. Xing, *J. Org. Chem.*, 2018, **83**, 7559–7565; (c) Z. Zeng, A. Feceu, N. Sivendran and L. J. Gooßen, *Adv. Synth. Catal.*, 2021, **363**, 2678–2722; (d) J. Schwarz and B. König, *Green Chem.*, 2018, **20**, 323–361; (e) S. Arshadi, S. Ebrahimiasl, A. Hosseinian, A. Monfared and E. Vessally, *RSC Adv.*, 2019, **9**, 8964–8976; (f) N. Rodríguez and L. J. Goossen, *Chem. Soc. Rev*., 2011, **40**, 5030–5048; (g) P. Liu, G. Zhang and P. Sun, *Org. Biomol. Chem*., 2016, **14**, 10763–10777.

(2) J. Xuan, Z.-G. Zhang and W.-J. Xiao, *Angew. Chem. Int. Ed*., 2015, **54**, 15632–15641.

(3) (a) J. D. Bell and J. A. Murphy, *Chem. Soc. Rev*., 2021, **50**, 9540–9685; (b) W.-M. Cheng and R. Shang, *ACS Catal*., 2020, **10**, 9170–9196; (c) Y. Lang, C.-J. Li and H. Zeng, *Org. Chem. Front*., 2021, **8**, 3594–3613; (d) J.-R. Chen, X.-Q. Hu, L.-Q. Lu and W.-J. Xiao, *Chem. Soc. Rev*., 2016, **45**, 2044–2056.

(4) (a) L. Candish, M. Teders and F. Glorius, *J. Am. Chem. Soc*., 2017, **139**, 7440–7443; (b) J. Yang, M. Song, H. Zhou, Y. Qi, B. Ma and X.-C. Wang, *Green Chem*., 2021, **23**, 5806–5811; (c) Y. Zhang, J. Qian, M. Wang, Y. Huang and P. Hu, *Org. Lett*., 2022, **24**, 5972–5976; (d) V. D. Nguyen, G. C. Haug, S. G. Greco, R. Trevino, G. B. Karki, H. D. Arman and O. V. Larionov, *Angew. Chem. Int. Ed*., 2022, **61**, e202210525; (e) S. Rajput, R. Kaur and N. Jain, *Org. Biomol. Chem*., 2022, **20**, 1453–1461.

(5) (a) V. T. Nguyen, V. D. Nguyen, G. C. Haug, N. T. H. Vuong, H. T. Dang, H. D. Arman and O. V. Larionov, *Angew. Chem. Int. Ed*., 2020, **59**, 7921–7927; (b) G. Feng, X. Wang and J. Jin, *Eur. J. Org. Chem*., 2019, **2019**, 6728–6732.

(6) J. Liu, Q. Liu, H. Yi, C. Qin, R. Bai, X. Qi, Y. Lan and A. Lei, *Angew. Chem. Int. Ed*., 2014, **53**, 502–506.

(7) Q. Y. Li, S. N. Gockel, G. A. Lutovsky, K. S. DeGlopper, N. J. Baldwin, M. W. Bundesmann, J. W. Tucker, S. W. Bagley and T. P. Yoon, *Nat. Chem*., 2022, **14**, 94–99.

(8) P. Xu, W. Su and T. Ritter, *Chem. Sci*., 2022, **13**, 13611–13616.

(9) (a) A. J. Borah and G. Yan, *Org. Biomol. Chem*., 2015, **13**, 8094–8115; (b) S. Chand, A. K. Sharma, A. K. Pandey and K. N. Singh, *Org. Lett*., 2022, **24**, 6423–6427; (c) L. Liu, D. Zhou, J. Dong, Y. Zhou, S.-F. Yin and L.-B. Han, *J. Org. Chem*., 2018, **83**, 4190–4196; (d) S. Peng, N. Chen, H. Zhang, M. He, H. Li, M. Lang and J. Wang, *Org. Lett*., 2020, **22**, 5589–5593; (e) D. Zhang, Z.-L. Tang, X.-H. Ouyang, R.-J. Song and J.-H. Li, *Chem.*

Commun., 2020, **56**, 14055–14058; (f) G. Li, T. Wang, F. Fei, Y.-M. Su, Y. Li, Q. Lan and X.-S. Wang, *Angew. Chem. Int. Ed*., 2016, **55**, 3491–3495; (g) H. Li, S. H. H. Younes, S. Chen, P. Duan, C. Cui, R. Wever, W. Zhang and F. Hollmann, *ACS Catal.*, 2022, **12**, 4554–4559.

(10) X.-J. Wei, W. Boon, V. Hessel and T. Noël, *ACS Catal*., 2017, **7**, 7136–7140.

(11) H.-F. Qian, C.-K. Li, Z.-H. Zhou, Z.-K. Tao, A. Shoberu and J.-P. Zou, *Org. Lett*., 2018, **20**, 5947–5951.

(12) S. Cai, Y. Xu, D. Chen, L. Li, Q. Chen, M. Huang and W. Weng, *Org. Lett*., 2016, **18**, 2990–2993.

(13) S. Chand, A. K. Pandey, R. Singh and K. N. Singh, *J. Org. Chem.*, 2021, **86**, 6486–6493.

(14) (a) Y. Tu, P. Shi and C. Bolm, *Org. Lett*., 2022, **24**, 907–911; (b) Y. Tu, D. Zhang, P. Shi, C. Wang, D. Ma and C. Bolm, *Org. Biomol. Chem*., 2021, **19**, 8096–8101.

(15)(a) S. Baranwal, S. Gupta and J. Kandasamy, *Asian J. Org. Chem.*, 2021, **10**, 1835–1845; (b) T. Meng, J. Han, P. Zhang, J. Hu, J. Fu and J. Yin, *Chem. Sci*., 2019, **10**, 7156–7162.

(16) A. Zupanc and M. Jereb, *J. Org. Chem*., 2021, **86**, 5991–6000.

(17) J. R. Dehli and C. Bolm, *Adv. Synth. Catal*., 2005, **347**, 239–242.

(18) G. Shukla, T. Alam, H. K. Srivastava, R. Kumar and B. K. Patel, *Org. Lett*., 2019, **21**, 3543–3547.

(19) B. Sahoo, M. N. Hopkinson and F. Glorius, *Angew. Chem. Int. Ed*., 2015, **54**, 15545–15549.

(20) Y. Tu, P. Shi and C. Bolm, *Org. Lett*., 2022, **24**, 907–911.

(21) (a) X.-J. Shang, Z. Li and Z.-Q. Liu, *Tetrahedron Lett*., 2015, **56**, 233–235; (b) J.-D. Guo, X.-L. Yang, B. Chen, C.-H. Tung and L.-Z. Wu, *Green Chem*., 2021, **23**, 7193–7198; (c) X. Zeng, C. Miao, S. Wang, C. Xia and W. Sun, *RSC Adv*., 2013, **3**, 9666–9669.

Chapter III

PIDA/I_2-Mediated Photo-Induced Aerobic N-Acylation of Sulfoximines with Methylarenes

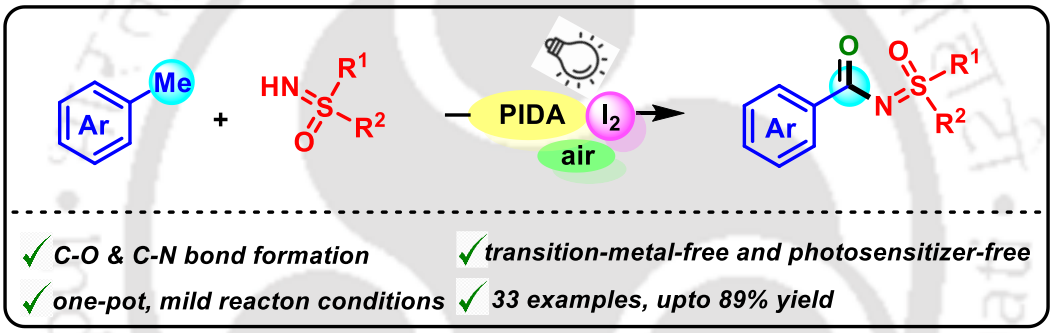

Organic & Biomolecular Chemistry
ROYAL SOCIETY OF CHEMISTRY
COMMUNICATION
View Article Online
View Journal | View Issue
Org. Biomol. Chem., 2024, **22**, 2375–2379

Abstract: *A visible-light-promoted, PIDA/I_2-mediated acylation of NH-sulfoximines with methylarenes as an acyl source has been achieved. This transition metal, photosensitizer-free approach provides easy access to N-acylsulfoximines via oxidative coupling of sulfoximines with easily available methylarenes without using any peroxide source. Mechanistic investigations suggest the intermediacy of radicals and the importance of molecular oxygen.*

भारतीय प्रौद्योगिकी संस्थान गुवाहाटी
Indian Institute of Technology Guwahati

CHAPTER III

PIDA/I_2-Mediated Photo-Induced Aerobic *N*-Acylation of Sulfoximines with Methylarenes

III.1. Introduction:

The pursuit of developing practical and efficient methodologies for forming C–C and C–heteroatom bonds *via* C–H functionalization reactions has garnered significant attention over the past few decades.[1] In this regard, hydrocarbons stand out as the most cost-effective and readily available starting materials for synthesizing essential chemicals. Harnessing easily accessible hydrocarbons not only offers a practical, potent, and straightforward alternative but also presents an excellent opportunity to expand our chemical understanding in a relatively unexplored domain. In this context, methylarenes are versatile starting material that widely finds application as a solvent, industrial feedstock, and a constituent of gasoline. In the realm of synthesis, they are particularly appealing for constructing intricate molecules, including pharmaceuticals, polymers, agrochemicals, and commodity chemicals.[2] Over time, a myriad of methodologies has been established to facilitate direct transformations of benzylic C−H bonds of methylarenes to C−C, and C−heteroatom bonds.[2] Moreover, methylarenes serve as a commonly available and inexpensive acyl surrogate. The sp^3 C–H bond of methylarenes can be efficiently oxidized in the presence of transition metal catalysts and oxidants.[3]

III.1.1. Representative Examples of Methylarenes as an Acylating Agent:

Jiao group reported a Pd-catalyzed aerobic oxidative acylation of *o*-methyloximes and pyridine derivatives with methylarenes in the presence of molecular oxygen as the terminal oxidant. The mechanistic investigations suggest the involvement of a Pd^{II}/Pd^{IV} catalytic cycle (Scheme III.1.1.1).[3d]

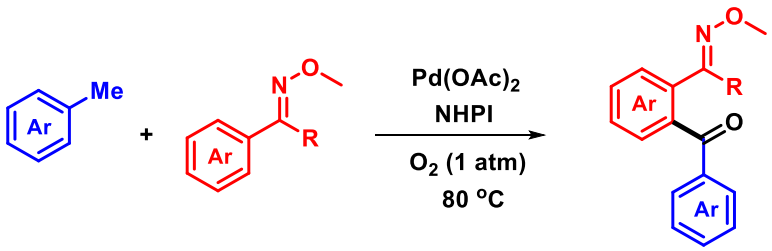

Scheme III.1.1.1. *Acylation of o-methyloximes.*

Sharma and Eycken reported an operationally simple and efficient method for C2-acylation of indoles, employing palladium catalysis. The protocol employed low-toxic, stable, and commercially available toluene derivatives as the acyl source, TBHP as the oxidant, and PivOH as an additive, and demonstrated a satisfying functional group tolerance (Scheme III.1.1.2).[3e]

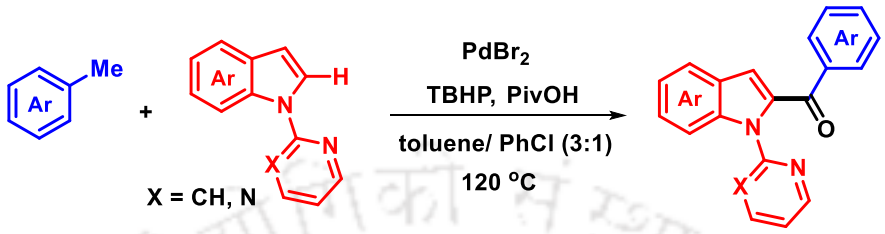

Scheme III.1.1.2. *Benzoylation of electron-deficient N-heterocycles.*

A nickel(II)-catalyzed regioselective C–H acylation of chelating arenes using toluene derivatives as the acylation reagent was developed by Cai *et al.* in 2019. This protocol is notable for its low cost, excellent regioselectivity, easy availability of starting materials, broad applicability to a range of substrates, and good yields (Scheme III.1.1.3).[3f]

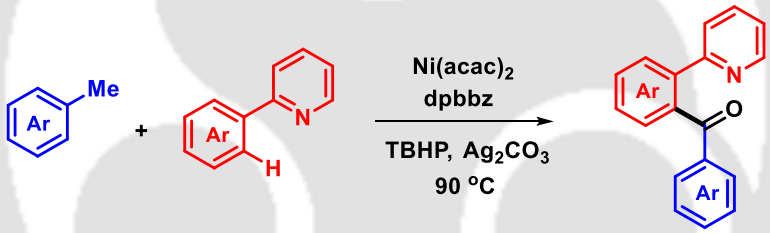

Scheme III.1.1.3. *Cai's Ni(II)-catalyzed ortho-acylation of 2-phenylpyridine.*

Our group has had a history of exploring methylarene chemistry and disclosed numerous strategies involving it as an acyl source.[3b,g,h] A novel copper-catalyzed cross-dehydrogenative coupling (CDC) strategy for the synthesis of thioesters was disclosed in 2014. This process involves the successive formation of C–S and C–O bonds, utilizing three sp^3 C–H bonds of the alkylbenzene and one sp^3 S–H bond of the thiol (Scheme III.1.1.4).[3g]

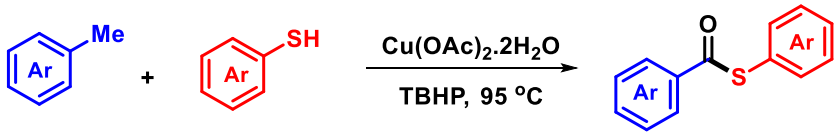

Scheme III.1.1.4. *Cu(II)-catalyzed thioesterification of alkylbenzenes with thiols.*

In 2015, our group reported a regioselective cross-dehydrogenative coupling between methylarenes and electron-deficient *N*-heterocycles (such as isoquinolines, quinolines, and

quinoxalines). This Minisci-type reaction proceeds *via* regiospecific C−aroylation, using $AlCl_3$ as the catalyst and TBHP as the oxidant (Scheme III.1.1.5).[3h]

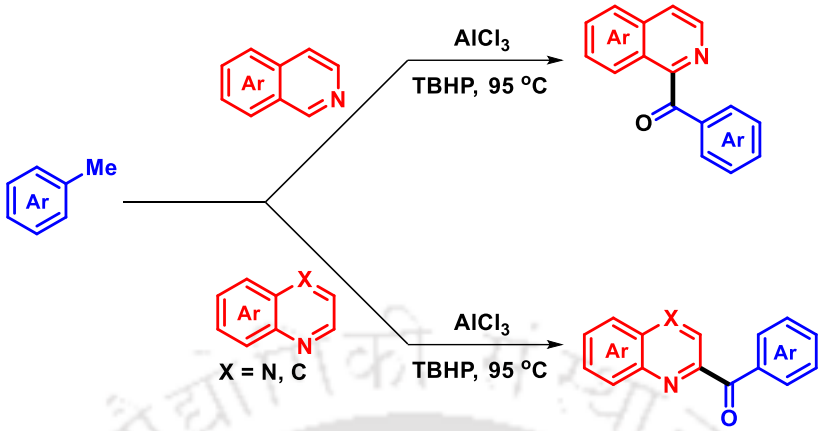

Scheme III.1.1.5. *Benzoylation of electron-deficient N-heterocycles with methylbenzenes.*

III.2. Previous Approaches on *N*-Acylation of Sulfoximines with Methylarenes:

The acylation of nitrogen atoms stands as one of the most extensively employed chemical transformations in organic synthesis. This reaction holds significant prominence as approximately 20% of all medicinal chemistry experiments rely on this reaction.[4] The *N*-acylation of sulfoximines is also an area of interest, as to date, there are few biologically active *N*-acylated sulfoximines (Figure III.2.1),[5] and the development of newer protocols will lead to their further expansion and utilization in related areas.

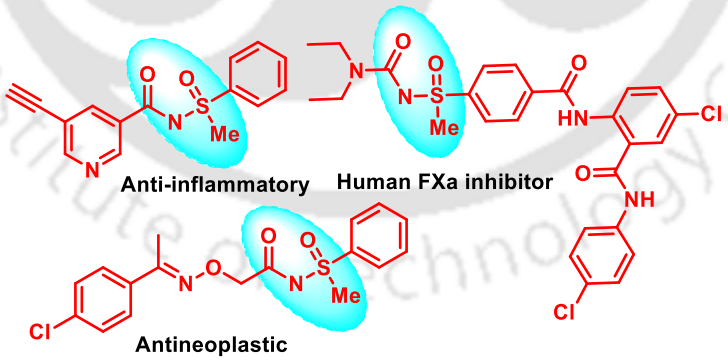

Figure III.2.1. *Representational examples of bioactive N-acylated sulfoximines.*

The conventional acylation of sulfoximines with methylarenes requires an appropriate peroxide source and high reaction temperatures and proceeds in the presence of transition metals or additives. One of the earlier examples of *N*-aroylation of sulfoximines was disclosed by Bolm and colleagues in 2014, which involved the MnO_2-promoted C–H bond activation of

methylarenes. This generated the aroylated intermediate, which, on reaction with *N*-chlorosulfoximine, produced a series of *N*-acylsulfoxime in good yields (Scheme III.2.1).[6]

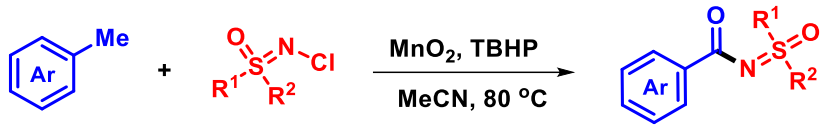

Scheme III.2.1. *MnO_2-mediated N-acylation of sulfoximines with methylarenes.*

In the subsequent year, the Zhao group reported an I_2-catalyzed, Fe(III)-promoted strategy for *N*-acylation of sulfoximines under neat conditions (Scheme III.2.2).[7]

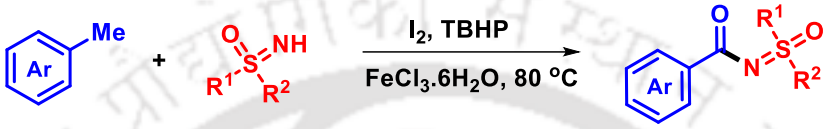

Scheme III.2.2. *I_2-catalyzed N-acylation of sulfoximines with methylarenes.*

The first metal-free approach for the N-aroylation of sulfoximines utilizing methyl arenes as the aroyl source was reported by An *et al*. The reaction proceeds in the presence of elemental iodine, Na_2CO_3, and TBHP without the requirement of any additional solvent (Scheme III.2.3).[8]

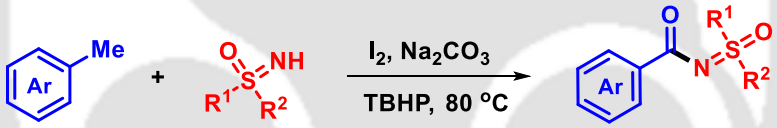

Scheme III.2.3. *Metal-free N-acylation of sulfoximines with methylarenes.*

III.3. Present Work:

Our group is actively engaged in exploring sulfoximine chemistry and as a part of the ongoing research, we envisioned designing a strategy between methylarenes and NH-sulfoximines under the influence of visible light. To synchronize this assumption, a reaction was carried out between *S*-phenyl-*S*-methylsulfoximine (**a**, 1 equiv), toluene (**1**, 5 equiv) in the presence of diacetoxyiodobenzene (PIDA) (3 equiv), and I_2 (1 equiv) in DCM (3 mL) under the irradiation of 2 x 10 W white LEDs at room temperature. After around 30 h a new product was isolated in 86% yield. The spectroscopic evidence (^{1}H and ^{13}C{^{1}H} NMR and X-ray diffraction) revealed the structure of the product to be *N*-(methyl(oxo)(phenyl)-λ^6-sulfaneylidene)benzamide (**1a**). The formation of *N*-acylsulfoximines through oxidative cross-coupling of sulfoximine with methylarene under photochemical and peroxide-free conditions appeared interesting from both a mechanistic and synthetic point of view.

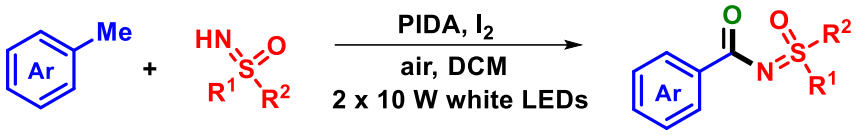

Scheme III.3.1. *Our approach.*

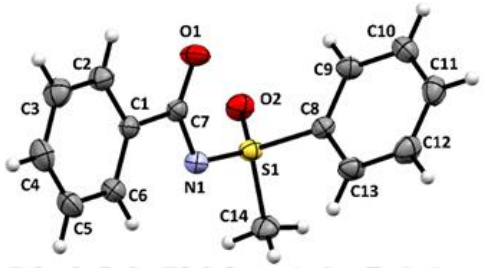

Figure.III.3.1. *ORTEP structure of **1a** with 30% ellipsoid probability* (CCDC 2302382).

III.3.1. Optimization of Reaction Conditions:

Inspired by this, extensive optimization studies involving the selection of different reaction conditions were carried out. Initially, different oxidant systems such as only PIDA, only I_2, and *N*-iodosuccinimide (NIS), were screened. However, in all three cases the anticipated product, **1a** was not formed at all (Table III.3.1, entries 2-4). Further, a trace amount of product was obtained when a 3:1 combination of NIS: I_2 was used (Table III.3.1, entry 5). Next, to optimize the loading of PIDA and I_2, reactions were performed with different concentrations of PIDA: I_2 (Table III.3.1, entries 6-7). Decreasing the loading of PIDA to 1 equiv and 2 equiv was detrimental for the reaction whereas increasing it to 5 equiv had no major impact on the reaction (Table III.3.1, entry 6). Further, changing the concentration of I_2 to 0.5 equiv lowered the product yield, whereas increasing it to 2 equiv made no significant difference in the product formation (Table III.3.1, entry 7). Thus, all further reactions were conducted with the original condition using PIDA: I_2 in a ratio of 3:1. Next, to check the effect of solvent in the given transformation, different solvents such as DCE, CH_3CN, DMSO, DMF, EtOH, and 1,2-dioxane were screened. However, except for DCE (71%) and CH_3CN (54%), the reaction did not proceed at all for other solvents (Table III.3.1, entries 8-9). To check the effect of wavelength and intensity of light, the standard reaction was carried out in 4 x 5 W blue (448 nm) and green (534 nm) LEDs. Both the lights failed to improve the reaction yield (Table III.3.1, entries 10 and 11). Hence, the optimized condition for this reaction is the use of NH-sulfoximine (1 equiv), toluene (5 equiv), PIDA (3 equiv), I_2 (1 equiv) in DCM (3 mL) in open air at room temperature under 2 x 10 W white LEDs (46 mW/cm^2) (Table III.3.1, entry 1).

Table III.3.1 *Optimization of the reaction conditions*[a,b]

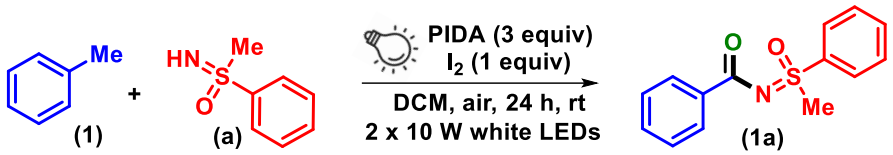

(1) + (a) → (1a)

entry	variation from optimal conditions[a]	yield (%)[b]
1.	None	86
2.	Only PIDA (3 equiv)	N.D.
3.	Only I_2 (1 equiv)	N.D.
4.	NIS (1 equiv)	N.D.
5.	NIS and I_2 (3:1)	trace
6.	PIDA (1 equiv), (2 equiv), (5 equiv)	42, 67, 87
7.	I_2 (0.5 equiv), (2 equiv)	61, 85
8.	CH_3CN, DCE instead of DCM	54, 71
9.	DMSO, THF, EtOH, 1,2-dioxane instead of DCM	N.D.
10.	4 x 5 W blue LEDs	78
11.	4 x 5 W green LEDs	37

[a]Reaction condition: **a** (0.4 mmol), **1** (2.0 mmol), PIDA (1.2 mmol), I_2 (0.4 mmol) in DCM (3 mL) in open air for 24 h in 2 x 10 W white LED's.
[b]Isolated pure product. N.D. = not detected.

III.3.2. Substrate Scope:

With the optimized condition in hand, the scope of this protocol was extended to a variety of methylarenes and NH-sulfoximines which are summarized in Schemes III.3.2.1 and III.3.2.2. We began our investigation by varying different substituents on methylarenes (**1**–**15**) keeping the *S*-aryl-*S*-methyl sulfoximine (**a**) counterpart fixed. Methylarenes with electron-neutral (**1**), and electron-donating substituents such as *p*-Me (**2**) and *m*-Me (**3**), underwent successful conversion to the products **1a**, **2a**, and **3a** in 86%, 82%, and 79% yields, respectively. The structure of **1a** was ascertained by single-crystal X-ray crystallography (CCDC 2302382). Similarly, the presence of moderately electron-withdrawing groups in the para and meta position as in *p*-Cl (**4**), *p*-Br (**5**), *p*-I (**6**), and *m*-I (**7**), successfully yielded the products **4a**–**7a** in good yields of 72–84%. The present protocol was successful for strongly electron-withdrawing groups such as –CN (**8** and **9**) and $–NO_2$ (**10**), resulting in the products **8a** (78%), **9a** (73%), and **10a** (68%), respectively. Further, di-substituted methylarenes as in

3,5-di-Me (**11**), 3-iodo-5-Me (**12**), and 3-bromo-4-CN (**13**) resulted in the corresponding *N*-acylsulfoximines in appreciable yields, **11a** (67%), **12a** (66%), and **13a** (63%). Further, to demonstrate the applicability of the protocol, we extended the scope of methylarenes to biphenylic systems, **14** and **15**. To our delight, both these substrates were successfully converted to the acylated products **14a** and **15a** in substantial yields of 71% and 69%, respectively.

Scheme III.3.2.1. *Substrate scope for methylarenes.*[a,b]

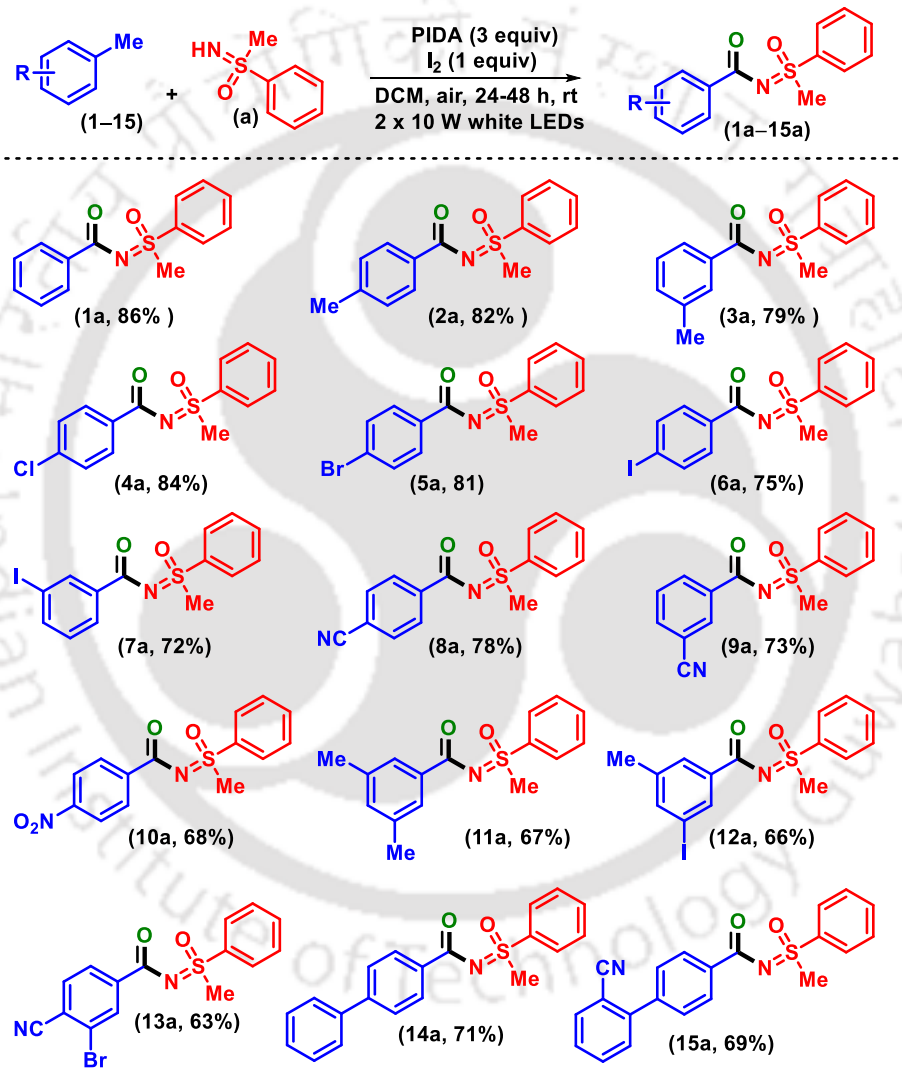

[a]Reaction conditions: Performed on a 0.4 mmol scale of NH-sulfoximine (**a**) (1 equiv), (**1**–**15**) (2.0 mmol, 5 equiv), PIDA (1.2 mmol, 3 equiv), I_2 (0.4 mmol, 1 equiv), DCM (3 mL) at rt for 24–48 h in open air under 2 x 10 W white LEDs (flux = 46 mW/cm^2). [b]Yield of the isolated product.

Scheme III.3.2.2. *Substrate scope for NH-sulfoximines.*[a,b]

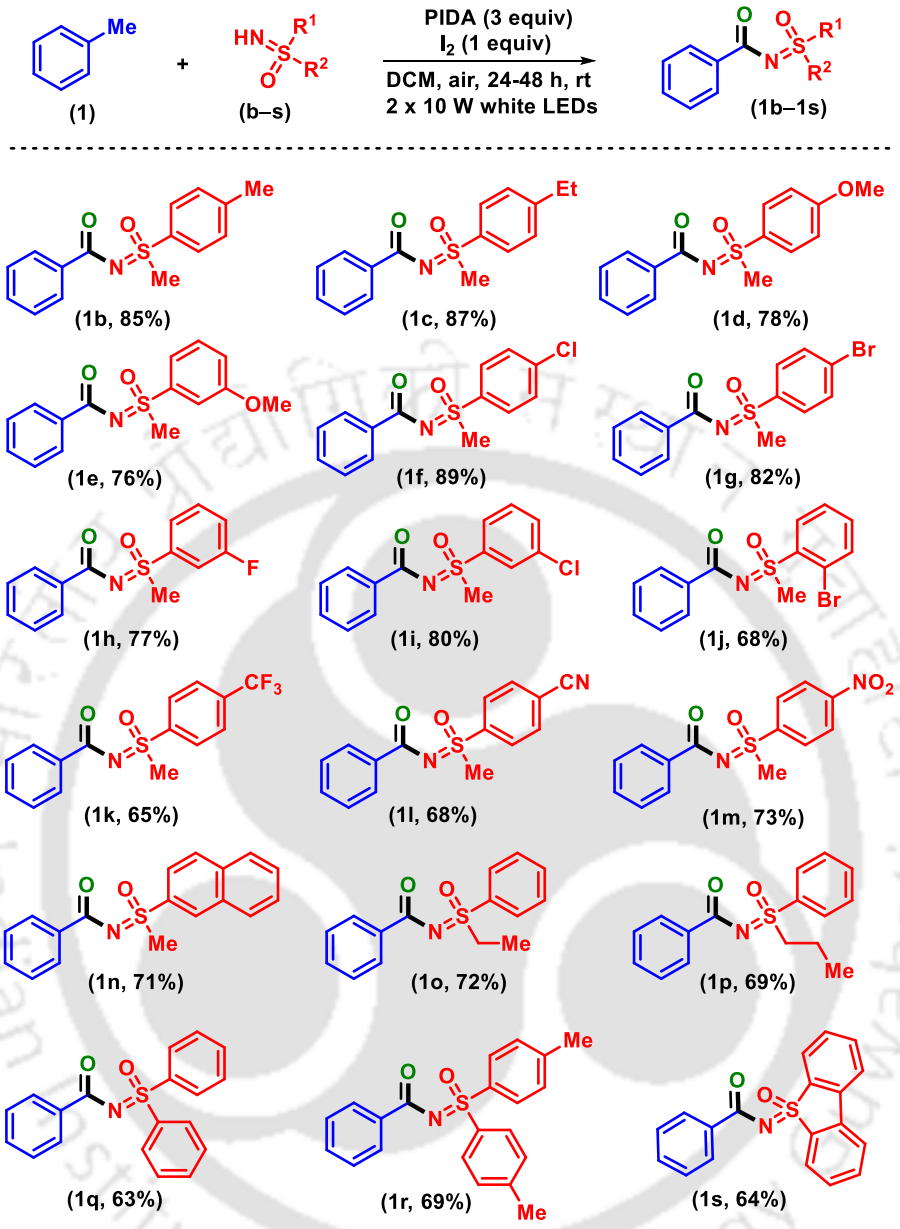

[a]Reaction conditions: (Performed on a 0.4 mmol scale of NH-sulfoximine (**b**–**s**) (1 equiv), (**1**) (2.0 mmol, 5 equiv) PIDA (1.2 mmol, 3 equiv), I_2 (0.4 mmol, 1 equiv), DCM (3 mL) at rt for 24–48 h in open air under 2 x 10 W white LEDs (flux = 46 mW/cm^2). [b]Yield of the isolated product.

Next, the scope of different NH-sulfoximines (**b**–**s**) bearing electron-donating (EDGs), as well as electron-withdrawing groups (EWGs), were investigated, which are presented in Scheme III.3.2.2. *S*-Aryl-*S*-methyl sulfoximines, having diverse electronic and steric effects, underwent successful conversion to their respective products. Electron-donating groups such as *p*-Me (**b**), *p*-Et (c), *p*-OMe (**d**), and *m*-OMe (**e**) in the phenyl ring of *S*-aryl-*S*-methyl sulfoximine successfully yielded the products in good yields, **1b** (85%), **1c** (87%), **1d** (78%),

and **1e** (76%), respectively. Similarly, diverse electron-withdrawing groups such as –F, –Cl, and –Br in the *p*-, *m*- and *o*- position were well compatible under the standard condition and resulted in the products *p*-Cl (**1f**, 89%), *p*-Br (**1g**, 82%), *m*-F (**1h**, 77%), *m*-Cl (**1i**, 80%), *o*-Br (**1j**, 68%). The given transformation proceeded smoothly in the presence of strongly electron-withdrawing groups *p*-CF_3 (**k**), *p*-CN (**l**), and *p*-NO_2 (**m**), affording the product in moderate yields of 65%–73%. Further, the reaction was favourable for polyaromatic-containing sulfoximine such as *S*-naphthyl-*S*-methyl sulfoximine (**n**) affording the *N*-acylated product (**1n**) in 71% yield. Moreover, *S*-aryl-*S*-ethyl (**o**) and *S*-aryl-*S*-propyl sulfoximine (**p**) were also successful in delivering the products **1o** and **1p** in appreciable yields of 72% and 69%. The sterically congested sulfoximines containing a diphenyl unit **q** and **r** were successful in this protocol, resulting in the product, albeit in a lower yield of 63% and 69%. Finally, dibenzothiophene-derived sulfoximine **s**, when applied to the present protocol, underwent successful conversion to product **1s** (64%).

III.3.3. Mechanistic Investigations:

To gain insight into the active mechanistic steps involved in this photoinduced strategy, various control experiments were conducted, taking toluene (**1**) and *S*-phenyl-*S*-methyl sulfoximine (**a**) as model substrates. As discussed above, under the standard optimized reaction condition, 86% of the desired product (**1a**) was formed, however, conducting the reaction without irradiation of light completely failed to result in **1a** {Scheme III.3.3.1(b)}. This suggested the crucial involvement of light in the overall strategy. Further, the reaction did not proceed at all when carried out in anhydrous DCM under an atmosphere of N_2 {Scheme III.3.3.1(c)}. However, when conducted under an atmosphere of oxygen, a better yield of 89% was obtained {Scheme III.3.3.1(d)}. Moreover, the reaction failed in the absence of either PIDA or I_2 {Scheme III.3.3.1(e, f)}, implying that a combination of both these reagents is essential for the transformation.

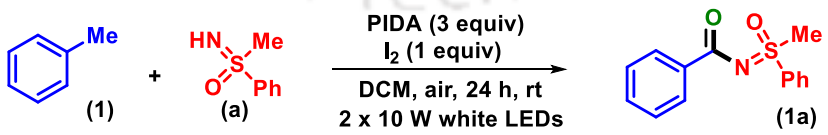

(a) Standard Condition	Formation of 1a (86%)
(b) Without irradiation	No reaction
(c) With anhydrous DCM in N_2	No reaction
(d) Under O_2 instead of air	Formation of 1a (89%)
(e) Without PIDA	No reaction
(f) Without I_2	No reaction

Scheme III.3.3.1. *Preliminary investigations.*

To understand the nature of the reaction, two identical reactions were conducted in the presence of radical scavengers, 2,2,6,6-tetramethylpiperidine-1-oxyl (TEMPO, 1 equiv) and 1,1-diphenylethylene (1 equiv) (Scheme III.3.3.2). Failure of the reaction under the standard reaction conditions suggests the radical nature of the reaction. Further, a small aliquot of the reaction mixture was withdrawn at approximately 12 h, diluted with acetonitrile (1 mL), and subjected to HRMS. The HRMS analysis of this reaction aliquot shows HRMS values corresponding to diphenylethylene-sulfoximine adduct (**a''**). which confirms the presence of N-centered sulfoximine radical in the reactive cycle (Figure III.3.3.1).

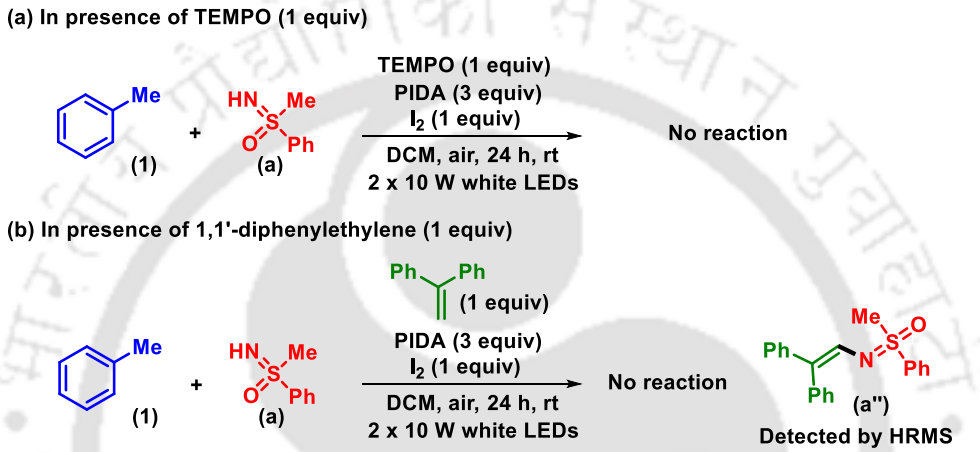

Scheme III.3.3.2. *Radical trapping experiments.*

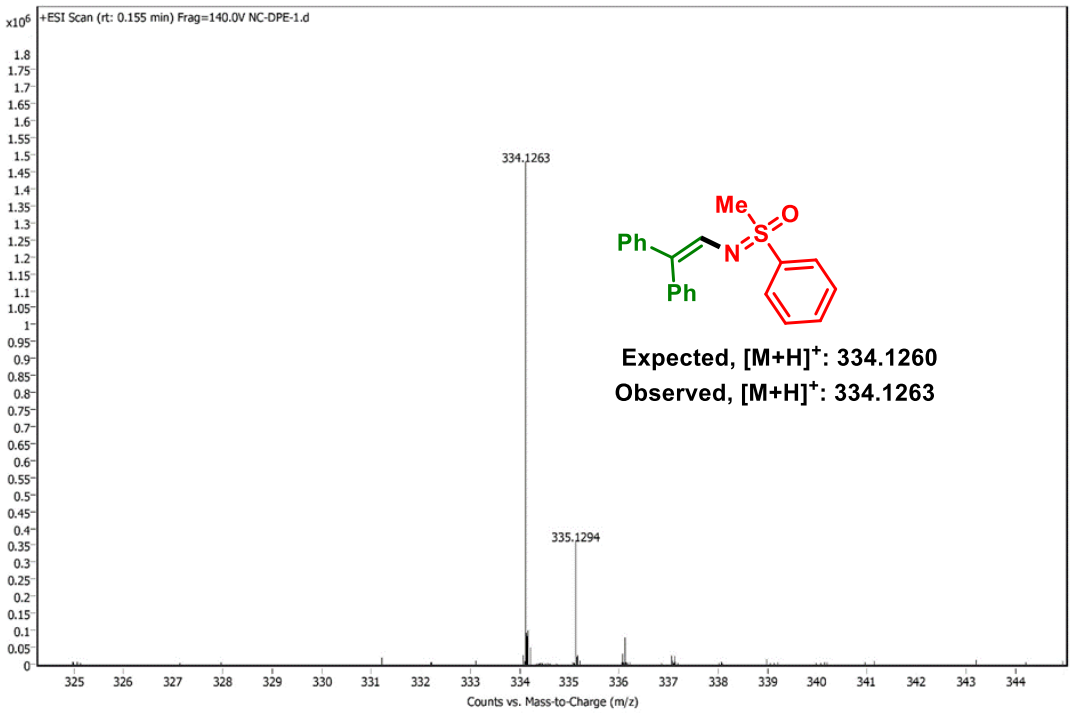

Figure III.3.3.1. *HRMS analysis of diphenylethylene-sulfoximine adduct* (**a''**).

The carbonyl oxygen in the product can either arise from moisture or atmospheric oxygen, hence to ascertain this, a reaction was carried out in the presence of H_2O^{18} (2 equiv) keeping the other reaction conditions fixed (Scheme III.3.3.3). The separated product was subjected to HRMS and ^{13}C NMR analysis. However, it was observed that in the HRMS, there was only one peak for O^{16} labelled product {$[M + H]^+$ calculated for $C_{14}H_{13}NO_2S$, 260.0740, found 260.0741} and no peak was found for O^{18} labelled product (Figure III.3.3.2). Similarly, the single peak at 174.5 in the ^{13}C NMR spectrum suggested no presence of O^{18} in the product (Figure III.3.3.3). Both these observations ruled out the involvement of moisture as the source of carbonyl oxygen.

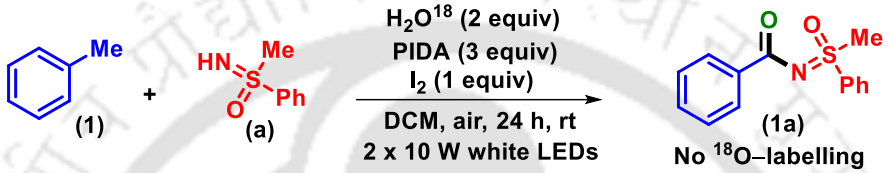

Scheme III.3.3.3. *H_2O^{18}-labelling experiment.*

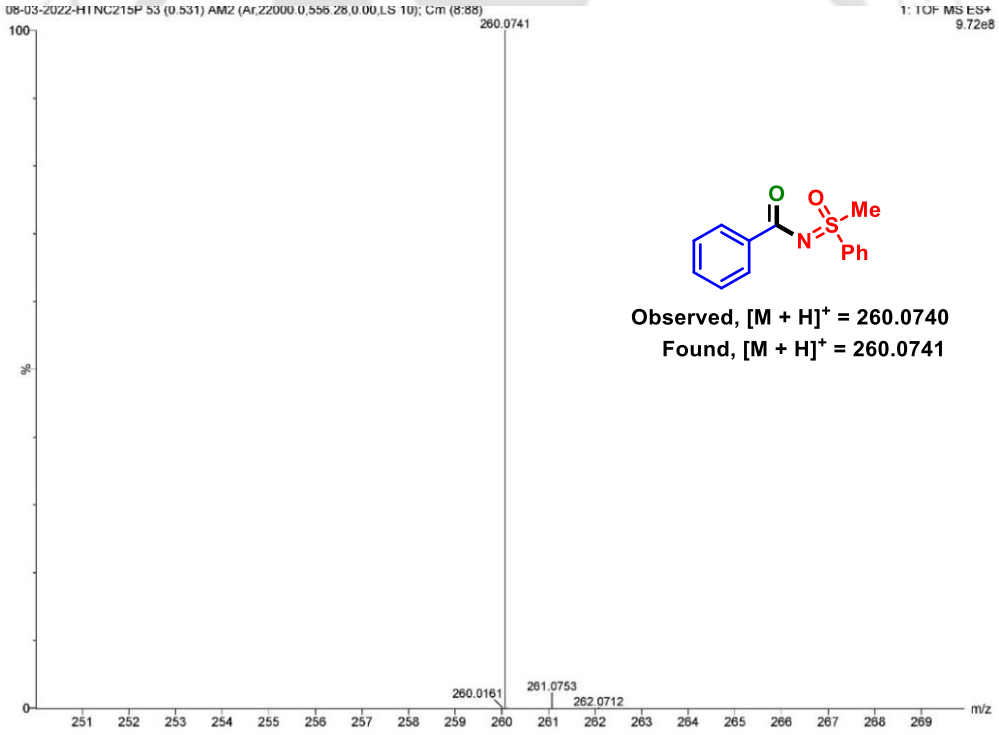

Figure III.3.3.2. *HRMS of labelled N-acylsulfoximines* (**1a**).

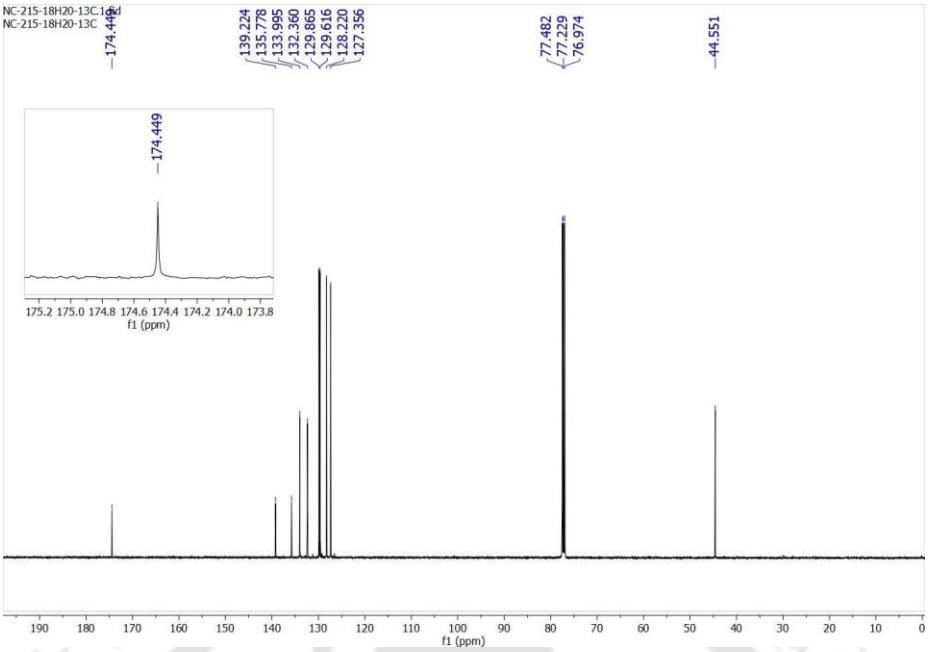

Figure III.3.3.3. *$^{13}C\{^{1}H\}$ spectrum of labelled N-acylsulfoximines* (**1a**).

From the literature precedents, it is apparent that *N*-iodosulfoximine (**A**) is one of the active intermediates,[9] hence to further confirm its involvement, a reaction was carried out between presynthesized **A**[10] and **1** keeping other reaction conditions fixed (Scheme III.3.3.4). The successful formation of **1a** confirms the involvement of **A** as the reactive intermediate in this visible-light-promoted protocol.

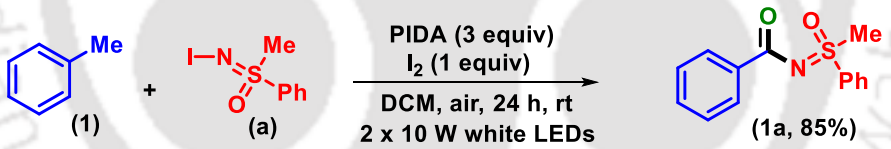

Scheme III.3.3.4. *Intermediacy of N-iodosulfoximine (**A**).*

Further, it was initially assumed that the reaction proceeded through the formation of *N*-benzylsulfoximine (**X**) followed by subsequent oxidation at the benzylic position to afford *N*-acylsulfoximine (**1a**). Hence to corroborate this supposition, a presynthesized *N*-benzylsulfoximine (**X**)[11] was subjected to the standard reaction condition (Scheme III.3.3.5). However, only a trace of the product was obtained, and this observation ruled out the involvement of **X** as an intermediate.

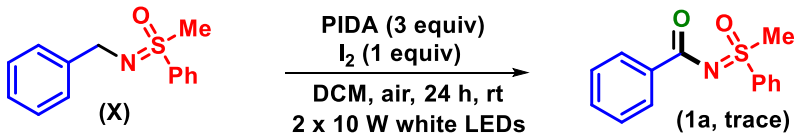

Scheme III.3.3.5. *Intermediacy of N-benzylsulfoximine (**X**).*

The above experiment suggested that initially, oxidation of the C(sp^3)–H bond of toluene takes place, followed by coupling with *N*-iodosulfoximine **A**. Thus, to further confirm this hypothesis, a reaction was conducted between intermediate **A** and benzaldehyde **D** under the irradiation of white light without PIDA and I_2 (Scheme III.3.3.6). To our delight, product **1a** was formed in 87% yield, thus suggesting that the reaction proceeds through benzaldehyde intermediate **D**. Further, this experiment also corroborated that both these oxidants have a potential role during the toluene oxidation step and no involvement in the final coupling step.

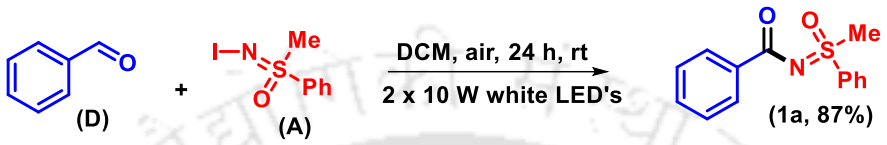

Scheme III.3.3.6. *Intermediacy of benzaldehyde (**D**).*

III.3.4. Plausible Mechanism:

Based on the control experiments and literature precedents, we suggest the reaction path as shown in Scheme III.3.4.[9,12,13] Initially, the N-iodination of NH-sulfoximine (**a**) takes place in the presence of IOAc which is generated *in situ* from PIDA and I_2 and gives the key intermediate *N*-iodosulfoximine (**A**).[12] The intermediate A serves as the energy-absorbing species (λ_{max} = 363 nm) under visible light irradiation and undergoes a homolytic N−I bond cleavage resulting in the N-centered sulfoximidoyl radical (**a′**), and iodine radical.[9c] The iodo radical abstracts a proton from the benzylic C(sp^3)–H bond of toluene and generates the benzylic radical intermediate (**B**) and HI. Intermediate **B** captures O_2 from the atmosphere, along with concurrent abstraction of a proton from HI, resulting in the peroxo intermediate **C** and regenerating the iodo radical.[9a,b] The loss of H_2O from **C** gives the benzaldehyde intermediate **D**, which in the presence of iodo radical forms intermediate **E**. The final product **1a** is a result of the coupling between **E** and **a′**.[13]

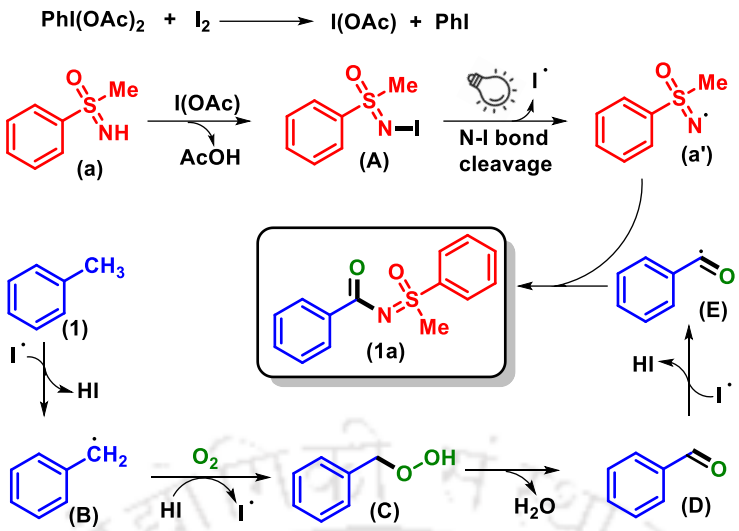

III.3.4. *Plausible mechanism.*

III.3.5. Scale-up Reaction:

To demonstrate the scalability of this protocol, a large-scale reaction was conducted in an identical reaction setup (**a**, 5 mmol, 775 mg), which successfully resulted in product **1a** in 63% yield (Scheme III.3.5).

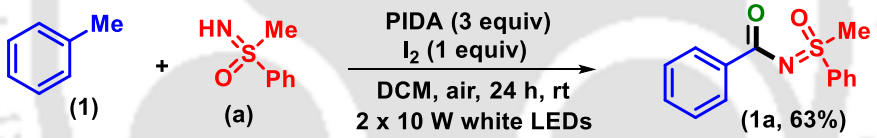

Scheme III.3.5. *Scale-up reaction for the synthesis of N-acyl sulfoximines (**1a**).*

III.3.6. Conclusion:

In conclusion, a visible-light-induced transition metal and photocatalyst-free approach for *N*-acylation of sulfoximines has been disclosed. This PIDA/I_2-mediated acylation approach utilizes methylarenes as the acyl donor without using highly oxygenated peroxide sources. The reaction involves *in situ* generated IOAc for the generation of the reactive intermediate *N*-iodosulfoximine, which drives out the entire reaction without any external photocatalyst. Operational simplicity, scalability, and good functional group tolerance are the main features of this strategy.

III.4. Experimental Section:

III.4.1. General Information:

All the reagents were commercial grade and purified according to the established procedures. All the reactions were carried out in oven-dried glassware. The highest commercial quality reagents were purchased and were used without further purification unless otherwise stated. All the cinnamic acids used in this protocol were commercially purchased from Sigma Aldrich and BLD Pharma. Reactions were monitored by thin layer chromatography (TLC) on 0.25 mm silica gel plates ($60F_{254}$) visualized under UV illumination at 254 nm. Organic extracts were dried over anhydrous sodium sulfate (Na_2SO_4). Solvents were removed using a rotary evaporator under reduced pressure. Column chromatography was performed to purify the crude product on silica gel 60–120 mesh using a mixture of hexane and ethyl acetate as eluent. The isolated compounds were characterized by spectroscopic [^{1}H, ^{13}C{1H} NMR, and IR] techniques and HRMS analysis. NMR spectra were recorded in deuterochloroform ($CDCl_3$). ^{1}H, ^{13}C{^{1}H} were recorded in 400 (100), 500 (125) or 600 (150) MHz spectrometers and were calibrated using tetramethylsilane or residual undeuterated solvent for ^{1}H NMR, deuterochloroform for ^{13}C NMR as an internal reference {$Si(CH_3)_4$: 0.00 ppm or $CHCl_3$: 7.260 ppm for ^{1}H NMR and 77.230 ppm for ^{13}C{1H}. ^{19}F NMR was calibrated without any internal standard in $CDCl_3$ in a 370, 471 or 565 MHz spectrometer. The chemical shifts are quoted in δ units, parts per million (ppm). ^{1}H NMR data is represented as follows: Chemical shift, multiplicity (s = singlet, d = doublet, t = triplet, q = quartet, dd = doublet of doublets, m = multiplet), integration and coupling constant(s) *J* in hertz (Hz). High-resolution mass spectra (HRMS) were recorded on a mass spectrometer using electrospray ionization-time of flight (ESI-TOF) reflection experiments. FT-IR spectra were recorded in neat and reported in the frequency of absorption (cm^{-1}).

III.4.2. Light Information and Reaction Setup:

Philips 2 x 10 W white LEDs (flux = 46mW/cm^2) bulb was used as the light source for this light-induced reaction, and no filter was used. Borosilicate round bottom glass was used as the reaction vessel. The distance from the light source to the irradiation vessel was ~3-5 cm. A regular fan was used to ventilate the area to maintain the room temperature (25–30 ^{o}C). The reaction setup for this photochemical strategy is shown below (Figure III.4.2).

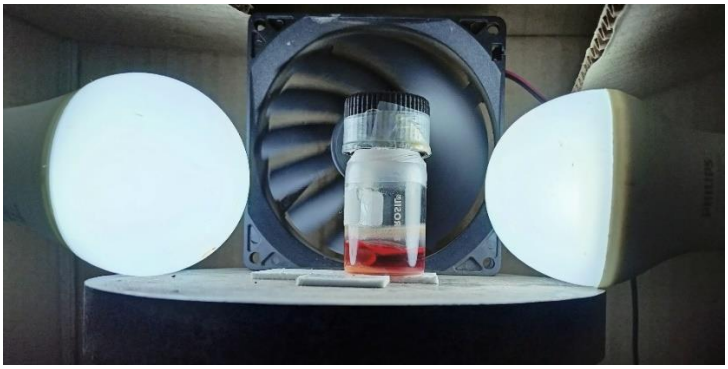

Figure III.4.2. *Photochemical reaction set-up.*

III.4.3. Crystallographic Information:

Crystallographic information of *N-(methyl(oxo)(phenyl)-λ⁶-sulfaneylidene)benzamide* (1a):

(i) Sample Preparation: The single crystal of compound **1a** was prepared by the slow evaporation method for which 25 mg of the compound (**1a**) was dissolved in 1 mL of DCM in a clean and dry 10 mL glass vial. MeOH (0.5 mL) was added to this solution slowly with a dropper. The mouth of the glass vial was covered with a cap having a small hole and kept for slow evaporation at room temperature. Crystals of **1a** were obtained after approximately 3-4 days as a transparent block-shaped crystal.

(ii) Data Collection: Diffraction data were collected at 292 K with MoKα radiation (λ = 0.71073 Å) using a Bruker Nonius SMART APEX CCD diffractometer equipped with graphite monochromator and Apex CD camera. The SMART software was used for data collection and for indexing the reflections and determining the unit cell parameters. Data reduction and cell refinement were performed using SAINT software and the space groups of these crystals were determined from systematic absences by XPREP and further justified by the refinement results. The structures were solved by direct methods and refined by full-matrix least-squares calculations using SHELXTL-973 software. All the non-H atoms were refined in the anisotropic approximation against F2 of all reflections.

(iii) Crystallographic description of *N*-(methyl(oxo)(phenyl)-λ⁶-sulfaneylidene)benzamide (1a):

$C_{14}H_{13}NO_2S$, colourless block shaped crystal; crystal dimensions 0.06 x 0.05 x 0.05 mm, M_r = 259.312, Triclinic space group P -1; a = 5.8219 (4) Å, b = 8.6182 (5) Å, c = 13.5458 (8) Å, α = 81.096 (2) °, β = 88.255 (2)°, γ = 73.391 (2)°, V = 643.38 (7) Å^3, Z = 2, ρ_{calcd} = 1.339 g/cm^3, μ = 0.244 mm^{-1}, F(000)= 272.0, reflection collected / unique = 3160 / 2525, refinement method = full-matrix least-squares on F^2, final R indices [I> 2\s(I)]: R_1 = 0.0552, wR_2 = 0.1069, R

indices (all data): R_1 = 0.0769, wR_2 = 0.1180, goodness of fit = 1.139. **CCDC**-2302382 for *N*-(methyl(oxo)(phenyl)-λ^6-sulfaneylidene)benzamide (**1a**) contains the supplementary crystallographic data for this paper. These data can be obtained free of charge from The Cambridge Crystallographic Data Centre via www.ccdc.cam.ac.uk/data_request/cif.

III.4.4. General Procedure:

III.4.4.1. Procedure for the Synthesis of *N*-Acylsulfoximine (1a):

NH-sulfoximine (**a**) (0.4 mmol, 1 equiv, 62 mg), toluene (**1**) (2 mmol, 5 equiv, 184 mg), and phenyliododiacetate (PIDA) (1.2 mmol, 3 equiv, 386 mg), molecular iodine I_2 (0.4 mmol, 1 equiv, 102 mg) in 3 mL of DCM were added to an oven-dried 10 mL borosilicate vial and stirred in open air at room temperature, approximately at a distance of ~3−5 cm from two 10 W white LED bulbs. After completion of the reaction (monitored by TLC analysis), the reaction mixture was added ethyl acetate (25 mL) and washed with 5% aqueous $Na_2S_2O_3$ (1 x 10 mL) solution followed by saturated brine solution (1 x 10 mL). The organic layer was dried over anhydrous Na_2SO_4, and then the solvent was evaporated under reduced pressure. The crude product obtained was purified over a column of silica gel using (1:4) mixture of ethyl acetate in hexane to afford the *N*-acyl sulfoximine (**1a**) in 82% yield. The identity and purity of the product were confirmed by spectroscopic analysis (Scheme III.4.4.1).

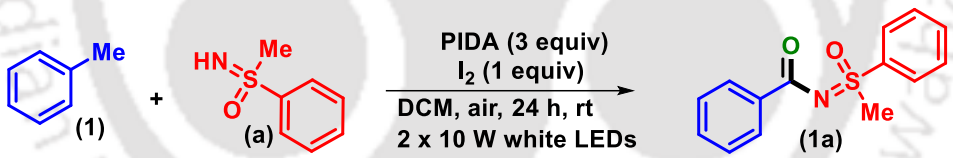

Scheme III.4.4.1. *Preparation of N-acyl sulfoximines (**1a**).*

III.4.4.2. Procedure for the Synthesis of (Benzylimino)(methyl)(phenyl)-λ^6-sulfanone X:[11]

A 25 mL oven-dried round bottom flask was charged with a magnetic stirbar, *S*-phenyl-*S*-methylsulfoximine **a** (2 mmol, 1 equiv, 310 mg) and KOH (4 mmol, 2 equiv, 224 mg) were added. Maintaining an atmosphere of nitrogen, anhydrous DMSO (4 mL) was added to the reaction mixture followed by a dropwise addition of benzylbromide (3.0 mmol, 1.5 equiv, 513 mg). The resultant reaction mixture was further stirred at room temperature and the progress of the reaction was monitored by TLC. Once all the sulfoximine was consumed, the reaction mixture was added ethyl acetate (25 mL) and washed with saturated brine solution (1 x 10 mL). The organic layer was dried over anhydrous Na_2SO_4, and then the solvent was evaporated under reduced pressure. The crude product obtained was purified over a column of silica gel using

(4:1) ethyl acetate in hexane to afford the *N*-benzylsulfoximine (**X**) in 87% yield. The identity and purity of the product was confirmed by spectroscopic analysis (Scheme III.4.4.2).

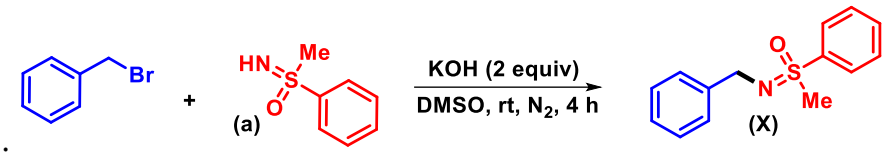

Scheme III.4.4.2. *Preparation of intermediate **X**.*

III.4.5. Mechanistic Investigations:

III.4.5.1. Radical-Trapping Experiment:

NH-sulfoximine (**a**) (0.4 mmol, 1 equiv, 62 mg), toluene (**1**) (2 mmol, 5 equiv, 184 mg), phenyliododiacetate (PIDA) (1.2 mmol, 3 equiv, 386 mg), molecular iodine I_2 (0.4 mmol, 1 equiv, 102 mg), and 1,1-dephenylethylene (0.4 mmol, 1 equiv, 72 mg) in 3 mL of DCM were added to an oven-dried 10 mL borosilicate vial and stirred in open air at room temperature, approximately at a distance of ~3−5 cm from two 10 W white LED bulbs. A small aliquot of the reaction mixture was withdrawn at approximately 12 h and diluted with acetonitrile (1 mL) and subjected to HRMS. The HRMS analysis of this reaction aliquot shows HRMS values corresponding to diphenylethylene-sulfoximine adduct (**a''**).

III.4.5.2. H_2O^{18}-Labelling Experiment:

NH-sulfoximine (**a**) (1 mmol, 1 equiv, 155 mg), toluene (**1**) (5 mmol, 5 equiv, 460 mg), phenyliododiacetate (PIDA) (3 mmol, 3 equiv, 966 mg), molecular iodine I_2 (1 mmol, 1 equiv, 254 mg) and H_2O^{18} (2 mmol, 2 equiv, 40 mg) in 4 mL of DCM were added to an oven-dried 10 mL borosilicate vial and stirred in open air at room temperature, approximately at a distance of ~3−5 cm from two 10 W white LED bulbs. After completion of the reaction (monitored by TLC analysis), the mixture was admixed with 20 mL ethyl acetate and sequentially washed with 5% aqueous $Na_2S_2O_3$ (1 x 10 mL) and brine solution (1 x 10 mL). The organic layer was dried over anhydrous Na_2SO_4, and the solvent was evaporated under reduced pressure. The crude residue thus obtained was purified by column chromatography over silica gel (60-120 mesh) using hexane and ethyl acetate (4:1) as eluent to afford *N*-acylsulfoximine (**1a**) in 85% yield.

III.5. Spectral Data:

N-(Methyl(oxo)(phenyl)-λ⁶-sulfaneylidene)benzamide (1a):

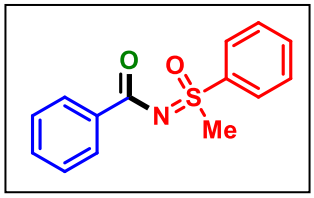

As yellow solid (89 mg, 86% yield); purified over a column of silica gel (25% EtOAc in hexane); ^{1}H NMR (500 MHz, $CDCl_3$): δ (ppm) 8.17 (d, 2H, J = 7.5 Hz), 8.06 (d, 2H, J = 8.0 Hz), 7.69 (t, 1H, J = 7.5 Hz), 7.62 (t, 2H, J = 7.5 Hz), 7.51 (t, 1H, J = 7.3 Hz), 7.41 (t, 2H, J = 7.5 Hz), 3.47 (s, 3H); ^{13}C NMR (125 MHz, $CDCl_3$): δ (ppm) 174.5, 139.3, 135.8, 134.0, 132.4, 129.9, 129.6, 128.2, 127.4, 44.6.

4-Methyl-N-(methyl(oxo)(phenyl)-λ⁶-sulfaneylidene)benzamide (2a):

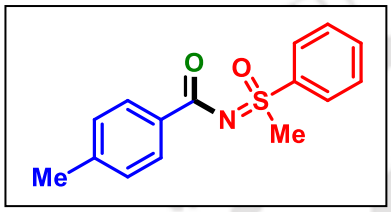

As dark brown solid (90 mg, 82% yield); purified over a column of silica gel (25% EtOAc in hexane); ^{1}H NMR (500 MHz, $CDCl_3$): δ (ppm) 8.06 (d, 4H, J = 6.5 Hz), 7.68 (t, 1H, J = 7.5 Hz), 7.61 (t, 2H, J = 7.8 Hz), 7.21 (d, 2H, J = 8.0 Hz), 3.46 (s, 3H), 2.40 (s, 3H); ^{13}C NMR (125 MHz, $CDCl_3$): δ (ppm) 174.5, 142.9, 139.4, 133.9, 133.1, 129.9, 129.7, 129.0, 127.4, 44.6, 21.8.

3-Methyl-N-(methyl(oxo)(phenyl)-λ⁶-sulfaneylidene)benzamide (3a):

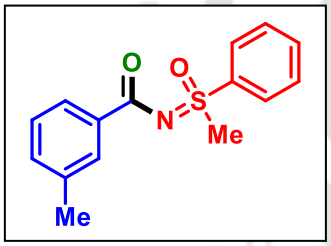

As light brown solid (86 mg, 79% yield); purified over a column of silica gel (25% EtOAc in hexane); ^{1}H NMR (500 MHz, $CDCl_3$): δ (ppm) 8.06 (d, 2H, J = 7.5 Hz), 7.97 (d, 2H, J = 8.5 Hz), 7.69 (t, 1H, J = 7.3 Hz,), 7.62 (t, 2H, J = 7.8 Hz), 7.33–7.29 (m, 2H), 3.47 (s, 3H), 2.40 (s, 3H); ^{13}C NMR (100 MHz, $CDCl_3$): δ (ppm) 174.7, 139.3, 137.9, 135.7, 134.0, 133.2, 130.2, 129.9, 128.2, 127.4, 126.8, 44.6, 21.5.

4-Chloro-N-(methyl(oxo)(phenyl)-λ⁶-sulfaneylidene)benzamide (4a):

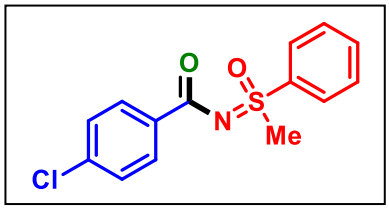

As brown solid (98 mg, 84% yield); purified over a column of silica gel (27% EtOAc in hexane); ^{1}H NMR (500 MHz, $CDCl_3$): δ (ppm) 8.10 (d, 2H, J = 8.5 Hz), 8.04 (d, 2H, J = 7.5 Hz), 7.70 (t, 1H, J = 7.5 Hz), 7.62 (t, 2H, J = 7.8 Hz), 7.38 (d, 2H, J = 8.5 Hz), 3.47 (s, 3H); ^{13}C NMR (100 MHz, $CDCl_3$): δ (ppm) 173.5, 139.0, 138.7, 134.3, 134.1, 131.1, 129.9, 128.5, 127.3, 44.6.

4-Bromo-N-(methyl(oxo)(phenyl)-λ⁶-sulfaneylidene)benzamide (5a):

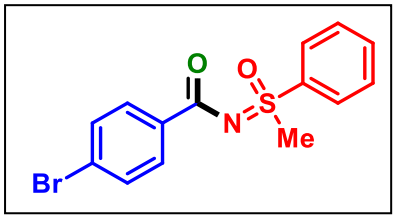

As yellow solid (109 mg, 81% yield); purified over a column of silica gel (27% EtOAc in hexane); ^{1}H NMR (500 MHz, $CDCl_3$): δ (ppm) 8.03 (t, 4H, J = 8.8 Hz), 7.70 (t, 1H, J = 7.5 Hz), 7.62 (t, 2H, J = 7.5 Hz), 7.54 (d, 2H, J = 8.5 Hz), 3.47 (s, 3H); ^{13}C NMR (100 MHz, $CDCl_3$): δ (ppm) 173.6, 139.0, 134.7, 134.1, 131.5, 131.3, 129.9, 127.4, 127.3, 44.6.

4-Iodo-N-(methyl(oxo)(phenyl)-λ⁶-sulfaneylidene)benzamide (6a):

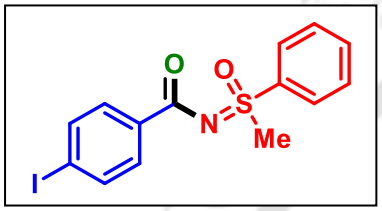

As pale yellow solid (115 mg, 75% yield); purified over a column of silica gel (25% EtOAc in hexane); ^{1}H NMR (500 MHz, $CDCl_3$): δ (ppm) 8.04 (d, 2H, J = 7.5 Hz), 7.87 (d, 2H, J = 8.5 Hz), 7.76 (d, 2H, J = 8.5 Hz), 7.70 (t, 1H, J = 7.5 Hz), 7.62 (t, 2H J = 7.8 Hz), 3.46 (s, 3H); ^{13}C NMR (125 MHz, $CDCl_3$): δ (ppm) 173.8, 139.0, 137.5, 135.3, 134.1, 131.3, 129.9, 127.3, 100.0, 44.6.

3-Iodo-N-(methyl(oxo)(phenyl)-λ⁶-sulfaneylidene)benzamide (7a):

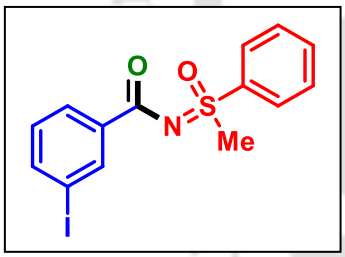

As brown solid (111 mg, 72% yield); purified over a column of silica gel (25% EtOAc in hexane); ^{1}H NMR (500 MHz, $CDCl_3$): δ (ppm) 8.51 (s, 1H), 8.11 (d, 1H, J = 7.5 Hz), 8.04 (d, 2H, J = 8.5 Hz), 7.83 (d, 1H, J = 8.0 Hz), 7.70 (t, 1H, J = 7.0 Hz), 7.63 (t, 2H, J = 7.5 Hz), 7.15 (t, 1H, J = 7.8 Hz), 3.46 (s, 3H); ^{13}C NMR (125 MHz, $CDCl_3$): δ (ppm) 172.8, 141.1, 139.0, 138.7, 137.8, 134.1, 130.0, 129.9, 128.8, 127.4, 93.9, 44.6.

4-Cyano-N-(methyl(oxo)(phenyl)-λ⁶-sulfaneylidene)benzamide (8a):

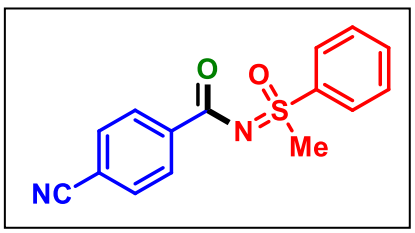

As brown gummy (88 mg, 78% yield);); purified over a column of silica gel (30% EtOAc in hexane); ^{1}H NMR (500 MHz, $CDCl_3$): δ (ppm) 8.24 (d, 2H, J = 8.0 Hz), 8.04 (d, 2H, J = 7.5 Hz), 7.73–7.69 (m, 3H), 7.64 (t, 2H, J = 7.8 Hz), 3.49 (s, 3H); ^{13}C NMR (125 MHz, $CDCl_3$): δ (ppm) 172.6, 139.7, 138.7, 134.3, 132.1, 130.1, 130.0, 127.3, 118.7, 115.6, 44.6.

3-Cyano-N-(methyl(oxo)(phenyl)-λ⁶-sulfaneylidene)benzamide (9a):

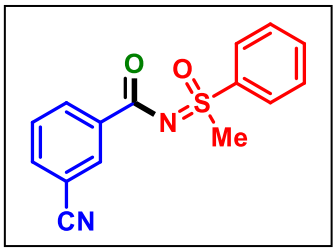

As brown gummy (83 mg, 73% yield); purified over a column of silica gel (30% EtOAc in hexane); ^{1}H NMR (500 MHz, $CDCl_3$): δ (ppm) 8.47 (s, 1H), 8.36 (d, 1H, J = 8.0 Hz), 8.05 (d, 2H, J = 8.0 Hz), 7.78 (d, 1H, J = 7.5 Hz), 7.72 (t, 1H, J = 7.5 Hz), 7.65 (t, 2H, J = 7.8 Hz), 7.53 (t, 1H, J = 7.8 Hz), 3.49 (s, 3H); ^{13}C NMR (125 MHz, $CDCl_3$): δ (ppm) 172.1, 138.7, 137.1, 135.3, 134.4, 133.7, 133.5, 130.1, 129.3, 127.3, 118.6, 112.6, 44.6.

N-(Methyl(oxo)(phenyl)-λ⁶-sulfaneylidene)-4-nitrobenzamide (10a):

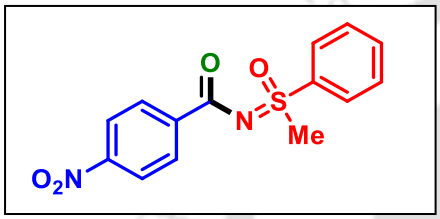

As dark brown solid (83 mg, 68% yield); purified over a column of silica gel (30% EtOAc in hexane); ^{1}H NMR (400 MHz, $CDCl_3$): δ (ppm) 8.31 (d, 2H J = 9.2 Hz), 8.24 (d, 2H, J = 8.8 Hz), 8.05 (d, 2H, J = 7.6 Hz), 7.73 (t, 1H, J = 7.4 Hz), 7.65 (t, 2H, J = 7.6 Hz), 3.50 (s, 3H); ^{13}C NMR (100 MHz, $CDCl_3$): δ (ppm) 172.3, 150.2, 141.2, 138.5, 134.4, 130.6, 130.1, 127.3, 123.4, 44.5.

3,5-Dimethyl-N-(methyl(oxo)(phenyl)-λ⁶-sulfaneylidene)benzamide (11a):

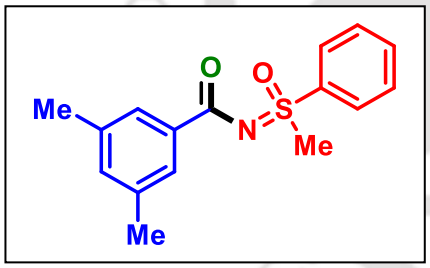

As pale yellow solid (77 mg, 67% yield); purified over a column of silica gel (22% EtOAc in hexane); ^{1}H NMR (500 MHz, $CDCl_3$): δ (ppm) 8.05 (d, 2H, J = 7.5 Hz), 7.78 (s, 2H), 7.68 (t, 1H, J = 7.5 Hz), 7.61 (t, 2H, J = 7.5 Hz), 7.15 (s, 1H), 3.46 (s, 3H), 2.35 (s, 6H); ^{13}C NMR (125 MHz, $CDCl_3$): δ (ppm) 174.9, 139.4, 137.8, 135.7, 134.1, 133.9, 129.9, 128.1, 127.4, 44.6, 21.4.

3-Iodo-5-methyl-N-(methyl(oxo)(phenyl)-λ⁶-sulfaneylidene)benzamide (12a):

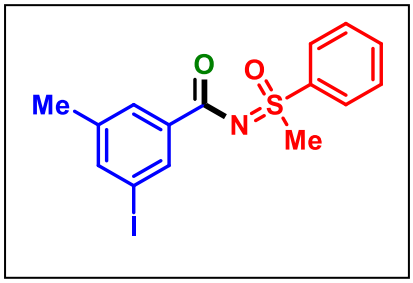

As orange solid (105 mg, 66% yield); purified over a column of silica gel (25% EtOAc in hexane); ^{1}H NMR (500 MHz, $CDCl_3$): δ (ppm) 8.30 (s, 1H), 8.03 (d, 2H, J = 8.0 Hz), 7.90 (s, 1H), 7.71–7.67 (m, 2H), 7.62 (t, 2H, J = 7.8 Hz), 3.45 (s, 3H), 2.34 (s, 3H); ^{13}C NMR (125 MHz, $CDCl_3$): δ (ppm) 173.0, 141.7, 140.2, 138.9, 137.5, 135.7, 134.1, 129.9, 129.5, 127.3, 93.9, 44.6, 21.1.

3-Bromo-4-cyano-N-(methyl(oxo)(phenyl)-λ⁶-sulfaneylidene)benzamide (13a):

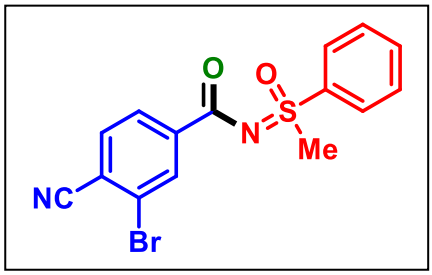

As brown solid (91 mg, 63% yield); m.p. 119–121 °C; purified over a column of silica gel (28% EtOAc in hexane); ^{1}H NMR (400 MHz, $CDCl_3$): δ (ppm) 8.45 (s, 1H), 8.16 (dd, 1H, J_1 = 8.0, J_2 = 1.5 Hz,), 8.03 (d, 2H, J = 7.6 Hz), 7.73–7.63 (m, 4H), 3.49 (s, 3H); ^{13}C NMR (125 MHz, $CDCl_3$): δ (ppm) 171.2, 140.9, 138.4, 134.5, 134.2, 134.0, 130.1, 128.4, 127.3, 125.3, 118.7, 117.1, 44.6; IR (neat, cm^{-1}): 3101, 2915, 2850, 2233, 1732, 1623, 1549, 1445, 1379, 1285, 1213, 1089; HRMS (ESI) m/z: $[M + H]^+$ Calcd for $C_{15}H_{12}BrN_2O_2S$ 362.9797; Found 362.9799.

N-(Methyl(oxo)(phenyl)-λ⁶-sulfaneylidene)-[1,1'-biphenyl]-4-carboxamide (14a):

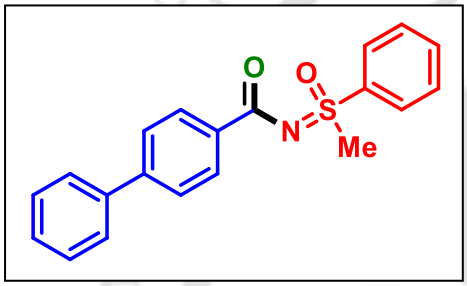

As pale yellow solid (95 mg, 71% yield); purified over a column of silica gel (22% EtOAc in hexane); ^{1}H NMR (400 MHz, $CDCl_3$): δ (ppm) 8.24 (d, 2H, J = 8.4 Hz), 8.08 (d, 2H, J = 7.2 Hz), 7.70 (t, 1H, J = 7.2 Hz), 7.66–7.61 (m, 6H), 7.46 (t, 2H, J = 7.4 Hz), 7.38 (t, 1H, J = 7.2 Hz), 3.49 (s, 3H); ^{13}C NMR (125 MHz, $CDCl_3$): δ (ppm) 174.3, 145.1, 140.6, 139.3, 134.7, 134.0, 130.2, 129.9, 129.1, 128.1, 127.5, 127.4, 127.0, 44.6;

2'-Cyano-N-(methyl(oxo)(phenyl)-λ⁶-sulfaneylidene)-[1,1'-biphenyl]-4-carboxamide (15a):

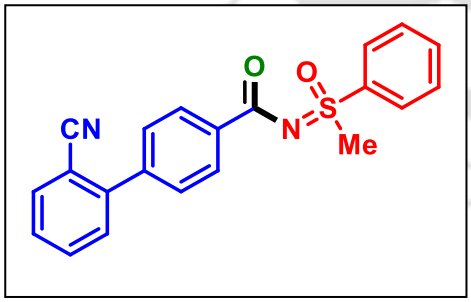

As brown solid (99 mg, 69% yield); m.p. 110–112 °C; purified over a column of silica gel (28% EtOAc in hexane); ^{1}H NMR (400 MHz, $CDCl_3$): δ (ppm) 8.29 (d, 2H, J = 8.4 Hz), 8.08 (d, 2H, J = 8.0 Hz), 7.79 (d, 1H, J = 7.6 Hz), 7.73–7.65 (m, 3H), 7.64–7.60 (m, 3H), 7.54 (d, 1H, J = 7.2 Hz), 7.48 (t, 1H, J = 7.6 Hz), 3.49 (s, 3H); ^{13}C NMR (125 MHz, $CDCl_3$): δ (ppm) 173.9, 144.9, 141.9, 139.0, 136.0, 134.1, 134.0, 133.1, 130.2, 130.1, 129.9, 128.8, 128.2, 127.4, 118.7, 111.5, 44.6; IR (neat, cm^{-1}): 3062, 3013, 2922, 2851, 2223, 1676, 1620, 1445, 1280, 1219, 1147, 1091; HRMS (ESI) m/z: $[M + H]^+$ Calcd for $C_{21}H_{17}N_2O_2S$, 361.1005; Found 361.1015.

N-(Methyl(oxo)(p-tolyl)-λ⁶-sulfaneylidene)benzamide (1b):

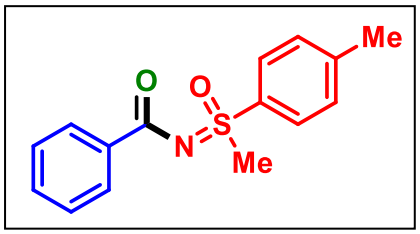

As pale-yellow solid (93 mg, 85% yield); purified over a column of silica gel (25% EtOAc in hexane); ^{1}H NMR (500 MHz, $CDCl_3$): δ (ppm) 8.17 (d, 2H, J = 6.5 Hz), 7.93 (d, 2H J = 8.0 Hz), 7.50 (t, 1H, J = 7.5 Hz), 7.40 (t, 4H, J = 7.5 Hz), 3.45 (s, 3H), 2.46 (s, 3H); ^{13}C NMR (125 MHz, $CDCl_3$): δ (ppm) 174.4, 145.1, 136.3, 136.0, 132.3, 130.5, 129.6, 128.2, 127.4, 44.7, 21.8.

N-((4-Ethylphenyl)(methyl)(oxo)-λ⁶-sulfaneylidene)benzamide (1c):

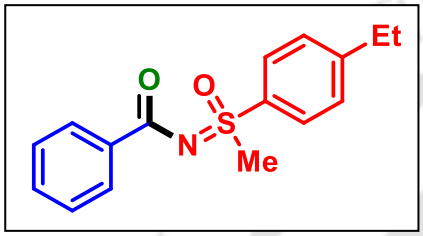

As brown solid (100 mg, 87% yield); m.p. 84–86 °C; purified over a column of silica gel (25% EtOAc in hexane); ^{1}H NMR (500 MHz, $CDCl_3$): δ (ppm) 8.17 (d, 2H, J = 8.0 Hz), 7.96 (d, 2H, J = 8.0 Hz), 7.50 (t, 1H, J = 7.3 Hz), 7.43–7.39 (m, 4H), 3.46 (s, 3H), 2.75 (q, 2H, J = 7.6 Hz), 1.28 (t, 3H, J = 7.8 Hz); ^{13}C NMR (125 MHz, $CDCl_3$): δ (ppm) 174.5, 151.2, 136.3, 135.9, 132.3, 129.6, 129.4, 128.2, 127.5, 44.7, 29.1, 15.3; IR (neat, cm^{-1}): 3021, 2963, 2927, 1740, 1615, 1574, 1450, 1404, 1318, 1274, 1208, 1135; HRMS (ESI) m/z: $[M + H]^+$ Calcd for $C_{16}H_{18}NO_2S$, 288.1053; Found 288.1065.

N-((4-Methoxyphenyl)(methyl)(oxo)-λ⁶-sulfaneylidene)benzamide (1d):

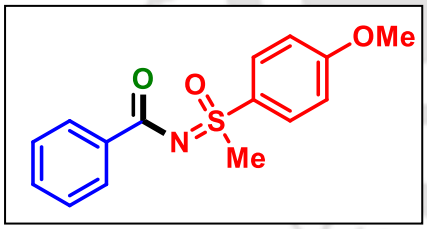

As brown solid (90 mg, 78% yield); purified over a column of silica gel (25% EtOAc in hexane); ^{1}H NMR (500 MHz, $CDCl_3$): δ (ppm) 8.17 (d, 2H, J = 7.5 Hz), 7.98 (d, 2H, J = 9.0 Hz), 7.50 (t, 1H, J = 7.5 Hz), 7.40 (t, 2H, J = 7.5 Hz), 7.06 (d, 2H, J = 8.5 Hz), 3.88 (s, 3H), 3.45 (s, 3H); ^{13}C NMR (125 MHz, $CDCl_3$): δ (ppm) 174.4, 164.1, 136.0, 132.2, 130.3, 129.6, 129.5, 128.2, 115.1, 55.9, 44.9.

N-((3-Methoxyphenyl)(methyl)(oxo)-λ⁶-sulfaneylidene)benzamide (1e):

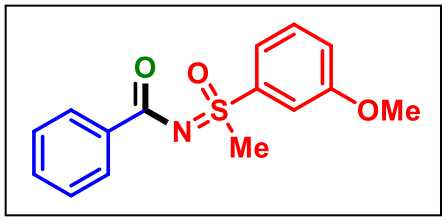

As orange solid (88 mg, 76% yield); purified over a column of silica gel (25% EtOAc in hexane); ^{1}H NMR (500 MHz, $CDCl_3$): δ (ppm) 8.17 (d, 2H, J = 7.0 Hz), 7.61 (d, 1H, J = 8.0 Hz), 7.57 (s, 1H), 7.52–7.49 (m, 2H), 7.41 (t, 2H, J = 7.5 Hz), 7.19 (dd, 1H, J_1 = 8.5 Hz, J_2 = 2.5 Hz), 3.88 (s, 3H), 3.46 (s, 3H); ^{13}C NMR

(125 MHz, $CDCl_3$): δ (ppm) 174.5, 160.6, 140.5, 135.8, 132.4, 131.0, 129.6, 128.2, 120.3, 119.3, 112.3, 56.0, 44.6.

N-((4-Chlorophenyl)(methyl)(oxo)-λ⁶-sulfaneylidene)benzamide (1f):

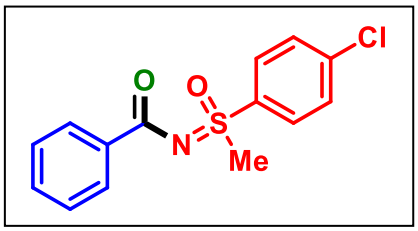

As brown solid (104 mg, 89% yield); purified over a column of silica gel (25% EtOAc in hexane); ^{1}H NMR (500 MHz, $CDCl_3$): δ (ppm) 8.15 (d, 2H, J = 7.5 Hz), 7.99 (d, 2H, J = 8.0 Hz), 7.59 (d, 2H, J = 8.0 Hz), 7.52 (t, 1H, J = 7.3 Hz), 7.42 (t, 2H, J = 7.8 Hz), 3.46 (s, 3H); ^{13}C NMR (100 MHz, $CDCl_3$): δ (ppm) 174.4, 140.9, 137.7, 135.5, 132.6, 130.3, 129.7, 128.9, 128.3, 44.6.

N-((4-Bromophenyl)(methyl)(oxo)-λ⁶-sulfaneylidene)benzamide (1g):

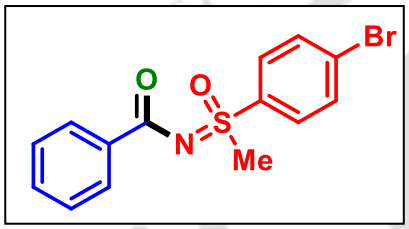

As brown solid (110 mg, 82% yield); purified over a column of silica gel (28% EtOAc in hexane); ^{1}H NMR (500 MHz, $CDCl_3$): δ (ppm) 8.14 (d, 2H, J = 7.0 Hz), 7.91 (d, 2H, J = 8.0 Hz), 7.74 (d, 2H, J = 8.5 Hz), 7.52 (t, 1H, J = 7.3 Hz), 7.41 (t, 2H, J = 7.5 Hz), 3.45 (s, 3H); ^{13}C NMR (125 MHz, $CDCl_3$): δ (ppm) 174.4, 138.3, 135.5, 133.2, 132.5, 129.6, 129.4, 128.9, 128.3, 44.6.

N-((3-Fluorophenyl)(methyl)(oxo)-λ⁶-sulfaneylidene)benzamide (1h):

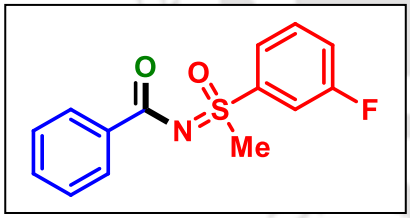

As brown solid (85 mg, 77% yield); purified over a column of silica gel (28% EtOAc in hexane); ^{1}H NMR (400 MHz, $CDCl_3$): δ (ppm) 8.15 (d, 2H, J = 6.8 Hz), 7.85 (d, 1H, J = 7.6 Hz), 7.79–7.76 (m, 1H), 7.64–7.58 (m, 1H), 7.52 (t, 1H, J = 7.4 Hz), 7.44–7.36 (m, 3H), 3.46 (s, 3H); ^{13}C NMR (100 MHz, $CDCl_3$): δ (ppm) 174.4, 162.9 (d, J = 251.5 Hz), 141.3 (d, J = 6.7 Hz), 135.4, 132.6, 131.8(d, J = 7.8 Hz), 129.7, 128.3, 123.2 (d, J = 3.3 Hz), 121.4 (d, J = 21.2 Hz), 115.0 (d, J = 24.9 Hz), 44.5; ^{19}F NMR (471 MHz, $CDCl_3$): δ (ppm) -108.2.

N-((3-Chlorophenyl)(methyl)(oxo)-λ⁶-sulfaneylidene)benzamide (1i):

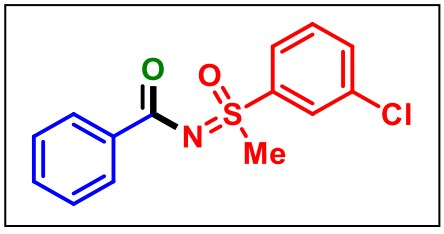

As brown solid (94 mg, 80% yield); purified over a column of silica gel (25% EtOAc in hexane); ^{1}H NMR (500 MHz, $CDCl_3$): δ (ppm) 8.15 (d, 2H, J = 7.0 Hz), 8.04 (s, 1H), 7.93 (d, 1H, J = 8.0 Hz), 7.65 (d, 1H, J = 9.0 Hz),

7.57–7.51 (m, 2H), 7.42 (t, 2H, *J* = 7.8 Hz), 3.46 (s, 3H); ^{13}C NMR (125 MHz, $CDCl_3$): δ (ppm) 174.4, 141.1, 136.2, 135.5, 134.2, 132.6, 131.2, 129.7, 128.3, 127.5, 125.5, 44.6.

N-((2-Bromophenyl)(methyl)(oxo)-λ^6-sulfaneylidene)benzamide (1j):

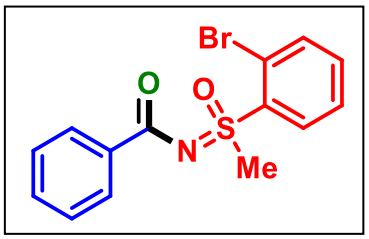

As dark brown solid (92 mg, 68% yield); purified over a column of silica gel (28% EtOAc in hexane); ^{1}H NMR (500 MHz, $CDCl_3$): δ (ppm) 8.37 (d, 1H, *J* = 8.0 Hz), 8.14 (d, 2H, *J* = 7.5 Hz), 7.77 (d, 1H, *J* = 7.5 Hz), 7.62 (t, 1H, *J* = 7.8 Hz), 7.50 (t, 2H, *J* = 8.0 Hz), 7.39 (t, 2H, *J* = 7.5Hz), 3.61 (s, 3H); ^{13}C NMR (125 MHz, $CDCl_3$): δ (ppm) 173.9, 138.3, 135.9, 135.5, 134.9, 132.4, 132.1, 129.8, 128.7, 128.2, 119.7, 42.2.

N-(Methyl(oxo)(4-(trifluoromethyl)phenyl)-λ^6-sulfaneylidene)benzamide (1k):

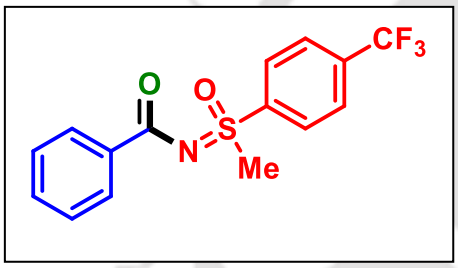

As yellow solid (85 mg, 65% yield); purified over a column of silica gel (30% EtOAc in hexane); ^{1}H NMR (500 MHz, $CDCl_3$): δ (ppm) 8.19 (d, 2H, *J* = 8.5 Hz), 8.15 (d, 2H, *J* = 7.0 Hz), 7.88 (d, 2H**,** *J* = 8.5 Hz), 7.53 (t, 1H, *J* = 7.5 Hz), 7.42 (t, 2H, *J* = 7.5 Hz), 3.47 (s, 3H); ^{13}C NMR (125 MHz, $CDCl_3$): δ (ppm) 174.2, 142.9, 135.9, 135.7, 135.4, 135.1, 132.5, 129.5, 128.1, 127.9, 126.9 (q, *J* = 3.7 Hz), 124.2, 122.0, 44.2; ^{19}F NMR (471 MHz, $CDCl_3$): δ (ppm) -63.2.

N-((4-Cyanophenyl)(methyl)(oxo)-λ^6-sulfaneylidene)benzamide (1l):

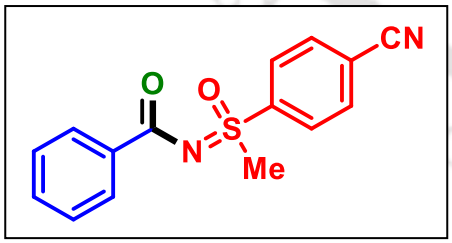

As brown solid (77 mg, 68% yield); purified over a column of silica gel (32% EtOAc in hexane); ^{1}H NMR (500 MHz, $CDCl_3$): δ (ppm) 8.15 (d, 2H, *J* = 9.0 Hz), 8.11 (d, 2H, *J* = 7.0 Hz), 7.88 (d, 2H, *J* = 9.0 Hz), 7.52 (t, 1H, *J* = 7.3 Hz), 7.41 (t, 2H, *J* = 7.8 Hz), 3.44 (s, 3H); ^{13}C NMR (125 MHz, $CDCl_3$): δ (ppm) 174.3, 143.7, 135.0, 133.6, 132.8, 129.6, 128.3, 128.2, 117.7, 117.2, 44.1.

N-(Methyl(4-nitrophenyl)(oxo)-λ⁶-sulfaneylidene)benzamide (1m):

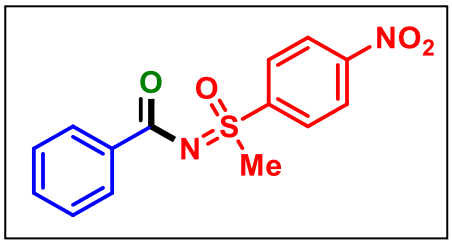

As pale yellow solid (89 mg, 73% yield); purified over a column of silica gel (30% EtOAc in hexane); ^{1}H NMR (500 MHz, $CDCl_3$): δ (ppm) 8.44 (d, 2H, J = 9.0 Hz), 8.24 (d, 2H, J =9.0 Hz), 8.12 (d, 2H, J = 7.0 Hz), 7.53 (t, 1H, J = 7.3 Hz), 7.42 (t, 2H, J = 7.8 Hz), 3.48 (s, 3H); ^{13}C NMR (125 MHz, $CDCl_3$): δ (ppm) 174.3, 151.0, 145.3, 135.0, 132.9, 129.7, 128.9, 128.4, 125.1, 44.2.

N-(Methyl(naphthalen-2-yl)(oxo)-λ⁶-sulfaneylidene)benzamide (1n):

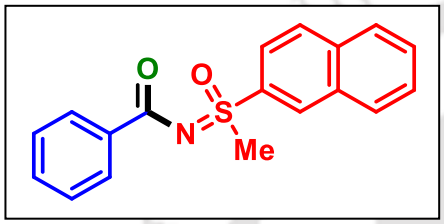

As pale yellow solid (88 mg, 71% yield); purified over a column of silica gel (27% EtOAc in hexane); ^{1}H NMR (500 MHz, $CDCl_3$): δ (ppm) 8.66 (s, 1H), 8.20 (d, 2H, J = 7.0 Hz), 8.04 (t, 2H, J = 8.5 Hz), 7.96 (t, 2H, J = 8.3 Hz), 7.71–7.64 (m, 2H), 7.52 (t, 1H, J = 7.5 Hz), 7.43 (t, 2H, J = 7.5 Hz), 3.54 (s, 3H); ^{13}C NMR (125 MHz, $CDCl_3$): δ (ppm) 174.5, 136.0, 135.8, 135.6, 132.6, 132.4, 130.3, 129.7, 129.67, 129.4, 128.3, 128.2, 128.1, 121.8, 44.6.

N-(Ethyl(oxo)(phenyl)-λ⁶-sulfaneylidene)benzamide (1o):

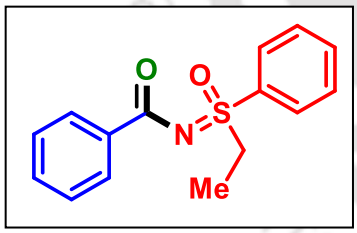

As brown solid (79 mg, 72% yield); purified over a column of silica gel (25% EtOAc in hexane); ^{1}H NMR (500 MHz, $CDCl_3$): δ (ppm) 8.18 (d, 2H, J = 7.5 Hz), 8.01 (d, 2H, J = 7.5 Hz), 7.68 (t, 1H, J = 7.5 Hz), 7.61 (t, 2H, J = 7.8 Hz), 7.51 (t, 1H, J = 7.5 Hz), 7.41 (t, 2H, J = 7.5 Hz), 3.62 (q, 2H, J = 7.5 Hz), 1.32 (t, 3H, J = 7.5 Hz); ^{13}C NMR (125 MHz, $CDCl_3$): δ (ppm) 174.4, 136.9, 136.0, 133.9, 132.3, 129.8, 129.7, 128.24, 128.22, 50.9, 7.5.

N-(Oxo(phenyl)(propyl)-λ⁶-sulfaneylidene)benzamide (1p):

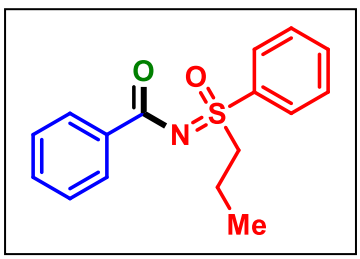

As dark brown solid (79 mg, 69% yield); m.p. 80–82 °C; purified over a column of silica gel (22% EtOAc in hexane); ^{1}H NMR (500 MHz, $CDCl_3$): δ (ppm) 8.17 (d, 2H, J = 7.5 Hz), 8.01 (d, 2H, J = 7.5 Hz), 7.67 (t, 1H J = 7.3 Hz), 7.60 (t, 2H, J = 7.8 Hz), 7.50 (t, 1H, J = 7.3 Hz), 7.41 (t, 2H, J = 7.8 Hz), 3.62–3.48 (m, 2H), 1.88–1.69 (m, 2H), 1.01 (t, 3H, J = 7.5 Hz); ^{13}C NMR (125 MHz, $CDCl_3$): δ (ppm)

174.4, 137.5, 136.0, 133.9, 132.3, 129.8, 129.6, 128.2, 128.1, 57.9, 16.5, 12.9; IR (neat, cm^{-1}): 3059, 2968, 2930, 2876, 1714, 1620, 1575, 1447, 1313, 1275, 1193, 1132, 1086, 929; HRMS (ESI) m/z: $[M + H]^+$ Calcd for $C_{16}H_{18}NO_2S$, 288.1053; Found 288.1070.

N-(Oxodiphenyl-λ⁶-sulfaneylidene)benzamide (1q):

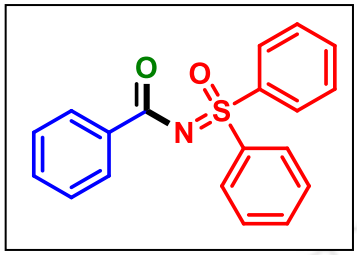

As brown solid (81 mg, 63% yield); purified over a column of silica gel (15% EtOAc in hexane); ^{1}H NMR (400 MHz, $CDCl_3$): δ (ppm) 8.25 (d, 2H, J = 6.8 Hz), 8.09–8.06 (m, 4H), 7.59–7.52 (m, 7H), 7.44 (t, 2H, J = 7.6 Hz); ^{13}C NMR (100 MHz, $CDCl_3$): δ (ppm) 174.1, 140.1, 136.0, 133.5, 132.4, 129.75, 129.73, 128.3, 127.8.

N-(Oxodi-p-tolyl-λ⁶-sulfaneylidene)benzamide (1r):

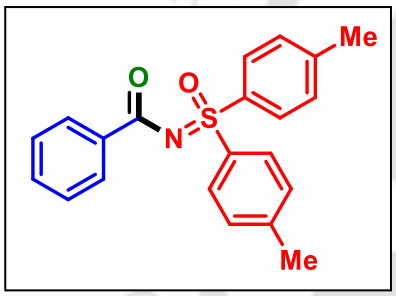

As brown gummy (96 mg, 69% yield); purified over a column of silica gel (18% EtOAc in hexane); ^{1}H NMR (500 MHz, $CDCl_3$): δ (ppm) 8.24 (d, 2H, J = 7.5 Hz), 7.93 (d, 4H, J = 8.0 Hz), 7.52 (t, 1H, J = 7.3 Hz), 7.43 (t, 2H, J = 7.5 Hz), 7.31 (d, 4H, J = 8.5 Hz), 2.39 (s, 6H); ^{13}C NMR (125 MHz, $CDCl_3$): δ (ppm) 174.1, 144.3, 137.3, 136.2, 132.3, 130.4, 129.7, 128.2, 127.7, 21.7.

N-(5-Oxido-5λ⁴-dibenzo[b,d]thiophen-5-ylidene)benzamide (1s):

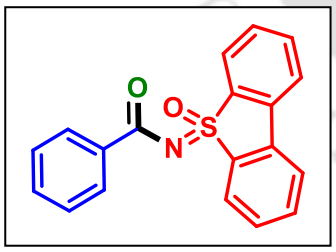

As white solid (82 mg, 64% yield); purified over a column of silica gel (25% EtOAc in hexane); ^{1}H NMR (400 MHz, $CDCl_3$): δ (ppm) 8.34 (d, 2H, J = 7.6 Hz), 8.13 (d, 2H, J = 6.8 Hz), 7.85 (d, 2H, J = 7.6 Hz), 7.70 (t, 2H, J = 7.6 Hz), 7.59 (t, 2H, J = 7.6 Hz), 7.47 (t, 1H, J = 7.2 Hz), 7.37 (t, 2H, J = 7.6 Hz); ^{13}C NMR (125 MHz, $CDCl_3$): δ (ppm) 175.3, 137.4, 135.3, 134.6, 133.3, 132.5, 130.8, 129.8, 128.2, 125.8, 121.9.

***(Iodoimino)(methyl)(phenyl)-λ⁶-sulfanone* (A):**

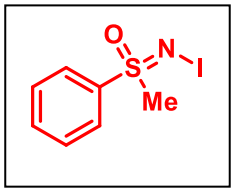

As white solid (233 mg, 83% yield); ^{1}H NMR (600 MHz, $CDCl_3$); δ (ppm) 7.85 (d, 2H, J = 7.2 Hz), 7.68 (t, 1H, J = 7.8 Hz), 7.60 (t, 2H, J = 7.8 Hz), 3.33 (s, 3H); ^{13}C NMR (150 MHz, $CDCl_3$): δ (ppm) 140.1, 133.9, 129.8, 128.5, 42.9.

(Benzylimino)(methyl)(phenyl)-λ⁶-sulfanone (X):

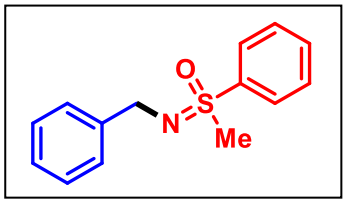

As yellow gummy (426 mg, 87% yield); purified over a column of silica gel (25% EtOAc in hexane); ^{1}H NMR (500 MHz, $CDCl_3$): δ (ppm) 7.94 (d, 2H, J = 7.0 Hz), 7.62 (t, 1H, J = 7.3 Hz), 7.56 (t, 2H, J = 7.5 Hz), 7.35 (d, 2H, J = 7.5 Hz), 7.29 (t, 2H, J = 7.5 Hz), 7.21 (t, 1H, J = 7.3 Hz), 4.20 (d, 1H, J = 14.0 Hz), 3.98 (d, 1H, J = 14.5 Hz), 3.15 (s, 3H); ^{13}C NMR (125 MHz, $CDCl_3$): δ (ppm) 141.4, 139.7, 133.1, 129.7, 128.9, 128.5, 127.8, 126.8, 47.6, 45.5.

III.6. Representative NMR Spectra:

***N-(Methyl(oxo)(phenyl)-λ⁶-sulfaneylidene)benzamide (1a)*: ^{1}H NMR (500 MHz, $CDCl_3$)**

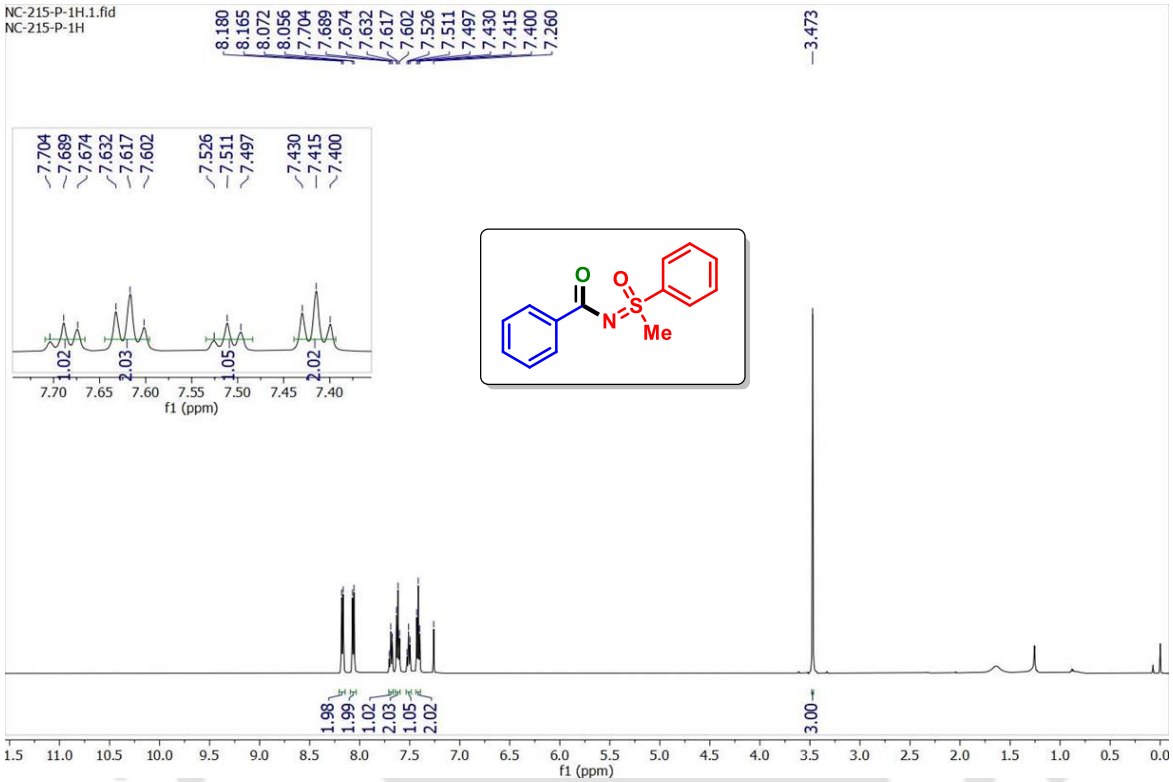

***N-(Methyl(oxo)(phenyl)-λ⁶-sulfaneylidene)benzamide (1a)*: ^{13}C NMR (125 MHz, $CDCl_3$)**

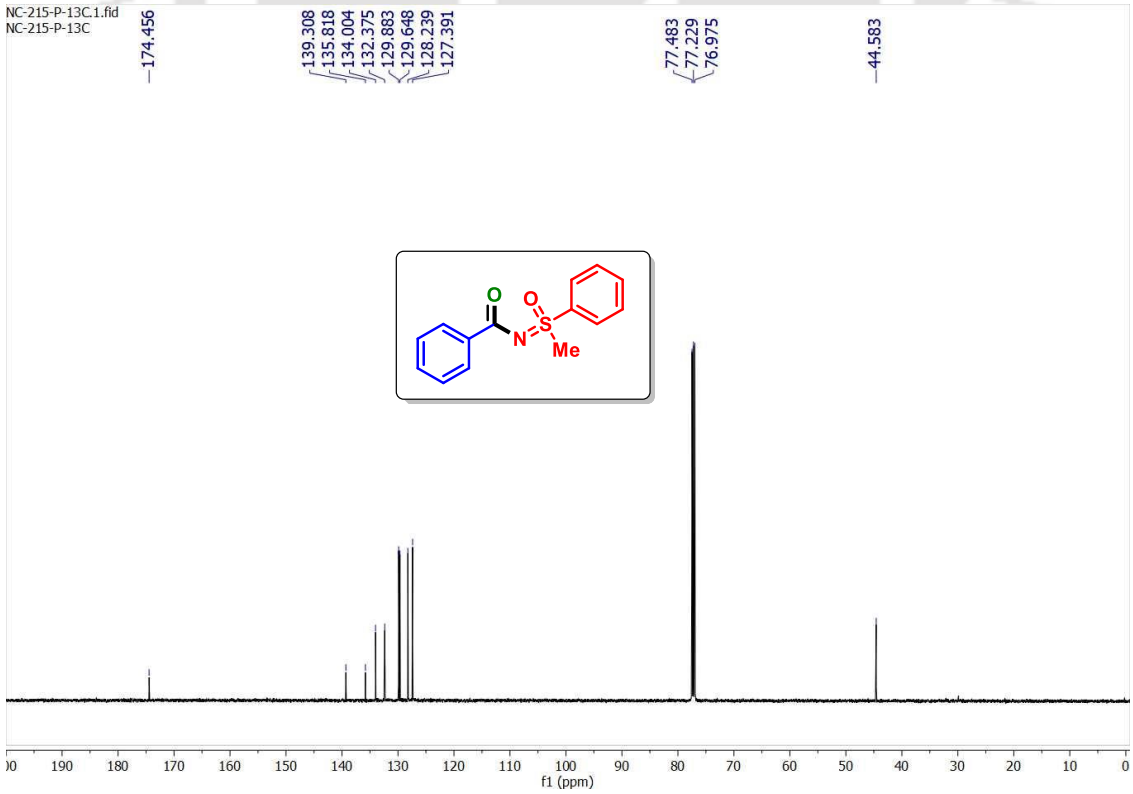

3-Methyl-N-(methyl(oxo)(phenyl)-λ⁶-sulfaneylidene)benzamide (3a): **^{1}H NMR (500 MHz, $CDCl_3$)**

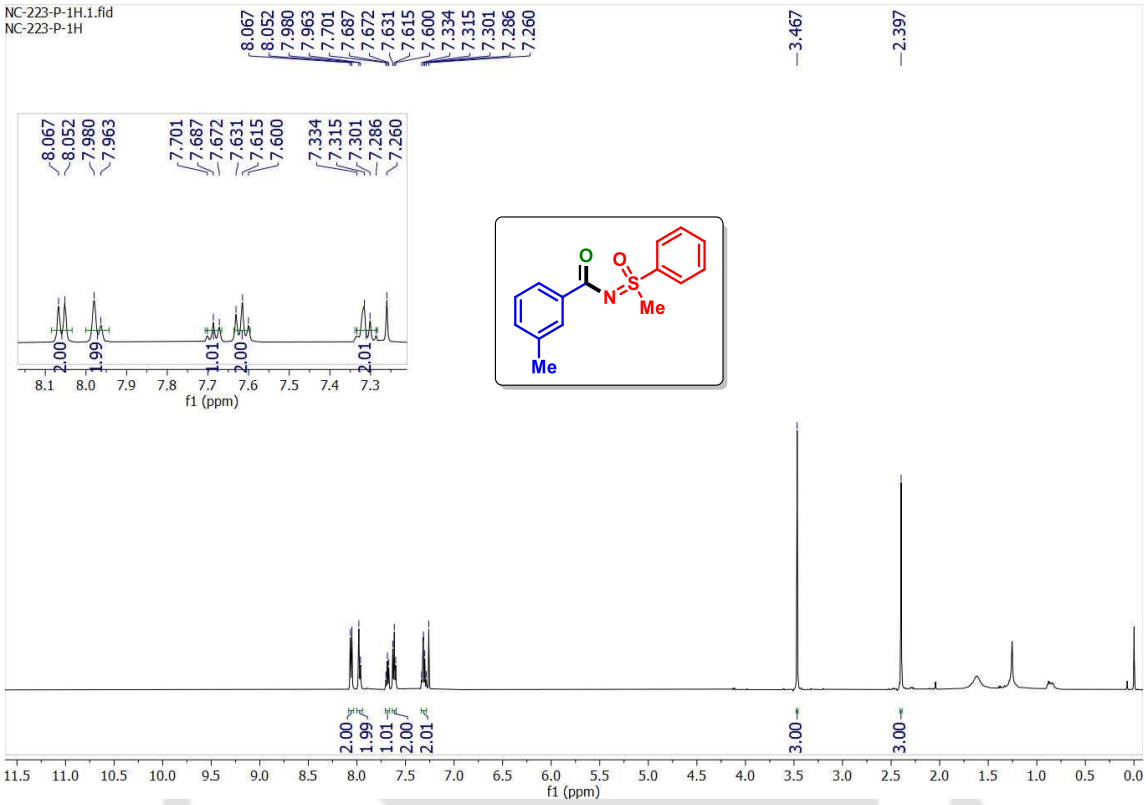

3-Methyl-N-(methyl(oxo)(phenyl)-λ⁶-sulfaneylidene)benzamide (3a): **^{13}C NMR (100 MHz, $CDCl_3$)**

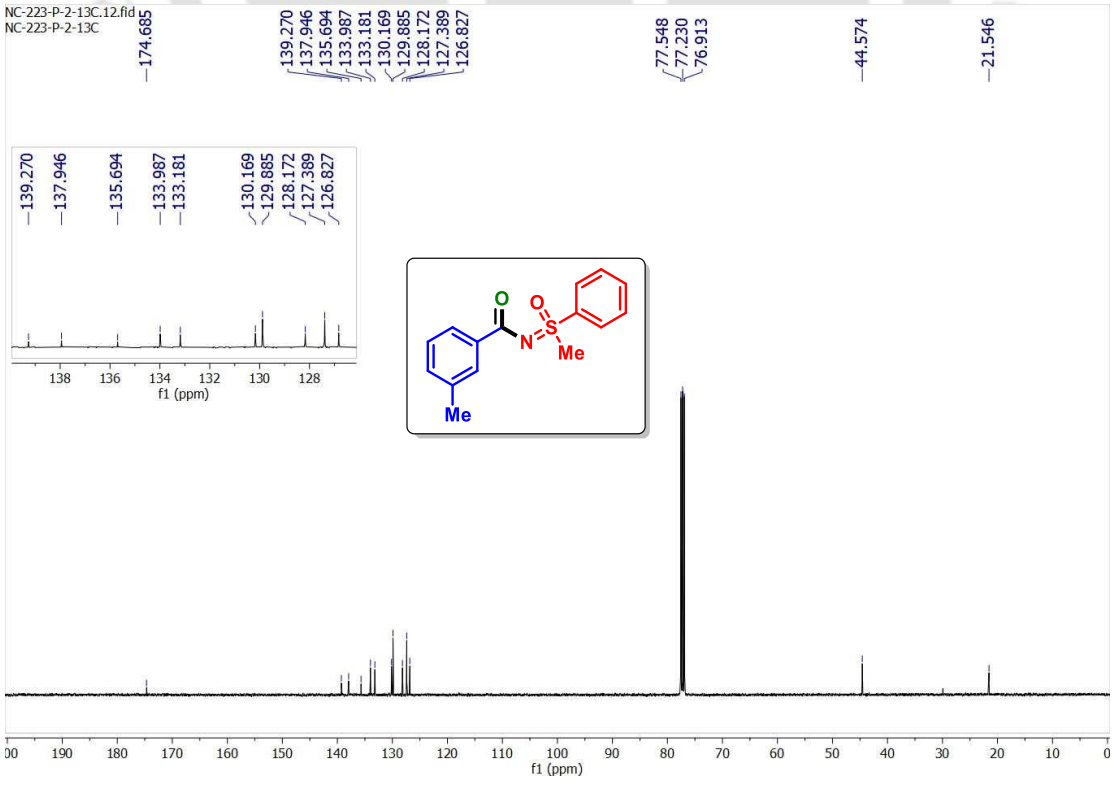

***N-(Methyl(oxo)(phenyl)-λ⁶-sulfaneylidene)-4-nitrobenzamide (10a)*: ^{1}H NMR (400 MHz, CDCl$_3$)**

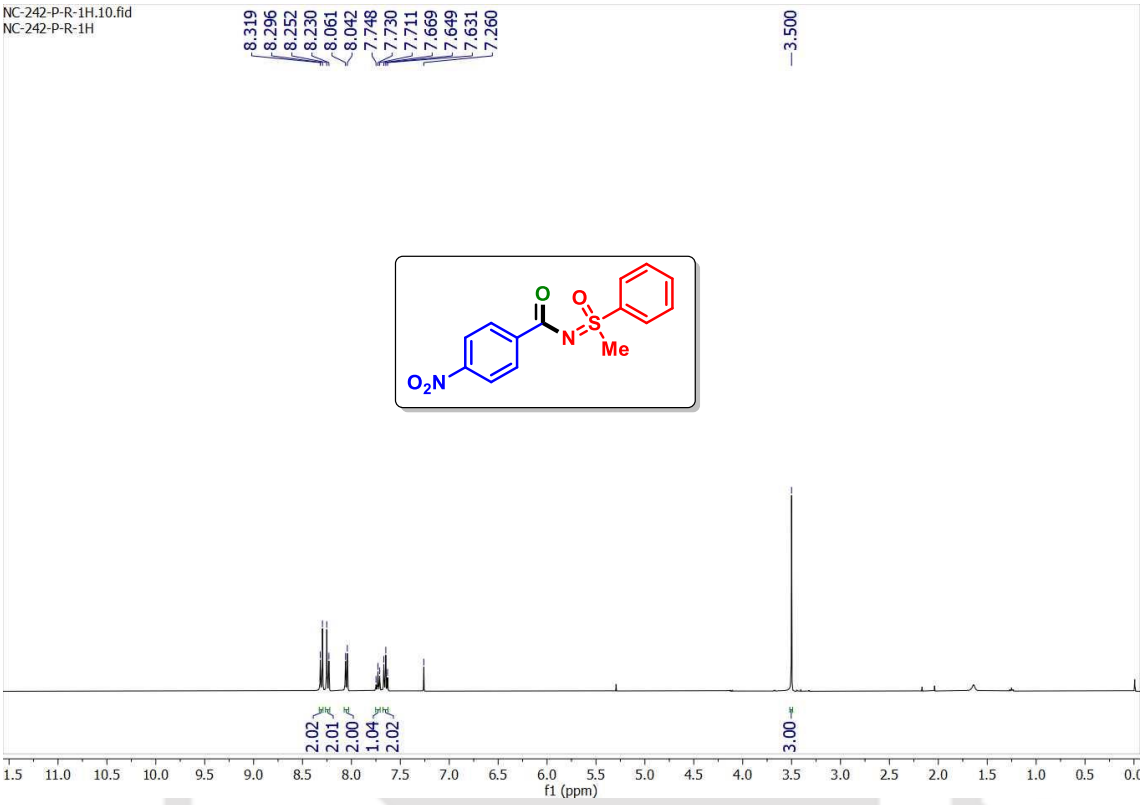

***N-(Methyl(oxo)(phenyl)-λ⁶-sulfaneylidene)-4-nitrobenzamide (10a)*: ^{13}C NMR (100 MHz, CDCl$_3$)**

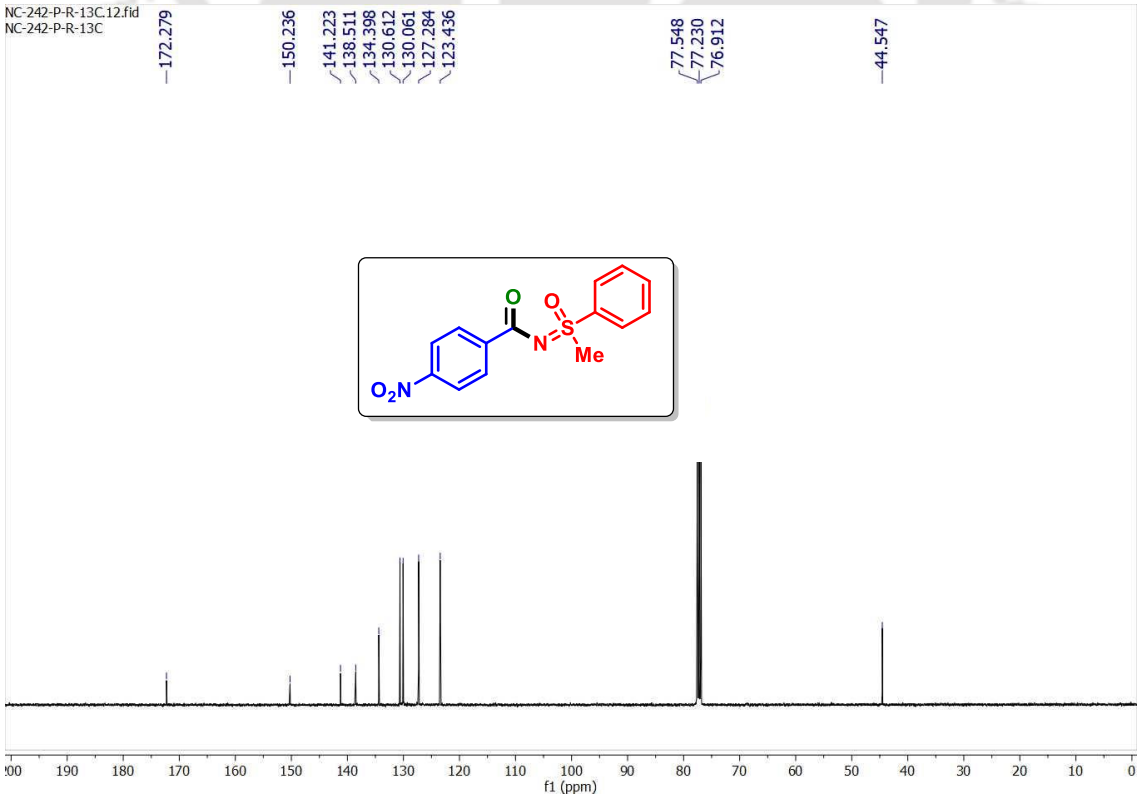

***N-((4-Ethylphenyl)(methyl)(oxo)-λ⁶-sulfaneylidene)benzamide (1c)*: ^{1}H NMR (500 MHz, $CDCl_3$)**

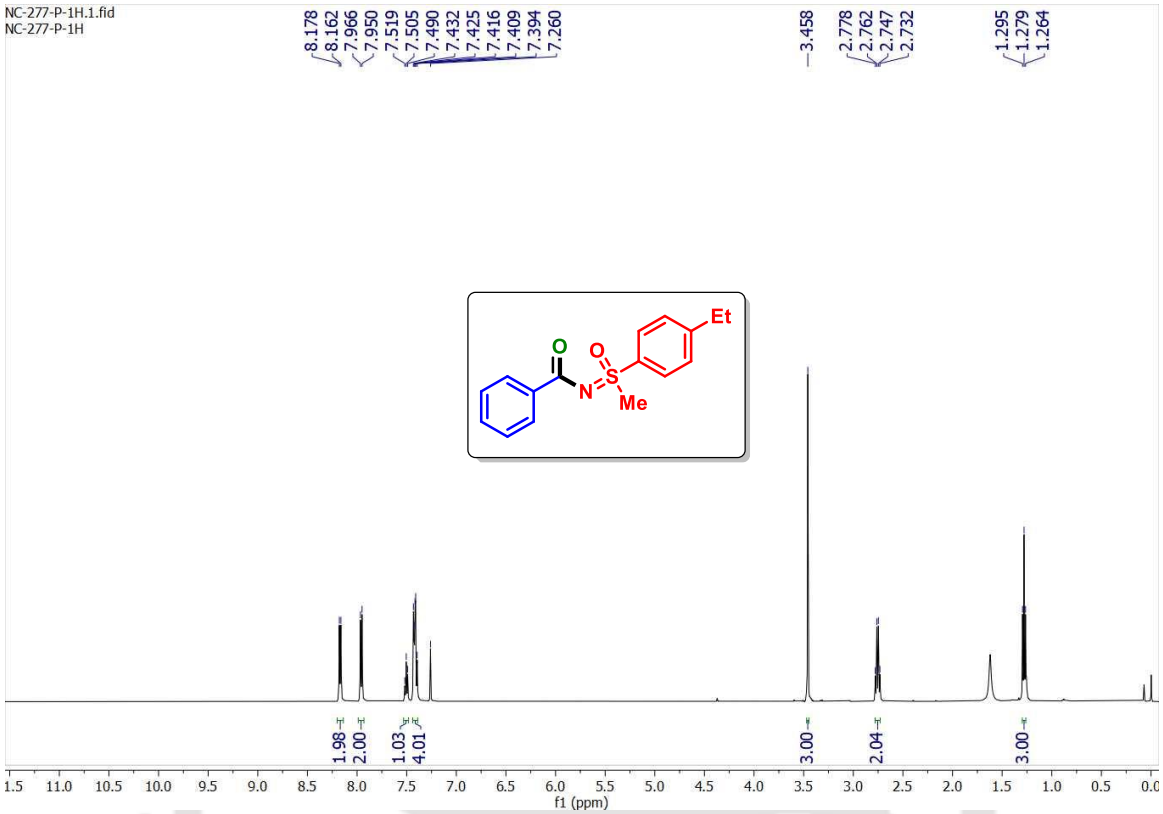

***N-((4-Ethylphenyl)(methyl)(oxo)-λ⁶-sulfaneylidene)benzamide (1c)*: ^{13}C NMR (125 MHz, $CDCl_3$)**

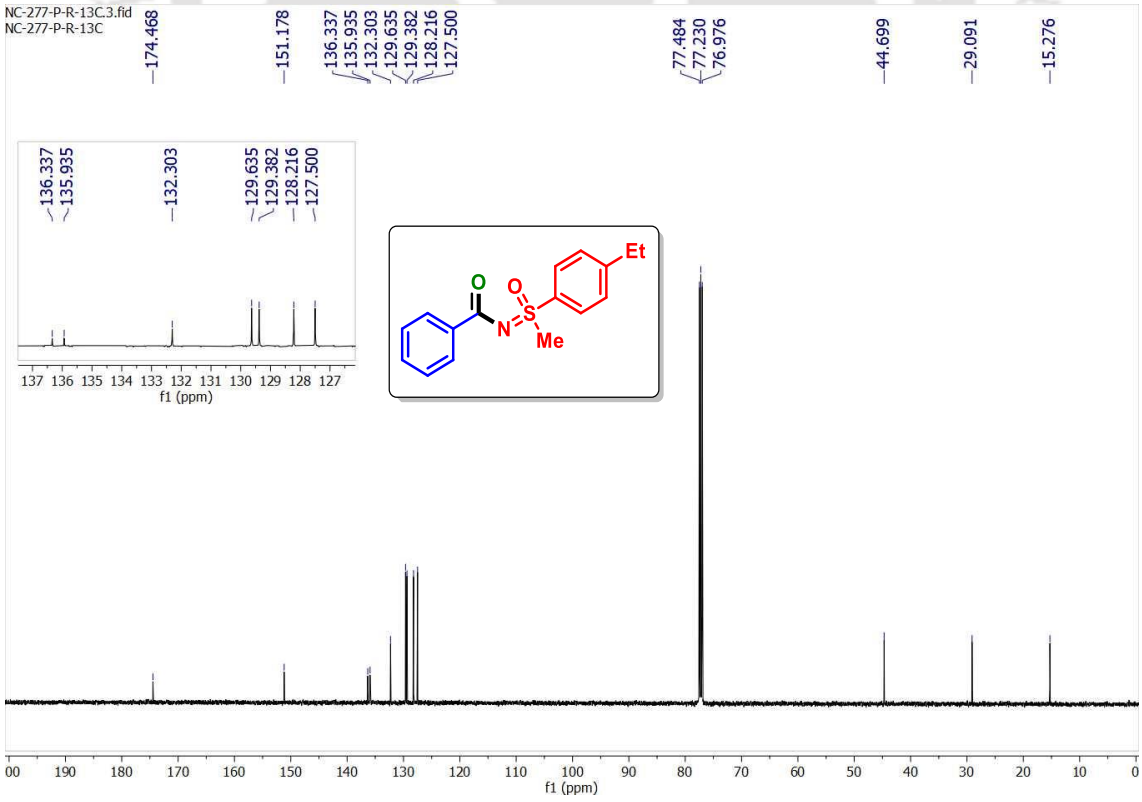

***N-(5-Oxido-5λ⁴-dibenzo[b,d]thiophen-5-ylidene)benzamide (1s)*: ^{1}H NMR (500 MHz, $CDCl_3$)**

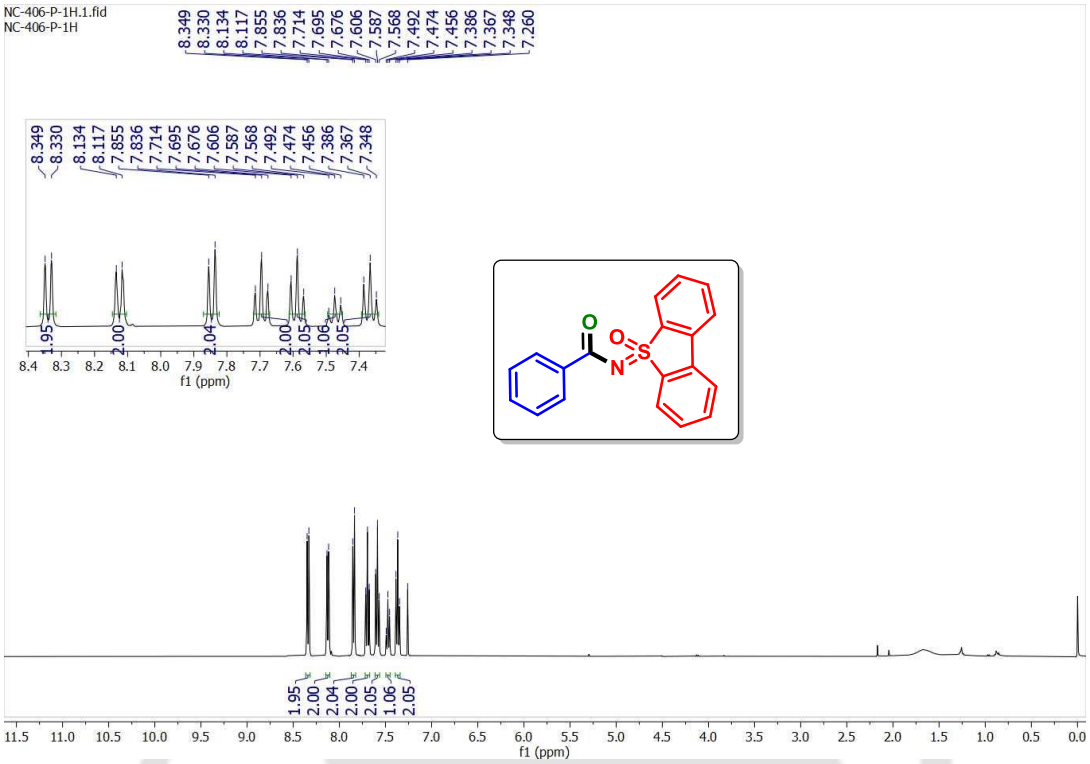

***N-(5-Oxido-5λ⁴-dibenzo[b,d]thiophen-5-ylidene)benzamide (1s)*: ^{13}C NMR (125 MHz, $CDCl_3$)**

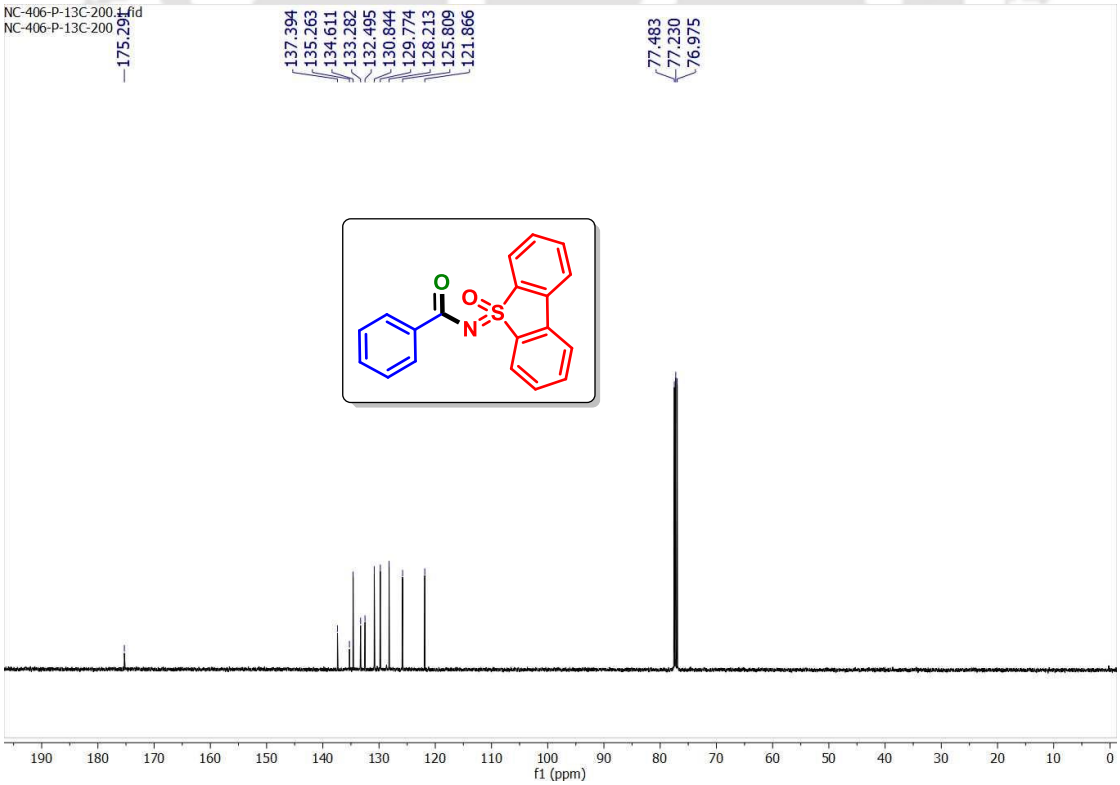

III.7. References:

(1)(a) H. M. L. Davies and D. Morton, *J. Org. Chem.*, 2016, **81**, 343–350; (b) D. J. Abrams, P. A. Provencher and E. J. Sorensen, *Chem. Soc. Rev.*, 2018, **47**, 8925–8967; (c) L. Guillemard, N. Kaplaneris, L. Ackermann and M. J. Johansson, *Nat. Rev. Chem.*, 2021, **5**, 522–545; (d) N. Holmberg-Douglas and D. A. Nicewicz, *Chem. Rev.*, 2022, **122**, 1925–2016; (e) B. Li, A. I. M. Ali and H. Ge, *Chem*, 2020, **6**, 2591–2657.

(2)(a) R. Vanjari and K. N. Singh, *Chem. Soc. Rev.*, 2015, **44**, 8062–8096; (b) G. Majji, S. K. Rout, S. Rajamanickam, S. Guin and B. K. Patel, *Org. Biomol. Chem.*, 2016, **14**, 8178–8211; (c) H. Yu, Z. Li and C. Bolm, *Org. Lett.*, 2018, **20**, 2076–2079; (d) L. Hu, J. Yuan, J. Fu, T. Zhang, L. Gao, Y. Xiao, P. Mao and L. Qu, *Eur. J. Org. Chem.*, 2018, **2018**, 4113–4120; (e) J. Dong, Q. Su, D. Li and J. Mo, *Org. Lett.*, 2022, **24**, 8447–8451.

(3)(a) A. Joshi, Z. Iqbal, J. L. Jat and S. R. De, *ChemistrySelect*, 2021, **6**, 12383–12406; (b) G. Majji, S. Guin, A. Gogoi, S. K. Rout and B. K. Patel, *Chem. Commun.*, 2013, **49**, 3031–3033; (c) C. D. Clinton, C. D. Prasad, H. D. Khanal and Y. R. Lee, *Asian J. Org. Chem.*, 2021, **10**, 241–244; (d) Y.-F. Liang, X. Li, X. Wang, Y. Yan, P. Feng and N. Jiao, *ACS Catal.*, 2015, **5**, 1956–1963; (e) Y. Zhao, U. K. Sharma, F. Schröder, N. Sharma, G. Song and E. V. Van der Eycken, *RSC Adv.*, 2017, **7**, 32559–32563; (f) Z.-L. Li, P.-Y. Wu, K.-K. Sun and C. Cai, *New J Chem*, 2019, **43**, 12152–12158; (g) W. Ali, S. Guin, S. K. Rout, A. Gogoi and B. K. Patel, *Adv. Synth. Catal.*, 2014, **356**, 3099–3105; (h) W. Ali, A. Behera, S. Guin and B. K. Patel, *J. Org. Chem.*, 2015, **80**, 5625–5632.

(4) S. D. Roughley and A. M. Jordan, *J. Med. Chem.*, 2011, **54**, 3451–3479.

(5)W. Huang, S. Wang, M. Li, L. Zhao, M. Peng, C. Kang, G. Jiang and F. Ji, *J. Org. Chem.*, 2023, **88**, 17511–17520.

(6)D. L. Priebbenow and C. Bolm, *Org. Lett.*, 2014, **16**, 1650–1652.

(7)Z. Zhao, T. Wang, L. Yuan, X. Jia and J. Zhao, *RSC Adv.*, 2015, **5**, 75386–75389

(8)Y. Zou, J. Xiao, Z. Peng, W. Dong and D. An, *Chem. Commun. (Camb.)*, 2015, **51**, 14889–14892.

(9)(a) Y. Tu, P. Shi and C. Bolm, *Org. Lett.*, 2022, **24**, 907–911; (b) Y. Tu, D. Zhang, P. Shi, C. Wang, D. Ma and C. Bolm, *Org. Biomol. Chem.*, 2021, **19**, 8096–8101; (c) N. Chakraborty, K. K. Rajbongshi, A. Dahiya, B. Das, A. Vaishnani and B. K. Patel, *Chem. Commun.*, 2023, **59**, 2779–2782

(10) A. Zupanc and M. Jereb, *J. Org. Chem.*, 2021, **86**, 5991–6000.

(11) C. M. M. Hendriks, R. A. Bohmann, M. Bohlem and C. Bolm, *Adv. Synth. Catal*., 2014, **356**, 1847–1852.

(12) (a) Y. Zhu, L.-D. Shao, Z.-T. Deng, Y. Bao, X. Shi and Q.-S. Zhao, *J. Org. Chem*., 2018, **83**, 10166–10174; (b) T. K. Achar, S. Maiti and P. Mal, *Org. Biomol. Chem*., 2016, **14**, 4654–4663; (c) T. Kuribara, M. Nakajima and T. Nemoto, *Org. Lett*., 2020, **22**, 2235–2239.

(13) (a) Z. Liu, J. Zhang, S. Chen, E. Shi, Y. Xu and X. Wan, *Angew. Chem. Int. Ed.*, 2012, **51**, 3231–3235; (b) T. Alam and B. K. Patel, *Chem. Eur. J*., 2023, **30**, e202303444.

Chapter IV

Base-Promoted Synthesis of S-Arylisothiazolones via Intramolecular Dehydrative Cyclization of α-Keto-N-acylsulfoximines

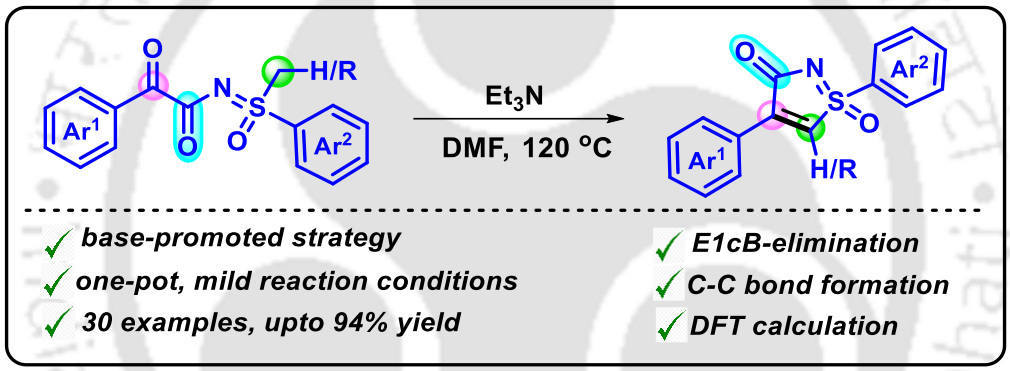

JOC The Journal of Organic Chemistry

J. Org. Chem., 2023, **89**, 778-783

Abstract: *A base (Et_3N)-promoted synthesis of 1,4-diarylisothiazolones from α-keto-N-acylsulfoximines has been achieved. The reaction proceeds via α-hydrogen abstraction from sulfoximine, followed by an intramolecular nucleophilic attack at the keto carbonyl to form a tert-hydroxy isothiazolone intermediate. The 1,4-substituted isothiazolone is obtained after dehydration via an E1cB path. This one-pot synthesis of isothiazolinones has a broad substrate scope, high atom economy, and provides products with good yields. The $\Delta E_{LUMO-HOMO}$ is calculated using Gaussian 16 at the B3LYP/6-31G (d, p) level of theory.*

भारतीय प्रौद्योगिकी संस्थान गुवाहाटी
Indian Institute of Technology Guwahati

CHAPTER IV

Base-Promoted Synthesis of *S*-Arylisothiazolones *via* Intramolecular Dehydrative Cyclization of α-Keto-*N*-acylsulfoximines

IV.1. Introduction:

Heterocyclic skeletons having sulfur and nitrogen as core elements are the subject of long-standing interest owing to their widespread presence in different pharmaceuticals, bioactive compounds, and functional materials.[1] In this context, isothiazole exhibits valuable biological properties, including antimicrobial, antibacterial, antifungal, antiviral, anticancer, and anti-inflammatory activities. Structurally, isothiazoles are 5-membered heterocycles, having two electronegative atoms (sulfur and nitrogen) in a 1,2-relationship. This subtle structure contributes to their distinct properties and versatile applications in various scientific and industrial domains. Over time, isothiazoles have been identified as inhibitors of proteases for treating anxiety and depression, as well as inhibitors of aldose reductase and 5-hydroxytryptamine receptor antagonists.[2] The significant biological effects observed for isothiazole-containing compounds have sparked interest in drug discovery programs. This has led to a steady increase in related patent applications and the successful introduction of isothiazole-based derivatives in the market.[2]

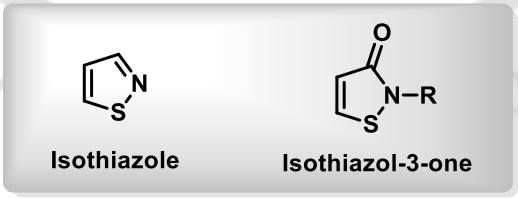

Figure IV.1.1. *Representative structure of isothiazole and isothiazol-3-one.*

Among the derivatives of isothiazoles, isothiazolin-3-ones finds extensive application in industries, including pharmaceuticals and agrochemicals, and as reactive intermediates in the synthesis of various organic compounds. Isothiazol-3-ones are renowned for their notable antifungal and antibacterial properties, making them extensively utilized biocides in various industrial water treatment applications to control microbial growth and biofouling. They are

also used as preservatives to inhibit fungal growth in various manufactured goods, including emulsion paints, wood varnishes, adhesives, and natural and artificial leather. Commonly found isothiazolones in commercial applications, either alone or in combination, include methylisothiazolinone (MI), methylchloroisothiazolinone (MCI), benzisothiazolinone (BIT), octylisothiazolione (OIT), and dichlorocthylisothiazolinone (DCOIT) (Figure IV.1.2).[3]

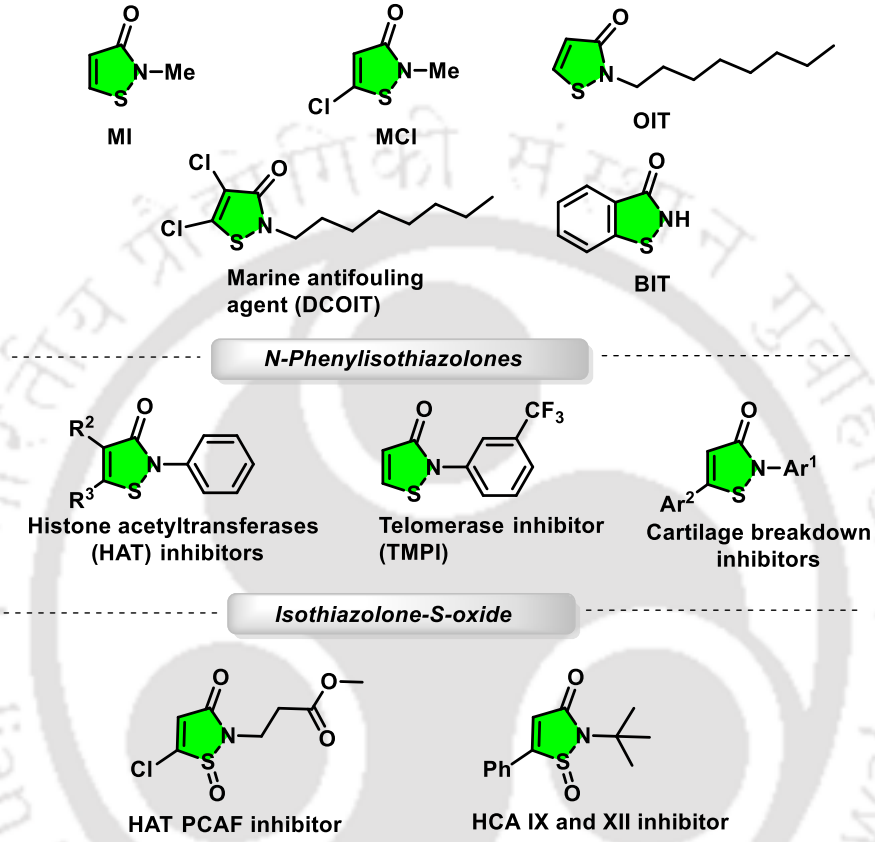

Figure IV.1.2. *Representative example of bioactive isothiazolone-containing compounds.*

Methylisothiazolinone (MI) is frequently used in wastewater treatment processes, cosmetics, paints, and detergents, often combined with MCI (in a 3:1 ratio) as a critical component of the commercial biocide Kathon. Although BIT and OIT are prohibited in cosmetics, they are commonly employed in cleaning and leather products, respectively, and in antifouling coating agents. DCOIT, found in SeaNine 211, is a widely utilized antifouling agent to combat the undesirable biofouling phenomenon.[3] Further, substituted *N*-phenylisothiazolones act as inhibitors of histone acetyltransferase, telomerase, and cartilage destruction enzymes.[4] Moreover, isothiazolone-*S*-oxides also exhibit numerous biological activities, with a potential role in the inhibition of PCAF histone acetyltransferase and tumor-associated carbonic anhydrase (hCA IX and XII).[5]

IV.2. Previous Approaches to Access Isothiazolones:

The rich chemistry, biological properties, and profound application of these heterocycles have garnered enormous interest in developing more sustainable, efficient, and cost-effective methodologies for their synthesis. Over time, researchers have disclosed diverse multistep strategies to access substituted isothiazolones, from various prefunctionalized starting materials.[2a,6] The traditional synthetic methods for producing isothiazolinones involve various oxidative cyclization reactions. These methods include the oxidative cyclization of 3,3'-dithiopropionamides using oxidants such as Cl_2, $SOCl_2$, or SO_2Cl_2. Another approach is the reaction of 3-aroylpropionic amides with $SOCl_2$ (Scheme IV.2.1).[6]

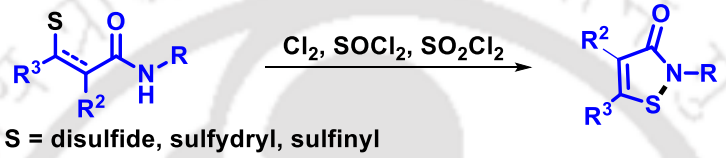

Scheme IV.2.1. *Traditional approaches using various reagents.*

In 2017, the Reddy group disclosed that ynamides can undergo thiocyanation with KSCN, followed by decyanative intramolecular amido cyclization to form isothiazolones (Scheme IV.2.2).[7]

Scheme IV.2.2. *Synthesis of isothiazolones from ynamides.*

Zhang's group, in 2019, reported a Cu(II)-catalyzed thioannulation of propynamides with sodium sulfide as an effective strategy for the synthesis of 5-substituted isothiazolones. The reaction proceeds *via* nucleophilic addition and intramolecular cross-dehydrogenative coupling resulting in the desired products with good functional group tolerance. (Scheme IV.2.3).[8]

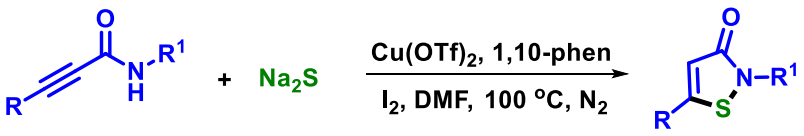

Scheme IV.2.3. *Intramolecular thioannulation of propynamides.*

In 2019, Besset *et al.* disclosed a methodology for synthesizing isothiazolones *via* Pd-catalyzed C–H bond functionalization of acrylamides. The reaction utilizes an electrophilic

SCN source leading to an array of functionalized isothiazolones in good yields. (Scheme IV.2.4).[9]

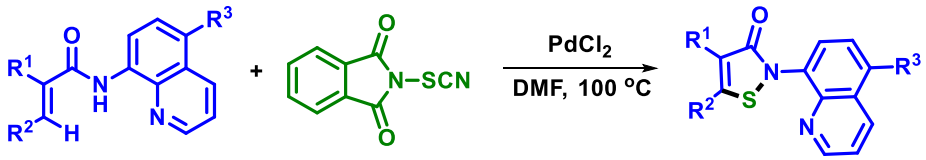

Scheme IV.2.4. *C–H functionalization of acrylamides.*

Li and Song in 2021, developed an efficient protocol for forming highly substituted isothiazolones *via* Selectfluor-mediated intramolecular oxidative annulation of α-carbamoyl ketene dithioacetals. This metal-free approach utilizes water during the new N–S bond formation and the elimination of the alkyl group from the S atom. (Scheme IV.2.5).[6c]

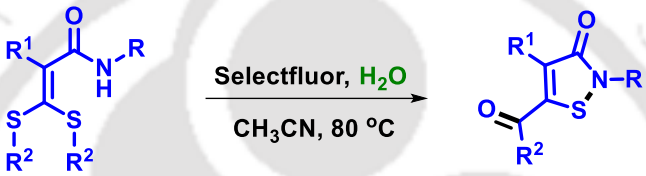

Scheme IV.2.5. *Selectfluor-mediated synthesis of highly substituted isothiazolones.*

IV.3. Present Work:

Although notable developments have been achieved in this field, the exploration of efficient methodologies to access isothiazolones with structural variations at the sulfur site remains elusive. Hence, leveraging from the previous reports, we envisioned a strategy for the synthesis of isothiazolones *via* base-promoted intramolecular cyclization of our previously synthesized α-keto-*N*-acylsulfoximine which has an acidic proton (*S*-methyl) and an appropriately placed electrophilic carbonyl functionality. For the initial reaction, a mild base was selected, which was based on the fact that a strongly electron-withdrawing dicarbonyl group would enhance the acidity of the α-carbon, facilitating its easy deprotonation. To synchronize this assumption, a reaction was carried out with α-keto-*N*-acylsulfoximine (**10**) in the presence of Et_3N (2 equiv) in DMF at 100 °C. As envisaged, a new product was obtained in 66% yield after being heated for 24 h. The spectroscopic analysis (^1H and $^{13}C\{^1H\}$ NMR and X-ray diffraction) revealed the structure of the product to be 1-(3-chlorophenyl)-4-phenyl-3H-1λ^6-isothiazol-3-one 1-oxide (**10a**). The formation of this novel class of isothiazolone with variation at the C–4 and S–positions is appealing, considering the unique structural attributes and rich chemistry of the moiety.

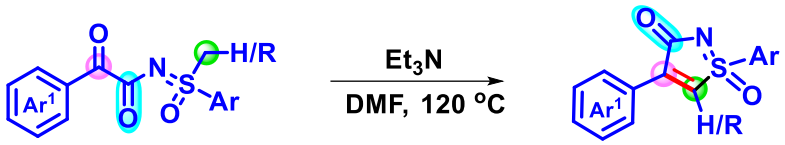

Scheme IV.3.1. *Our approach.*

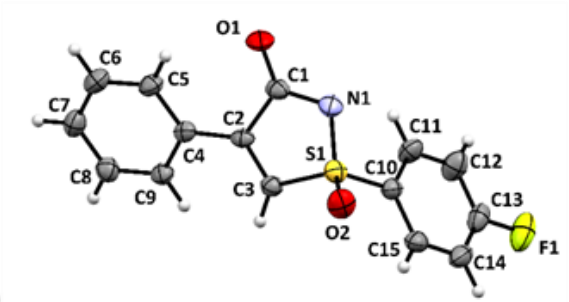

Figure IV.3.1. ORTEP diagram ***1-(4-fluorophenyl)-4-phenyl-3H-1λ^6-isothiazol-3-one 1-oxide*** (**6a**) with 30% ellipsoid probability (CCDC 2289663).

IV.3.1. Optimization of Reaction Conditions:

Intrigued by this outcome, further optimization of various reaction parameters such as base, solvent, and temperature were carried out using *N*-((3-chlorophenyl)(methyl)(oxo)- λ^6-sulfaneylidene)-2-oxo-2-phenylacetamide (**10**) as the test substrate. Initially, we began our investigation by varying different bases, including both organic and inorganic bases such as *N*,*N*-diisopropylethylamine (DIPEA), 1,4-diazabicylco[2.2.2]octane (DABCO), 1,8-diazabicyclo[5.4.0]undec-7-ene (DBU), pyridine, Cs_2CO_3, KOH, and KO^{t}Bu (Table IV.3.1, entries 2-8). Amongst the organic bases screened, DIPEA and DABCO, which have comparable basic character to Et_3N were successful in forming the products in lower yields, but DBU and pyridine completely failed to result in the product. The possible reason for the failure of the latter two bases could be the lower basicity of pyridine and steric congestion in DBU making it difficult for proton abstraction. Inorganic bases, such as Cs_2CO_3, KOH, and KO^{t}Bu, completely failed to form the isothiazolone product. The reaction failure for Cs_2CO_3 and KOH can be attributed to competing nucleophilic reactions with the carbonyl functionality. In the case of KO^{t}Bu, the reaction may fail because of steric reasons. Next, changing the amount of the Et_3N had a major effect on the product yield and the reaction time. Increasing the base loading to 5 equiv, 7 equiv, and 10 equiv led to the improvement in the product yield to 76%, 83%, and 86%, respectively, along with a subsequent decrease in the reaction time (Table IV.3.1, entries 9-11). Hence, all further optimization of different reaction parameters was carried out by using 7 equiv of Et_3N. Next, different solvents such as DMSO, CH_3CN,

EtOH, DCE, 1,4-dioxane, and toluene were screened (Table IV.3.1, entries 12-17). However, none of these solvents proved to be beneficial for the transformation and hence DMF was considered to be the best compatible solvent for this protocol.

Table IV.3.1. *Optimization of the reaction conditions*[a,b]

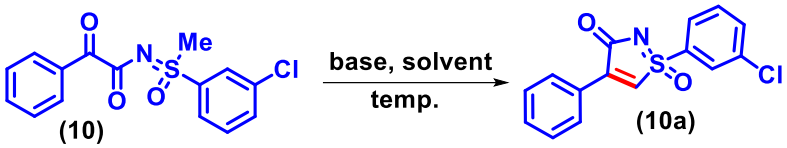

(10) (10a)

entry	base (equiv)	solvent	temperature (°C)	yield (%)[b]
1	Et_3N (2)	DMF	100	66
2	DIPEA (2)	DMF	100	42
3	DABCO (2)	DMF	100	39
4	DBU (2)	DMF	100	n.d.
5	Pyridine (2)	DMF	100	n.d
6	Cs_2CO_3 (2)	DMF	100	n.d
7	KOH (2)	DMF	100	n.d
8	KO^{t}Bu (2)	DMF	100	trace
9	Et_3N (5)	DMF	100	76
10	Et_3N (7)	DMF	100	83
11	Et_3N (10)	DMF	100	86
12	Et_3N (7)	DMSO	100	75
13	Et_3N (7)	CH_3CN	100	59
14	Et_3N (7)	EtOH	100	38
15	Et_3N (7)	DCE	100	trace
16	Et_3N (7)	1,4-Dioxane	100	trace
17	Et_3N (7)	Toluene	100	43
18	Et_3N (7)	DMF	60	trace
19	Et_3N (7)	DMF	80	54
20	**Et_3N (7)**	**DMF**	**120**	**92**
21	Et_3N (7)	DMF	140	78

[a]Reaction conditions: (**10**) (0.2 mmol), base (equiv), solvent (1.5 mL) for 6 h in a sealed tube under air. [b]Yield of the isolated product. n.d. = not detected.

To check the effect of temperature, the reaction was performed both at higher and lower temperatures, such as 60 °C, 80 °C, 120 °C, and 140 °C (Table IV.3.1, entries 18-21). Lowering the temperature to 60 °C had a detrimental effect on the reaction, with no product formation within the stipulated time. Performing the reaction at 80 °C led to a decrease in the product yield (54%), while increasing the temperature to 120 °C was beneficial for the transformation resulting in product **10a** in 92% yield. However, a further increase of the temperature to 140 °C gave a multitude of side products. Therefore, after a detailed optimization study it was concluded that the best condition for this base-promoted cyclization is the use of α–keto-*N*-acylsulfoximine (**10**) (1 equiv), Et_3N (7 equiv) in 1.5 mL DMF at 120 °C.

IV.3.2. Substrate Scope:

With the set conditions, the scope of this intramolecular dehydrative cyclization protocol was explored for a variety of α-keto-*N*-acylsulfoximines. We began our investigation by analyzing the effect of substituents on the phenyl ring toward the sulfoximidoyl part of α-keto-*N*-acylsulfoximines while keeping the other phenyl ring fixed (Scheme IV.3.2.1). Electron-neutral (**1**), as well as electron-donating substituents such as *p*-Me (**2**), *p*-Et (**3**), *m*-OMe (**4**), and sterically congested *o*-Me (**5**), successfully resulted in the respective products **1a**–**5a** in good yields of 85–91%. The methodology was equally successful for moderately electron-withdrawing halo-groups, *p*-F (**6**), *p*-Cl (**7**), *p*-Br (**8**), *m*-F (**9**), *m*-Cl (**10**) resulting in the products with good to excellent yields, **6a** (83%), **7a** (91%), **8a** (87%), **9a** (91%), and **10a** (92%), respectively. The structure of **6a** has been ascertained by single-crystal X-ray crystallography (CCDC 2289663) and is presented in Figure IV.3.1. Further, the efficacy of the reaction was tested with strongly electron-withdrawing substituents such as *p*-CF_3 (**11**), *p*-CN (**12**), and *p*-NO_2 (**13**), all of which led to the products in good yields (**11a**, 88%, **12a**, 94% and **13a**, 81%). These observations indicated that the transformation proceeded well for all types of substituents on R^1 having diverse electronic or steric effects. This protocol was also successful for polyaromatic-derived sulfoximine **14**, containing a naphthyl analogue resulting in product **14a** in 87% yield. Moreover, α-keto-*N*-acylsulfoximines having a secondary carbon center adjacent to the *S*-atom, that is, benzylic, also underwent smooth conversion to the isothiazolone products. However, the reactivity in such substrates greatly depended on the electronic nature of the substituents attached to the phenyl ring. For instance, electron-donating *p*-Me substituted substrate (**15**) resulted in the product **15a** in 69% yield, but electron-withdrawing *p*-F (**16**) and *p*-CF_3 (**17**) substrates efficiently delivered the corresponding

isothiazolone (**16a**, 78% and **17a**, 85%) in comparatively higher yields. However, the reaction was unsuccessful for the *S*-ethyl (**18**) and *S*-propyl (**19**) derived substrates. The possible reason for such failures could be the decrease in the carbanion stability of the α–carbon attached to the *S*-atom (Scheme IV.3.2.1).

Scheme IV.3.2.1. *Substrate scope of various* α*-Keto-N-acylsulfoximines*[a,b]

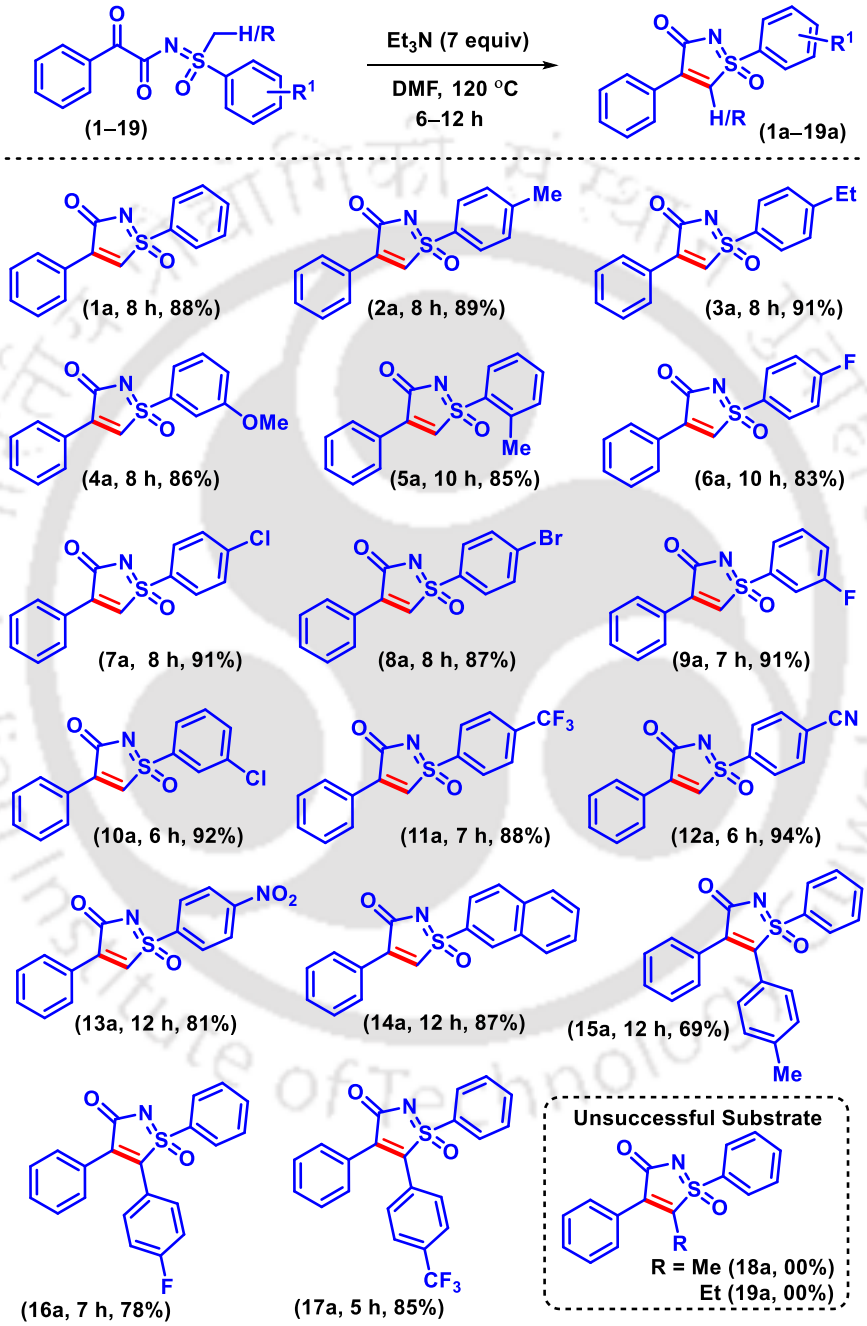

[a]Reaction conditions: (**1**–**19**) (0.2 mmol), Et_3N (1.4 mmol), DMF (1.5 mL) at 120 °C for 6–12 h in a sealed tube under air. [b]Yield of the isolated product.

Next, the effect of substituents on the phenyl ring on the carbonyl side of α-keto-*N*-acylsulfoximines was investigated and presented in Scheme IV.3.2.2. Electron-donating groups such as *p*-Me (**20**), *m*-Me (**21**), *p*-OMe (**22**), and *m*-OMe (**23**) successfully resulted in the products **20a** (78%), **21a** (81%), **22a** (77%), and **23a** (83%), respectively. Moderately electron-withdrawing groups such as *p*-F (**24**) and *p*-Br (**25**) underwent successful conversion to the products **24a** (82%) and **25a** (71%), respectively. The presence of an electron-withdrawing group in a sterically hindered position such as in *o*-Br (**26**) resulted in product **26a** albeit in a slightly lower yield of 57%.

Scheme IV.3.2.2. *Substrate scope of various* α*-Keto-N-acylsulfoximines*[a,b]

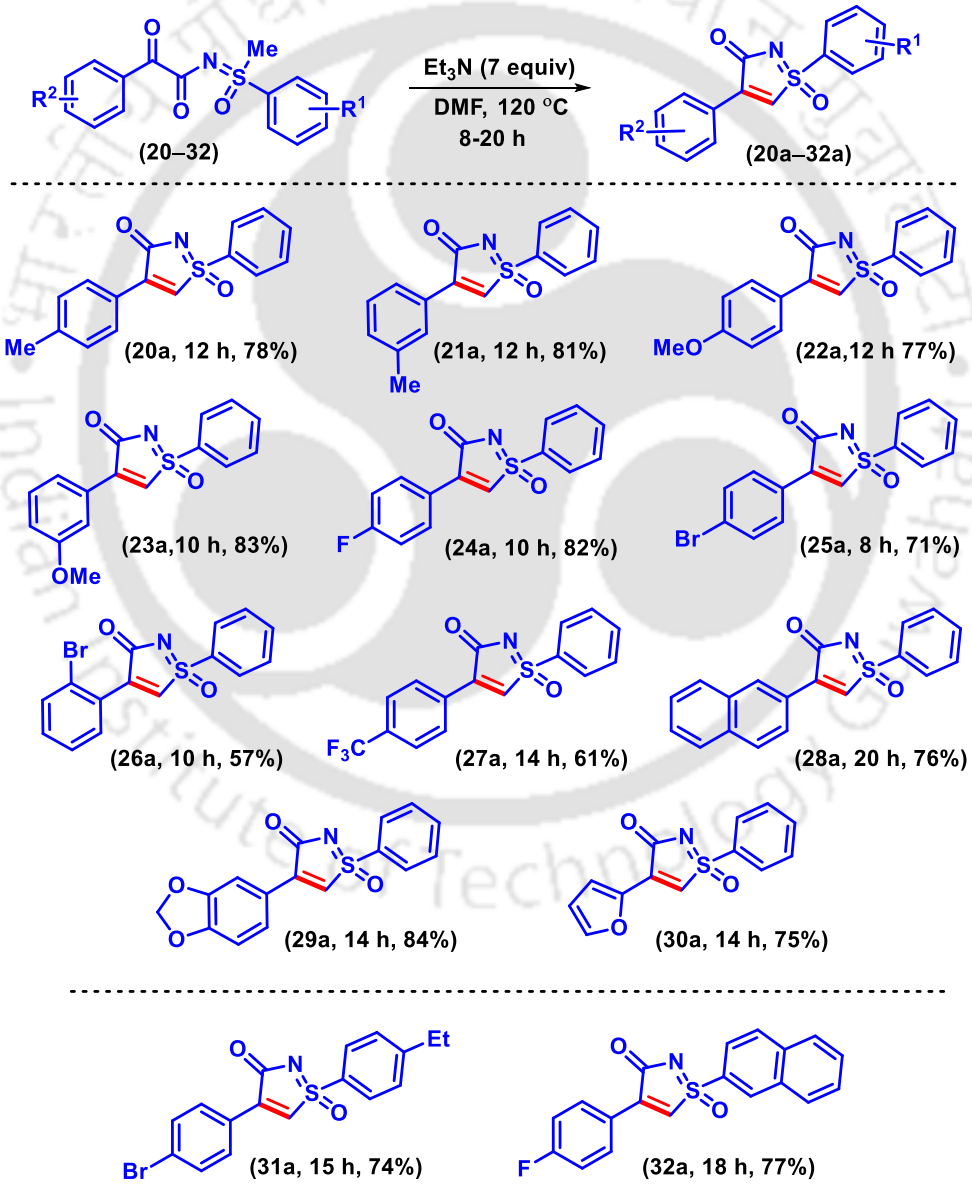

[a]Reaction conditions: (**20**–**32**) (0.2 mmol), Et_3N (1.4 mmol), and DMF (1.5 mL) at 120 °C for 8–20 h in a sealed tube under air. [b]Yield of the isolated product.

The given transformation efficaciously proceeded for a strongly electron-withdrawing –CF_3 group (**27**) forming the product **27a** in 61% yield (Scheme IV.3.2.2). Furthermore, the given transformation was successful for polyaromatic derived substrates having a naphthyl group (**28**) as well as for methylene dioxy-containing substrate (**29**), yielding the products **28a** and **29a** in good yields of 76% and 84%. Moreover, heteroaryl-derived α-keto-*N*-acylsulfoximine (**30**) resulted in the desired isothiazolone **30a** in 75% yield. α-Keto-*N*-acylsulfoximines with variations on both of the phenyl rings such as *p*-Br/*p*-Et (**31**) and *p*-F/naphth (**32**) were well compatible under the given set of conditions and resulted in the isothiazolones **31a** and **32a** in 74% and 77% yields, respectively (Scheme IV.3.2.2).

IV.3.4. Plausible Mechanism:

The possible mechanistic rationale of this intramolecular cyclization protocol is as follows (Scheme IV.3.4).[10,11] In the presence of Et_3N one of the protons on the *S*-methyl is deprotonated to form a carbanionic intermediate **A**.[11] The C-nucleophile (carbanion) then attacks the more electrophilic keto-carbonyl group intramolecularly and forms the cyclic intermediate **B**. The formation of either intermediate **A** and/or **B** has been confirmed by HRMS analysis of the reaction mixture (Figure IV.4.4). Protonation of the anionic counterpart with elimination of Et_3N gives the intermediate **C**. The formation of product **1a** from hydroxy intermediate **C** proceeds *via* an E1cB mechanism, wherein, the abstraction of another α-H results in the carbanion intermediate **D**, which is stabilized by the neighboring sulfoxide group.[11d] Finally, the leaving –OH group departs from **D** to give the isothiazolone (**1a**).

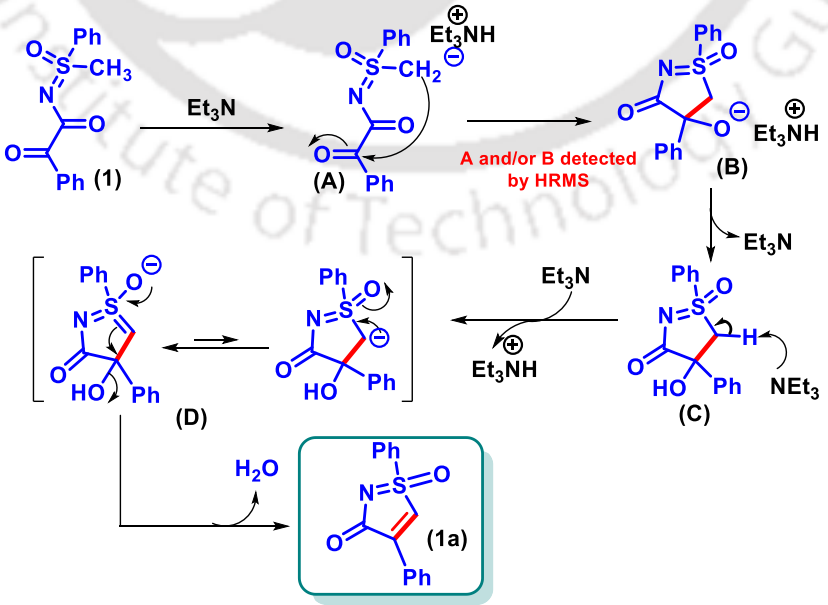

IV.3.4. *Plausible mechanistic rationale.*

IV.3.5. Scale-up Reaction:

To demonstrate the scalability of the reaction, a gram-scale reaction of **1** (3.5 mmol, 1.004 g) was conducted in an identical reaction setup. To our delight, the reaction successfully resulted in product **1a** in 71% yield (Scheme IV.3.5).

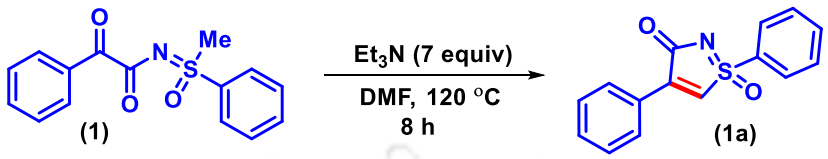

Scheme IV.3.5. *Scale-up reaction for the synthesis of isothiazolone (**1a**).*

IV.3.6. DFT Calculation:

To gain insight into the geometry and electronic structure of the isothiazolone core, density functional theory (DFT) calculations were performed with a B3LYP/6-31G (d, p) level of theory in DMF solvent modeled by the polarizable continuum model (PCM) approach (the Gaussian 16 program).[12] The density functional theory (DFT) calculation of **1a** reveals that the electron density in the highest occupied molecular orbital (HOMO) is mainly localized at the phenyl ring on the 4-position of isothiazolone with minor contributions from the central isothiazolone core (Figure IV.3.6.1). The lowest unoccupied molecular orbital (LUMO) is localized at the central isothiazolone core with minor contributions from the two phenyl rings. The computed HOMO−LUMO energy gap of **1a** is found to be 4.35 eV. Because the HOMO is localized at the C-4 phenyl moiety, the presence of electron-donating substituents such as *p*−OMe (**22a**) *via* a +I or +M effect is expected to decrease the HOMO−LUMO energy gap in **22a** as compared to the unsubstituted analogue (**1a**). On the contrary, an electron-withdrawing group such as *p*-CF_3 (**27a**) due to its strong -I effect would increase the energy gap. The computed HOMO−LUMO energy gap of **22a** and **27a** is thus found to be 3.80 and 4.48 eV, respectively, which corroborates our supposition. The energy gap between the frontier orbitals of a few other substituted isothiazolones (**4a**, **11a**, and **23a**) was found to be in the range of 3.79−4.29 eV (Figure IV.3.6.2)

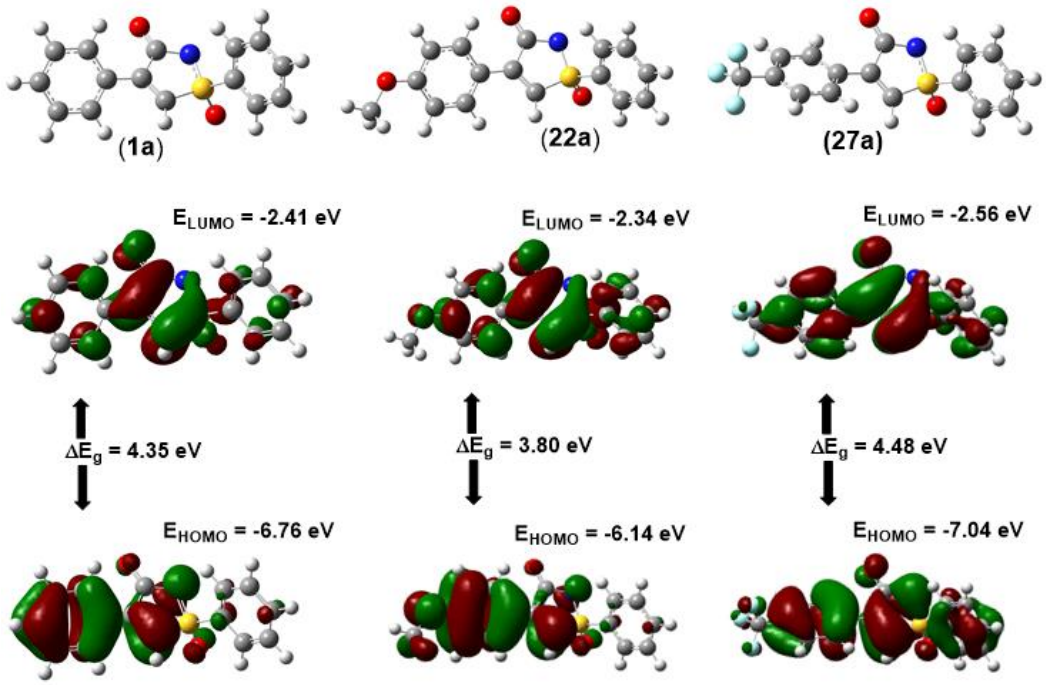

Figure IV.3.6.1. *DFT Optimized structure and Molecular orbital amplitude plots of HOMO and LUMO of **1a**, **22a**, **27a** using DFT calculation at the B3LYP/6-31G (d, p) level of theory in DMF solvent modeled by the PCM approach.*

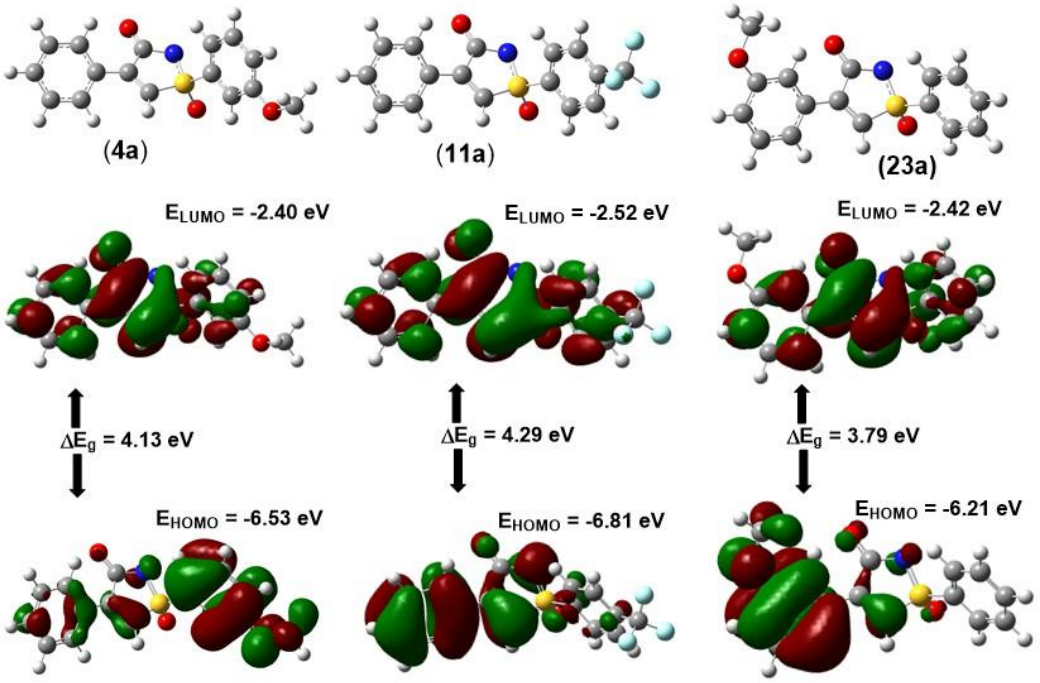

Figure IV.3.6.2. *DFT Optimized structure and Molecular orbital amplitude plots of HOMO and LUMO of **4a**, **11a**, **23a** using DFT calculation at the B3LYP/6-31G (d, p) level of theory in DMF solvent modeled by the PCM approach.*

IV.3.7. UV-Vis Measurements:

The UV−vis absorption spectra of some of the synthesized compounds **1a**, **4a**, **11a**, **12a**, **15a**, **22a**, **23a**, **27a**, and **31a** were recorded in 0.05 mM DMF solution (Figure IV.3.7). As evident from the UV−vis spectra, most compounds exhibited two distinct absorption maxima, one in the region of 270–280 nm, and the other in the 315–350 nm region. Further, the UV absorption maximum (wavelength) is in close correlation with the computationally determined $\Delta E_{\text{LUMO–HOMO}}$ values.

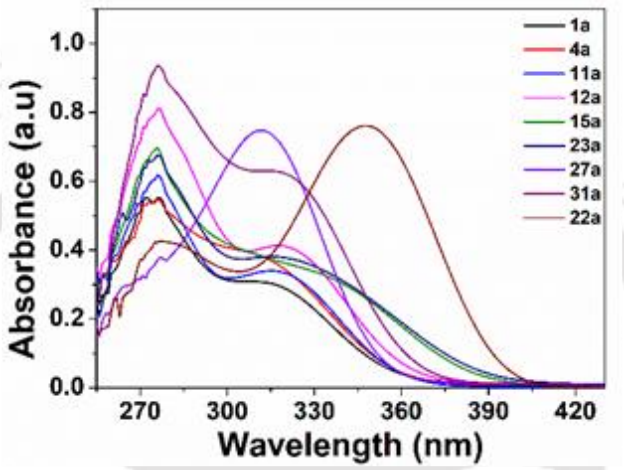

Figure IV.3.7. *UV-vis absorption spectra of a few isothiazolone derivatives in 0.05 mM DMF solution.*

IV.3.8. Conclusion:

In conclusion, an efficient method to synthesize *S*-substituted isothiazolones *via* a base-promoted intramolecular dehydrative cyclization of α-keto-*N*-acylsulfoximines is presented. The developed protocol explores the intrinsic reactivity of the α-C–H in *N*-substituted sulfoximines in the presence of triethylamine. The reaction is driven by the strongly electron-withdrawing dicarbonyl group in the starting material, which enhances the acidity of the protons for easy deprotonation. The calculated HOMO-LUMO energy gap is found in the range of 3.79–4.48 eV which is in agreement with the experimentally determined values. Isothiazolones with structural variations at the C4, and the S sites are less explored moieties and may possess notable properties and find application in diverse fields of research.

IV.4. Experimental Section:

IV.4.1. General Information:

All the reagents were commercial grade and purified according to the established procedures. All the reactions were carried out in oven-dried glassware. The highest commercial quality reagents were purchased and were used without further purification unless otherwise stated. All the cinnamic acids used in this protocol were commercially purchased from Sigma Aldrich and BLD Pharma. Reactions were monitored by thin layer chromatography (TLC) on 0.25 mm silica gel plates ($60F_{254}$) visualized under UV illumination at 254 nm. Organic extracts were dried over anhydrous sodium sulfate (Na_2SO_4). Solvents were removed using a rotary evaporator under reduced pressure. Column chromatography was performed to purify the crude product on silica gel 60–120 mesh using a mixture of hexane and ethyl acetate as eluent. The isolated compounds were characterized by spectroscopic [^{1}H, ^{13}C{1H} NMR, and IR] techniques and HRMS analysis. NMR spectra were recorded in deuterochloroform ($CDCl_3$). ^{1}H, ^{13}C{^{1}H} were recorded in 400 (100), 500 (125) or 600 (150) MHz spectrometers and were calibrated using tetramethylsilane or residual undeuterated solvent for ^{1}H NMR, deuterochloroform for ^{13}C NMR as an internal reference {$Si(CH_3)_4$: 0.00 ppm or $CHCl_3$: 7.260 ppm for ^{1}H NMR and 77.230 ppm for ^{13}C{1H}. ^{19}F NMR was calibrated without any internal standard in $CDCl_3$ in a 370, 471 or 565 MHz spectrometer. The chemical shifts are quoted in δ units, parts per million (ppm). ^{1}H NMR data is represented as follows: Chemical shift, multiplicity (s = singlet, d = doublet, t = triplet, q = quartet, dd = doublet of doublets, m = multiplet), integration and coupling constant(s) *J* in hertz (Hz). High-resolution mass spectra (HRMS) were recorded on a mass spectrometer using electrospray ionization-time of flight (ESI-TOF) reflection experiments. FT-IR spectra were recorded in neat and reported in the frequency of absorption (cm^{-1}).

IV.4.2. Crystallographic Information:

Crystallographic information of *1-(4-fluorophenyl)-4-phenyl-3H-1λ^6-isothiazol-3-one 1-oxide* (**6a**)

(i) Sample Preparation: The single crystal of compound **6a** was prepared by the slow evaporation method for which 10 mg of the compound (**6a**) was dissolved in 2 mL of hexane and 0.5 mL of EtOAc in a clean and dry 10 mL glass vial. To it, a few drops of MeOH was added. The mouth of the glass vial was covered with a cap having a small hole and kept for

slow evaporation at room temperature. Crystals of **6a** were obtained after approximately 3-4 days as a transparent block-shaped crystal.

(ii) Data Collection: Diffraction data were collected at 292 K with MoKα radiation (λ = 0.71073 Å) using a Bruker Nonius SMART APEX CCD diffractometer equipped with graphite monochromator and Apex CD camera. The SMART software was used for data collection and for indexing the reflections and determining the unit cell parameters. Data reduction and cell refinement were performed using SAINT software and the space groups of these crystals were determined from systematic absences by XPREP and further justified by the refinement results. The structures were solved by direct methods and refined by full-matrix least-squares calculations using SHELXTL-973 software. All the non-H atoms were refined in the anisotropic approximation against F2 of all reflections.

(iii) Crystallographic description of *1-(4-fluorophenyl)-4-phenyl-3H-1λ⁶-isothiazol-3-one 1-oxide* (6a)

$C_{15}H_{13}NO_3S$, colourless block shaped crystal; crystal dimensions 0.05 x 0.04 x 0.04 mm, M_r = 287.30, Orthorhombicic, space group P b c a; a = 7.418 (2), b = 11.799 (4), c = 29.299 (9) Å, α = 90°, β = 90°, γ = 90°, V = 2564.4 (14) Å^3, Z = 8, ρ_{calcd} = 1.488 g/cm^3, μ = 0.264 mm^{-1}, F(000)= 1184.0, reflection collected / unique = 2257/ 1674, refinement method = full-matrix least-squares on F^2, final R indices [I> 2\s(I)]: R_1 = 0.0423, wR_2 = 0.1341, R indices (all data): R_1 = 0.0629, wR_2 = 0.1466, goodness of fit = 1.050. **CCDC**-2289663 for *1-(4-fluorophenyl)-4-phenyl-3H-1λ⁶-isothiazol-3-one 1-oxide* (**6a**) contains the supplementary crystallographic data for this paper. These data can be obtained free of charge from The Cambridge Crystallographic Data Centre via www.ccdc.cam.ac.uk/data_request/cif.

IV.4.3. General Procedure:

IV.4.3.1. Procedure for the synthesis of α-keto-*N*-acyl sulfoximines (1):[13]

α-Keto-*N*-acyl sulfoximines are synthesized according to the two given literature procedures:

IV.4.3.2. General procedure for the synthesis of 1,4-diphenyl-3*H*-1λ⁶-isothiazol-3-one 1-oxide (1a):

To an oven-dried 15 mL pressure tube equipped with a magnetic bar was added *N*-(methyl(oxo)(phenyl)-λ⁶-sulfaneylidene)-2-oxo-2-phenylacetamide (**1**) (0.2 mmol, 57.4 mg), Et_3N (7 equiv, 1.4 mmol, 141 mg) and 1.5 mL DMF. The reaction mixture was allowed to stir at 120 °C for 8 h. After completion of the reaction as confirmed by TLC monitoring, the crude mixture was diluted by adding 20 mL ethyl acetate and washed with ice-cold water (1 x 10

mL) followed by brine solution (1 x 5 mL). The organic layer was dried over anhydrous Na_2SO_4 and concentrated under reduced pressure. The crude product thus obtained was purified over a column of silica gel using hexane and ethyl acetate (5:1) to give pure product **1a** in 88% yield (47 mg) (Scheme IV.4.3.2).

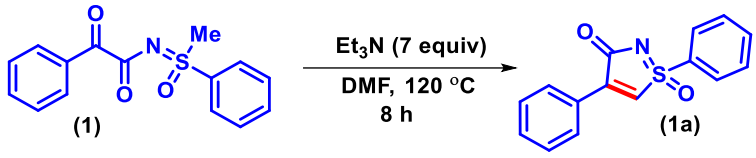

Scheme IV.4.3.2. *Synthesis of 1,4-diphenyl-3H-1λ⁶-isothiazol-3-one 1-oxide (**1a**).*

IV.4.4. Mechanistic Investigations:

Intermediate-trapping experiment:

To an oven-dried 15 mL pressure tube equipped with a magnetic bar was added *N*-(methyl(oxo)(phenyl)-λ6-sulfaneylidene)-2-oxo-2-phenylacetamide (**1**) (0.2 mmol, 57.4 mg), Et_3N (3 equiv, 0.6 mmol, 60 mg) and 1.5 mL DMF. The reaction mixture was allowed to stir at 120 °C for 3 h. A small aliquot of the reaction mixture was withdrawn at approximately 3 h and diluted with acetonitrile (1 mL) and subjected to HRMS. The HRMS analysis of this reaction aliquot shows HRMS values corresponding to intermediate **A** and/or cyclic triethylamine adduct (**B**). This observation infers the involvement of intermediate **A** or **B** in the reaction (Figure IV.4.4).

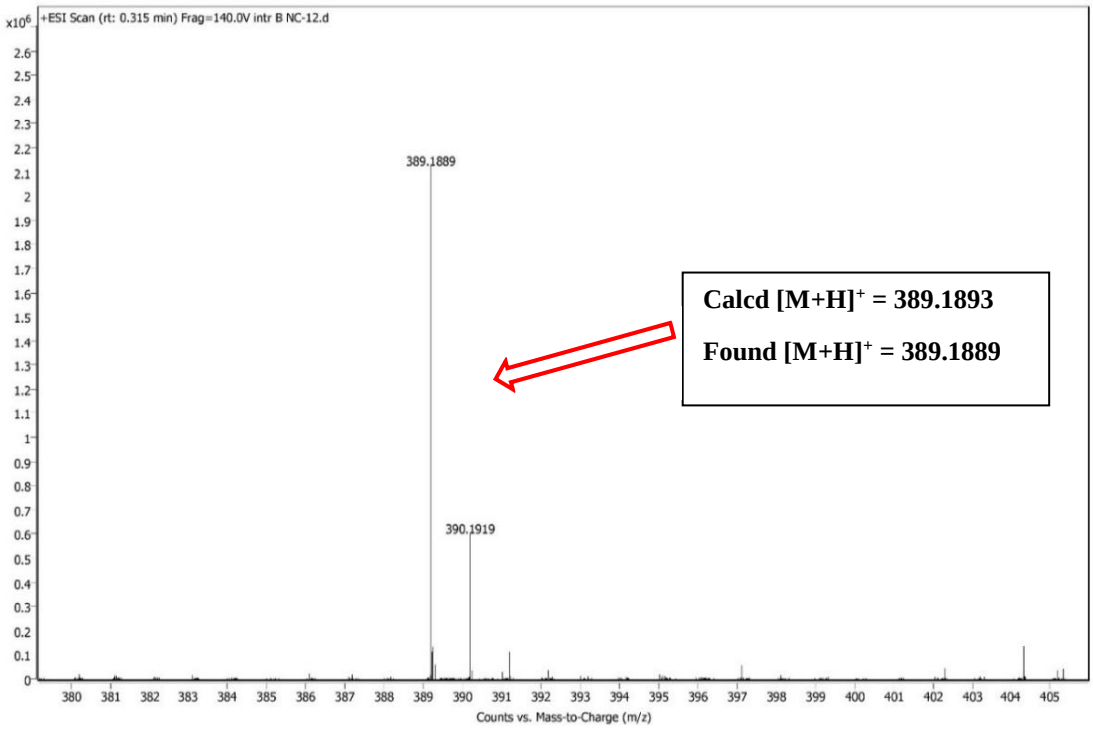

Figure IV.4.4. *HRMS of intermediate **A** or **B**.*

IV.5. Spectral Data:

1,4-Diphenyl-3H-1λ⁶-isothiazol-3-one 1-oxide (1a):

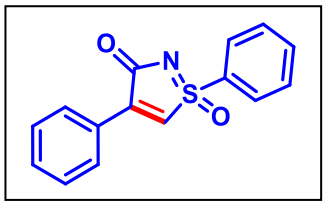

As brownish white solid (47 mg, 88% yield); m.p. 128-130 °C; purified over a column of silica gel (20% EtOAc in hexane); ^{1}H NMR ($CDCl_3$, 500 MHz): δ (ppm) 7.98 (d, 2H, J = 7.5 Hz), 7.92 (d, 2H, J = 7.5 Hz), 7.74 (t, 1H, J = 7.5 Hz), 7.64 (t, 2H, J = 8.0 Hz), 7.61 (s, 1H), 7.51 (t, 1H, J = 7.5 Hz), 7.45 (t, 2H, J = 8.0 Hz); ^{13}C{^{1}H} NMR ($CDCl_3$, 125 MHz): δ (ppm) 173.0, 149.4, 135.3, 133.7, 133.5, 132.1, 130.3, 130.1, 129.1, 128.9, 128.2; IR (neat, cm^{-1}): 3356, 3103, 2922, 2851, 1683, 1593, 1569, 1486, 1445, 1243, 1194, 1132, 1091, 988; HRMS (ESI) m/z: $[M + H]^+$ Calcd for $C_{15}H_{12}NO_2S$ 270.0583; Found 270.0597.

4-Phenyl-1-(p-tolyl)-3H-1λ⁶-isothiazol-3-one 1-oxide (2a):

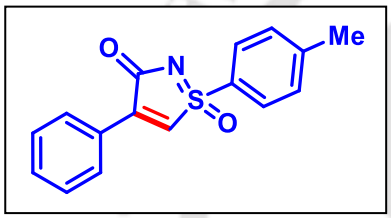

As dark brown solid (51 mg, 89% yield); m.p. 134-136 °C; purified over a column of silica gel (20% EtOAc in hexane); ^{1}H NMR ($CDCl_3$, 400 MHz): δ (ppm) 7.91 (d, 2H, J = 6.8 Hz), 7.85 (d, 2H, J = 8.4 Hz), 7.58 (s, 1H), 7.50 (t, 1H, J = 7.6 Hz), 7.46–7.41 (m, 4H), 2.48 (s, 3H); ^{13}C{^{1}H} NMR ($CDCl_3$, 125 MHz): δ (ppm) 173.2, 148.8, 146.9, 133.9, 132.0, 131.0, 130.3, 130.1, 129.1, 128.9, 128.3, 21.9; IR (neat, cm^{-1}): 3373, 3081, 2923, 2858, 1685, 1589, 1446, 1488, 1236, 1189, 1128, 1091, 994; HRMS (ESI) m/z: $[M + Na]^+$ Calcd for $C_{16}H_{13}NO_2SNa$ 306.0559; Found 306.0574.

1-(4-Ethylphenyl)-4-phenyl-3H-1λ⁶-isothiazol-3-one 1-oxide (3a):

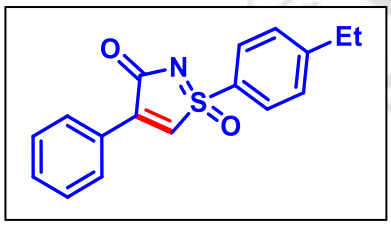

As light brown solid (54 mg, 91% yield); m.p. 110-112 °C; purified over a column of silica gel (20% EtOAc in hexane); ^{1}H NMR ($CDCl_3$, 500 MHz): δ (ppm) 7.91 (d, 2H, J = 7.5 Hz), 7.88 (d, 2H, J = 8.5 Hz), 7.58 (s, 1H), 7.50 (t, 1H, J = 7.0 Hz), 7.46–7.43 (m, 4H), 2.77 (q, 2H, J = 7.5 Hz), 1.28 (t, 3H, J = 8.0 Hz); ^{13}C{^{1}H} NMR ($CDCl_3$, 125 MHz): δ (ppm) 173.1, 152.9, 148.8, 133.9, 132.0, 130.4, 130.1, 129.9, 129.1, 129.0, 128.3, 29.2, 15.2; IR (neat, cm^{-1}): 3386, 3064, 2965, 1688, 1588, 1488, 1447, 1407, 1240, 1194, 1133, 1095, 994; HRMS (ESI) m/z: $[M + H]^+$ Calcd for $C_{17}H_{16}NO_2S$ 298.0896; Found 298.0905.

1-(3-Methoxyphenyl)-4-phenyl-3H-1λ⁶-isothiazol-3-one 1-oxide (4a):

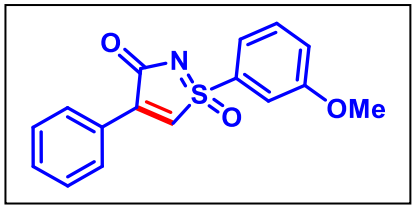

As off-white solid (51 mg, 86% yield); m.p. 125-127 °C; purified over a column of silica gel (22% EtOAc in hexane); ^{1}H NMR ($CDCl_3$, 500 MHz): δ (ppm) 7.90 (d, 2H, J = 7.5 Hz), 7.64 (s, 1H), 7.53–7.47 (m, 3H), 7.44–7.41 (m, 3H), 7.23 (dt, 1H, J_1 = 7.5 Hz, J_2 = 2.0 Hz), 3.85 (s, 3H); ^{13}C{^{1}H} NMR ($CDCl_3$, 125 MHz): δ (ppm) 173.0, 160.8, 149.1, 134.7, 133.5, 132.0, 131.3, 130.1, 129.0, 128.2, 121.8, 120.8, 113.0, 56.1; IR (neat, cm^{-1}): 3102, 2952, 2849, 2850, 1684, 1588, 1478, 1430, 1287, 1237, 1191, 1131, 1035, 987; HRMS (ESI) m/z: $[M + H]^+$ Calcd for $C_{16}H_{14}NO_3S$ 300.0689; Found 300.0702.

4-Phenyl-1-(o-tolyl)-3H-1λ⁶-isothiazol-3-one 1-oxide (5a):

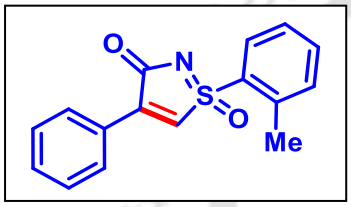

As yellow solid (43 mg, 85% yield); m.p. 146-148 °C; purified over a column of silica gel (20% EtOAc in hexane); ^{1}H NMR ($CDCl_3$, 400 MHz): δ (ppm) 8.18 (d, 1H, J = 8.0 Hz), 7.92 (d, 2H, J = 7.2 Hz), 7.70 (s, 1H), 7.62 (t, 1H, J = 6.8 Hz), 7.51 (t, 1H, J = 7.2 Hz), 7.47–7.40 (m, 4H), 2.67 (s, 3H); ^{13}C{^{1}H} NMR ($CDCl_3$, 125 MHz): δ (ppm) 172.5, 150.1, 139.5, 135.2, 133.6, 132.3, 132.2, 132.0, 129.9, 129.8, 129.0, 128.2, 127.5, 20.3; IR (neat, cm^{-1}): 3352, 3043, 2925, 2854, 1682, 1591,1530, 1445, 1240, 1196, 1152, 1066, 993; HRMS (ESI) m/z: $[M + H]^+$ Calcd for $C_{16}H_{14}NO_2S$ 284.0740; Found 284.0745.

1-(4-Fluorophenyl)-4-phenyl-3H-1λ⁶-isothiazol-3-one 1-oxide (6a):

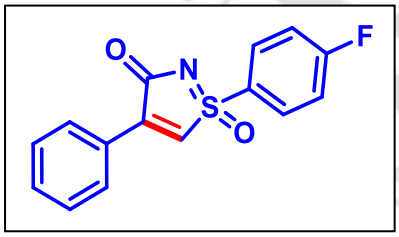

As brown solid (48 mg, 83% yield); m.p. 119-121 °C; purified over a column of silica gel (22% EtOAc in hexane); ^{1}H NMR ($CDCl_3$, 500 MHz): δ (ppm) 8.02–7.99 (m, 2H) 7.92 (d, 2H, J = 7.5 Hz), 7.62 (s, 1H), 7.51 (t, 1H, J = 7.5 Hz), 7.45 (t, 2H, J = 7.5 Hz), 7.31 (t, 2H, J = 8.5 Hz); ^{13}C{^{1}H} NMR ($CDCl_3$, 125 MHz): δ (ppm) 172.9, 167.0 (d, J = 258.1 Hz), 149.3 133.4, 132.2, 131.9 (d, J = 9.9 Hz), 130.1, 129.4 (d, J = 3.0 Hz), 129.1, 128.1, 117.8 (d, J = 22.8 Hz); ^{19}F NMR ($CDCl_3$, 565 MHz): δ (ppm) –100.4 ; IR (neat, cm^{-1}): 3373, 3113, 3056, 2920, 2853, 2337, 1687, 1583, 1487, 1147, 1232, 1195, 1135, 1093, 993; HRMS (ESI) m/z: $[M + H]^+$ Calcd for $C_{15}H_{11}FNO_2S$ 288.0489; Found 288.0489.

1-(4-Chlorophenyl)-4-phenyl-3H-1λ⁶-isothiazol-3-one 1-oxide (7a):

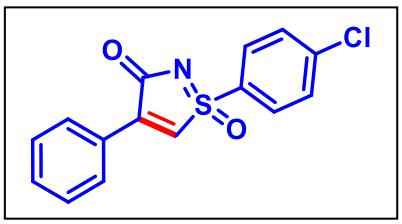

As dark yellow solid (55 mg, 91% yield); m.p. 97-99 °C; purified over a column of silica gel (22% EtOAc in hexane); ^{1}H NMR ($CDCl_3$, 500 MHz): δ (ppm) 7.92–7.90 (m, 4H), 7.61 (s, 2H), 7.59 (s, 1H), 7.51 (t, 1H, J = 7.5 Hz), 7.45 (t, 2H, J = 7.5 Hz); ^{13}C{^{1}H} NMR ($CDCl_3$, 125 MHz): δ (ppm) 172.8, 149.6, 142.5, 133.2, 132.3, 132.2, 130.7, 130.3, 130.1, 129.2, 128.1; IR (neat, cm^{-1}): 3035, 2920, 2854, 1687, 1571, 1444, 1472, 1395, 1257, 1195, 1240, 1135, 1083, 991; HRMS (ESI) m/z: $[M + H]^+$ Calcd for $C_{15}H_{11}ClNO_2S$ 304.0194; Found 304.0194.

1-(4-Bromophenyl)-4-phenyl-3H-1λ⁶-isothiazol-3-one 1-oxide (8a):

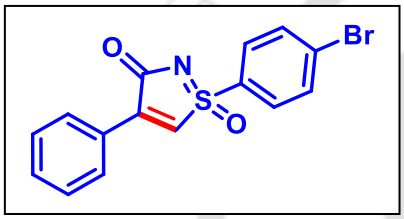

As pale yellow solid (60 mg, 87% yield); m.p. 147-149 °C; purified over a column of silica gel (22% EtOAc in hexane); ^{1}H NMR ($CDCl_3$, 400 MHz): δ (ppm) 7.92 (d, 2H, J = 7.2 Hz), 7.83 (d, 2H, J = 8.8 Hz), 7.77 (d, 2H, J = 8.8 Hz), 7.61 (s, 1H), 7.52 (t, 1H, J = 7.6 Hz), 7.46 (t, 2H, J = 8.0 Hz); ^{13}C{^{1}H} NMR ($CDCl_3$, 125 MHz): δ (ppm) 172.8, 149.6, 133.7, 133.1, 132.8, 132.3, 131.1, 130.3, 130.1, 129.2, 128.0; IR (neat, cm^{-1}): 3360, 3030, 2922, 2853, 1685, 1685, 1567, 1468, 1388, 1241, 1193, 1137, 1093, 989; HRMS (ESI) m/z: $[M + H]^+$ Calcd for $C_{15}H_{11}BrNO_2S$ 347.9688; Found 347.9699.

1-(3-Fluorophenyl)-4-phenyl-3H-1λ⁶-isothiazol-3-one 1-oxide (9a):

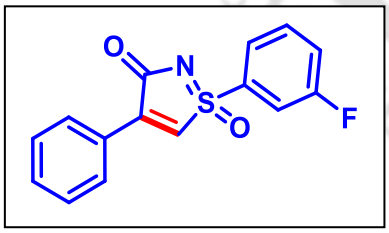

As pale yellow solid (52 mg, 91% yield); m.p. 155-157 °C; purified over a column of silica gel (20% EtOAc in hexane); ^{1}H NMR ($CDCl_3$, 500 MHz): δ (ppm) 7.92 (d, 2H, J = 8.5 Hz), 7.77 (d, 1H, J = 8.0 Hz), 7.69–7.66 (m, 2H), 7.64–7.60 (m, 1H), 7.50 (t, 1H, J = 7.0 Hz), 7.46–7.41 (m, 3H); ^{13}C{^{1}H} NMR ($CDCl_3$, 125 MHz): δ (ppm) 172.7, 162.9 (d, J = 252.8 Hz), 149.9, 136.0 (d, J = 7.0 Hz), 132.9, 132.3, 132.2 (d, J = 7.8 Hz), 130.1, 129.1, 128.0, 124.7 (d, J = 3.5 Hz), 122.7 (d, J = 21.0 Hz), 116.2 (d, J = 25.3 Hz), ^{19}F NMR ($CDCl_3$, 471 MHz): δ (ppm) –107.2; IR (neat, cm^{-1}): 3099, 2920, 2850, 1683, 1588, 1473, 1426, 1243, 1194, 1132, 990; HRMS (ESI) m/z: $[M + H]^+$ Calcd for $C_{15}H_{11}FNO_2S$ 288.0489; Found 288.0492.

1-(3-Chlorophenyl)-4-phenyl-3H-1λ⁶-isothiazol-3-one 1-oxide (10a):

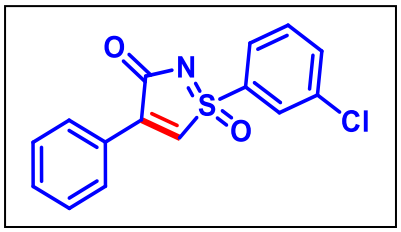

As brownish white solid (56 mg, 92% yield); m.p. 145-147 °C; purified over a column of silica gel (20% EtOAc in hexane); ^{1}H NMR ($CDCl_3$, 400 MHz): δ (ppm) 7.96–7.92 (m, 3H), 7.86 (d, 1H, J = 8.0 Hz), 7.70 (d, 1H, J = 9.2 Hz), 7.63(s, 1H), 7.58 (t, 1H, J = 8.0 Hz), 7.52 (t, 1H, J = 7.6 Hz), 7.46 (t, 2H, J = 7.6 Hz); ^{13}C{^{1}H} NMR ($CDCl_3$, 125 MHz): δ (ppm) 172.7, 149.9, 136.5, 135.7, 135.4, 132.9, 132.3, 131.5, 130.1, 129.1, 128.7, 127.9, 126.9; IR (neat, cm^{-1}): 3029, 1691, 1567, 1468, 1403, 1257, 1194, 1120, 1010, 993; HRMS (ESI) m/z: $[M + H]^+$ Calcd for $C_{15}H_{11}ClNO_2S$ 304.0194; Found 304.0203.

4-Phenyl-1-(4-(trifluoromethyl)phenyl)-3H-1λ⁶-isothiazol-3-one 1-oxide (11a):

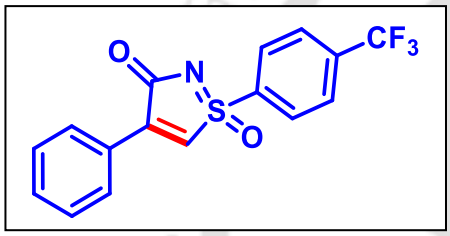

As pale yellow solid (59 mg, 88% yield); m.p. 170-172 °C; purified over a column of silica gel (25% EtOAc in hexane); ^{1}H NMR ($CDCl_3$, 500 MHz): δ (ppm) 8.13 (d, 2H, J = 8.0 Hz), 7.93 (d, 2H, J = 7.0 Hz), 7.89 (d, 2H, J = 8.0 Hz), 7.65 (s, 1H), 7.53 (t, 1H, J = 8.0 Hz), 7.46 (t, 2H, J = 7.5 Hz); ^{13}C{^{1}H} NMR ($CDCl_3$, 125 MHz): δ (ppm) 172.5, 150.5, 138.1, 136.9, (q, J = 33.5 Hz), 132.6, 132.5, 130.2, 129.6, 129.2, 127.9, 127.4 (q, J = 3.6 Hz), 123.0 (q, J = 271.9 Hz); ^{19}F NMR ($CDCl_3$, 565 MHz): δ (ppm) –63.3; IR (neat, cm^{-1}): 3369, 3097, 2920, 1692, 1588, 1565, 1491, 1448,, 1404, 1239, 1322, 1116, 1059, 994; HRMS (ESI) m/z: $[M + H]^+$ Calcd for $C_{16}H_{11}F_3NO_2S$ 338.0457; Found 338.0460.

4-(1-Oxido-3-oxo-4-phenyl-3H-1λ⁶-isothiazol-1-yl)benzonitrile (12a):

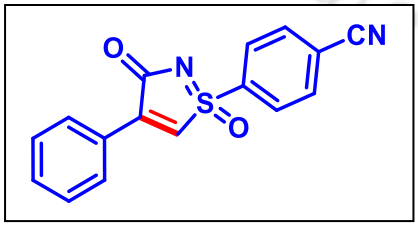

As yellow solid (55 mg, 94% yield); m.p. 205-207 °C; purified over a column of silica gel (28% EtOAc in hexane); ^{1}H NMR ($CDCl_3$, 500 MHz): δ (ppm) 8.11 (d, 2H, J = 8.5 Hz), 7.94–7.92 (m, 4H), 7.63 (s, 1H), 7.54 (t, 1H, J = 7.5 Hz), 7.47 (t, 2H, J = 8.0 Hz); ^{13}C{^{1}H} NMR ($CDCl_3$, 125 MHz): δ (ppm) 172.3, 151.0, 138.8, 133.9, 132.7, 132.1, 130.3, 129.6, 129.3, 127.8, 119.0, 116.9; IR (neat, cm^{-1}): 3358, 3108, 2955, 2913, 2239, 1692, 1484, 1444, 1392; HRMS (ESI) m/z: $[M + H]^+$ Calcd for $C_{16}H_{11}N_2O_2S$ 295.0536; Found 295.0549.

1-(4-Nitrophenyl)-4-phenyl-3H-1λ⁶-isothiazol-3-one 1-oxide (13a):

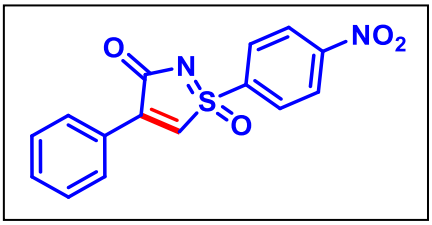

As dark yellow solid (51 mg, 81% yield); m.p. 199-201 °C; purified over a column of silica gel (28% EtOAc in hexane); ^{1}H NMR ($CDCl_3$, 500 MHz): δ (ppm) 8.46 (d, 2H, J = 8.5 Hz), 8.19 (d, 2H, J = 9.0 Hz), 7.95 (d, 2H, J = 7.5 Hz), 7.64 (s, 1H), 7.56 (t, 1H, J = 7.0 Hz), 7.49 (t, 2H, J = 8.0 Hz); ^{13}C{^{1}H} NMR ($CDCl_3$, 125 MHz): δ (ppm) 172.2, 151.8, 151.2, 140.5, 132.8, 132.0, 130.4, 130.3, 129.3, 127.8, 125.4; IR (neat, cm^{-1}): 3097, 2955, 2917, 2851, 1691, 1586, 1525, 1491, 1445, 1342, 1239, 1239, 1191, 1145, 1089, 995; HRMS (ESI) m/z: $[M + H]^+$ Calcd for $C_{15}H_{11}N_2O_4S$ 315.0434; Found 315.0442.

1-(Naphthalen-2-yl)-4-phenyl-3H-1λ⁶-isothiazol-3-one 1-oxide (14a):

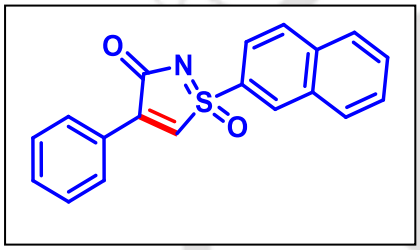

As pale yellow solid (55.5 mg, 87% yield); m.p. 131-133 °C; purified over a column of silica gel (22% EtOAc in hexane); ^{1}H NMR ($CDCl_3$, 500 MHz): δ (ppm) 8.65 (d, 1H, J = 2.5 Hz), 8.05 (d, 1H, J = 8.5 Hz), 8.00 (d, 1H, J = 8.0 Hz), 7.96–7.91 (m, 3H), 7.79 (dd, 1H, J_1 = 9.0 Hz, J_2 = 2.0 Hz), 7.23 (t, 1H, J = 8.0 Hz), 7.68–7.64 (m, 2H), 7.50 (t, 1H, J = 7.0 Hz), 7.45 (t, 2H, J = 7.5 Hz); ^{13}C{^{1}H} NMR ($CDCl_3$, 125 MHz): δ (ppm) 173.1, 149.3, 136.0, 133.6, 132.6, 132.1, 131.6, 130.8, 130.5, 130.1, 130.0, 129.7, 129.1, 128.5, 128.3, 128.2, 122.3; IR (neat, cm^{-1}): 3032, 2918, 2850, 1680, 1590, 1490, 1446, 1247, 1193, 1144, 1071, 996; HRMS (ESI) m/z: $[M + H]^+$ Calcd for $C_{19}H_{14}NO_2S$ 320.0740; Found 320.0745.

1,4-Diphenyl-5-(p-tolyl)-3H-1λ⁶-isothiazol-3-one 1-oxide (15a):

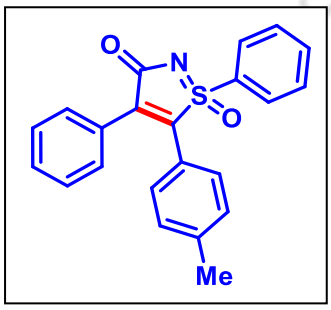

As yellow solid (50 mg, 69% yield); m.p. 174-176 °C; purified over a column of silica gel (25% EtOAc in hexane) ^{1}H NMR ($CDCl_3$, 500 MHz): δ (ppm) 7.85 (d, 2H, J = 8.0 Hz), 7.67 (t, 1H, J = 7.2 Hz), 7.54 (t, 2H, J = 7.7 Hz), 7.49 (d, 2H, J = 7.8 Hz), 7.38 (t, 1H, J = 7.3 Hz), 7.33 (t, 2H, J = 7.6 Hz), 7.09 (q, 4H, J = 8.1 Hz), 2.31 (s, 3H); ^{13}C{^{1}H} NMR ($CDCl_3$, 125 MHz): δ (ppm) 173.5, 148.4, 141.4, 141.3, 135.1, 133.2, 130.6, 130.5, 130.2, 130.0, 129.2, 129.0, 128.8, 128.7, 123.2, 21.7; IR (neat, cm^{-1}): 2955, 2928, 2851, 1763, 1692, 1638, 1607, 1445, 1304, 1228,

1159, 1091, 1009, 998; HRMS (ESI) m/z: $[M + H]^+$ Calcd for $C_{22}H_{18}NO_2S$ 360.1053; Found 360.1058.

5-(4-Fluorophenyl)-1,4-diphenyl-3H-1λ⁶-isothiazol-3-one 1-oxide (16a):

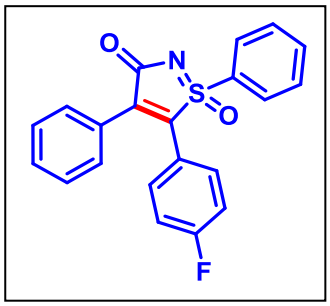

As white solid (57 mg, 78% yield); m.p. 176-178 °C; purified over a column of silica gel (20% EtOAc in hexane) ^{1}H NMR ($CDCl_3$, 500 MHz): δ (ppm) 7.84 (d, 2H, J = 8.0 Hz), 7.69 (t, 1H, J = 7.5 Hz), 7.56 (t, 2H, J = 7.8 Hz), 7.48 (d, 2H, J = 7.0 Hz), 7.40 (t, 1H, J = 7.4 Hz), 7.34 (t, 2H, J = 7.5 Hz), 7.23 (dd, 2H, J_1 = 8.7 Hz, J_2 = 5.4 Hz), 6.99 (t, 2H, J = 8.5 Hz); ^{13}C{^{1}H} NMR ($CDCl_3$, 125 MHz): δ (ppm) 173.1, 164.0 (d, J = 251.9 Hz), 147.3, 142.0, 135.3, 132.9, 131.3 (d, J = 8.6 Hz), 130.8, 130.5, 130.2, 129.2, 128.8, 128.4, 122.3 (d, J = 3.6 Hz), 116.9 (d, J = 22.0 Hz); ^{19}F NMR ($CDCl_3$, 471 MHz): δ (ppm) –107.6; IR (neat, cm^{-1}): 2918, 1690, 1598, 1505, 1448, 1308, 1233, 1160, 1096, 1012, 992; HRMS (ESI) m/z: $[M + H]^+$ Calcd for $C_{21}H_{15}FNO_2S$ 364.0802; Found 364.0819.

1,4-Diphenyl-5-(4-(trifluoromethyl)phenyl)-3H-1λ⁶-isothiazol-3-one 1-oxide (17a):

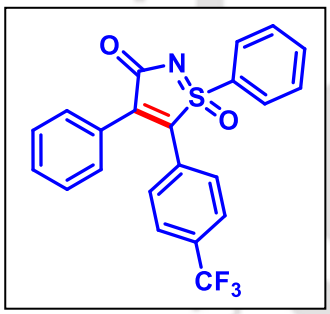

As white solid (70 mg, 85% yield); m.p. 170-172 °C; purified over a column of silica gel (22% EtOAc in hexane) ^{1}H NMR ($CDCl_3$, 500 MHz): δ (ppm) 7.84 (d, 2H, J = 7.5 Hz), 7.70 (t, 1H, J = 7.4 Hz), 7.58–7.54 (m, 4H), 7.46 (d, 2H, J = 7.5 Hz), 7.40 (t, 1H, J = 7.4 Hz), 7.34 (t, 4H, J = 7.8 Hz); ^{13}C{^{1}H} NMR ($CDCl_3$, 125 MHz): δ (ppm) 172.7, 146.7, 143.3, 135.5, 132.6, 131.1, 130.6, 130.3, 130.2, 129.6, 129.2, 128.9, 128.0, 126.4 (q, J = 3.6 Hz), 124.7, 122.5; ^{19}F NMR ($CDCl_3$, 471 MHz): δ (ppm) –63.1; IR (neat, cm^{-1}): 2955, 1695, 1646, 1447, 1326, 1231, 1160, 1128, 1094, 1068, 906; HRMS (ESI) m/z: $[M + H]^+$ Calcd for $C_{22}H_{15}F_3NO_2S$ 414.0770; Found 414.0787.

1-Phenyl-4-(p-tolyl)-3H-1λ⁶-isothiazol-3-one 1-oxide (20a):

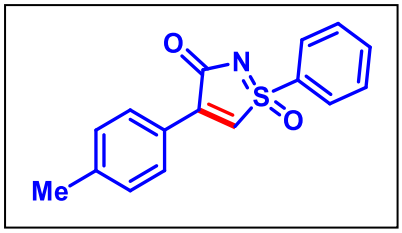

As off white solid (44 mg, 78% yield); m.p. 143-145 °C; purified over a column of silica gel (20% EtOAc in hexane) ^{1}H NMR ($CDCl_3$, 500 MHz): δ (ppm) 7.98 (d, 2H, J = 7.5 Hz), 7.86 (d, 2H, J = 8.5 Hz), 7.74 (t, 1H, J = 7.5 Hz), 7.63 (t, 2H, J = 8.0 Hz), 7.55 (s, 1H), 7.26 (d, 2H, J = 8.0 Hz), 2.40 (s, 3H); ^{13}C{^{1}H} NMR ($CDCl_3$, 125 MHz): δ (ppm) 173.2, 149.3, 143.0, 135.2, 134.0, 132.1,

130.3. 130.1, 129.9, 128.8, 125.4, 21.8; IR (neat, cm^{-1}): 3079, 2921, 2856, 2326, 1681, 1587, 1505, 1446, 1241, 1192, 1192, 11233, 1091, 989; HRMS (ESI) m/z: $[M + H]^+$ Calcd for $C_{16}H_{14}NO_2S$ 284.0740; Found 284.0737.

1-Phenyl-4-(m-tolyl)-3H-1λ⁶-isothiazol-3-one 1-oxide (21a):

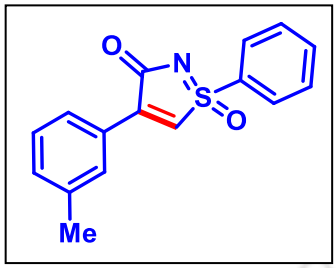

As yellow solid (46 mg, 81% yield); m.p. 98-100 °C; purified over a column of silica gel (20% EtOAc in hexane); ^1H NMR ($CDCl_3$, 500 MHz): δ (ppm) 7.97 (d, 2H, J = 7.5 Hz), 7.76–7.70 (m. 3H), 7.63 (t, 2H, J = 7.8 Hz), 7.59 (s, 1H), 7.35–7.30 (m, 2H), 2.38 (s, 3H); $^{13}C\{^1H\}$ NMR ($CDCl_3$, 125 MHz): δ (ppm) 173.1, 149.6, 138.9, 135.2, 133.8, 133.3, 133.0, 130.6, 130.3, 129.0, 128.8, 128.1, 127.2, 21.6; IR (neat, cm^{-1}): 3350, 3074, 2920, 2853, 1678, 1586, 1446, 1241, 1130, 1089, 986; HRMS (ESI) m/z: $[M + H]^+$ Calcd for $C_{16}H_{14}NO_2S$ 284.0740; Found 284.0755.

4-(4-Methoxyphenyl)-1-phenyl-3H-1λ⁶-isothiazol-3-one 1-oxide (22a):

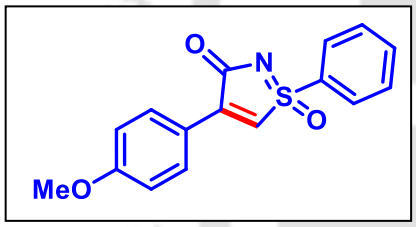

As pale yellow solid (46 mg, 77% yield); m.p. 170-172 °C; purified over a column of silica gel (22% EtOAc in hexane); ^1H NMR ($CDCl_3$, 500 MHz): δ (ppm) 7.97 (dd, 4H, J_1 = 10.5 Hz, J_2 = 8.7 Hz), 7.72 (t, 1H, J = 7.5 Hz), 7.61 (t, 2H, J = 8.0 Hz), 7.47 (s, 1H), 6.94 (d, 2H, J = 9.0 Hz), 3.85 (s, 3H); $^{13}C\{^1H\}$ NMR ($CDCl_3$, 125 MHz): δ (ppm) 173.4, 163.0, 148.7, 135.1, 134.2, 132.2, 130.2, 130.1, 128.7, 120.7, 114.7, 55.7; IR (neat, cm^{-1}): 3330, 3049, 2921, 2848, 2338,1669, 1600, 1504, 1439, 1243, 1188, 1143, 1087, 985; HRMS (ESI) m/z: $[M + H]^+$ Calcd for $C_{16}H_{14}NO_3S$ 300.0689; Found 300.0700.

4-(3-Methoxyphenyl)-1-phenyl-3H-1λ⁶-isothiazol-3-one 1-oxide (23a):

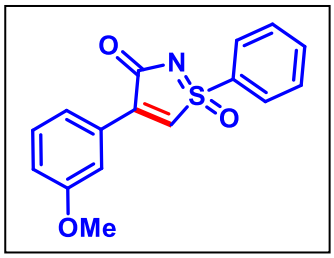

As brown gummy solid (50 mg, 83% yield); purified over a column of silica gel (15% EtOAc in hexane); ^1H NMR ($CDCl_3$, 500 MHz): δ (ppm) 7.98 (d, 2H, J = 7.5 Hz), 7.75 (t, 1H, J = 7.5 Hz), 7.63 (t, 2H, J = 7.7 Hz), 7.60 (s, 1H), 7.52 (s, 1H), 7.46 (d, 1H, J = 8.0 Hz), 7.35 (t, 1H, J = 8.0 Hz), 7.04 (dd, 1H, J_1 = 8.0 Hz, J_2 = 2.5 Hz), 3.84 (s, 3H); $^{13}C\{^1H\}$ NMR ($CDCl_3$, 125 MHz): δ (ppm) 172.9, 159.9, 149.2, 135.3, 133.8, 133.7, 130.3, 130.1, 129.4, 128.9, 122.4, 118.3, 115.1, 55.7; IR (neat, cm^{-1}): 3325, 3047, 2923,

2850, 2338, 1667, 1601, 1508, 1440, 1241, 1187, 1141, 1087, 986; HRMS (ESI) m/z: $[M + H]^+$ Calcd for $C_{16}H_{14}NO_3S$ 300.0689; Found 300.0698.

4-(4-Fluorophenyl)-1-phenyl-3H-1λ⁶-isothiazol-3-one 1-oxide (24a):

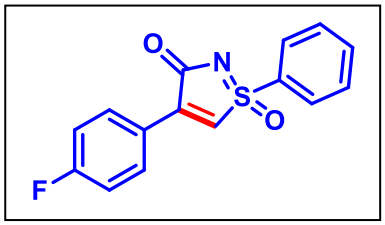

As brown solid (47 mg, 82% yield); m.p. 98-100 °C; purified over a column of silica gel (20% EtOAc in hexane); ^{1}H NMR ($CDCl_3$, 500 MHz): δ (ppm) 8.00–7.96 (m, 4H), 7.75 (t, 1H, J = 7.4 Hz), 7.63 (t, 2H, J = 8.0 Hz), 7.61 (s, 1H), 7.13 (t, 2H, J = 8.7 Hz); ^{13}C{^{1}H} NMR ($CDCl_3$, 125 MHz): δ (ppm) 172.9, 165.1 (d, J = 253.3 Hz), 148.0, 135.4, 133.6, 133.1 (d, J = 2.0 Hz), 132.5 (d, J = 8.9 Hz), 130.3, 128.8, 124.4 (d, J = 3.5 Hz), 116.4 (d, J = 21.5 Hz); ^{19}F NMR ($CDCl_3$, 471 MHz): δ (ppm) –106.2; IR (neat, cm^{-1}): 3355, 3061, 2922, 2853, 2328, 1905, 1677, 1594, 1501, 1445, 1239, 1136, 991; HRMS (ESI) m/z: $[M + H]^+$ Calcd for $C_{15}H_{11}FNO_2S$ 288.0489; Found 288.0495.

4-(4-Bromophenyl)-1-phenyl-3H-1λ⁶-isothiazol-3-one 1-oxide (25a):

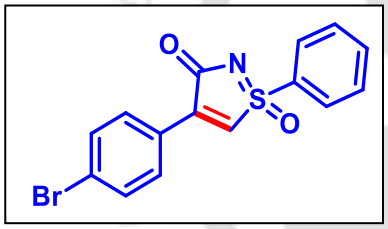

As yellow solid (49 mg, 71% yield); m.p. 194-196 °C; purified over a column of silica gel (20% EtOAc in hexane); ^{1}H NMR ($CDCl_3$, 400 MHz): δ (ppm) 7.98 (d, 2H, J = 7.6 Hz), 7.82 (d, 2H, J = 8.4 Hz), 7.73 (t, 1H, J = 7.5 Hz), 7.66 (d, 2H, J = 8.0 Hz), 7.63 (s, 1H), 7.60 (d, 2H, J = 8.6 Hz); ^{13}C{^{1}H} NMR ($CDCl_3$, 125 MHz): δ (ppm) 172.7, 148.0, 135.5, 133.9, 133.4, 132.4, 131.5, 130.4, 128.9, 127.2, 127.0; IR (neat, cm^{-1}): 3351, 3049, 2921, 2855, 2328, 1679, 1587,1481, 1446, 1245, 1193, 1141, 1088, 992; HRMS (ESI) m/z: $[M + H]^+$ Calcd for $C_{15}H_{11}BrNO_2S$ 347.9688; Found 347.9697.

4-(2-Bromophenyl)-1-phenyl-3H-1λ⁶-isothiazol-3-one 1-oxide (26a):

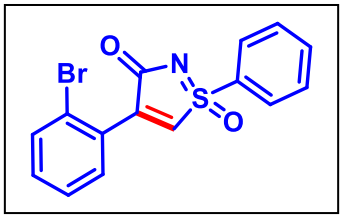

As off white solid (40 mg, 57% yield); m.p. 148-150 °C; purified over a column of silica gel (20% EtOAc in hexane); ^{1}H NMR ($CDCl_3$, 500 MHz): δ (ppm) 8.02 (d, 2H, J = 8.0 Hz), 7.82 (s, 1H), 7.78 (t, 1H, J = 7.5 Hz), 7.69–7.66 (m, 3H), 7.58 (d, 1H, J = 8.0 Hz), 7.43 (t, 1H, J = 7.7 Hz), 7.32 (t, 1H, J = 7.7 Hz); ^{13}C{^{1}H} NMR ($CDCl_3$, 125 MHz): δ (ppm) 172.4, 149.2, 138.6, 135.5, 133.8, 133.3, 132.2, 132.0, 130.4, 129.2, 129.0, 127.7, 123.2; IR (neat, cm^{-1}): 3352, 3062, 2918, 2327, 1682, 1622, 1577,

1290, 1243, 1135, 1091, 986; HRMS (ESI) m/z: $[M + Na]^+$ Calcd for $C_{15}H_{10}BrNO_2SNa$ 369.9508; Found 369.9508.

1-Phenyl-4-(4-(trifluoromethyl)phenyl)-3H-1λ⁶-isothiazol-3-one 1-oxide (27a):

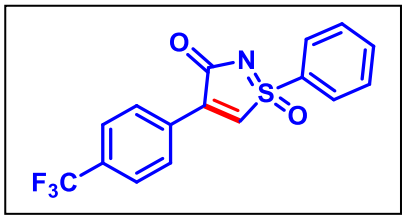

As pale yellow solid (41 mg, 61% yield); m.p. 198-200 °C; purified over a column of silica gel (28% EtOAc in hexane); ^{1}H NMR ($CDCl_3$, 400 MHz): δ (ppm) 7.74 (d, 2H, J = 8.0 Hz), 7.62 (dd, 2H, J_1 = 8.0 Hz, J_2 = 1.6 Hz), 7.57 (d, 2H, J = 8.0 Hz), 7.48–7.42 (m, 3H), 7.35 (s, 1H); ^{13}C{^{1}H} NMR ($CDCl_3$, 125 MHz): δ (ppm) 167.7, 147.1, 141.9, 137.2, 131.4, 130.6, 129.6, 129.4, 128.5, 127.5, 126.2 (q, J = 3.9 Hz), 125.0; ^{19}F NMR ($CDCl_3$, 565 MHz): δ (ppm) –62.7; IR (neat, cm^{-1}): 3361, 3168, 2922, 1643, 1612, 1547, 1396, 1326, 1111, 1067,825; HRMS (ESI) m/z: $[M + H]^+$ Calcd for $C_{16}H_{11}F_3NO_2S$ 338.0457; Found 338.0459.

4-(Naphthalen-2-yl)-1-phenyl-3H-1λ⁶-isothiazol-3-one 1-oxide (28a):

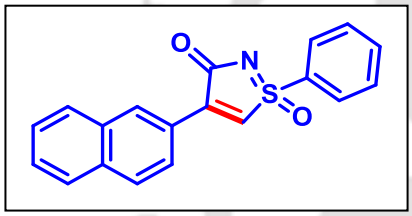

As dark yellow solid (49 mg, 76% yield); m.p. 190-192 °C; purified over a column of silica gel (25% EtOAc in hexane); ^{1}H NMR ($CDCl_3$, 500 MHz): δ (ppm) 8.83 (s, 1H), 8.02 (d, 2H, J = 8.5 Hz), 7.96 (d, 1H, J = 8.0 Hz), 7.88–7.84 (m, 2H), 7.77–7.72 (m, 2H), 7.70 (s, 1H), 7.66 (t, 2H, J = 7.5 Hz), 7.60–7.54 (m, 2H); ^{13}C{^{1}H} NMR ($CDCl_3$, 125 MHz): δ (ppm) 173.2, 149.0, 135.3, 134.9, 133.9, 133.1, 132.0, 130.4, 129.8, 129.0, 128.9, 128.7, 127.9, 127.2, 125.7, 125.4; IR (neat, cm^{-1}): 3031, 2919, 2852, 1683, 1556, 1445, 1370, 1237, 1142, 1093, 992; HRMS (ESI) m/z: $[M + H]^+$ Calcd for $C_{19}H_{14}NO_2S$ 320.0740; Found 320.0743.

4-(Benzo[d][1,3]dioxol-5-yl)-1-phenyl-3H-1λ⁶-isothiazol-3-one 1-oxide (29a):

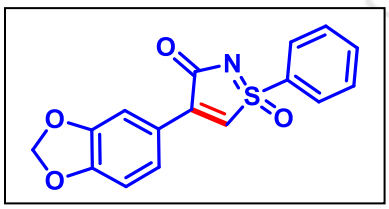

As pale yellow solid (55 mg, 84% yield); m.p. 178-180 °C; purified over a column of silica gel (30% EtOAc in hexane); ^{1}H NMR ($CDCl_3$, 500 MHz): δ (ppm) 7.95 (d, 2H, J = 7.0 Hz), 7.73 (t, 1H, J = 7.3 Hz), 7.64–7.60 (m, 3H), 7.46 (s, 1H), 7.43 (d, 1H, J = 1.5 Hz), 6.68 (d, 1H, J = 8.0 Hz), 6.02 (s, 2H); ^{13}C{^{1}H} NMR ($CDCl_3$, 125 MHz): δ (ppm) 173.1, 151.3, 148.6, 148.4, 135.1, 134.0, 130.9, 130.3, 128.7, 126.0, 122.1, 109.8, 109.0, 102.1; IR (neat, cm^{-1}): 3343, 3065, 2912. 2327, 1675, 1566, 1500, 1445, 1241, 1195, 1093, 1039, 973; HRMS (ESI) m/z: $[M + H]^+$ Calcd for $C_{16}H_{12}NO_4S$ 314.0482; Found 314.0487.

4-(Furan-2-yl)-1-phenyl-3H-1λ⁶-isothiazol-3-one 1-oxide (30a):

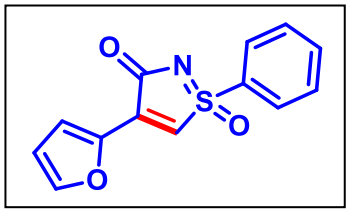

As brownish black solid (39 mg, 75% yield); m.p. 160-162 °C; purified over a column of silica gel (27% EtOAc in hexane); ^{1}H NMR ($CDCl_3$, 500 MHz): δ (ppm) 7.95 (d, 2H, J = 7.5 Hz), 7.80 (d, 1H, J = 3.5 Hz), 7.73 (t, 1H, J = 7.5 Hz), 7.63–7.60 (m, 3H), 7.46 (s, 1H), 6.62–6.61 (m, 1H); ^{13}C{^{1}H} NMR ($CDCl_3$, 125 MHz): δ (ppm) 171.3, 147.6, 144.8, 138.0, 135.1, 134.2, 130.3, 128.7, 127.1, 121.0, 113.7; IR (neat, cm^{-1}): 3374, 3097, 2920, 2855, 1692, 1615, 1530, 1447, 1303, 1201, 1119, 1088, 1014, 964; HRMS (ESI) m/z: [M + H]$^{+}$ Calcd for $C_{13}H_{10}NO_3S$ 260.0376; Found 260.0381.

4-(4-Bromophenyl)-1-(4-ethylphenyl)-3H-1λ⁶-isothiazol-3-one 1-oxide (31a):

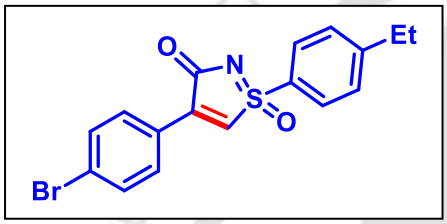

As off-white solid (56 mg, 74% yield); m.p. 164-166 °C; purified over a column of silica gel (24% EtOAc in hexane); ^{1}H NMR ($CDCl_3$, 400 MHz): δ (ppm) 7.86 (d, 2H, J = 8.8 Hz), 7.80 (d, 2H, J = 8.8 Hz), 7.64 (s, 1H), 7.57 (d, 2H, J = 8.4 Hz), 7.44 (d, 2H, J = 8.4 Hz), 2.76 (q, 2H, J = 7.6 Hz), 1.27 (t, 3H, J = 7.6 Hz); ^{13}C{^{1}H} NMR ($CDCl_3$, 125 MHz): δ (ppm) 172.9, 153.1, 147.4, 134.2, 132.4, 131.5, 130.1, 129.9, 129.1, 127.1, 127.0, 29.2, 15.2; IR (neat, cm^{-1}): 3363, 3064, 2966, 2930, 1922, 1690,1591, 1485, 1242, 1138, 1094, 996; HRMS (ESI) m/z: [M + H]$^{+}$ Calcd for $C_{17}H_{15}BrNO_2S$ 376.0001; Found 376.0006.

4-(4-Fluorophenyl)-1-(naphthalen-2-yl)-3H-1λ⁶-isothiazol-3-one 1-oxide (32a):

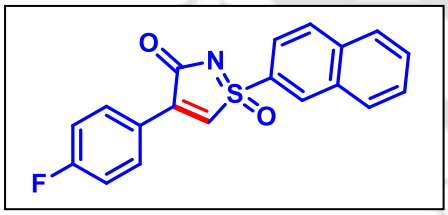

As yellow solid (52 mg, 77% yield); m.p. 171-173 °C; purified over a column of silica gel (20% EtOAc in hexane); ^{1}H NMR ($CDCl_3$, 400 MHz): δ (ppm) 8.65 (s, 1H), 8.05 (d, 1H, J = 8.8 Hz), 8.02–7.98 (m, 3H), 7.95 (d, 1H, J = 8.0 Hz), 7.79 (dd, 1H, J_1 = 8.8 Hz, J_2 = 2.0 Hz), 7.76–7.71 (m, 1H), 7.70–7.66 (m, 1H), 7.64 (s, 1H), 7.14 (t, 2H, J = 8.6 Hz); ^{13}C{^{1}H} NMR ($CDCl_3$, 125 MHz): δ (ppm) 173.1, 165.2 (d, J = 253.3 Hz), 148.0, 136.1, 133.2 (d, J = 2.0 Hz), 132.7, 132.5 (d, J = 8.6 Hz), 131.6, 130.8, 130.5, 130.0, 129.7, 128.5, 128.4, 124.5 (d, J = 3.6 Hz), 122.3, 116.4 (d, J = 21.8 Hz); ^{19}F NMR ($CDCl_3$, 565 MHz): δ (ppm) –106.1; IR (neat, cm^{-1}): 3364, 3035, 2918, 1853, 1684, 1591, 1497, 1230, 1193, 1150, 1070, 1001; HRMS (ESI) m/z: [M + H]$^{+}$ Calcd for $C_{19}H_{13}FNO_2S$ 338.0646; Found 338.0646.

IV.6. Representative NMR Spectra:

***1,4-Diphenyl-3H-1λ⁶-isothiazol-3-one 1-oxide (1a)*: ^{1}H NMR (500 MHz, $CDCl_3$)**

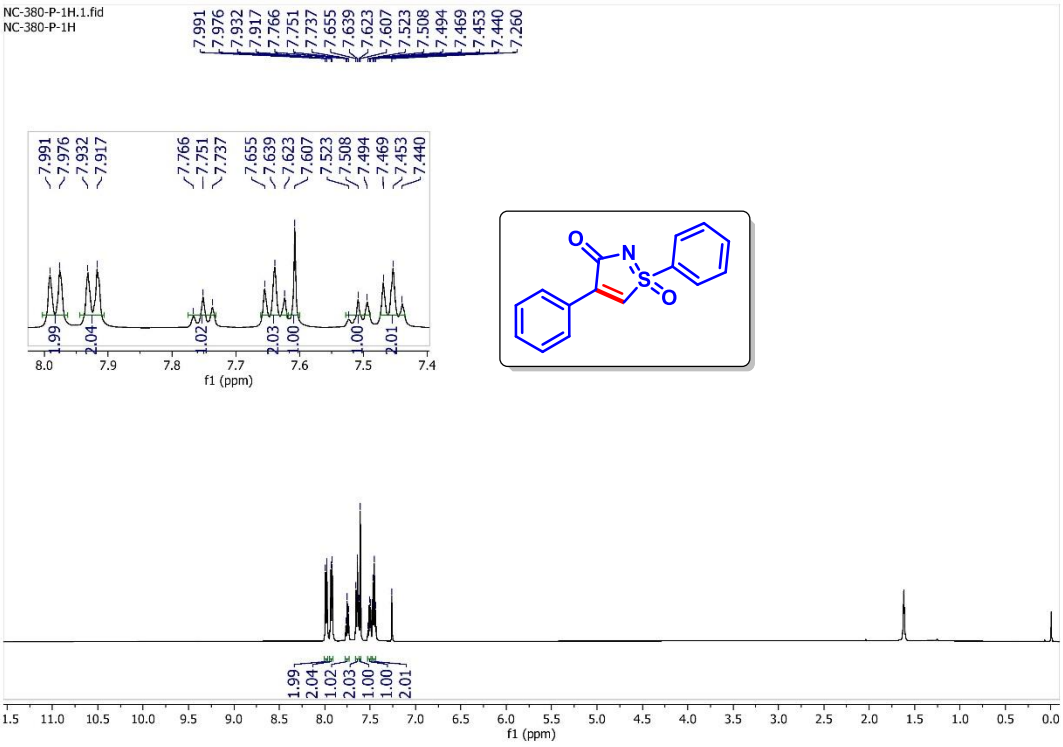

***1,4-Diphenyl-3H-1λ⁶-isothiazol-3-one 1-oxide (1a)*: ^{13}C{^{1}H} NMR (125 MHz, $CDCl_3$)**

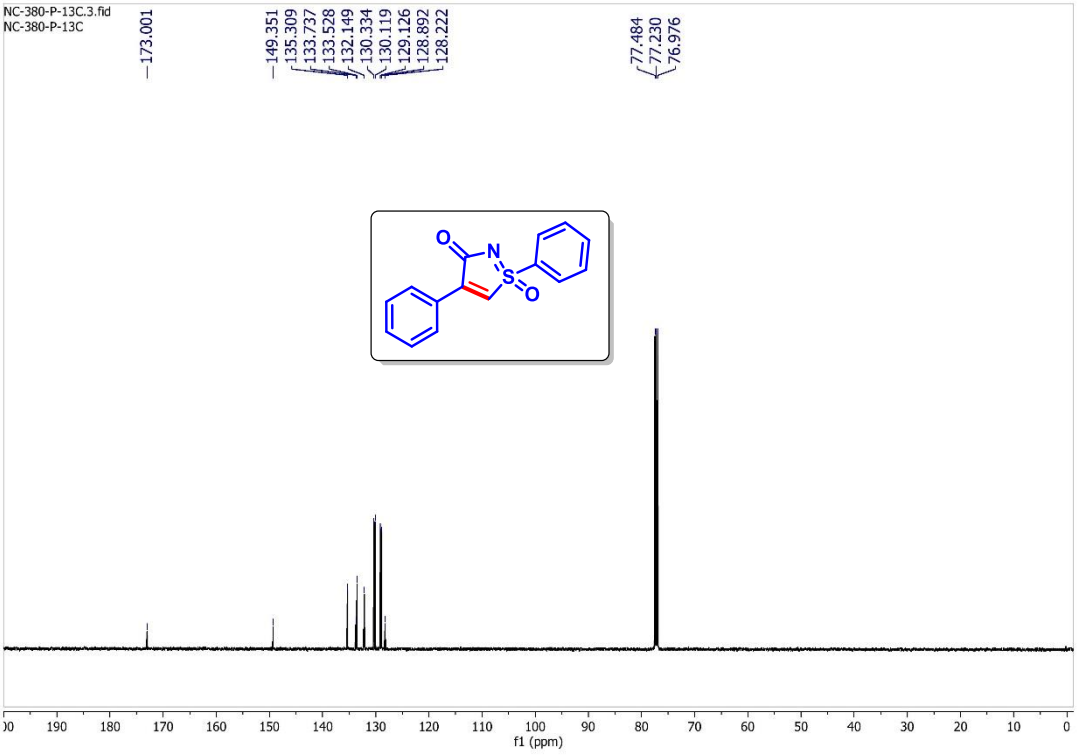

1-(3-Methoxyphenyl)-4-phenyl-3H-1λ⁶-isothiazol-3-one 1-oxide (4a): **^{1}H NMR (500 MHz, $CDCl_3$)**

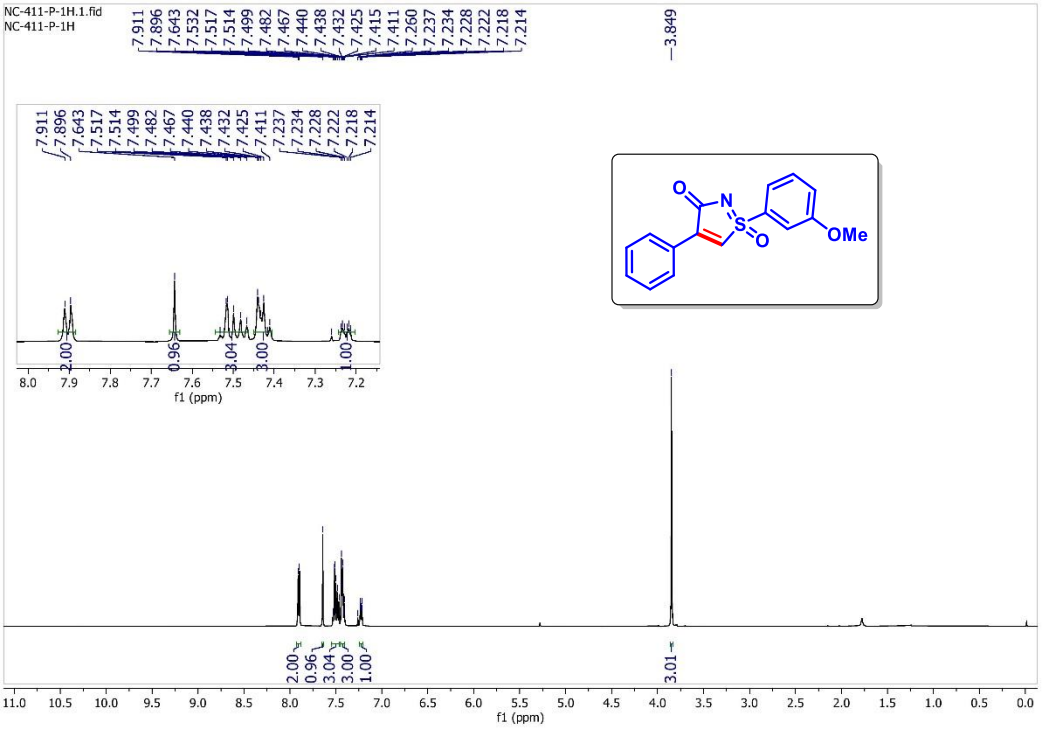

1-(3-Methoxyphenyl)-4-phenyl-3H-1λ⁶-isothiazol-3-one 1-oxide (4a): **^{13}C{^{1}H} NMR (125 MHz, $CDCl_3$)**

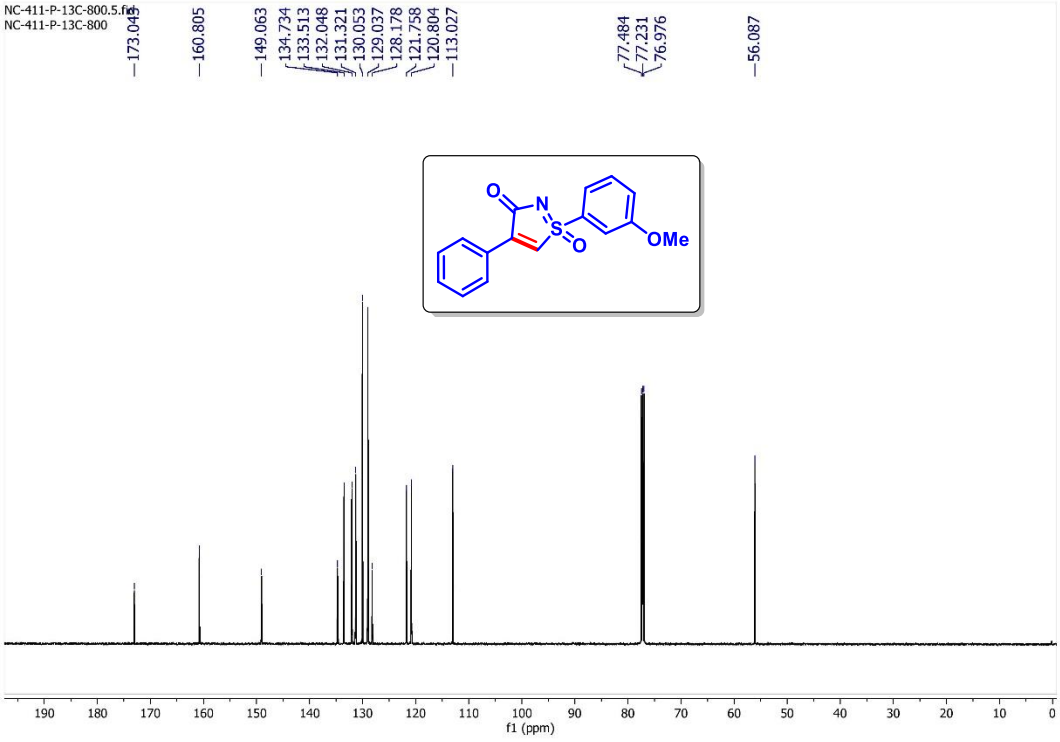

4-(1-Oxido-3-oxo-4-phenyl-3H-1λ⁶-isothiazol-1-yl)benzonitrile (12a): **^{1}H NMR (500 MHz, $CDCl_3$)**

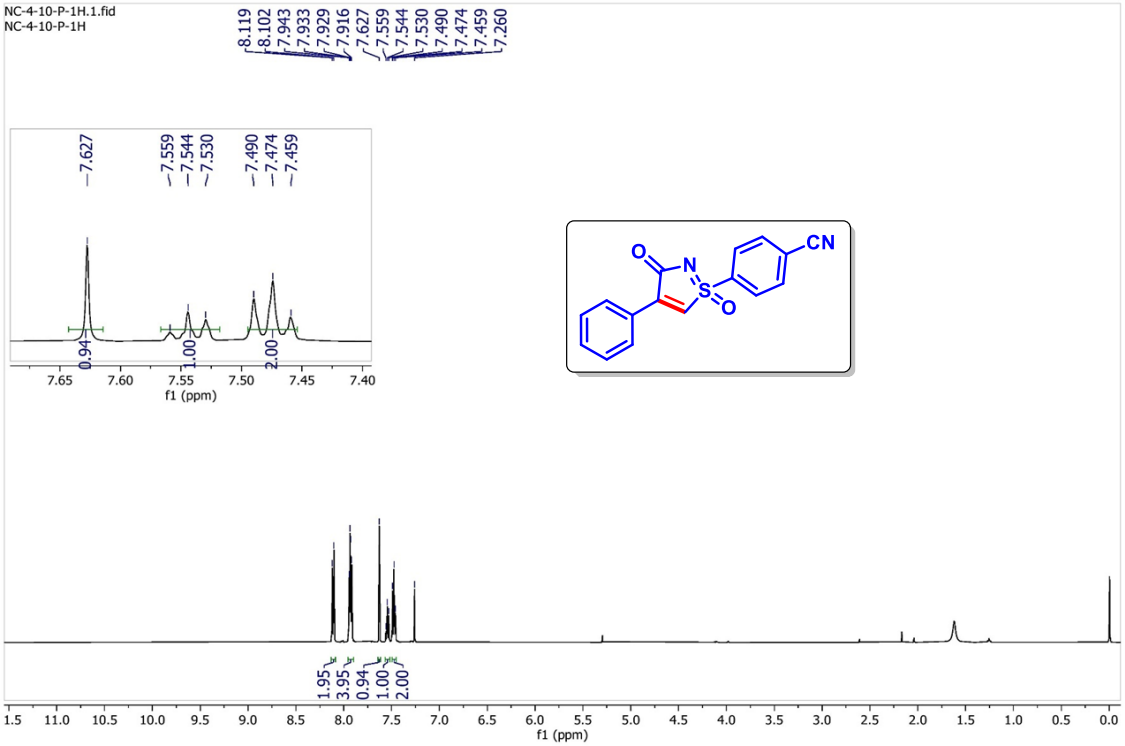

4-(1-Oxido-3-oxo-4-phenyl-3H-1λ⁶-isothiazol-1-yl)benzonitrile (12a): **^{13}C{^{1}H} NMR (125 MHz, $CDCl_3$)**

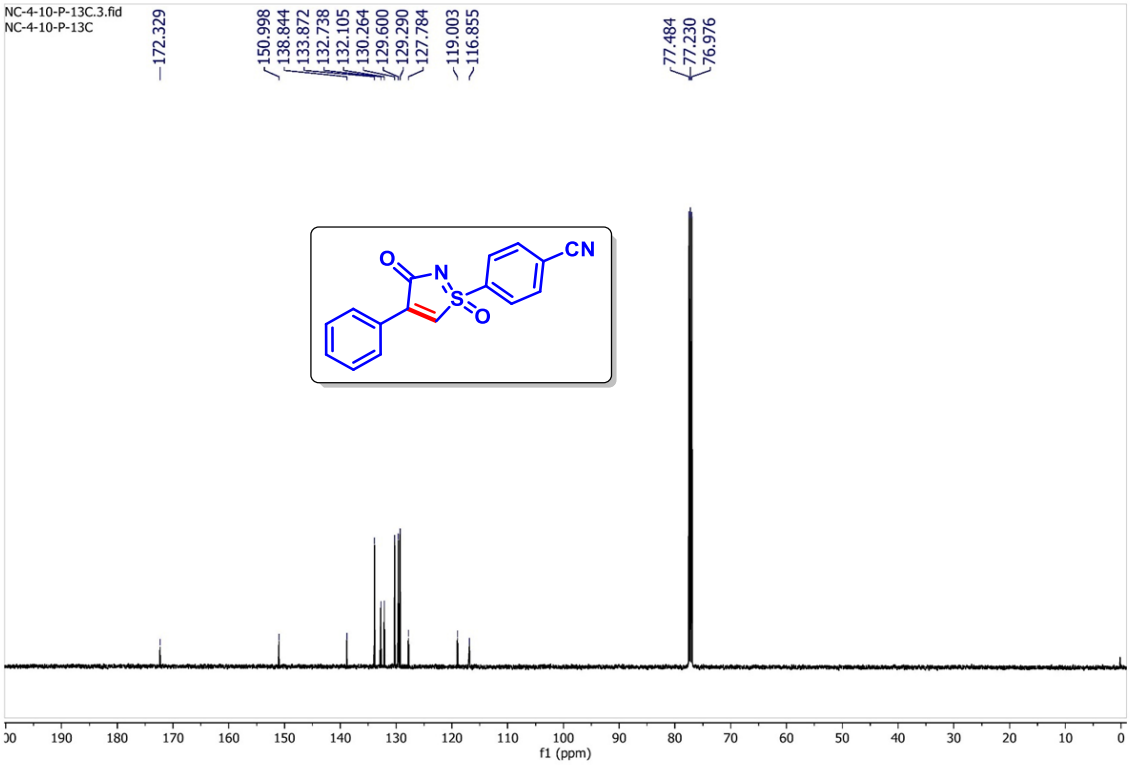

1,4-Diphenyl-5-(p-tolyl)-3H-1λ⁶-isothiazol-3-one 1-oxide (15a): **^{1}H NMR (500 MHz, $CDCl_3$)**

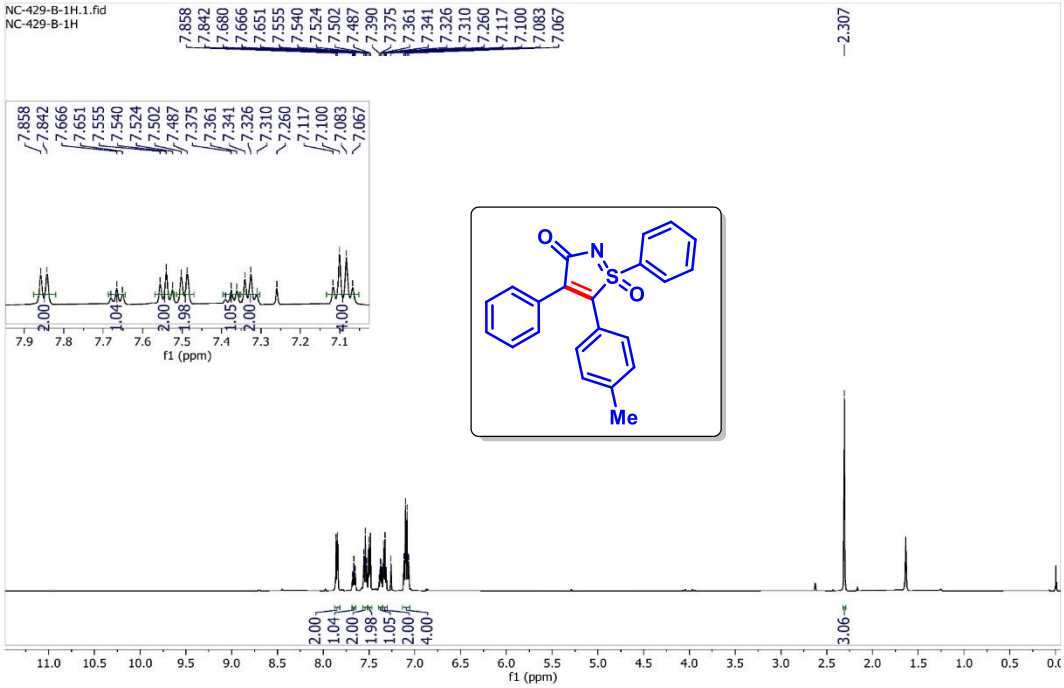

1,4-Diphenyl-5-(p-tolyl)-3H-1λ⁶-isothiazol-3-one 1-oxide (15a): **^{13}C{^{1}H} NMR (125 MHz, $CDCl_3$)**

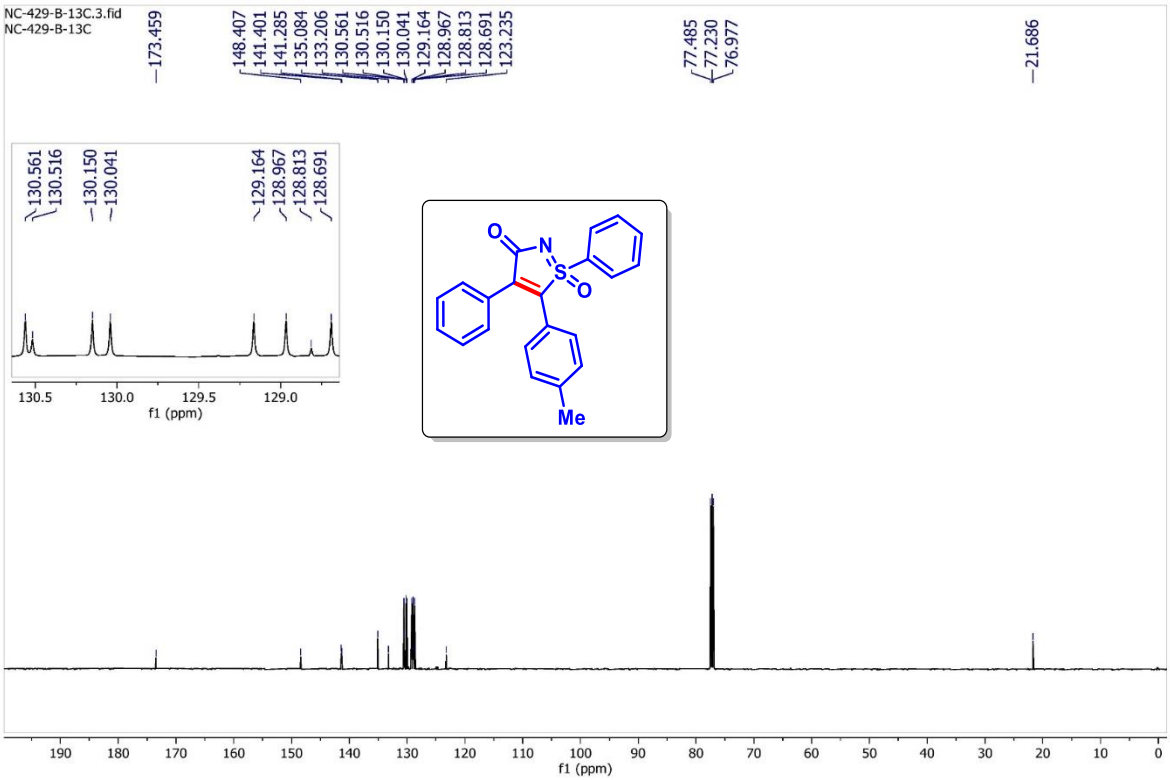

4-(Benzo[d][1,3]dioxol-5-yl)-1-phenyl-3H-1λ⁶-isothiazol-3-one 1-oxide (29a): **^{1}H NMR (500 MHz, $CDCl_3$)**

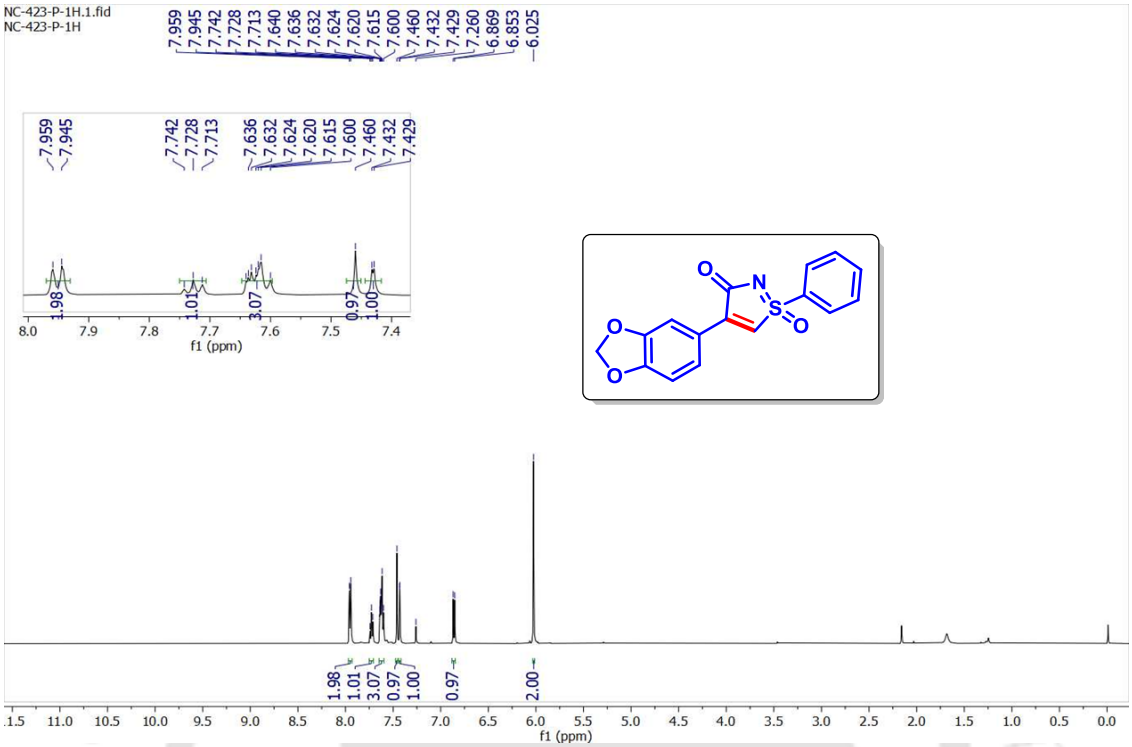

4-(Benzo[d][1,3]dioxol-5-yl)-1-phenyl-3H-1λ⁶-isothiazol-3-one 1-oxide (29a): **^{13}C{^{1}H} NMR (125 MHz, $CDCl_3$)**

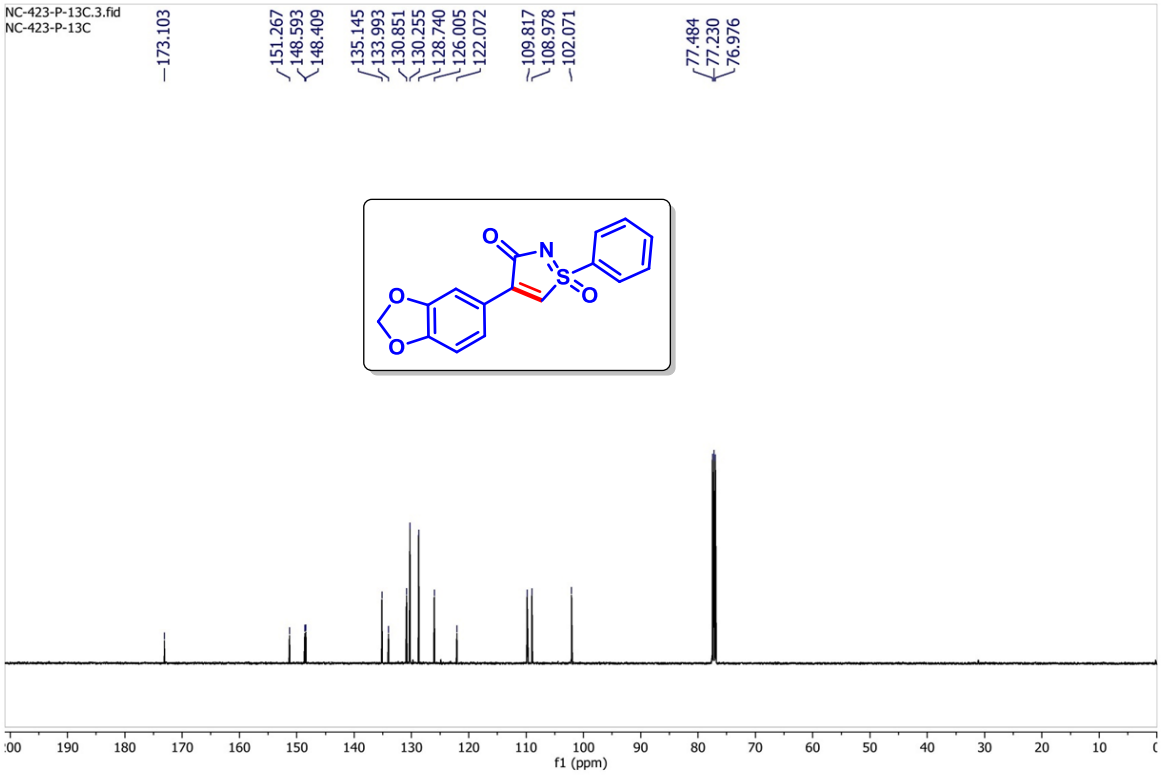

IV.7 References:

(1) (a) S. Carradori, P. Guglielmi, G. Luisi and D. Secci, in *Handbook of Oxidative Stress in Cancer: Mechanistic Aspects*, Springer Singapore, Singapore, 2021, pp. 1–18; (b) S. Badshah and A. Naeem, *Molecules*, 2016, **21**, 1054; (c) K. Laxmikeshav, P. Kumari and N. Shankaraiah, *Med. Res. Rev.*, 2022, **42**, 513–575.

(2) (a) A. De Oliveira Silva, J. McQuade and M. Szostak, *Adv. Synth. Catal.*, 2019, **361**, 3050–3067; (b) A. V. Kletskov, N. A. Bumagin, F. I. Zubkov, D. G. Grudinin and V. I. Potkin, *Synthesis*, 2020, **52**, 159–188.

(3) (a) V. Silva, C. Silva, P. Soares, E. M. Garrido, F. Borges and J. Garrido, *Molecules*, 2020, **25**, 991; (b) K. Taubert, S. Kraus and B. Schulze, *Sulfur Rep.*, 2002, **23**, 79–121; (c) J. F. Schwensen and J. D. Johansen, in *Kanerva's Occupational Dermatology*, Springer International Publishing, Cham, 2018, pp. 1–14.

(4) (a) S. Gorsuch, V. Bavetsias, M. G. Rowlands, G. W. Aherne, P. Workman, M. Jarman and E. McDonald, *Bioorg. Med. Chem.*, 2009, **17**, 467–474; (b) L. Stimson, M. G. Rowlands, Y. M. Newbatt, N. F. Smith, F. I. Raynaud, P. Rogers, V. Bavetsias, S. Gorsuch, M. Jarman, A. Bannister, T. Kouzarides, E. McDonald, P. Workman and G. W. Aherne, *Mol. Cancer Ther.*, 2005, **4**, 1521–1532; (c) N. Hayakawa, K. Nozawa, A. Ogawa, N. Kato, K. Yoshida, K.-I. Akamatsu, M. Tsuchiya, A. Nagasaka and S. Yoshida, *Biochemistry*, 1999, **38**, 11501–11507; (d) S. W. Wright, J. J. Petraitis, B. Freimark, J. V. Giannaras, M. A. Pratta, S. R. Sherk, J. M. Williams, R. L. Magolda and E. C. Arner, *Bioorg. Med. Chem.*, 1996, **4**, 851–858.

(5) (a) M. Ghizzoni, H. J. Haisma and F. J. Dekker, *Eur. J. Med. Chem.*, 2009, **44**, 4855–4861; (b) B. Cornelio, M. Laronze-Cochard, R. Miambo, M. De Grandis, R. Riccioni, B. Borisova, D. Dontchev, C. Machado, M. Ceruso, A. Fontana, C. T. Supuran and J. Sapi, *Eur. J. Med. Chem.*, 2019, **175**, 40–48.

(6) (a) S. N. Lewis, G. A. Miller, M. Hausman and E. C. Szamborski, *J. Heterocycl. Chem.*, 1971, **8**, 571–580; (b) A. S. Bell, C. W. G. Fishwick and J. E. Reed, *Tetrahedron Lett.*, 1994, **35**, 6551–6554; (c) Z. Liu, Y. Wang, J. Huo, X.-J. Li, S. Li and X. Song, *J. Org. Chem.*, 2021, **86**, 5506–5517.

(7) V. Dwivedi, M. Rajesh, R. Kumar, R. Kant and M. Sridhar Reddy, *Chem. Commun.*, 2017, **53**, 11060–11063.

(8) S.-Q. Wang, B.-L. Hu and X.-G. Zhang, *Adv. Synth. Catal.*, 2019, **361**, 1459–1462.

(9) M.-Y. Chen, X. Pannecoucke, P. Jubault and T. Besset, *J. Org. Chem.*, 2019, **84**, 13194–13202.

(10) D. Ma, D. Kong, C. Wang, K.-N. Truong, K. Rissanen and C. Bolm, *Org. Lett.*, 2021, **23**, 8287–8290.

(11) (a) G. Brahmachari, N. Nayek, K. Nurjamal, I. Karmakar and S. Begam, *Synthesis*, 2018, **50**, 4145–4164; (b) Y.-X. Lu, X.-J. Lv, C. Liu and Y.-K. Liu, *Org. Lett.*, 2023, **25**, 4033–4037; (c) H. H. Choi, Y. H. Son, M. S. Jung and E. J. Kang, *Tetrahedron Lett.*, 2011, **52**, 2312–2315; (d) J. Clayden, N. Greeves and S. Warren, *Organic chemistry*, Oxford University Press, London, England, 2012.

(12) M. J. Frisch, G. W. Trucks, H. B. Schlegel, G. E. Scuseria, M. A. Robb, J. R. Cheeseman, G. Scalmani, V. Barone, G. A. Petersson, H. Nakatsuji, X. Li, M. Caricato, A. V. Marenich, J. Bloino, B. G. Janesko, R. Gomperts, B. Mennucci, H. P. Hratchian, J. V. Ortiz, A. F. Izmaylov, J. L. Sonnenberg, D. Williams-Young, F. Ding, F. Lipparini, F. Egidi, J. Goings, B. Peng, A. Petrone, T. Henderson, D. Ranasinghe, V. G. Zakrzewski, J. Gao, N. Rega, G. Zheng, W. Liang, M. Hada, M. Ehara, K. Toyota, R. Fukuda, J. Hasegawa, M. Ishida, T. Nakajima, Y. Honda, O. Kitao, H. Nakai, T. Vreven, K. Throssell, J. A. Montgomery, Jr., J. E. Peralta, F. Ogliaro, M. J. Bearpark, J. J. Heyd, E. N. Brothers, K. N. Kudin, V. N. Staroverov, T. A. Keith, R. Kobayashi, J. Normand, K. Raghavachari, A. P. Rendell, J. C. Burant, S. S. Iyengar, J. Tomasi, M. Cossi, J. M. Millam, M. Klene, C. Adamo, R. Cammi, J. W. Ochterski, R. L. Martin, K. Morokuma, O. Farkas, J. B. Foresman, and D. J. Fox, Gaussian 16, Revision C.01, Gaussian, Inc., Wallingford CT, 2019.

(13) (a) N. Chakraborty, K. K. Rajbongshi, A. Dahiya, B. Das, A. Vaishnani and B. K. Patel, *Chem. Commun.*, 2023, **59**, 2779–2782; (b) S. Baranwal, S. Gupta and J. Kandasamy, *Asian J. Org. Chem.*, 2021, **10**, 1835–1845.

Chapter V

An Expedient Route to Tricyanovinylindoles and Indolylmaleimides from o-Alkynylanilines Utilising DMSO as a One-Carbon Synthon

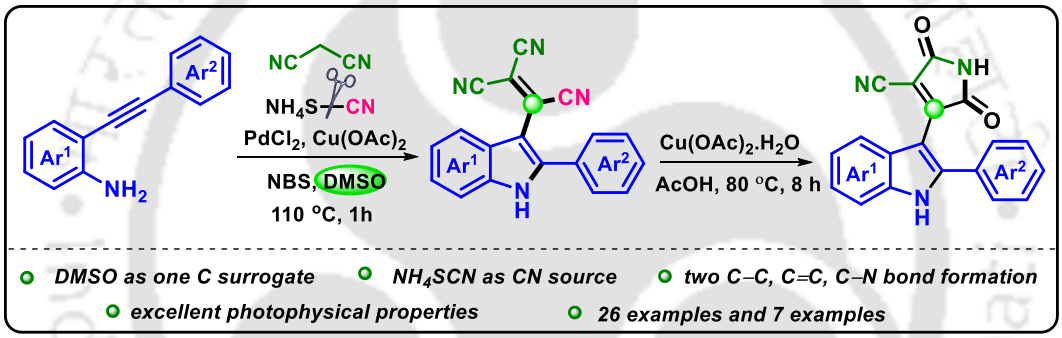

Organic & Biomolecular Chemistry

ROYAL SOCIETY OF CHEMISTRY

PAPER

View Article Online
View Journal | View Issue

Org. Biomol. Chem., 2021, **19**, 6847–6857

Abstract: *A Pd(II)/Cu(II) catalyzed domino synthesis of tricyanovinylindoles has been achieved using DMSO as a one-carbon synthon and NH_4SCN as the cyano source. The reaction proceeds via the construction of 2-aryl-3-formyl indole followed by sequential addition of malononitrile and a CN resulting in two C–C, one C=C and one C–N bond in the final product. Furthermore, post-synthetic modification results in the unprecedented formation of 4-cyano-3-indolylmaleimides. Photophysical studies of selected compounds show emission in the visible range.*

भारतीय प्रौद्योगिकी संस्थान गुवाहाटी
Indian Institute of Technology Guwahati

CHAPTER V

An Expedient Route to Tricyanovinylindoles and Indolylmaleimides from *o*-Alkynylanilines Utilizing DMSO as a One-Carbon Synthon

V.1. Introduction:

Heterocycles have long intrigued synthetic chemists due to their unique properties and diverse applications. Over the years, developing novel methodologies for the stereoselective synthesis of hetero-polycyclic ring systems has become a pivotal aspect of synthetic organic chemistry. The efficiency of constructing these heterocyclic moieties holds significance from both economic and ecological point of view. The increase in molecular complexity as one progresses from a simple starting material to complex products can give a measure of the competency of the reaction. Further, factors such as the number of steps involved, less toxic reagents, and waste reduction are crucial in evaluating the sustainability of synthetic processes.

Considering all these aspects, domino or cascade reactions have become an attractive and promising approach for constructing these complex molecules.[1] Precisely, cascade reactions are those transformations where the product of the first step acts as the substrate for the next step, and so on. Unlike traditional synthesis, where intermediates are purified or isolated at each step, cascade reactions enable the seamless formation of multiple bonds in a single operation without the need for purification of the intermediates. The success of a cascade reaction depends on its ability to efficiently form bonds, increase structural complexity, and be applicable across various substrates.[1] In this regard, several internal alkyne-based molecules possessing nucleophiles at appropriate positions have proven to be remarkable precursors for the domino synthesis of various heterocycles. Among various internal alkynes, *o*-alkynylanilines have become effective substrates and synthesized diverse heterocyclic motifs. This discussion has already been included in the introductory section (Chapter 1B).

Another exciting aspect of organic synthesis is the involvement of solvents as a reactive partner. Over the years, numerous reports have discussed the participation of solvents as an essential reagent in multi-component reactions.[2] In this context, DMSO has attracted considerable attention as a single or dual synthon in new molecule synthesis.[3] Dimethyl sulfoxide has a long history of being used as a polar aprotic solvent in synthetic chemistry.

However, over the past few decades, the reactivity of DMSO has been explored, and it is found to be a versatile reagent serving as a potential source of O, Me, SOMe, SO_2Me, $MeSCH_2$, $MeSOCH_2$, CH_2, CN, CHO, etc.[3] This aspect of DMSO is quite interesting and attractive. Considering the vastness of the topic, we limit the discussion to only the utility of DMSO as a one-carbon synthon.

V.2. Dimethyl Sulfoxide as a One-Carbon Source:

In 2019, Wang *et al*. disclosed a methodology for the synthesis of disubstituted 2-aryl-indoles and benzofurans from readily available starting materials under a base-mediated method using dimethyl sulfoxide (DMSO) as the carbon source. Here, DMSO plays a dual role, serving both as a solvent and a reactant for the *in situ* generation of sulfoxide under basic conditions. Mechanistic investigations suggest an anionic pathway comprising of four steps encompassing aldol condensation, Michael addition, dehydrosulfenylation, and isomerization reactions (Scheme V.2.1).[4]

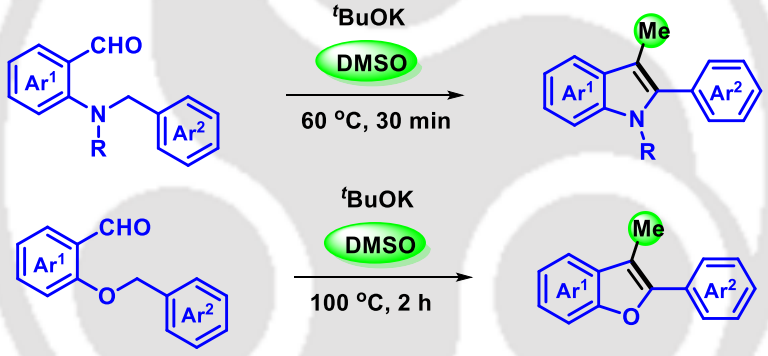

Scheme V.2.1. *DMSO as a one-carbon source in synthesizing disubstituted 2-aryl-indoles and benzofurans.*

In 2020, the Ma group employed DMSO as a carbon source in the synthesis of phenanthridines by a one-pot cascade Suzuki coupling and annulation between aryl boronic acids and *o*-bromo arylamides (Scheme V.2.2).[5]

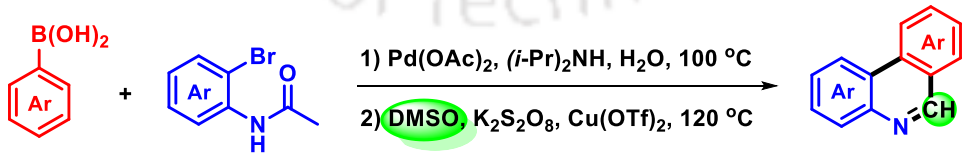

Scheme V.2.2. *Synthesis of phenanthridines using DMSO as a one-carbon synthon.*

Many reports have focused on employing DMSO as a formyl donor utilizing atmospheric oxygen as the oxidant.[6] Nevertheless, the use of DMSO as a formylating agent provides a more efficient approach to form the formylated product which can undergo various rearrangements to construct other highly functionalized molecular frameworks. In 2015, Cao

et al. developed a copper-catalyzed C3-formylation of imidazo[1,2-*a*]pyridine, enabling the direct generation of 3-formyl imidazo[1,2-*a*]pyridine derivatives (Scheme V.2.3).[6a]

Scheme V.2.3. *DMSO as a formylating agent under oxidative conditions.*

A Fe(III)-catalyzed synthesis of α-formylpyrroles *via* domino oxidation/formylation reaction of readily available 2,3-dihydro-*1H*-pyrroles in DMSO under an air atmosphere was reported by Zhang and Zhang. The reaction was compatible with a wide range of substrates resulting in the formylated products in moderate to good yields (Scheme V.2.4).[6b]

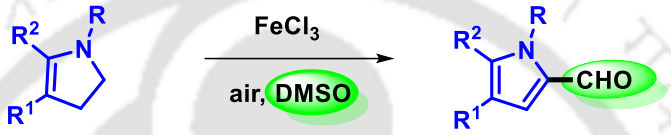

Scheme V.2.4. *DMSO as a formylating agent.*

V.3. Present Work:

As has already been discussed in the introductory chapter (Chapter 1B), our group is actively involved in the domino synthesis of different *N*-heterocycles such as 3-aroylindole, benzofuran[3,2-*c*]quinolin-6[5*H*]ones, indolo[2,3-*b*]quinolones and quinoline-4(1*H*)-thiones utilizing *o*-alkynylanilines as the synthetic precursor. To further explore *o*-alkynylanilines, we commenced our investigation by treating 2-(phenylethynyl)aniline (**1**) (1 equiv.) with malononitrile (**a**) (2 equiv) in the presence of KSCN (2 equiv), CuBr (15 mol%) and NBS (1 equiv) in DMSO at 110 °C in open air (Scheme V.3.1). After 6 hours, complete consumption of **1** with the appearance of a sharp orange colour spot in the TLC marked the completion of the reaction. The spectroscopic analysis of the isolated product (43%) and single-crystal X-ray diffraction studies of one of its derivatives confirmed the structure to be 2-(2-phenyl-1*H*-indol-3-yl)ethene-1,1,2-tricarbonitrile (**1a**). The presence of multiple –CN groups in conjugated heterocycles enhances its electron acceptor and solvatochromic properties, and such compounds can serve as essential components in non-linear optical, luminescence, and photovoltaic devices.[7] Despite the importance, not enough work is reported on the synthesis of tricyanovinylated indoles, and those reported involve the reaction of pre-synthesised indoles with tetracyanoethylene.[8] To the best of our knowledge, this is the only example of the cascade synthesis of 2-(2-phenyl-1*H*-indol-3-yl)ethene-1,1,2-tricarbonitrile employing *o*-alkynylaniline and malononitrile.

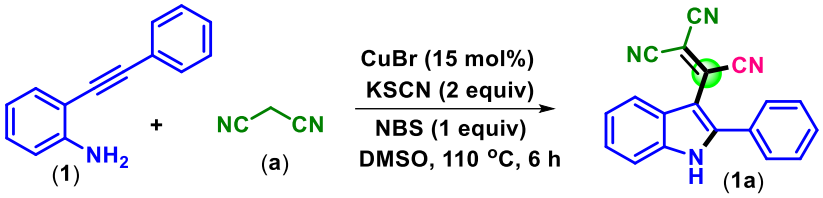

Scheme V.3.1. *Our initial reaction.*

V.3.1. Optimization of Reaction Conditions:

Captivated by the formation of the tricyanovinyl indole, further optimization of the reaction parameters was carried out using 2-(phenylethynyl)aniline (**1**) and malononitrile (**a**) to improve the overall yield. Initially, we began with a range of different copper salts such as CuBr, $Cu(OTf)_2$, CuI, CuO, and $Cu(OAc)_2$, out of which $Cu(OAc)_2$ gave a better yield of 49% (Table V.3.1, entries 1–5). Using alkynophilic silver salts such as Ag_2O and AgCl, instead of copper salts, showed no significant increase in the product yield (Table V.3.1, entries 6 and 7). To improve the reaction outcome, Pd salts such as $Pd(OAc)_2$, and $PdCl_2$ were also tested, but it resulted in a lower product yield (Table V.3.1, entries 8 and 9). Interestingly, the combination of $PdCl_2$ (7 mol%) and $Cu(OAc)_2$ (7 mol%) increased the yield to 61% and reduced the reaction time from 6 h to 1 h (Table V.3.1, entry 10). Next, a range of oxidants, such as *N*-chlorosuccinimide (NCS), ceric ammonium nitrate (CAN), and potassium persulfate ($K_2S_2O_8$) were screened. Still, none resulted in the successful formation of the desired product (**1a**) compared to NBS (Table V.3.1, entries 11–13). Lowering the oxidant loading further decreased the product yield (Table V.3.1, entry 14). Inorganic bases such as K_2CO_3, K^tOBu were examined in place of KSCN, but they all failed to give the desired product (Table V.3.1, entries 15 and 16). Replacing KSCN with NH_4SCN further improved the product yield to 66% (Table V.3.1, entry 17). Solvents such as CH_3CN, toluene, 1,4-dioxane, DCE (Table V.3.1, entries 18–21), etc., resulted in no product formation, whereas < 22% of the product (**1a**) was formed using DMF (21%) and DMA (17%) (Table V.3.1, entries 22 and 23). Failure of the reaction in all other solvents except those with similar characteristics as DMSO *i.e.*, DMF and DMA, which are known to serve as –Me source, hints towards the crucial involvement of solvent in this strategy. However, compared to all, a better product yield was obtained using DMSO (66%). To check the effect of the temperature, the reaction was performed at higher and lower temperatures, such as 130 °C and 90 °C. Lowering the temperature to 90 °C led to a decrease in the product yield, while increasing the temperature to 130 °C gave many side products (Table V.3.1, entries 24 and 25). A poor conversion at a higher temperature may be due to the decomposition of the product/intermediate or some other competitive reactions.

Table V.3.1. *Optimization of the reaction conditions*[a,b]

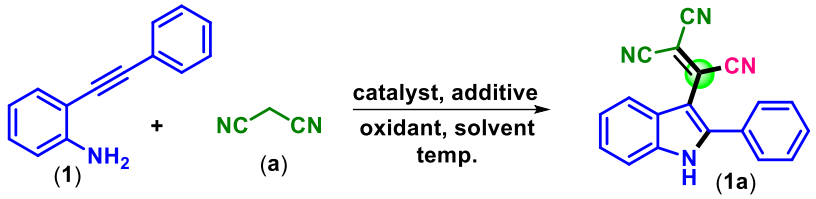

Entry	Catalyst (mol%)	Oxidant (equiv)	Additive (2 equiv)	Solvent	Yield (%)[b]
1	CuBr (15)	NBS (1)	KSCN	DMSO	43
2	$Cu(OTf)_2$ (15)	NBS (1)	KSCN	DMSO	38
3	CuI (15)	NBS (1)	KSCN	DMSO	35
4	CuO (15)	NBS (1)	KSCN	DMSO	40
5	$Cu(OAc)_2$ (15)	NBS (1)	KSCN	DMSO	49
6	Ag_2O (15)	NBS (1)	KSCN	DMSO	51
7	AgCl (15)	NBS (1)	KSCN	DMSO	44
8	$Pd(OAc)_2$ (10)	NBS (1)	KSCN	DMSO	15
9	$PdCl_2$ (10)	NBS (1)	KSCN	DMSO	19
10	$PdCl_2$ (7) + $Cu(OAc)_2$ (7)	NBS (1)	KSCN	DMSO	61
11	$PdCl_2$ (7) + $Cu(OAc)_2$ (7)	NCS (1)	KSCN	DMSO	32
12	$PdCl_2$ (7) + $Cu(OAc)_2$ (7)	CAN (1)	KSCN	DMSO	n.d.
13	$PdCl_2$ (7) + $Cu(OAc)_2$ (7)	$K_2S_2O_8$ (1)	KSCN	DMSO	46
14	$PdCl_2$ (7) + $Cu(OAc)_2$ (7)	NBS (0.5)	KSCN	DMSO	50
15	$PdCl_2$ (7) + $Cu(OAc)_2$ (7)	NBS (1)	K_2CO_3	DMSO	n.d.
16	$PdCl_2$ (7) + $Cu(OAc)_2$ (7)	NBS (1)	KO^{t}Bu	DMSO	n.d.
17	$PdCl_2$ (7) + $Cu(OAc)_2$ (7)	NBS (1)	NH_4SCN	DMSO	66
18	$PdCl_2$ (7) + $Cu(OAc)_2$ (7)	NBS (1)	NH_4SCN	CH_3CN	n.d.
19	$PdCl_2$ (7) + $Cu(OAc)_2$ (7)	NBS (1)	NH_4SCN	toluene	n.d.
20	$PdCl_2$ (7) + $Cu(OAc)_2$ (7)	NBS (1)	NH_4SCN	1,4-dioxane	n.d.
21	$PdCl_2$ (7) + $Cu(OAc)_2$ (7)	NBS (1)	NH_4SCN	DCE	n.d.
22	$PdCl_2$ (7) + $Cu(OAc)_2$ (7)	NBS (1)	NH_4SCN	DMF	21
23	$PdCl_2$ (7) + $Cu(OAc)_2$ (7)	NBS (1)	NH_4SCN	DMA	17
24[c]	$PdCl_2$ (7) + $Cu(OAc)_2$ (7)	NBS (1)	NH_4SCN	DMSO	57
25[d]	$PdCl_2$ (7) + $Cu(OAc)_2$ (7)	NBS (1)	NH_4SCN	DMSO	47
26[e]	**$PdCl_2$ (7) + $Cu(OAc)_2$ (7)**	**NBS (1)**	**NH_4SCN**	**DMSO**	**72**

[a]Reaction conditions: (**1**) (0.25 mmol), (**a**) (0.5 mmol), catalyst (mol%), oxidant (equiv), base (equiv), solvent (1.5 mL) at 110 °C for 1 h under air. [b]Yield of the isolated product. [c]Reaction at 90 °C. [d]Reaction at 130 °C. [e]Reaction using (**a**) (4 equiv). n.d. = not detected

It was observed that increasing the concentration of malononitrile (**a**) to 4 equivalents proved to be beneficial for improving the yield up to 72% with lesser side-products (Table V.3.1, entry 26). Finally, the optimized condition for this transformation are the use of malononitrile (**a**) (4 equiv), $PdCl_2$ (7 mol%), $Cu(OAc)_2$ (7 mol%), NH_4SCN (2 equiv) and NBS (1 equiv) in 1.5 mL DMSO at 110 ^oC.

V.3.2. Substrate Scope:

With the optimized reaction conditions in hand, the scope of this novel cyclization-functionalization protocol was extended to a variety of *o*-alkynylanilines (Scheme V.3.2.1). Initially, we began our investigation to see the effect of substituents on the amine-containing phenyl ring of 2-(phenylethynyl)aniline (R^1). The presence of electron-donating groups resulted in good yields of the products **2a** (67%), **3a** (58%), and **4a** (70%); however, the yields obtained were found to be lower than the unsubstituted analogue **1a** (72%) (Scheme V.3.2.1). Electron-withdrawing groups such as *p*-F (**5**), *p*-Cl (**6**), *p*-Br (7), and *p*-CF_3 (**8**) resulted in the products (**5a–8a**) in 57%, 61%, 64%, and 49% yield, respectively. Next, the effect of substituents (R^2) on the phenyl ring towards the alkyne side was examined. Electron-donating groups (**9–11**) and electron-withdrawing groups (**12–15**) reacted efficiently to result in the desired products {**9a** (65%), **10a** (71%), **11a** (58%), **12a** (62%), **13a** (73%), **14a** (67%), **15a** (70%)} (Scheme V.3.2.1).

Next, the effects of substituents on both the phenyl rings, *i.e.*, the amine side and alkyne side of the substrate, were explored (Scheme V.3.2.2). When both the rings possess groups such as *p*-Me/*p*-Me (**16**), *p*-Me/*p*-^{t}Bu (**17**), *p*-Me/*p*-F (**18**), *p*-F/*p*-Me (**19**), *p*-Br/*p*-^{t}Bu (**20**) and *p*-F/*p*-F (**21**), the yields of products obtained were 68% (**16a**) and 70% (**17a**), 62% (**18a**), 59% (**19a**), 78% (**20a**) and 60% (**21a**) respectively. The structure of **19a** has been ascertained by single-crystal X-ray crystallography and is presented in Figure V.3.1. An unsymmetrical tri-substituted substrate (**22**), despite having two electron-withdrawing substituents on a single phenyl ring successfully formed the desired product (**22a**) in 55% yield. When aliphatic groups like *n*-butyl and cyclopropyl were used instead of the phenyl group on the alkyne side of the substrate, products **23a** and **24a** were obtained in 47% and 67% yield, respectively (Scheme V.3.2.2). Furthermore, the reaction proceeded smoothly when 2-(naphthalen-2-ylethynyl)aniline (**25**) and 2-(thiophen-2-ylethynyl)aniline (**26**) were employed, giving the corresponding tricyanovinyl indoles **25a** and **26a** in 46% and 59% yields, respectively. However, the present methodology failed when there was *p*-CN (**27**) and *p*-NO_2 (**28**) substitution on the R^1 and for 2-(pyridin-2-ylethynyl)aniline (**29**) (Scheme V.3.2.2). In all the

above substrates, no definite pattern of yields was observed which could be correlated to the electronic nature of the attached substituents.

Scheme V.3.2.1. *Substrate scope for substituted o-alkynylaniline.*[a,b]

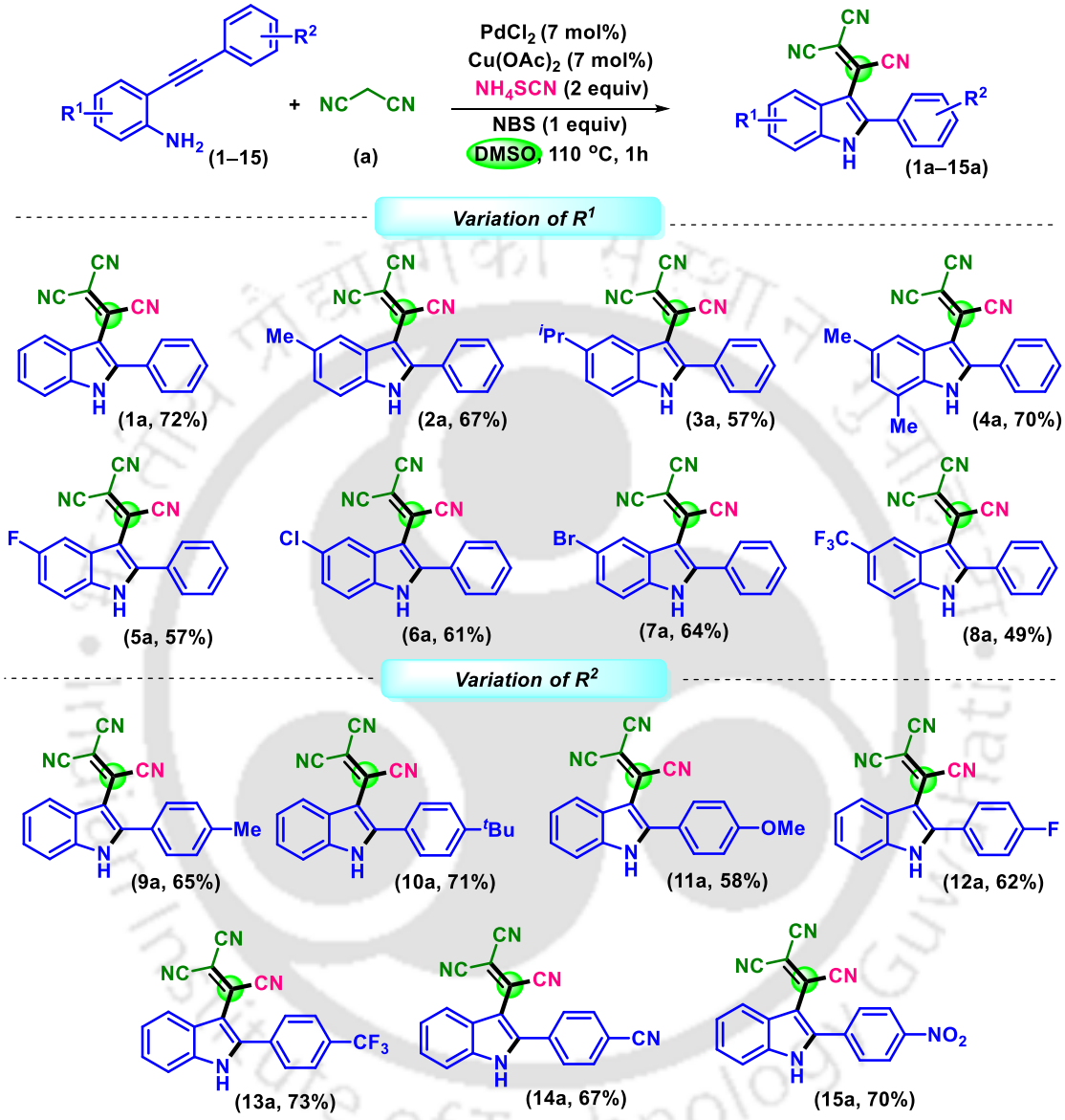

[a]Reaction conditions: Reaction conditions: (**1**–**15**) (0.25 mmol), (**a**) (1 mmol), $PdCl_2$ (7 mol%), $Cu(OAc)_2$ (7 mol%), NH_4SCN (0.5 mmol), NBS (0.25 mmol), DMSO (1.5 mL) at 110 °C for 1 h under air. [b]Yield of the isolated product.

Scheme V.3.2.2. *Substrate scope for substituted o-alkynylaniline.*[a,b]

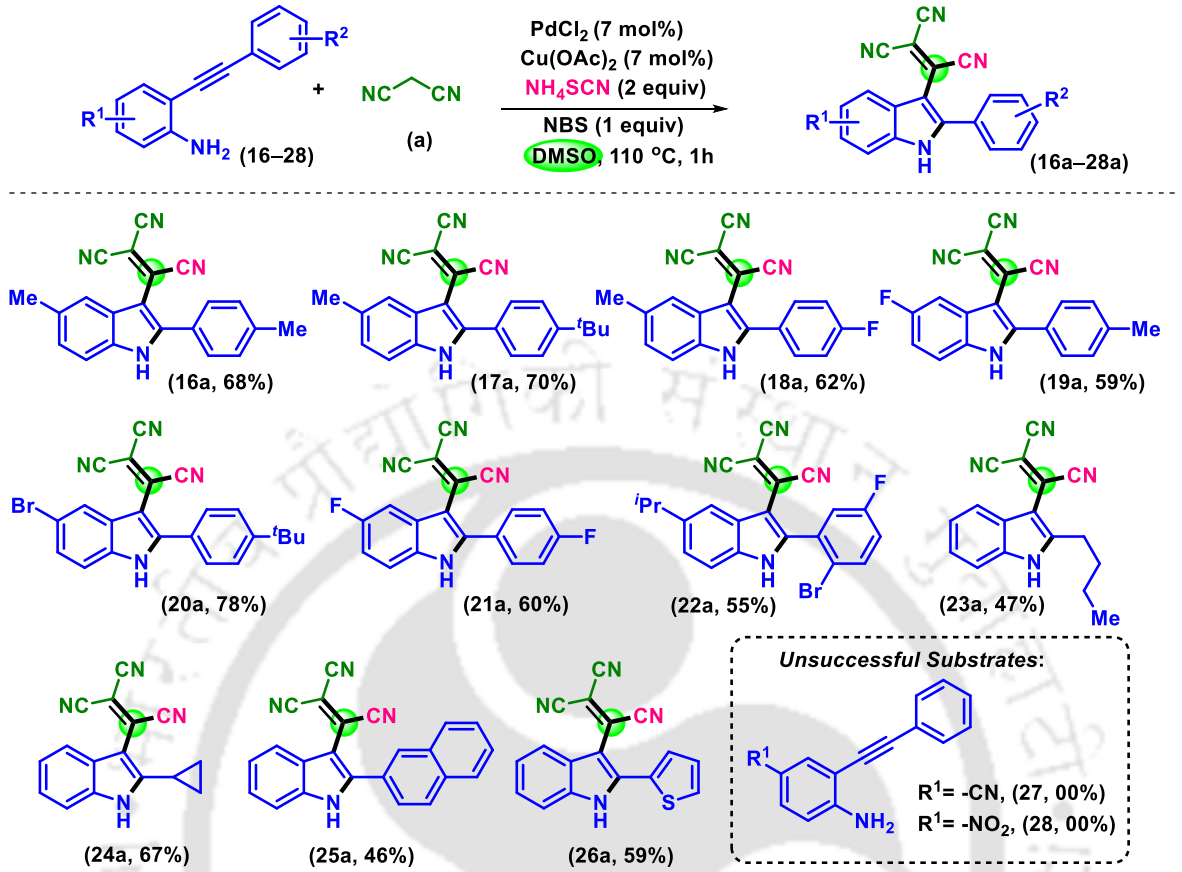

[a]Reaction conditions: (**16**–**28**) (0.25 mmol), (**a**) (1 mmol), $PdCl_2$ (7 mol%), $Cu(OAc)_2$ (7 mol%), NH_4SCN (0.5 mmol), NBS (0.25 mmol), DMSO (1.5 mL) at 110 °C for 1 h under air. [b]Yield of the isolated product.

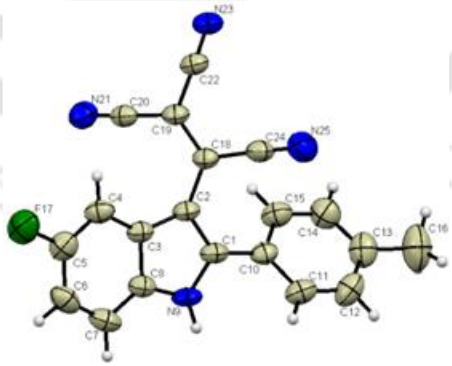

Figure V.3.2. *ORTEP structure of **19a** (CCDC 2051416).*

V.3.3. Mechanistic Investigations:

After successfully demonstrating the substrate scope on various *o*-alkynylanilines, various investigations were carried out to understand the mechanism of this unprecedented

reaction. Initially, we were curious to find the sources of the three –CN groups and the carbon attached to C–3 of the indole. From a few literature precedents, it was presumed that there might be a reaction between indole and tetracyanoethylene.[8] Hence, to determine whether the tricyanovinyl group is originating from the *in situ* dimerized malononitrile, a control reaction was carried out between **1** and tetracyanoethylene (**b**) (Scheme V.3.3.1). The failure to form the desired product rules out any involvement of tetracyanoethylene in the reaction.

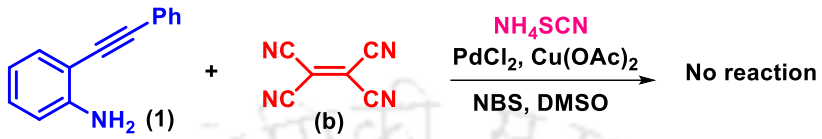

Scheme V.3.3.1. *Involvement of tetracyanoethylene in the reaction.*

Moreover, when a reaction was performed without thiocyanate, it failed to result in the anticipated product. This observation suggested the crucial involvement of –SCN in the overall strategy (Scheme V.3.3.2).

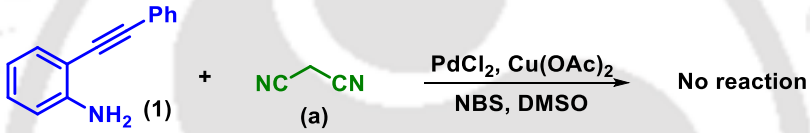

Scheme V.3.3.2. *Role of NH_4SCN.*

The above two experiments and the incompatibility of the reaction in solvents other than DMSO hinted towards the possible involvement of DMSO as one carbon source in the reaction. The exact function as to how the solvent participates as a formyl source is still not clear, and hence based on literature reports,[6] a few control experiments were carried out. To ascertain the radical nature of the reaction, identical reactions were conducted in the presence of radical scavengers, 2,2,6,6-tetramethylpiperidine-1-oxyl (TEMPO, 2 equiv) and 1,1'-diphenylethylene. Failure of the reaction under the standard reaction conditions, along with the formation of a multitude of products, approves the radical nature of the reaction (Scheme V.3.3.3). Moreover, the HRMS and ESI-MS analysis of both the reaction aliquots suggests the formation of a methylated TEMPO adduct (**1a'**) (Figure V.3.3.1) and a methylated 1,1-diphenylethylene adduct (**1a''**) (Scheme V.3.3.2), thereby confirming the generation of a methyl radical.

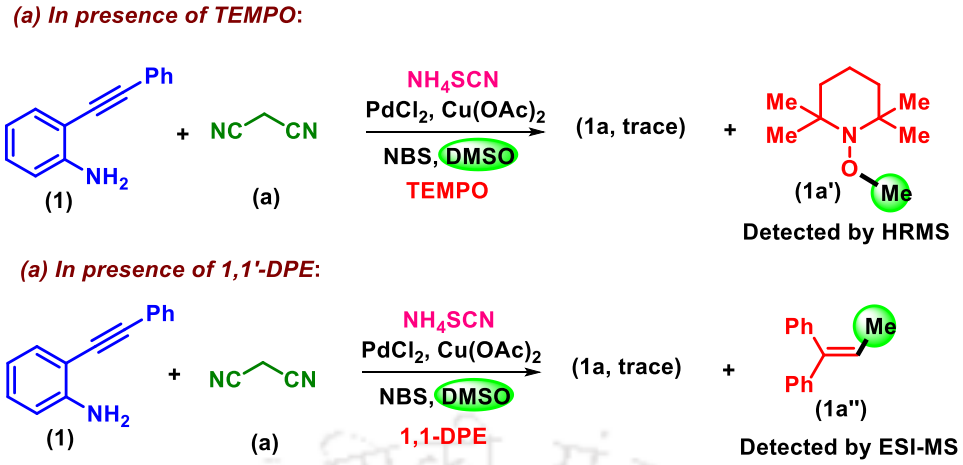

Scheme V.3.3.3. *Radical-trapping experiments.*

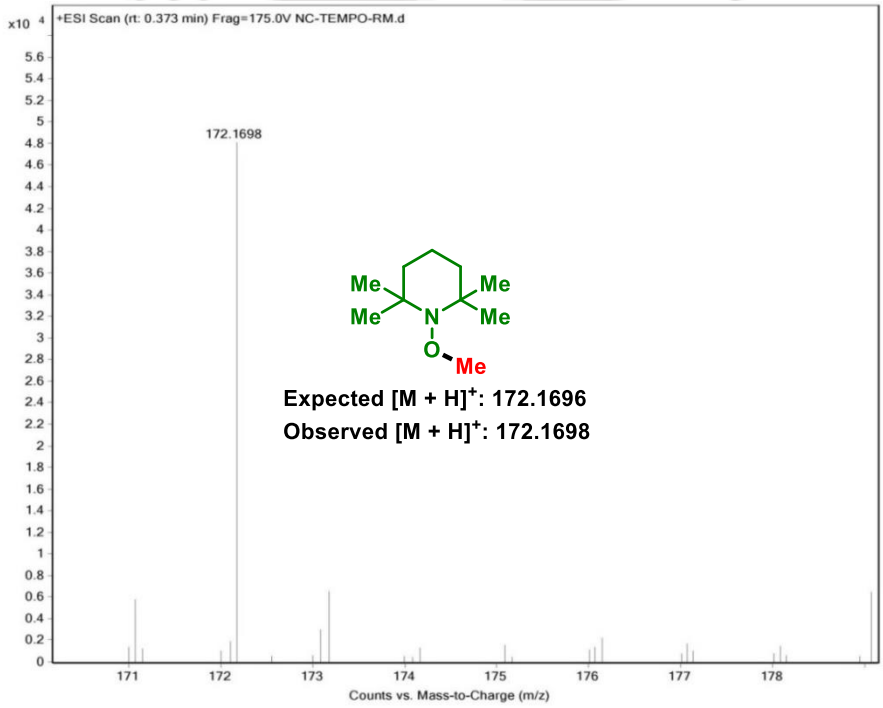

Figure V.3.3.1 *HRMS analysis of methylated-TEMPO adduct.*

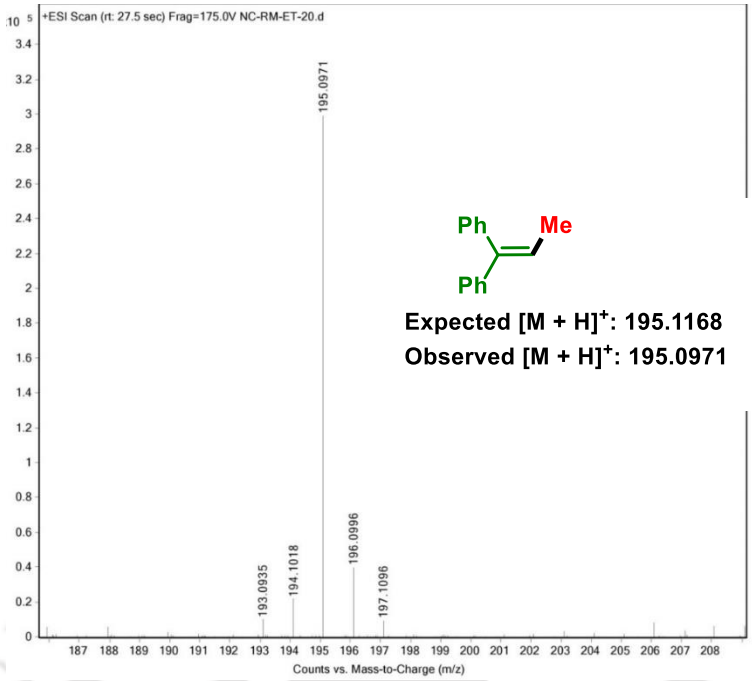

Figure V.3.3.2. *HRMS analysis of methylated-1,1-diphenylethylene adduct.*

To get better insight into the reaction mechanism, ^{1}H NMR and IR analysis of the reaction mixture was carried out at regular intervals during the reaction. The occurrence of peaks at δ 12.7 ppm (^{1}H NMR) and 1711 cm^{-1} (IR) indicated the generation of a carbonyl moiety as a plausible intermediate (Figure V.3.3.3 and V.3.3.4). This observation presented a new direction to this cascade strategy, suggesting the possible formation of 3-formylindole, followed by the Knoevenagel condensation with malononitrile as the possible reaction route. Further analysis of the ^{1}H NMR spectra of the reaction aliquots suggests the sequential appearance of –CH_3, –CH_2O, and –CHO peaks. This suggested the formation of peroxy intermediate followed by carbonyl intermediate. Further, the reaction aliquot was subjected to ESI-MS analysis, which gave ESI-MS values corresponding to the peroxo intermediate (Figure V.3.3.5).

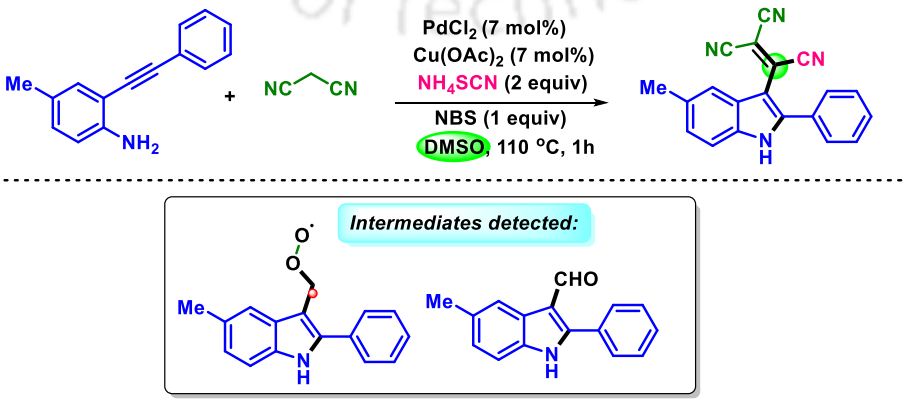

Scheme V.3.3.4. *Detection of reaction intermediates.*

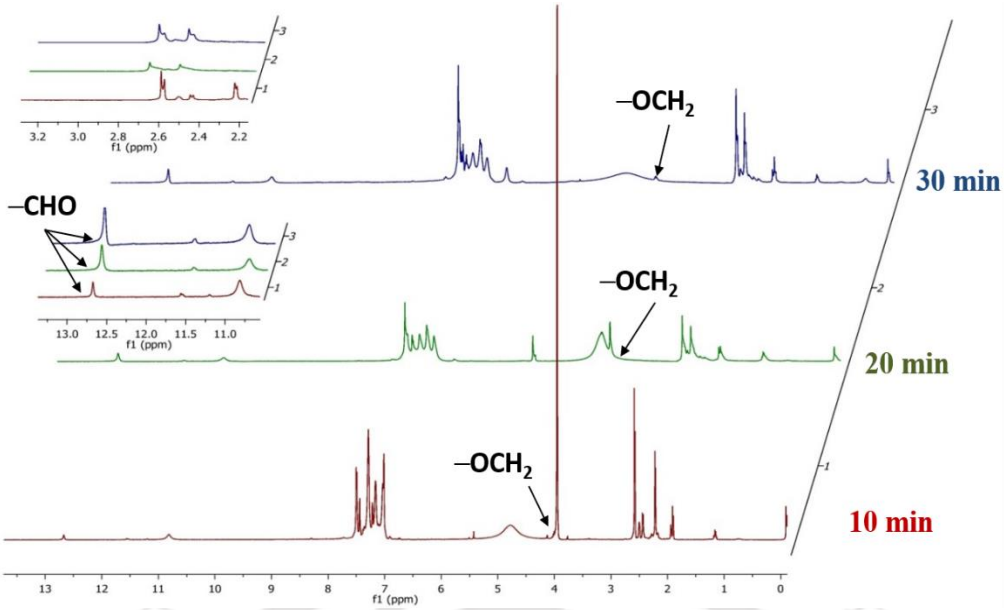

Figure V.3.3.3. *^{1}H NMR analysis of reaction aliquot.*

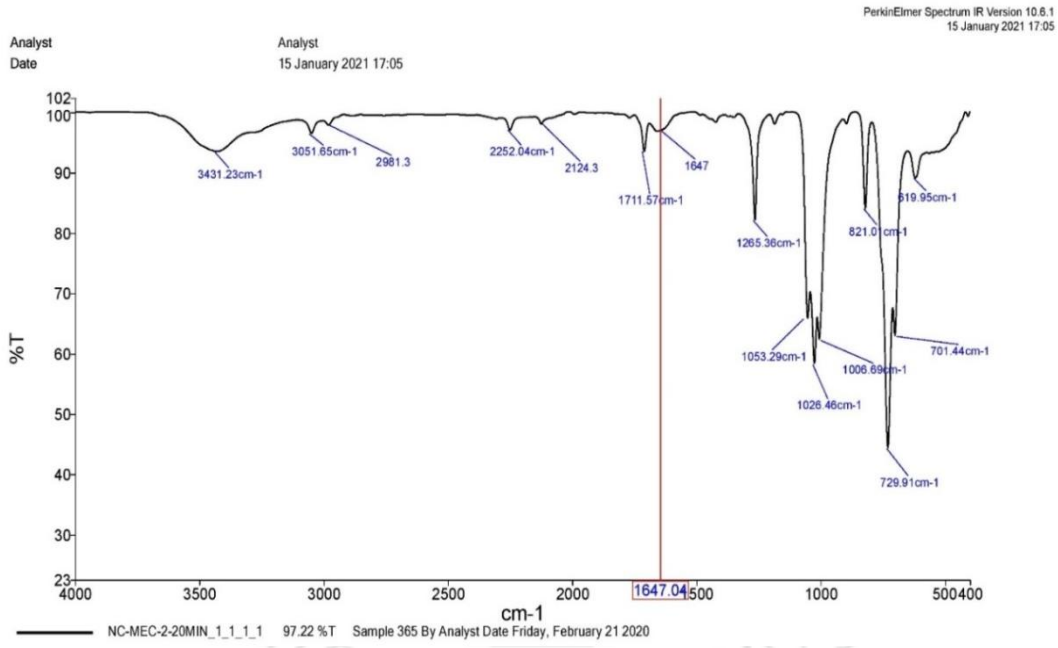

Figure V.3.3.4. *IR analysis of reaction aliquot.*

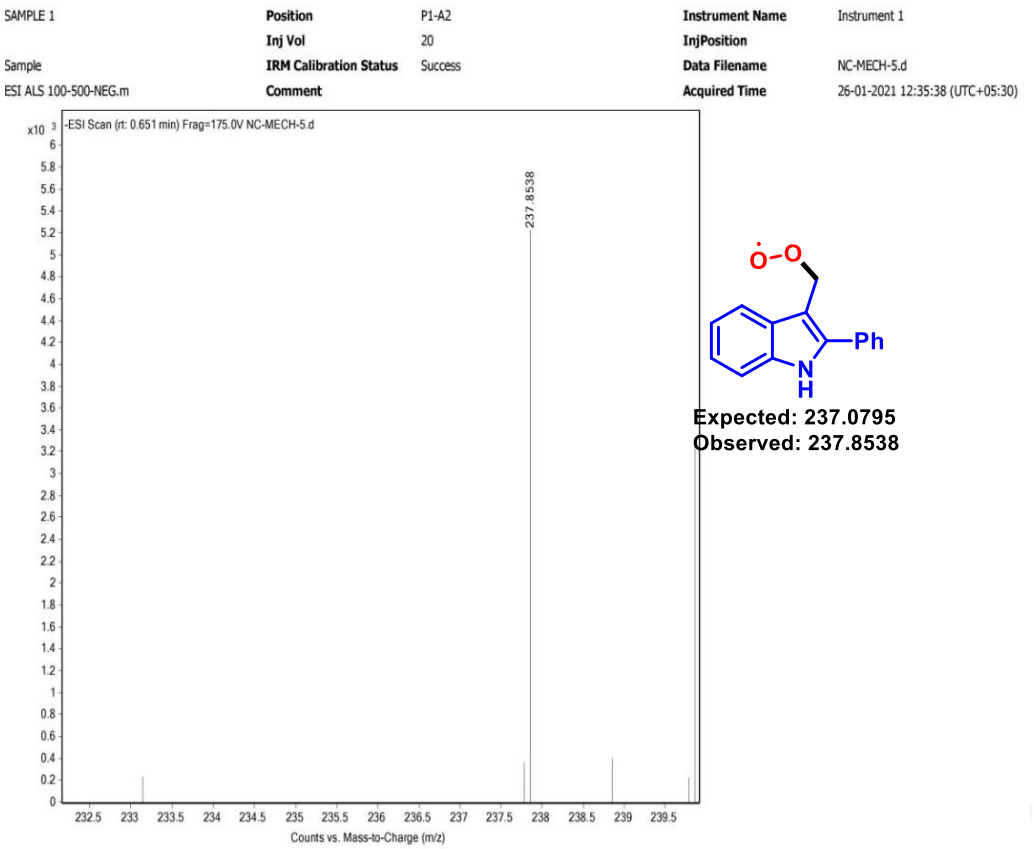

Figure V.3.3.5 *ESI-MS analysis of reaction intermediate.*

All the above control experiments suggested that the reaction proceeds through the formation of 3-formyl indole, where DMSO serves as the carbonyl source. For further confirmation, pre-synthesized 2-phenyl-3-formylindole (**G**)[9] was subjected to the optimized conditions, and the anticipated tricyanovinyl (**1a**) was obtained successfully (Scheme V.3.3.5).

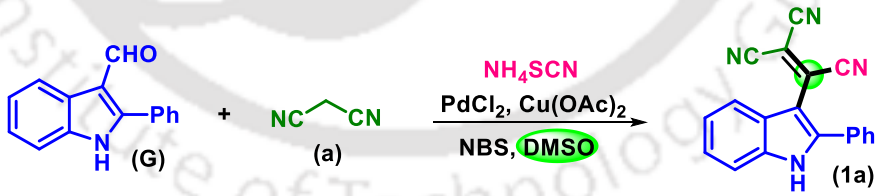

Scheme V.3.3.5. *Intermediacy of 2-phenyl-3-formylindole.*

The intermediate (**G**) would undergo Knoevenagel condensation with malononitrile (**a**) to give the dicyanovinylated indole intermediate (**H**). Thus, to further confirm its intermediacy, preformed **H**[10] was employed under the standard condition in the absence of malononitrile (**a**) (Scheme V.3.3.6). The successful formation of **1a** infers that the reaction proceeds *via* intermediate **H**.

Scheme V.3.3.6. *Formation of intermediate H.*

The above observation also pointed towards the fact that NH_4SCN must act as the source of the third nitrile group. Hence, to corroborate this supposition, a reaction was conducted between 2-methyl-1*H*-indole (**30**) in the absence of malononitrile keeping the other reaction conditions fixed. This led to the successful formation of 2-methyl-1*H*-indole-3-carbonitrile (**30b**), emphasizing the role of NH_4SCN as the third nitrile group under these reaction conditions (Scheme V.3.3.7).[11]

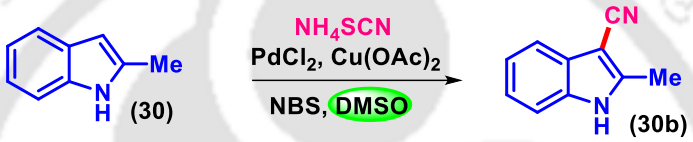

Scheme V.3.3.7. *Role of NH_4SCN.*

Next, the role of $PdCl_2$ and the intermediacy of **B** were tested by performing two independent reactions of 2-phenyl-1*H* indole (**B**) in the presence and absence of the Pd catalyst. Both reactions led to the formation of **1a** in 52% and 49% yields, respectively. This confirms the intermediacy of **B** and the role of $PdCl_2$ in the formation of **B** *via* 5-*endo-dig* cyclization of 2-(phenylethynyl)aniline (**1**) (Scheme V.3.3.8).[12]

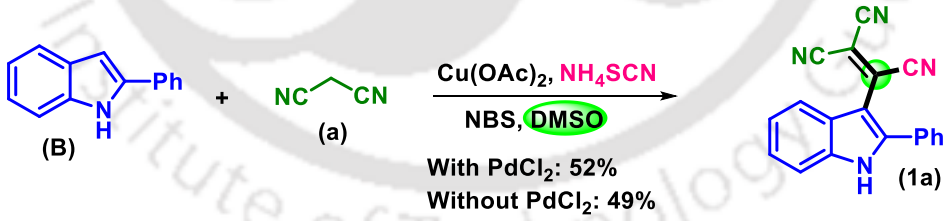

Scheme V.3.3.8. *Intermediacy of 2-phenylindole and role of $PdCl_2$.*

Further, when the reaction was conducted in the absence of *N*-bromo succinimide (NBS), a trace amount of the product was formed (Scheme V.3.3.9). This implied that NBS plays an essential role in the overall methodology.

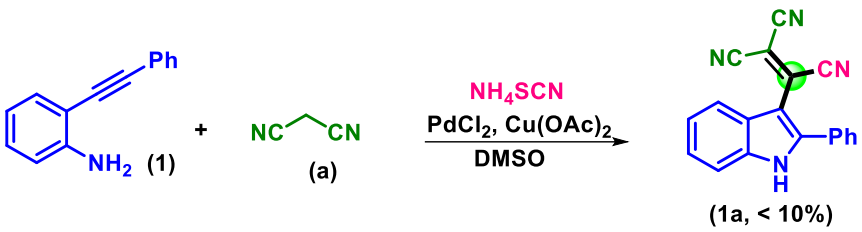

Scheme V.3.3.9. *Reaction in the absence of NBS.*

V.3.4. Plausible Mechanism:

Based on literature precedents,[6,11–14] control experiments, and detection of intermediates *via* ^{1}H NMR and HRMS analyses of the reaction at different time intervals, a plausible mechanism is proposed (Scheme V.3.4). Initially, 2-(phenylethynyl)aniline (**1**) undergoes 5-*endo-dig* cyclization *via* aminopalladation to give 2-phenyl indole (**B**).[12] This heterocycle **B** is oxidized to aminyl intermediate **C**. On the other hand, the heterolytic cleavage of DMSO to the CH_3 radical occurs in the presence of Cu^{II} and O_2.[6a]

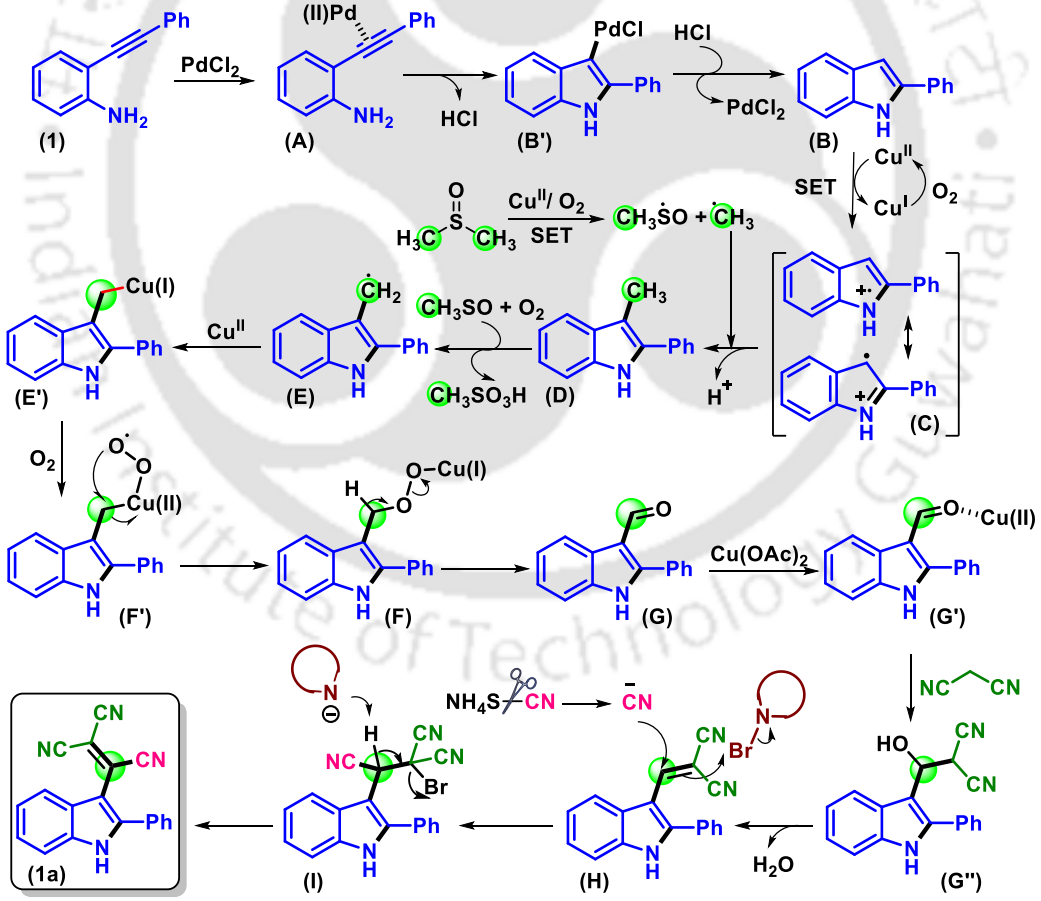

Scheme V.3.4. *Plausible mechanism.*

The radical coupling of intermediate **C** and the CH_3 radical gives 3-methyl-2-phenyl indole (**D**). Next, the CH_3SO species abstracts an H radical from intermediate **D** to give

intermediate **E** and methanesulfonic acid in the presence of oxygen.[13] Further oxidation of intermediate **E** in the presence of Cu^{II}/O_2 generates a peroxy species (**F**) *via* intermediate **F'**. The peroxy intermediate **F** generates a formyl intermediate (**G**), which subsequently undergoes Knoevenagel-type condensation with malononitrile to give intermediate **H**.[14] Next, the conjugate addition of the CN^- ion (obtained from NH_4SCN)[11] to intermediate **H** occurs with concurrent bromination utilizing NBS. The formation of the desired tricyanovinylindole (**1a**) is achieved *via* the elimination of HBr, which is facilitated by a succinimide anion (Scheme V.3.4).

V.3.5. DFT Calculation:

To account for the relative stability of intermediate 2-phenyl-3-methylindole (**D**) and its further oxidation even in the presence of methyl groups in other positions in the substrate (as in substrates **2** and **9**), DFT calculations were carried out using Gaussian-16 program package.[15] The calculation has been performed with the help of the density functional theory approach along with the M06-2X functional and the cc-pVTZ basis set for hydrogen, carbon and nitrogen atoms. The thermodynamic parameters for relative energy and enthalpy for these three radicals have been calculated and shown in Figure V.3.5, the values are expressed in kcal mol^{-1}. As can be seen from Figure V.3.5, the relative energy is lowest for radical_III, signifying its greater stability. Also, the methyl radical in 3-methyl-2-phenyl indole (**D**) is present on the pyrrole ring of indole, which is electronically rich compared to the other two radical species which are present on the electron-deficient benzene ring. These calculations suggest that the resultant methyl radical in 3-methyl-2-phenyl indole (**D**) is more stable than the corresponding radicals originating from methyl groups in other positions.

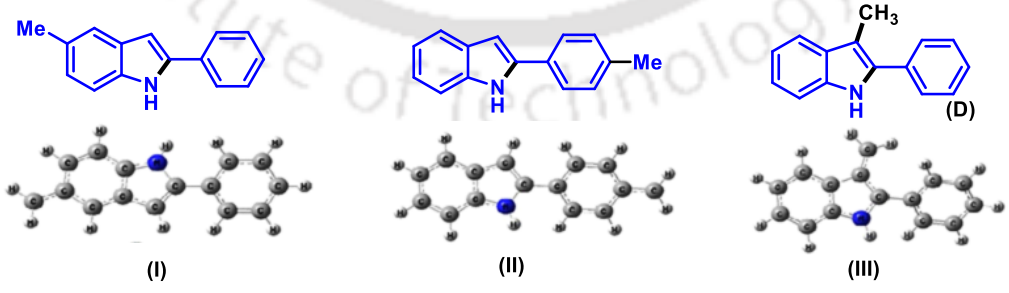

Species	Rel. E (kcal.mol^{-1})	Rel. H (kcal.mol^{-1})	Comment
Radical_I	0.00	0.00	Least stable
Radical_II	-1.56	-1.58	Gain stability
Radical_III	-2.51	-35.32	Most stable

Figure V.3.5. *DFT calculation for the relative stability of methyl-substituted indole.*

V.3.6. Post Synthetic Modification to Indolylmaleimides:

In an attempt to carry out further synthetic transformations of the product, selective hydrolysis was attempted to convert the nitrile functionality to an amide functionality.[16] Treatment of **2a** with $Cu(OAc)_2.H_2O$ in AcOH at 80 °C resulted in selective hydrolysis of one of the nitrile functionalities which is subsequently involved in the concomitant cyclization to form 4-(5-methyl-2-phenyl-1*H*-indol-3-yl)-2,5-dihydro-1*H*-pyrrole-3-carbonitrile (**2ab**) (57%) (Scheme V.3.6.1). Maleimides are a pivotal substructure in numerous pharmaceuticals, natural products, and material science. Consequently, newer methodologies for developing these scaffolds are in high demand.[17] This selective hydrolytic-cyclization protocol opened a new avenue for constructing nitrile-substituted indolylmaleimides, which are unexplored moieties.

Scheme V.3.6.1. *Post-synthetic modification to 3-cyano-4-indolylmaleimide.*[a,b]

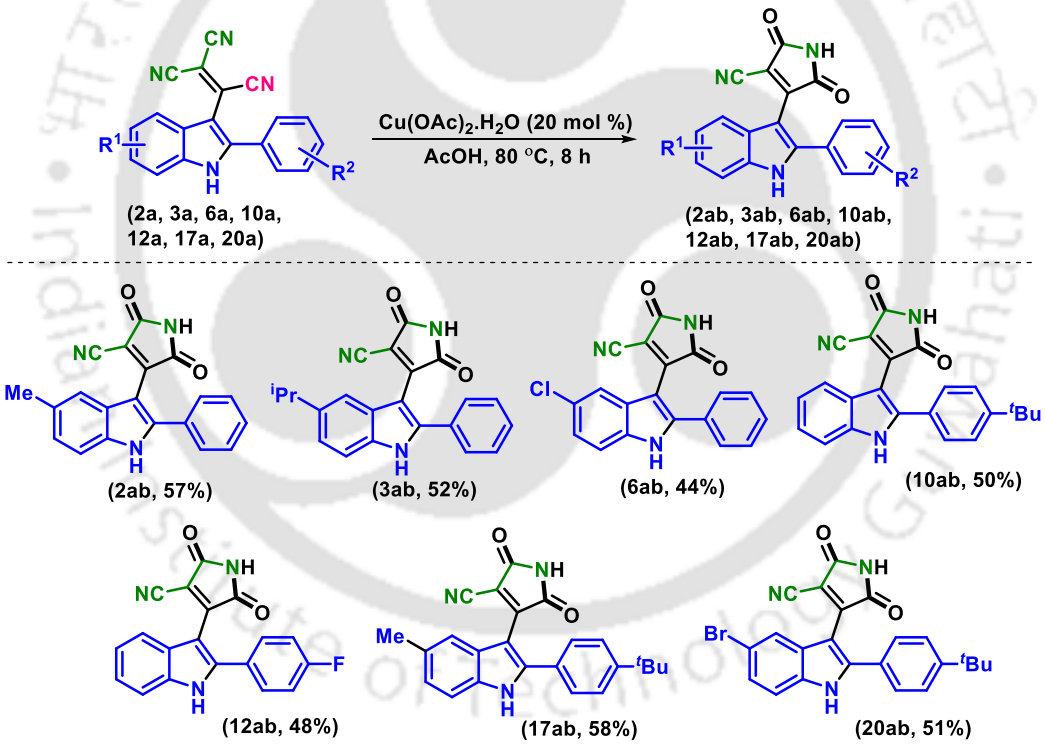

[a]Reaction conditions: (**2a**, **3a**, **6a, 10a, 12a, 17a, 20a**) (0.15 mmol), $Cu(OAc)_2.H_2O$ (20 mol %), AcOH (1.5 mL) at 80 °C for 8 h under air. [b]Yield of product.

With this remarkable outcome, the generality of this method was further extended, and various tricyanovinylindoles (**2a**, **3a**, **6a**, **10a**, **12a**, **17a**, **20a**) having different electronic effects were subjected to similar reaction conditions. Initially, the effect of substituents (R^1) on the benzene part of indole was explored. Indoles (**2a**, **3a**, **6a**) bearing electron-donating and

electron-withdrawing substituents in the phenyl ring reacted smoothly, giving their hydrolyzed products **2ab** (57%), **3ab** (52%), and **6ab** (44%) in good yields (Scheme V.3.6.1). Next, the substituents (R^2) on the 2-phenyl ring of indoles were varied. Both *p*-^{t}Bu (**10a**) and *p*-F (**12a**) gave their corresponding indolylmaleimides **10ab** (50%) and **12ab** (48%) in acceptable yields. When both the substituents (R^1 and R^2) were varied as *p*-Me/*p*-^{t}Bu (**17a**) and *p*-Br/*p*-^{t}Bu (**20a**), the corresponding products **17ab** (58%) and **20ab** (51%) were obtained in good yield (Scheme V.3.6.1).

In the proposed mechanism (Scheme V.3.6.2), the *cis*-cyano groups originating from malononitrile is selectively hydrolyzed in the presence of the other two cyano groups. This is due to the higher electron density owing to conjugation with the nitrogen atom of the pyrrole ring. Thus, the copper effectively binds at this site triggering the hydrolysis (Scheme V.3.6.2).

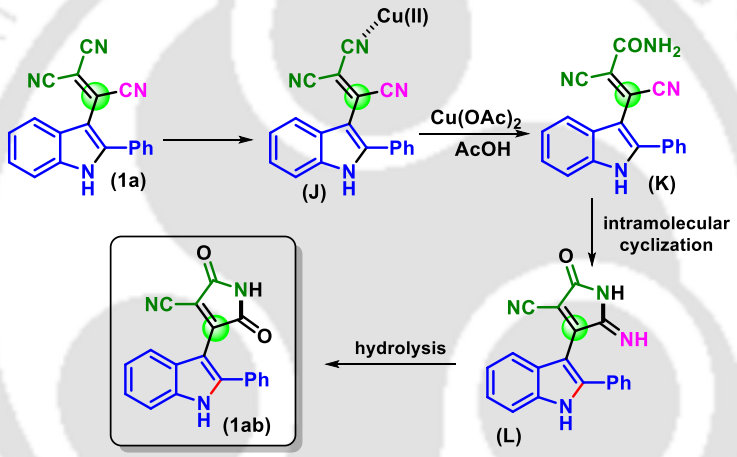

Scheme V.3.6.2. *Mechanism for the formation of 3-cyanoindolylmaleimides.*

V.3.7. Scale-up Reaction:

To demonstrate the scalability of this protocol, a gram-scale reaction (5 mmol, 1.035g) of 4-methyl-2-(phenylethynyl)aniline (**2**) resulted in the successful formation of **2a** in 49% yield. (Scheme V.3.7).

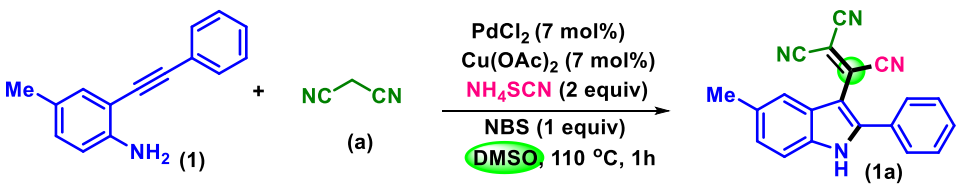

Scheme V.3.7. *Scale-up reaction for the synthesis of tricyanovinylindoles (**1a**).*

V.3.8. Photophysical Studies:

Next, photophysical studies such as UV-vis and photoluminescence were conducted on a few selected compounds. The absorption λ_{abs} and the emission λ_{em} spectra of the compounds were measured in 0.143 mM acetonitrile solution. The UV-vis and fluorescence emission spectra of these compounds (**2a**, **8a**, **9a**, **13a**, **22a**, **23a**, **25a**) are presented in Figure V.3.8. As evident from the UV-vis spectra, most compounds exhibit three distinct absorption maxima. The fluorescence emission spectra infer that the compounds **25a**, **8a**, and **9a** show the maximum fluorescence intensity, and thus they may find potential application in various fields of research (Figure V.3.8).

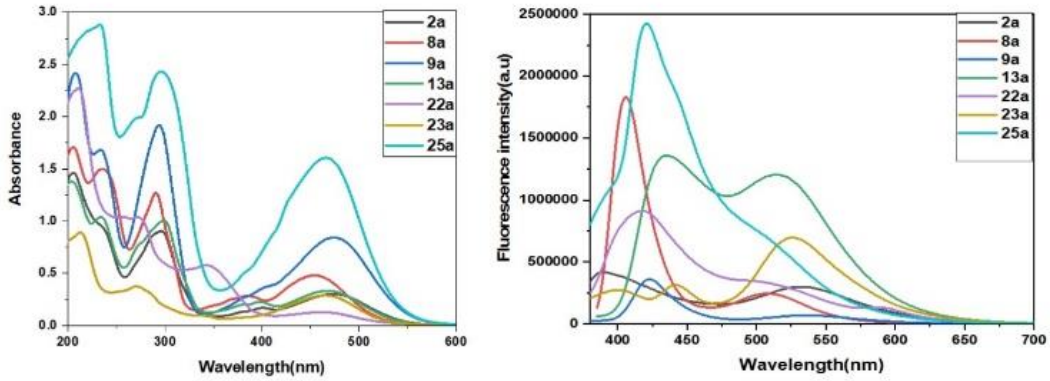

Figure V.3.8. *UV-vis spectra (left) and Photoluminescence spectra (right) of **2a**, **8a**, **9a**, **13a**, **22a**, **23a**, **25a** in 0.143 mM CH_3CN solution.*

Table V.3.8. *UV-vis and Photoluminescence Parameters*

Entry	Compound	Colour under UV lamp (365 nm)	λ_{abs} (nm)	$\varepsilon \times 10^3$ (L mol^{-1} cm^{-1})	λ_{em} (nm)
1	**2a**	Yellow	296, 399, 475	6.33, 1.17, 2.10	533
2	**8a**	Blue	233, 291, 454	10.48, 9.14, 3.36	410
3	**9a**	Orange red	234, 294, 474	11.85, 13.49, 5.90	422, 538
4	**13a**	Greenish yellow	233, 298, 468	7.27, 7.03, 2.32	435, 515
5	**22a**	Greenish yellow	272, 343, 464	7.37, 4.08, 0.89	417, 510
6	**23a**	Green	271, 465	2.66, 2.06	526
7	**25a**	Blue	233, 293, 462	20.13, 17.0, 11.18	421

V.3.9. Conclusion:

In conclusion, an efficient one-pot strategy for the synthesis of tricyanovinyl indoles utilising DMSO as a one-carbon surrogate has been developed. This operationally simple reaction leads to the formation of one C–N, one C–C and two C– C bonds. This cascade reaction undergoes sequential cyclization, formylation followed by cyanation to generate functionalized indoles. The post-synthetic modification resulted in the unprecedented formation of 4-cyano-3-indolylmaleimides. Photophysical studies on a few selected compounds indicate their future applicability in non-linear optics, light-emitting diodes, bio-imaging, and various other research fields.

V.4. Experimental Section:

V.4.1. General Information:

All the reagents were commercial grade and purified according to the established procedures. All the reactions were carried out in oven-dried glassware. The highest commercial quality reagents were purchased and were used without further purification unless otherwise stated. All the cinnamic acids used in this protocol were commercially purchased from Sigma Aldrich and BLD Pharma. Reactions were monitored by thin layer chromatography (TLC) on 0.25 mm silica gel plates ($60F_{254}$) visualized under UV illumination at 254 nm. Organic extracts were dried over anhydrous sodium sulfate (Na_2SO_4). Solvents were removed using a rotary evaporator under reduced pressure. Column chromatography was performed to purify the crude product on silica gel 60–120 mesh using a mixture of hexane and ethyl acetate as eluent. The isolated compounds were characterized by spectroscopic [^1H, $^{13}C\{1H\}$ NMR, and IR] techniques and HRMS analysis. NMR spectra were recorded in deuterochloroform ($CDCl_3$) and deuterated dimethylsulfoxide (DMSO-d_6). ^1H, $^{13}C\{^1H\}$ were recorded in 400 (100), 500 (125) or 600 (150) MHz spectrometers. The chemical shifts are quoted in δ units, parts per million (ppm). ^1H NMR data is represented as follows: Chemical shift, multiplicity (s = singlet, d = doublet, t = triplet, q = quartet, dd = doublet of doublets, m = multiplet), integration and coupling constant(s) *J* in hertz (Hz). HRMS spectra were recorded using ESI mode (Q-TOF type Mass Analyser). IR spectra were recorded in KBr or neat. All UV experiments were performed at a probe concentration of 0.143 mM in 1 mL quartz cuvettes of path length 1 cm at 25 ^oC in UV/VIS Spectrometer. Photoluminescence were carried out at a concentration of

0.143 mM in 1 mL quartz cuvettes at 25 ^{o}C in Spectrofluorometer in HPLC grade acetonitrile solution.

V.4.2. Crystallographic Information:

Crystallographic information of *2-(5-fluoro-2-(p-tolyl)-1H-indol-3-yl)ethene-1,1,2-tricarbonitrile (19a)*:

(i) Data Collection: Diffraction data were collected at 292 K with MoKα radiation (λ = 0.71073 Å) using a Bruker Nonius SMART APEX CCD diffractometer equipped with a graphite monochromator and Apex CD camera. The SMART software was used for data collection and for indexing the reflections and determining the unit cell parameters. Data reduction and cell refinement were performed using SAINT software and the space groups of these crystals were determined from systematic absences by XPREP and further justified by the refinement results. The structures were solved by direct methods and refined by full-matrix least-squares calculations using SHELXTL-973 software. All the non-H atoms were refined in the anisotropic approximation against F2 of all reflections.

(ii) Crystallographic description:

M.F. = $C_{20}H_{11}FN_4$, crystal dimensions 0.26 x 0.22 x 0.24 mm, M_r = 326.33, monoclinic space, group P 21/c, a = 11.4106 (7), b = 14.3958 (14), c = 9.9664 (5) Å, α = 90^{o}, β = 94.167^{o} (6) , γ = 90^{o}, V = 1632.8 (2) Å^3, Z = 4, ρ_{calcd} = 1.327 g/cm^3, μ = 0.090 mm^{-1}, F(000) = 672.0, refinement method = full-matrix least-squares on F^2, final R indices [$I > 2\sigma(I)$]: R_1 = 0.0521 (1842), wR_2 = 0.1383 (3709), goodness of fit = 1.000. CCDC No = 2051416 for 2-(5-fluoro-2-(*p*-tolyl)-1*H*-indol-3-yl)ethene-1,1,2-tricarbonitrile **(19a)** contains the supplementary crystallographic data for this paper. These data can be obtained free of charge from The Cambridge Crystallographic Data Centre via www.ccdc.cam.ac.uk/data_request/cif.

V.4.3. General Procedure:

V.4.3.1. Procedure for the Synthesis of Starting Substrates (1-29):

A 50 mL oven-dried round bottom flask was charged with a magnetic stir bar, [$Pd(PPh_3)_2Cl_2$] (0.04 mmol; 28 mg), CuI (0.08 mmol; 15.2 mg) and 2-iodo aniline (2 mmol; 438 mg). Maintaining an atmosphere of nitrogen, triethylamine (10 mL) was added to the reaction mixture followed by a dropwise addition of phenylacetylene (3.0 mmol; 306 mg). The resultant reaction mixture was further stirred at room temperature and the progress of the reaction was monitored by TLC. Once all the 2-iodoaniline was consumed, the mixture was diluted with ethyl acetate (10 mL), and filtered through a thin layer of Celite and washed with

ethyl acetate (2 x 5 mL). The filtrate was dried over anhydrous sodium sulfate and evaporated under reduced pressure. The compound was purified using a silica column to give the resultant product 2-(phenylethynyl)aniline in a quantitative yield (87%, 168 mg).

V.4.3.2. Procedure for the Synthesis of 2-(2-Phenyl-1*H*-indol-3-yl)ethane-1,1,2-tricarbonitrile (1a):

In an oven-dried round bottom flask, 2-(phenylethynyl)aniline (**1**) (0.25 mmol, 48 mg), malononitrile (**a**) (1 mmol, 66 mg), ammonium thiocyanate (0.5 mmol, 38 mg), $PdCl_2$ (7 mol%, 3 mg), $Cu(OAc)_2$ (7 mol%, 3 mg) and *N*-bromosuccinimide (0.25 mmol, 44 mg) were taken in DMSO (1.5 mL) and stirred on a preheated oil bath at 110 °C. After 1 h, when both the starting materials were completely consumed (as indicated by TLC), the reaction was stopped. After cooling to room temperature, the reaction mixture was filtered through a thin layer of Celite and admixed with ethyl acetate (20 mL). The organic layer was washed with brine solution (2 x 10 mL) and dried over anhydrous sodium sulfate and the solvent was evaporated under vacuum. The crude product obtained was purified using column chromatography and eluted with hexane : EtOAc (93 : 7) to afford 2-(2-phenyl-1*H*-indol-3-yl)ethane-1,1,2-tricarbonitrile (**1a**) in 72% yield (53 mg).

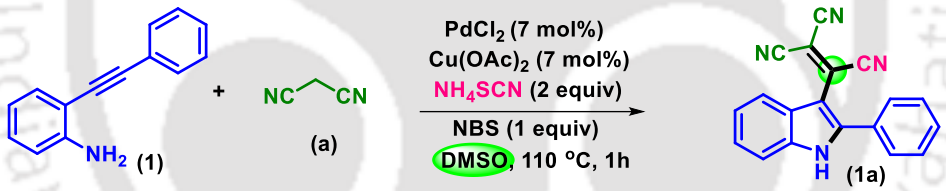

Scheme V.4.3.2. *Procedure for synthesis of tricyanovinyl indole (**1a**).*

V.4.3.3. Procedure for the Synthesis of 4-(5-Methyl-2-phenyl-1*H*-indol-3-yl)-2,5-dioxo-2,5-dihydro-1*H*-pyrrole-3-carbonitrile (2ab):

In a 5 mL oven-dried round bottom flask, 2-(5-methyl-2-phenyl-1*H*-indol-3-yl)ethene-1,1,2-tricarbonitrile (**2a**) (0.15 mmol, 46 mg) and $Cu(OAc)_2.H_2O$ (20 mol%, 6 mg) were taken in AcOH (1.5 mL) and stirred on a preheated oil bath at 80 °C. After 8 h, the reaction was stopped (as indicated by TLC). After cooling to room temperature, the reaction mixture was filtered through a layer of celite and admixed with ethyl acetate (10 mL). The organic layer was washed with saturated $NaHCO_3$ solution (2 x 10 mL) followed by brine solution (1 x 10 mL) and dried over anhydrous sodium sulfate and the solvent was evaporated under vacuum. The crude product obtained was purified using column chromatography and eluted with EtOAc : hexane (1 : 6) to afford 4-(5-methyl-2-phenyl-1*H*-indol-3-yl)-2,5-dioxo-2,5-dihydro-1*H*-pyrrole-3-carbonitrile (**2ab**) in 57% yield.

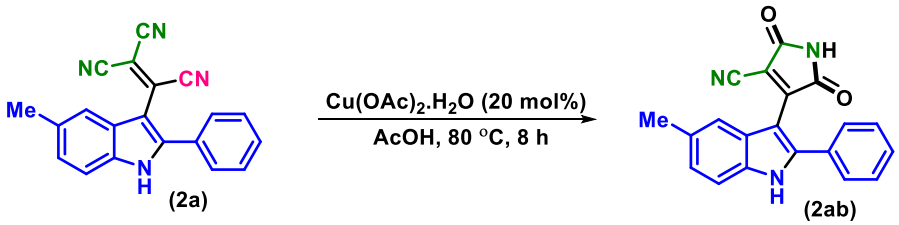

Scheme V.4.3.2. *Procedure for synthesis of 3-cyanoindolylmaleimide (**2ab**).*

V.4.3.4. General procedure for the synthesis of 2-Phenyl-1*H*-indole-3-carbaldehyde (G):[9]

Compound **G** was synthesized according to the previously reported literature procedure.

V.4.3.5. General procedure for the synthesis of 2-((2-Phenyl-1*H*-indol-3-yl)methylene)malononitrile (H):[10]

Compound **H** was synthesized according to the previously reported literature procedure.

V.4.4. Mechanistic Investigations:

V.4.4.1 *^{1}H NMR, IR and ESI-MS Analysis of Reaction Aliquots:*

To detect the intermediate species in the reaction mixture for this transformation ^{1}H NMR spectroscopy was performed. In this study (**2a**) was taken as a representative example. In a 5 mL oven-dried round bottom flask, 4-methyl-2-(phenylethynyl)aniline (**2**) (0.125 mmol, 26 mg), malanonitrile (**a**) (0.5 mmol, 33 mg), ammonium thiocyanate (0.25 mmol, 19 mg), $PdCl_2$ (7 mol%, 1.5 mg), $Cu(OAc)_2$ (7 mol%, 1.5mg) and *N*-bromosuccinimide (0.125 mmol, 22 mg) were taken in DMSO (1.0 mL) and was stirred on a preheated oil bath at 110 °C. Small aliquots of the reaction mixture were withdrawn at 10, 20, and 30 minutes. The crude product so obtained was used for ^{1}H NMR study in $CDCl_3$ with tetramethylsilane as the internal standard for ^{1}H NMR (400 MHz). The reaction crude was also subjected to IR and ESI-MS analysis.

V.4.4.2. Radical-Trapping Experiment:

(a) In presence of TEMPO:

In a 5 mL oven-dried round bottom flask, 2-(phenylethynyl)aniline (**1**) (0.125 mmol, 24 mg), malanonitrile (**a**) (0.5 mmol, 33 mg), ammonium thiocyanate (0.25 mmol, 19 mg), $PdCl_2$ (7 mol%, 1.5 mg), $Cu(OAc)_2$ (7 mol%, 1.5 mg), 2,2,6,6-tetramethylpiperidine-1-oxyl (TEMPO, 2 equiv., 39 mg), and *N*-bromosuccinimide (0.125 mmol, 22 mg) were taken in DMSO (1 mL) and was stirred on a preheated oil bath at 110 °C. A small aliquot of the reaction mixture was withdrawn at 1 h and diluted with 60:40 acetonitrile: water mixture (1 mL) and subjected to

HRMS. The HRMS analysis of this reaction aliquot shows HRMS values for methylated-TEMPO adduct (**1a'**).

(b) In the presence of 1,1-diphenylethylene:

In a 5 mL oven-dried round bottom flask, 2-(phenylethynyl)aniline (**1**) (0.125 mmol, 24 mg), malanonitrile (**a**) (0.5 mmol, 33 mg), ammonium thiocyanate (0.25 mmol, 19 mg), $PdCl_2$ (7 mol%, 1.5 mg), $Cu(OAc)_2$ (7 mol%, 1.5 mg), 1,1-diphenylethylene (1 equiv., 22.5 mg), and *N*-bromosuccinimide (0.125 mmol, 22 mg) were taken in DMSO (1 mL) and was stirred on a preheated oil bath at 110 °C. A small aliquot of the reaction mixture was withdrawn at 1 h and diluted with 60:40 acetonitrile : water mixture (1 mL) and subjected to ESI-MS. The ESI-MS analysis of this reaction aliquot shows ESI-MS values for methylated-1,1-diphenylethylene adduct (**1a''**).

V.5. Spectral Data:

2-(2-Phenyl-1H-indol-3-yl)ethene-1,1,2-tricarbonitrile (1a):

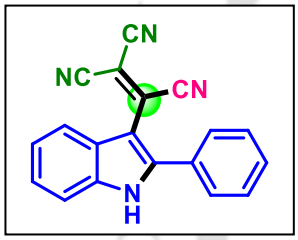

Dark red solid (53 mg, 72%); ^{1}H NMR (400 MHz, $CDCl_3$ + DMSO-d_6): δ (ppm) 7.25-7.30 (m, 4H), 7.44-7.49 (m, 3H), 7.65-7.68 (m, 2H), 12.49 (s, 1H); ^{13}C NMR (100 MHz, $CDCl_3$ + DMSO-d_6): δ (ppm) 86.5, 105.4, 112.5, 113.1, 113.7, 120.7, 122.5, 124.5, 124.9, 129.1, 129.4, 129.7, 130.6, 134.5, 136.8, 147.0; IR (cm^{-1}): 3260, 3057, 2190, 1611, 1450; HRMS (ESI): calculated for $C_{19}H_9N_4$ [M - H]$^-$: 293.0883, found 293.0877.

2-(5-Methyl-2-phenyl-1H-indol-3-yl)ethene-1,1,2-tricarbonitrile (2a):

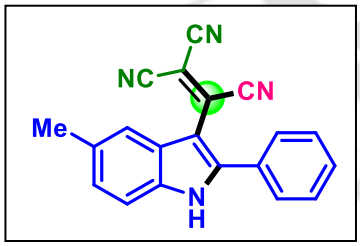

Red solid (52 mg, 67%); ^{1}H NMR (400 MHz, DMSO-d_6): δ (ppm) 2.45 (s, 3H), 7.21 (dd, 1H, J_1 = 8.4 Hz, J_2 = 1.2 Hz), 7.48 (d, 1H, J = 8.4 Hz). 7.57 (s, 1H), 7.60 (t, 3H, J = 6.4 Hz), 7.71–7.73 (m, 2H); ^{13}C NMR (100 MHz, DMSO-d_6): δ (ppm) 21.5, 87.0, 105.1, 112.9, 113.6, 114.0, 120.8, 125.1, 126.1, 129.2, 129.4, 130.0, 130.8, 131.9, 134.4, 135.0, 146.7; IR (cm^{-1}): 3306, 3062, 2924, 2852, 2222, 1590, 1457; HRMS (ESI): calculated for $C_{20}H_{11}N_4$ [M - H]$^-$: 307.0989, found 307.1008.

2-(5-Isopropyl-2-phenyl-1H-indol-3-yl)ethene-1,1,2-tricarbonitrile (3a):

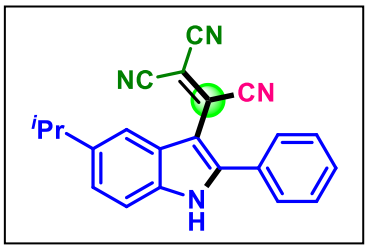

Red solid (48 mg, 57%); ^{1}H NMR (400 MHz, $CDCl_3$): δ (ppm) 1.35 (s, 3H), 1.36 (s, 3H), 3.07-3.13 (m, 1H), 7.30 (d, 1H, J = 8.4 Hz), 7.42 (d, 1H, J = 8.8 Hz), 7.50 (t, 2H, J = 6.8 Hz), 7.59 (t, 3H, J = 6.0 Hz), 7.63 (s, 1H), 9.20 (s, 1H); ^{13}C NMR (100 MHz, $CDCl_3$): δ (ppm) 24.7, 34.7, 88.4, 106.6, 112.2, 112.4, 112.6, 114.2, 118.3, 125.0, 125.9, 129.0, 129.9, 130.2, 131.4, 135.0, 135.6, 145.3, 146.5; IR (cm^{-1}): 3295, 3147, 2910, 2871, 2247, 1521, 1475; HRMS (ESI): calculated for $C_{22}H_{16}N_4$ [M - H]$^-$: 335.1302, found 335.1298.

2-(5,7-Dimethyl-2-phenyl-1H-indol-3-yl)ethene-1,1,2-tricarbonitrile (4a):

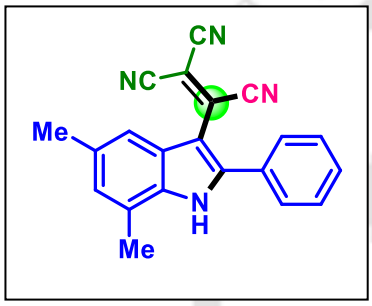

Dark red solid (56 mg, 70%); ^{1}H NMR (400 MHz, $CDCl_3$ + DMSO-d_6): δ (ppm) 2.43 (s, 3H), 2.53 (s, 3H), 7.02 (s, 1H), 7.41 (s, 1H), 7.62 (t, 3H, J = 6.4 Hz), 7.76 (dd, 2H, J_1 = 6.0 Hz, J_2 = 2.4 Hz), 12.90 (s, 1H); ^{13}C NMR (100 MHz, $CDCl_3$ + DMSO-d_6): δ (ppm) 16.4, 21.3, 83.9, 106.4, 112.0, 112.6, 113.3, 117.5, 122.5, 125.0, 127.0, 128.8, 129.4, 129.6, 130.2, 132.7, 134.5, 134.6, 147.4; IR (cm^{-1}): 3283, 2958, 2924, 2852, 2223, 1514, 1455; HRMS (ESI): calculated for $C_{21}H_{13}N_4$ [M - H]$^-$: 321.1146, found 321.1148.

2-(5-Fluoro-2-phenyl-1H-indol-3-yl)ethene-1,1,2-tricarbonitrile (5a):

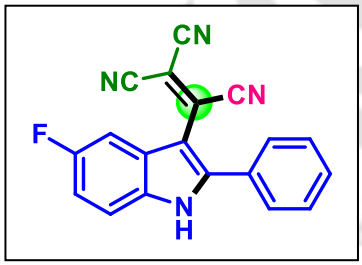

Brown solid (44 mg, 57%); ^{1}H NMR (400 MHz, DMSO-d_6): δ (ppm) 7.22–7.27 (m, 1H), 7.59 (d, 1H, J = 4.8 Hz), 7.62 (t, 3H, 6.4 Hz), 7.66 (d, 1H, J = 2.4 Hz) 7.76-7.79 (m, 2H), 13.29 (s, 1H); ^{13}C NMR (100 MHz, DMSO-d_6): δ (ppm) 89.4, 104.9 (d, J = 8.0 Hz), 106.6 (d, J = 26.0 Hz), 112.6, 112.8 (d, J = 10.5 Hz), 113.4, 113.8, 114.5 (d, J = 10.0 Hz), 125.6 (d, J = 11.0 Hz), 129.1, 129.3, 130.0, 131.0, 133.3, 134.1, 147.6, 157.3 (d, J = 235.0 Hz); ^{19}F NMR (DMSO): δ (ppm) -116.71; IR (cm^{-1}): 3304, 3062, 2960, 2226, 1587,1515, 1462; HRMS (ESI) calculated for $C_{19}H_7N_4F$ [M - H]$^-$: 311.0738, found 311.0745.

2-(5-Chloro-2-phenyl-1H-indol-3-yl)ethene-1,1,2-tricarbonitrile (6a):

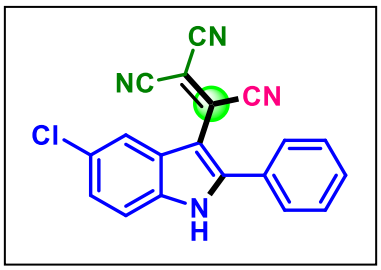

Red solid (50 mg, 61%); ^{1}H NMR (400 MHz, $CDCl_3$ + DMSO-d_6): δ (ppm) 7.22 (dd, 1H, J_1 = 8.4 Hz, J_2 = 1.2 Hz), 7.38 (d, 1H, J = 8.4 Hz), 7.48 (dd, 3H, J_1 = 7.2 Hz, J_2 = 3.6 Hz), 7.49 (s, 2H), 7.65 (s, 1H), 12.63 (s, 1H); ^{13}C NMR (100 MHz, $CDCl_3$ + DMSO-d_6): δ (ppm) 86.8, 105.2, 112.1, 112.5, 113.5, 114.3, 120.0, 125.2, 126.5, 129.0, 129.3, 129.6, 129.7, 131.0, 135.1, 135.5, 148.3; IR (cm^{-1}): 3055, 2986, 2302, 1548, 1422, 1264; HRMS (ESI) calculated for $C_{19}H_8N_4Cl$ $[M - H]^-$: 327.0443, found 327.0438.

2-(5-Bromo-2-phenyl-1H-indol-3-yl)ethene-1,1,2-tricarbonitrile (7a):

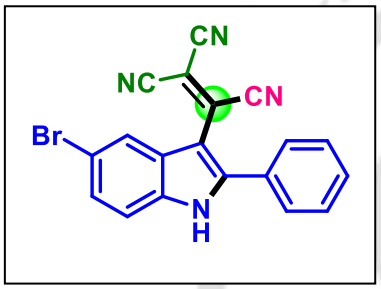

Red solid (59 mg, 64%); ^{1}H NMR (400 MHz, DMSO-d_6): δ (ppm) 7.50 (d, 1H, J = 8.4 Hz), 7.55 (d, 1H, J = 8.4 Hz), 7.62 (s, 3H), 7.77 (s, 2H), 8.06 (s, 1H), 13.3 (s, 1H); ^{13}C NMR (100 MHz, DMSO-d_6): δ (ppm) 90.3, 104.0, 112.7, 113.3, 113.8, 114.9, 115.0 123.4, 126.5, 127.1, 129.0, 129.3, 130.0, 131.0, 134.0, 135.4, 146.9; IR (cm^{-1}) 3059, 2926, 2222, 1514, 1460; HRMS (ESI) calculated for $C_{19}H_8N_4Br$ $[M - H]^-$: 370.9938, found 370.9942.

2-(2-Phenyl-5-trifluoromethyl-1H-indol-3-yl)ethene-1,1,2-tricarbonitrile (8a):

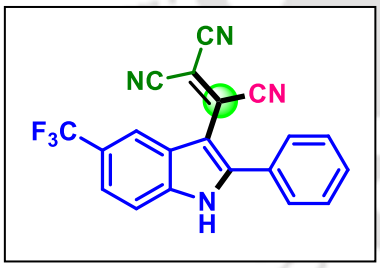

Red solid (44 mg, 49%); ^{1}H NMR (400 MHz, DMSO-d_6): δ (ppm) 7.65 (t, 3H, J = 6.0 Hz), 7.69 (d, 1H, J = 9.6 Hz), 7.78 (d, 1H, J = 8.4 Hz), 7.82 (dd, 2H, J_1 = 5.6 Hz, J_2 = 2.0 Hz), 8.29 (s, 1H), 13.47 (s, 1H); ^{13}C NMR (100 MHz, DMSO): δ (ppm) 91.8, 104.7, 112.5, 113.1, 113.9, 118.8 (q, J = 4.0 Hz), 120.7 (d, J = 13.6 Hz), 122.7, 123.0, 124.3, 128.8, 129.2, 130.1, 131.0, 133.9, 138.2, 147.5; ^{19}F NMR (DMSO-d_6): δ (ppm) -59.09; IR (cm^{-1}): 3303, 3062, 2925, 2229, 1518, 1427; HRMS (ESI) calculated for $C_{20}H_8N_4F_3$ $[M - H]^-$: 361.0707, found 361.0714.

2-(2-(p-Tolyl)-1H-indol-3-yl)ethene-1,1,2-tricarbonitrile (9a):

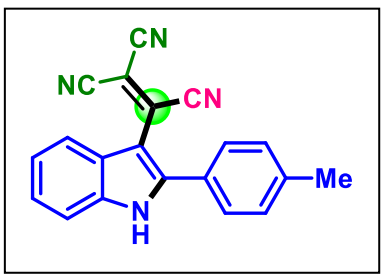

Red solid (50 mg, 65%); ^{1}H NMR (400 MHz, $CDCl_3$ + DMSO-d_6): δ (ppm) 2.21 (s, 3H), 7.09–7.14 (m, 4H), 7.22 (d, 2H, J = 7.6 Hz), 7.29 (dd, 1H, J_1 = 8.0 Hz, J_2 = 1.2 Hz), 7.48 (dd, 1H, J_1 = 5.6 Hz, J_2 = 1.2 Hz), 12.28 (s, 1H); ^{13}C NMR (100 MHz, $CDCl_3$ + DMSO-d_6): δ (ppm) 21.3, 84.6, 106.0, 112.3, 112.8,

113.0, 113.5, 120.3, 122.8, 124.5, 125.2, 126.8, 129.2, 129.9, 135.0, 137.0, 141.1, 148.0; IR (cm^{-1}): 3301, 3052, 2924, 2862, 2223, 1510, 1443; HRMS (ESI) calculated for $C_{20}H_{11}N_4$ [M - H]$^-$: 307.0989, found 307.0998.

2-(2-(4-(tert-Butyl)phenyl)-1H-indol-3-yl)ethene-1,1,2-tricarbonitrile (10a):

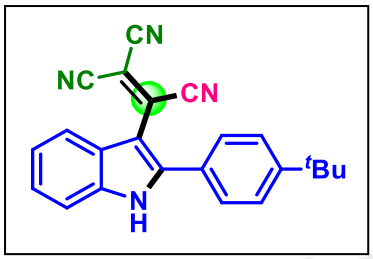

Red solid (62 mg, 71%); ^{1}H NMR (400 MHz, $CDCl_3$): δ (ppm) 1.37 (s, 9H), 7.38–7.44 (m, 4H), 7.47 (d, 1H, J = 8.4 Hz), 7.59 (d, 2H, J = 8.4 Hz), 7.79 (d, 1H, J = 7.6 Hz), 9.32 (s, 1H); ^{13}C NMR (100 MHz, $CDCl_3$): δ (ppm) 31.3, 35.3, 88.2, 106.2, 112.2, 112.6, 113.8, 120.8, 123.8, 125.5, 125.7, 126.7, 127.2, 128.7, 135.7, 136.3, 146.9, 155.3; IR (cm^{-1}): 3305, 2960, 2924, 2856, 2223, 1515, 1439. HRMS (ESI) calculated for $C_{23}H_{17}N_4$ [M - H]$^-$: 349.1459, found 349.1462.

2-(2-(4-Methoxyphenyl)-1H-indol-3-yl)ethene-1,1,2-tricarbonitrile (11a):

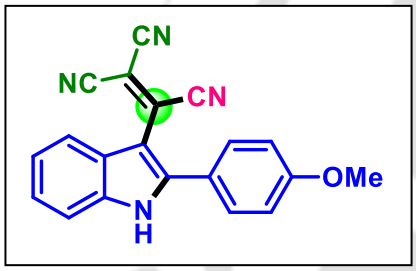

Red solid (47 mg, 58%); ^{1}H NMR (400 MHz, $CDCl_3$ + DMSO-d_6): δ (ppm) 3.84 (s, 3H), 7.04 (d, 2H, J = 7.6 Hz), 7.28 (t, 2H, J = 8.4 Hz), 7.47 (t, 3H, J = 7.2 Hz), 7.63 (t, 1H, J = 8.4 Hz), 12.63 (s, 1H); ^{13}C NMR (100 MHz, $CDCl_3$ + DMSO-d_6): δ (ppm) 55.0, 83.7, 105.7, 112.2, 112.7, 113.3, 114.4, 120.1, 121.4, 122.5, 124.2, 124.8, 130.7, 134.6, 136.7, 147.8, 161.3; IR (cm^{-1}): 3324, 2963, 2929, 2222, 1607, 1512, 1444; HRMS (ESI) calculated for $C_{20}H_{11}N_4O$ [M - H]$^-$: 323.0938, found 323.0943.

2-(2-(4-Fluorophenyl)-1H-indol-3-yl)ethene-1,1,2-tricarbonitrile (12a):

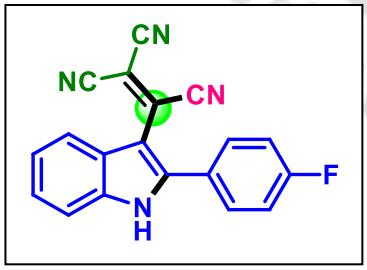

Black solid (48 mg, 62%); ^{1}H NMR (400 MHz, DMSO-d_6): δ (ppm) 7.34-7.41 (m, 2H), 7.47 (t, 2H, J = 8.8 Hz), 7.60 (d, 1H, J = 7.2 Hz), 7.80 (dd, 1H, J_1 = 7.2 Hz, J_2 = 1.2 Hz), 7.83-7.87 (m, 2H); ^{13}C NMR (100 MHz, DMSO): δ (ppm) 87.6, 105.5, 112.8, 113.2, 113.6, 114.0, 116.4 (d, J = 8.7 Hz), 121.0, 122.6, 124.7 (d, J = 1.2 Hz), 125.9 (d, J = 3.0 Hz), 132.4 (d, J = 8.8 Hz), 134.3, 136.7, 145.7, 163.7 (d, J = 247.9 Hz); ^{19}F NMR (DMSO-d_6): δ (ppm) -108.15; IR (cm^{-1}): 3416, 2922, 2857, 2221, 1512, 1445; HRMS (ESI) calculated for $C_{19}H_8N_4F$ [M - H]$^-$: 311.0738, found 311.0746.

2-(2-(4-Trifluoromethylphenyl)-1H-indol-3-yl)ethene-1,1,2-tricarbonitrile (13a):

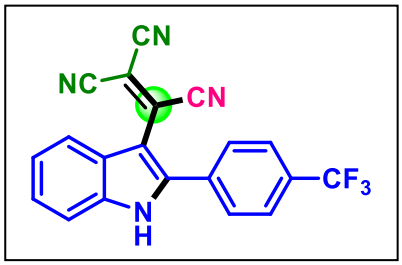

Red solid (66 mg, 73%); ^{1}H NMR (400 MHz, $CDCl_3$ + DMSO-d_6): δ (ppm) 8.62-8.67 (m, 2H), 8.81 (dd, 1H, J_1 = 5.2 Hz, J_2 = 2.8 Hz), 8.97 (t, 2H, J = 7.6 Hz), 9.02-9.05 (m, 1H), 9.08 (d, 2H, J = 7.6 Hz), 13.94 (s, 1H); ^{13}C NMR (100 MHz, $CDCl_3$ + DMSO): δ (ppm) 87.0, 106.5, 112.2, 112.5, 113.4, 113.7, 120.6, 123.6, 125.3, 125.5, 126.4 (q, J = 7.1 Hz), 129.8, 132.3, 133.8, 135.1, 137.2, 145.1, 169.9; ^{19}F NMR ($CDCl_3$ + DMSO-d_6): δ (ppm) -58.01; IR (cm^{-1}): 3298, 2958, 2927, 2854, 2226, 1520, 1442; HRMS (ESI) calculated for $C_{20}H_9N_4F_3$ $[M-H]^-$: 361.0707, found 361.0718.

2-(2-(4-Cyanophenyl)-1H-indol-3-yl)ethene-1,1,2-tricarbonitrile (14a):

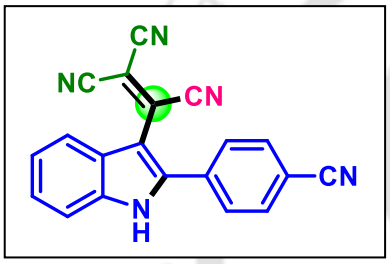

Red solid (53 mg, 67%); ^{1}H NMR (400 MHz, DMSO-d_6): δ (ppm) 7.31-7.39 (m, 2H), 7.59 (d, 1H, J = 7.6 Hz), 7.80 (d, 1H, J = 7.6 Hz), 7.94 (d, 2H, J = 8.0 Hz), 8.00 (d, 2H, J = 8.4 Hz), 13.32 (s, 1H); ^{13}C NMR (100 MHz, DMSO-d_6): δ (ppm) 89.5, 105.7, 112.6, 112.8, 113.3, 114.1, 118.4, 121.0, 122.8, 125.0, 125.1, 130.6, 133.0, 134.0, 134.1, 136.8, 143.6; IR (cm^{-1}): 3295, 3075, 2958, 2924, 2855, 2230, 1519, 1442; HRMS (ESI) calculated for $C_{20}H_8N_5$ $[M - H]^-$: 318.0785, found 318.0800.

2-(2-(4-Nitrophenyl)-1H-indol-3-yl)ethene-1,1,2-tricarbonitrile (15a):

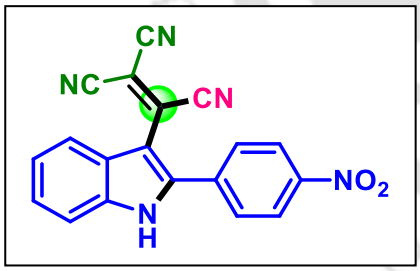

Red solid (59 mg, 70%); ^{1}H NMR (400 MHz, DMSO-d_6): δ (ppm) 7.37-7.45 (m, 2H), 7.64 (d, 1H, J = 8.0 Hz), 7.87 (d, 1H, J = 7.6 Hz), 8.10 (d, 2H, J = 8.4 Hz), 8.44 (d, 2H, J = 8.8 Hz), 13.52 (s, 1H); ^{13}C NMR (100 MHz, DMSO-d_6): δ (ppm) 89.8, 105.9, 112.6, 113.3, 113.4, 114.1, 121.0, 123.0, 124.2, 125.1, 125.2, 131.2, 134.1, 135.8, 136.9, 143.0, 148.3; IR (cm^{-1}): 3084, 2959, 2922, 2218, 2201, 1517, 1442; HRMS (ESI) calculated for $C_{19}H_8N_5O_2$ $[M - H]^-$: 338.0683, found 338.0687.

2-(5-Methyl-2-(p-tolyl)-1H-indol-3-yl)ethene-1,1,2-tricarbonitrile (16a):

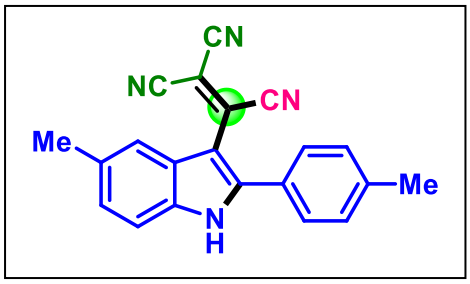

Red solid (55 mg, 68%); ^{1}H NMR (400 MHz, $CDCl_3$): δ (ppm) 2.45 (s, 3H), 2.53 (s, 3H), 7.20 (dd, 1H, J_1 = 8.4 Hz, J_2 = 1.6 Hz), 7.34 (d, 1H, J = 8.4 Hz), 7.37 (s, 4H), 7.57 (s, 1H), 9.16 (s, 1H); ^{13}C NMR (100 MHz, $CDCl_3$): δ (ppm) 21.8, 22.0, 87.6, 106.0, 112.2, 112.3, 112.7, 113.8, 120.7, 126.0, 126.9, 127.1, 128.8, 131.0, 133.8, 134.5, 135.6, 142.1, 146.8; IR (cm^{-1}): 3306, 3031, 2951, 2924, 2854, 2222, 1583, 1513, 1444; HRMS (ESI) calculated for $C_{21}H_{13}N_4$ $[M - H]^-$: 321.1146, found 321.1155.

2-(2-(4-(tert-Butyl)phenyl)-5-methyl-1H-indol-3-yl)ethene-1,1,2-tricarbonitrile (17a):

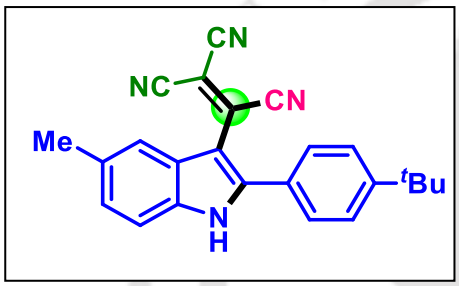

Black solid (64 mg, 70%); ^{1}H NMR (400 MHz, $CDCl_3$): δ (ppm) 1.38 (s, 9H), 2.54 (s, 3H), 7.22 (d, 1H, J = 8.4 Hz), 7.37 (d, 1H, J = 8.4 Hz), 7.43 (d, 2H, J = 8.4 Hz), 7.59 (t, 3H, J = 4 Hz), 8.97 (s, 1H); ^{13}C NMR (100 MHz, $CDCl_3$): δ (ppm) 22.0, 31.3, 35.3, 87.7, 106.0, 112.2, 112.3, 112.7, 113.8, 120.7, 126.0, 126.8, 127.1, 127.2, 128.6, 133.8, 134.5, 135.7, 146.8, 155.2; IR (cm^{-1}): 3440, 3194, 3017, 2919, 2852, 2221, 1634, 1400; HRMS (ESI) calculated for $C_{24}H_{19}N_4$ $[M - H]^-$: 363.1615, found 363.1620.

2-(2-(4-Fluorophenyl)-5-methyl-1H-indol-3-yl)ethene-1,1,2-tricarbonitrile (18a):

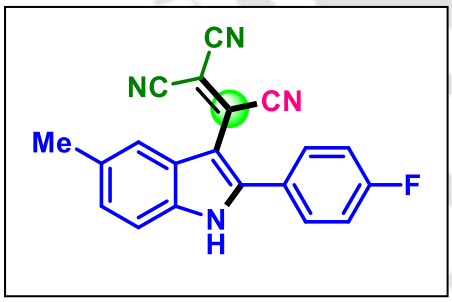

Dark red solid (50 mg, 62%); ^{1}H NMR (400 MHz, DMSO-d_6): δ (ppm) 2.47 (s, 3H), 7.19 (d, 1H, J = 7.2 Hz), 7.43 (dd, 3H, J_1 = 18.4 Hz, J_2 = 8.8 Hz), 7.5 (s, 1H), 7.80 (dd, 2H, J_1 = 8.8 Hz, J_2 = 5.2 Hz), 13.1 (s, 1H); ^{13}C NMR (100 MHz, DMSO-d_6): δ (ppm) 12.4, 77.7, 97.5, 104.2, 104.6, 105.5, 108.0 (d, J = 22.0 Hz), 112.2, 117.4, 118.1, 118.3 (d, J = 3.0 Hz), 123.3 (d, J = 9.0 Hz), 124.6, 126.8, 127.2, 138.0, 155.5 (d, J = 250.0 Hz); ^{19}F NMR (400 MHz, DMSO): δ (ppm) -107.72; IR (cm^{-1}): 3298, 2954, 2924, 2856, 2222, 1606, 1513, 1446; HRMS (ESI) calculated for $C_{20}H_{10}N_4F$ $[M - H]^-$: 325.0895, found 325.0908.

2-(5-Fluoro-2-(p-tolyl)-1H-indol-3-yl)ethene-1,1,2-tricarbonitrile (19a):

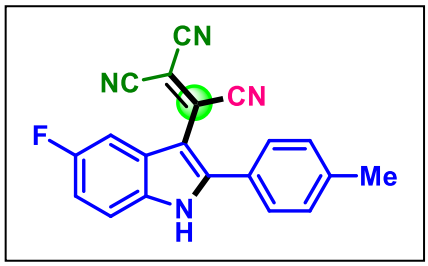

Dark red solid (48 mg, 59%); ^{1}H NMR (400 MHz, DMSO-d_6): δ (ppm) 2.43 (s, 3H), 7.21-7.26 (m, 1H), 7.44 (d, 2H, J = 8.0 Hz), 7.59 (dd, 1H, J_1 = 8.8 Hz, J_2 = 4.4 Hz), 7.63 (dd, 1H, J_1 = 10.0 Hz, J_2 = 2.4 Hz), 7.67 (d, 2H, J = 8.0 Hz), 13.21 (s, 1H); ^{13}C NMR (100 MHz, DMSO): δ (ppm) 21.0, 89.1, 104.6 (d, J = 4.1 Hz), 106.7 (d, J = 26.0 Hz), 112.6 (d, J = 26.0 Hz), 112.8, 113.6 (d, J = 41.4 Hz), 114.4 (d, J = 9.8 Hz), 125.6 (d, J = 11.0 Hz), 126.2, 129.8, 129.9, 133.2, 134.1, 141.0, 147.8, 158.4 (d, J = 235.0 Hz); ^{19}F NMR (400 MHz, DMSO-d_6): δ (ppm) -116.89; IR (cm^{-1}): 3298, 2960, 2924, 2853, 2224, 1516, 1443; HRMS (ESI) calculated for $C_{20}H_{10}N_4F$ [M - H]$^-$: 325.0895, found 325.0911.

2-(5-Bromo-2-(4-(tert-butyl)phenyl)-1H-indol-3-yl)ethene-1,1,2-tricarbonitrile (20a):

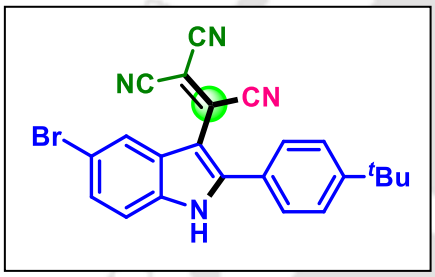

Red solid (83 mg, 78%); ^{1}H NMR (400 MHz, DMSO-d_6): δ (ppm) 1.35 (s, 9H), 7.50 (dd, 1H, J_1 = 8.4 Hz, J_2 = 1.6 Hz), 7.54 (d, 1H, J = 8.4 Hz), 7.64 (d, 2H, J = 8.4 Hz), 7.71 (d, 2H, J = 8.4 Hz), 8.06 (d, 1H, J = 1.6 Hz), 13.23 (s, 1H); ^{13}C NMR (100 MHz, DMSO-d_6): δ (ppm) 31.0, 34.9, 90.1, 104.0, 112.9, 113.4, 113.9, 115.0, 115.1, 123.5, 126.1, 126.2, 126.6, 127.2, 130.0, 134.1, 135.5, 147.3, 154.1; IR (cm^{-1}): 3054, 2959, 2664, 2730, 2221, 1507, 1444; HRMS (ESI) calculated for $C_{23}H_{16}N_4Br$ [M-Neutral] : 427.0558, found 427.0574.

2-(5-Fluoro-2-(4-fluorophenyl)-1H-indol-3-yl)ethene-1,1,2-tricarbonitrile (21a):

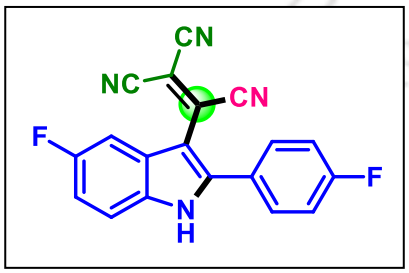

Red solid (49 mg, 60%); ^{1}H NMR (400 MHz, $CDCl_3$ + DMSO-d_6): δ (ppm) 7.00-7.05 (m, 1H), 7.22 (t, 2H, J = 8.4 Hz), 7.33-7.36 (m, 1H), 7.42 (dd, 1H, J_1 = 8.8 Hz, J_2 = 4.4 Hz), 7.49-7.53 (m, 2H), 12.76 (s, 1H); ^{13}C NMR (100 MHz, $CDCl_3$ + DMSO-d_6): δ (ppm) 85.9, 105.7 (d, J = 4.1 Hz), 106.2 (d, J = 25.8 Hz), 112.3 (d, J = 35.8 Hz), 112.9, 113.2, 113.3, 114.2 (d, J = 9.6 Hz), 116.6 (d, J = 21.9 Hz), 125.7 (d, J = 3.3 Hz), 125.9 (d, J = 10.5 Hz), 131.2 (d, J = 8.7 Hz), 133.3, 134.7, 147.3, 159.1 (d, J = 239.0 Hz), 164.0 (d, J = 251.0 Hz); ^{19}F NMR (400 MHz, $CDCl_3$ + DMSO-d_6): δ (ppm) -107.95, -117.61; IR (cm^{-1}): 3057,

2914, 2223, 1602, 1512, 1445; HRMS (ESI) calculated for $C_{19}H_7N_4F_2$ [M - H]$^-$: 329.0644, found 329.0647.

2-(2-(2-Bromo-5-fluorophenyl)5-isopropyl-1H-indol-3-yl)ethene-1,1,2-tricarbonitrile (22a):

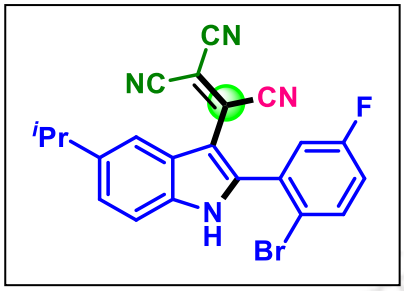

Red solid (59 mg, 55%); ^{1}H NMR (400 MHz, $CDCl_3$): δ (ppm) 1.35 (s, 3H), 1.37 (s, 3H), 3.06-3.15 (m, 1H), 7.15-7.19 (m, 2H), 7.34 (dd, 1H, J_1 = 8.4 Hz, J_2 = 1.2 Hz), 7.45 (d, 1H, J = 8.4 Hz), 7.65 (s, 1H), 7.74 (dd, 1H, J_1 = 9.6 Hz, J_2 = 5.2 Hz), 9.52 (s, 1H); ^{13}C NMR (100 MHz, $CDCl_3$): δ (ppm) 24.6, 34.7, 88.1, 108.1, 112.0, 112.5, 112.7, 113.3, 117.8 (d, J = 4.0 Hz), 118.5, 119.3 (d, J = 24.0 Hz), 119.9 (d, J = 22.0 Hz), 124.7, 125.5, 132.2 (d, J = 8.0 Hz), 134.5, 135.5, 135.9 (d, J = 8.0 Hz), 142.50 (d, J = 2.0 Hz), 145.5, 160.8 (d, J = 250 Hz); ^{19}F NMR (400 MHz, $CDCl_3$): δ (ppm) -111.64; IR (cm^{-1}): 3067, 2961, 2927, 2869, 2219, 1624, 1448; HRMS (ESI) calculated for $C_{22}H_{14}N_4FBr$ [M - H]$^-$: 431.0313, found 431.0310.

2-(2-Butyl-1H-indol-3-yl)ethene-1,1,2-tricarbonitrile (23a):

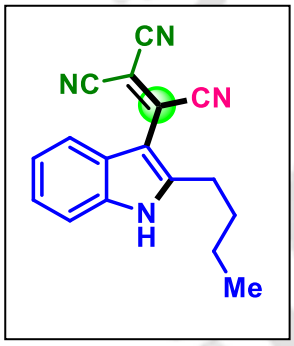

Red solid (32 mg, 47%); ^{1}H NMR (400 MHz, $CDCl_3$): δ (ppm) 0.99 (t, 3H, J = 7.6 Hz), 1.41-1.51 (m, 2H), 1.76–1.84 (m, 2H), 3.02 (t, 2H, J = 8.0 Hz), 7.33–7.38 (m, 2H), 7.41 (d, 1H, J= 8.4 Hz), 7.76 (d, 1H, J = 6.8 Hz), 9.35 (s, 1H). ^{13}C NMR (100 MHz, $CDCl_3$): δ (ppm) 13.9, 22.7, 28.6, 31.2, 85.9, 107.8, 112.2, 112.70, 112.73, 114.1, 120.9, 123.6, 124.9,125.2, 134.8, 135.6, 149.4; IR (cm^{-1}): 2961, 2932, 2872, 2219, 1495, 1452; HRMS (ESI) calculated for $C_{17}H_{13}N_4$ [M - H]$^-$: 273.1146, found 273.1151.

2-(2-Cyclopropyl-1H-indol-3-yl)ethene-1,1,2-tricarbonitrile (24a):

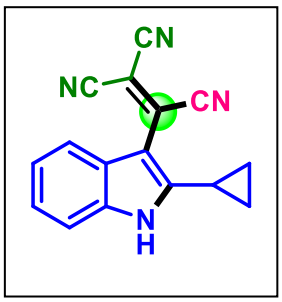

Dark red solid (43 mg, 67%); ^{1}H NMR (400 MHz, $CDCl_3$ + DMSO-d_6): δ (ppm) 0.95-0.99 (m, 2H), 1.19–1.24 (m, 2H), 2.07–2.13 (m, 1H), 7.11 (dd, 2H, J_1 = 5.2 Hz, J_2 = 1.6 Hz), 7.23 (dd, 1H, J_1 = 5.2 Hz, J_2 = 2.4 Hz), 7.53 (d, 1H, J = 6.4 Hz), 11.79 (s, 1H); ^{13}C NMR (100 MHz, $CDCl_3$ + DMSO-d_6): δ (ppm) 10.1, 10.9, 81.4, 108.9, 112.4, 113.0, 113.3, 114.2, 120.0, 122.7, 124.4, 124.8, 133.5, 136.2, 157.8; IR (cm^{-1}): 3054, 2218, 1445, 1268; HRMS (ESI) calculated for $C_{16}H_9N_4$ [M - H]$^-$: 257.0833, found 257.0846.

2-(2-(Naphthalen-2-yl)-1H-indol-3-yl)ethene-1,1,2-tricarbonitrile (25a):

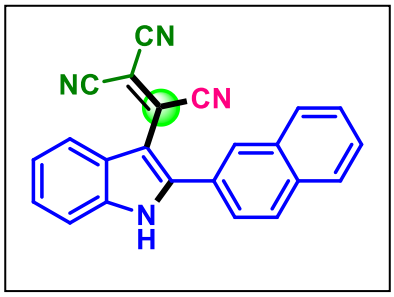

Red solid (39 mg, 46%); ^{1}H NMR (400 MHz, $CDCl_3$ + DMSO-d_6): δ (ppm) 7.48 (dd, 2H, J_1 = 7.6 Hz, J_2 = 3.6 Hz), 7.54–7.59 (m, 3H), 7.63 (dd, 2H, J_1 = 9.9 Hz, J_2 = 5.2 Hz), 7.73 (d, 1H, J = 7.6 Hz), 7.89 (dd, 1H, J_1 = 6.4 Hz, J_2 = 3.2 Hz), 7.99 (d, 1H, J = 7.2 Hz), 8.09 (d, 1H, J = 8.4 Hz), 9.47 (s, 1H); ^{13}C NMR (400 MHz, $CDCl_3$ + DMSO): δ (ppm) 108.8, 112.5, 113.0, 113.46, 113.51, 121.2, 123.4, 125.0, 125.1, 125.2, 125.6, 127.0, 127.5, 127.9, 128.9, 130.0, 131.5, 133.9, 134.0, 135.16, 135.24, 137.3, 146.7; IR (cm^{-1}): 3435, 3161, 3016, 2928, 2217, 1632, 1400; HRMS (ESI) calculated for $C_{23}H_{11}N_4$ $[M - H]^-$: 343.0989, found 343.1001.

2-(2-(Thiophen-2-yl)-1H-indol-3-yl)ethene-1,1,2-tricarbonitrile (26a):

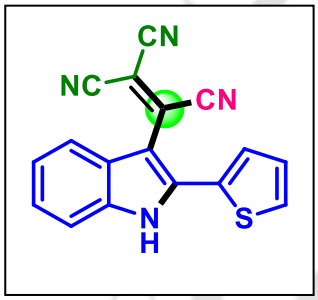

Black solid (44 mg, 59%); ^{1}H NMR (400 MHz, $CDCl_3$ + DMSO-d_6): δ (ppm) 7.28 (dd, 1H, J_1 = 4.8 Hz, J_2 = 3.6 Hz), 7.39–7.44 (m, 3H), 7.49 (dd, 1H, J_1 = 6.0 Hz, J_2 = 2.8 Hz), 7.67 (dd, 1H, J_1 = 5.2 Hz, J_2 = 1.2 Hz), 7.75–7.77 (m, 1H), 9.13 (s, 1H); ^{13}C NMR (100 MHz, $CDCl_3$ + DMSO): δ (ppm) 86.8, 107.0, 112.3, 112.8, 113.2, 113.6, 120.5, 123.4, 125.3, 125.4, 128.8, 130.1, 130.6, 131.2, 135.0, 137.1, 140.1; IR (cm^{-1}): 2954, 2924, 2854, 2221, 1520, 1456; HRMS (ESI) calculated for $C_{17}H_7N_4S$ $[M - H]^-$: 299.0397, found 299.0408.

4-(5-Methyl-2-phenyl-1H-indol-3-yl)-2,5-dioxo-2,5-dihydro-1H-pyrrole-3-carbonitrile (2ab):

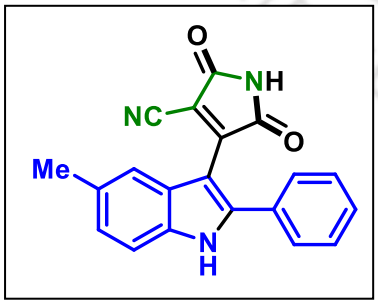

Red solid (28 mg, 57%); ^{1}H NMR (600 MHz, $CDCl_3$ + DMSO): δ (ppm) 2.43 (s, 3H), 7.12 (d, 1H, J = 7.8 Hz), 7.43 (t, 2H, J = 8.4 Hz), 7.48 (t, 3H, J = 7.8 Hz), 7.61 (d, 2H, J = 7.2 Hz), 11.51 (s, 1H), 12.56 (s, 1H); ^{13}C NMR (150 MHz, $CDCl_3$ + DMSO-d_6): δ (ppm) 21.5, 100.8, 105.9, 112.1, 112.5, 120.5, 125.0, 126.9, 128.9, 129.0, 130.4, 131.6, 135.2, 144.1, 149.7, 167.4, 168.4; IR (cm^{-1}): 3395, 2925, 2254, 1651, 1455, 1250; HRMS (ESI) calculated for $C_{20}H_{12}N_3O_2$ $[M - H]^-$: 326.0935, found 326.0943.

4-(5-Isopropyl-2-phenyl-1H-indol-3-yl)-2,5-dioxo-2,5-dihydro-1H-pyrrole-3-carbonitrile (3ab):

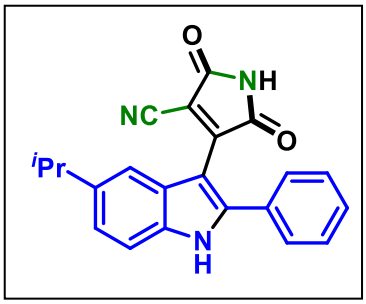

Red solid (28 mg, 52%); ^{1}H NMR (500 MHz, $CDCl_3$ + DMSO-d_6): δ (ppm) 1.33 (s, 3H), 1.34 (s, 3H), 3.03–3.08 (m, 1H), 7.19 (dd, 1H, J_1 = 8.0 Hz, J_2 = 1.5 Hz), 7.40–7.45 (m, 3H), 7.46–7.51 (m, 3H), 7.65 (s, 1H), 10.01 (s, 1H), 11.18 (s, 1H); ^{13}C NMR (125 MHz, $CDCl_3$ + DMSO-d_6): δ (ppm) 24.6, 34.5, 102.7, 105.2, 112.0, 118.5, 123.4, 127.4, 129.0, 129.2, 129.4, 132.5, 135.9, 143.5, 145.6, 150.1, 167.1, 168.2; IR (cm^{-1}): 3355, 3047, 2987, 2876, 2247, 1602, 1423, 1374; HRMS (ESI) calculated for $C_{22}H_{17}N_3O_2$ [M - H]$^-$: 354.1248, found 354.1233.

4-(5-Chloro-2-phenyl-1H-indol-3-yl)-2,5-dioxo-2,5-dihydro-1H-pyrrole-3-carbonitrile (6ab):

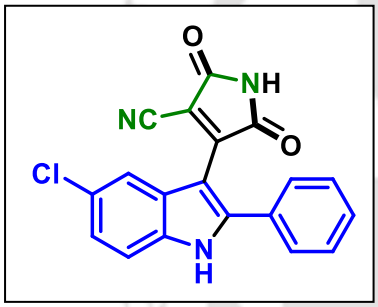

Red solid (23 mg, 44%); ^{1}H NMR (400 MHz, $CDCl_3$ + DMSO-d_6): δ (ppm) 8.47 (t, 1H, J = 6.8 Hz), 8.56 (d, 1H, J = 6.4 Hz), 8.66 (t, 1H, J = 7.2 Hz), 8.72 (s, 1H), 8.75 (d, 3H, J = 6.4 Hz), 9.02 (d, 1H, J = 5.2 Hz), 11.97 (s, 1H), 13.12 (s, 1H); ^{13}C NMR (100 MHz, $CDCl_3$ + DMSO-d_6): δ (ppm) 101.8, 106.0, 111.5, 113.5, 120.7, 124.2, 128.0, 128.1, 128.9, 129.4, 129.7, 131.7, 135.7, 146.5, 149.5, 166.9, 168.6; IR (cm^{-1}): 3054, 2981, 2305, 1605, 1422; HRMS (ESI) calculated for $C_{19}H_9N_3O_2Cl$ [M - H]$^-$: 346.0389, found 346.0387.

4-(2-(4-(tert-Butyl)phenyl)-1H-indol-3-yl)-2,5-dioxo-2,5-dihydro-1H-pyrrole-3-carbonitrile (10ab):

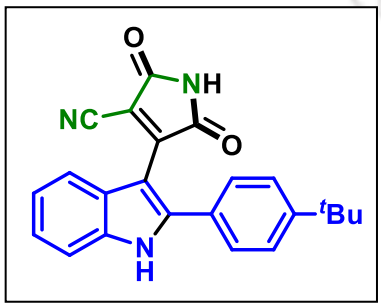

Red solid (27 mg, 50%); ^{1}H NMR (400 MHz, $CDCl_3$): δ (ppm) 1.35 (s, 9H), 7.34 (dd, 2H, J_1 = 6.0 Hz, J_2 = 3.2 Hz), 7.41 (d, 2H, J = 8.4 Hz), 7.46 (dd, 1H, J_1 = 5.6 Hz, J_2 = 1.6 Hz), 7.51 (d, 2H, J = 8.0 Hz), 7.80 (dd, 1H, J_1 = 6.4 Hz, J_2 = 3.2 Hz), 8.99 (s, 1H); ^{13}C NMR (100 MHz, $CDCl_3$ + DMSO-d_6): δ (ppm) 31.4, 35.1, 102.7, 106.2, 111.4, 112.1, 121.4, 123.1, 124.8, 126.8, 127.1 128.4, 128.7, 136.6, 145.6, 149.9, 153.7, 165.5, 167.0; IR (cm^{-1}): 3058, 2987, 2304, 1652, 1374; HRMS (ESI) calculated for $C_{23}H_{18}N_3O_2$ [M - H]$^-$: 368.1405, found 368.1415.

4-(2-(4-Fluorophenyl)-1H-indol-3-yl)-2,5-dioxo-2,5-dihydro-1H-pyrrole-3-carbonitrile (12ab):

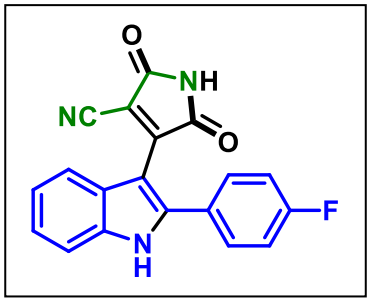

Red solid (24 mg, 48%); ^{1}H NMR (400 MHz, $CDCl_3$ + DMSO-d_6): δ (ppm) 7.13-7.19 (m, 2H), 7.25-7.29 (m, 2H), 7.46-7.53 (m, 3H), 7.77 (t, 1H, J = 8.8 Hz), 10.75 (s, 1H), 11.80 (s, 1H); ^{13}C NMR (100 MHz, $CDCl_3$ + DMSO-d_6): 102.5, 105.4, 111.9, 112.4, 116.2 (d, J = 21.6 Hz), 121.1, 122.3, 123.9, 127.0, 128.3 (d, J = 3.4 Hz), 130.8 (d, J = 8.4 Hz), 137.2, 144.2, 149.8, 163.3 (d, J = 248.8 Hz), 167.1, 168.4; ^{19}F NMR (400 MHz, $CDCl_3$ + DMSO-d_6): δ (ppm) -111.0; IR (cm^{-1}): 3055, 2981, 2305, 2223, 1601, 1451; HRMS (ESI) calculated for $C_{19}H_{10}N_3O_2F$ [M - H]$^-$: 330.0684, found 330.0683.

4-(2-(4-(tert-Butyl)phenyl)-5-methyl-1H-indol-3-yl)-2,5-dioxo-2,5-dihydro-1H-pyrrole-3-carbonitrile (17ab):

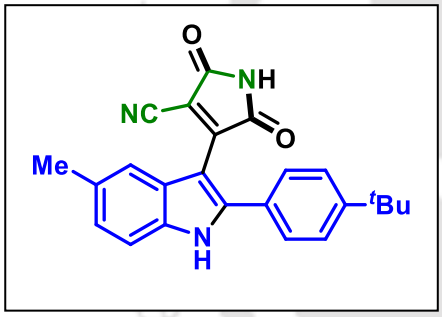

Red solid (33 mg, 58%); ^{1}H NMR (500 MHz, $CDCl_3$): δ (ppm) 1.35 (s, 9H), 2.50 (s, 3H), 7.14 (d, 1H, J = 8.0 Hz), 7.33 (d, 1H, J = 8.0 Hz), 7.39 (d, 2H, J = 8.0 Hz), 7.48 (d, 2H, J = 8.0 Hz), 7.58 (s, 1H), 8.11 (s, 1H), 9.30 (s, 1H); ^{13}C NMR (125 MHz, CDCl3): δ (ppm) 22.0, 31.4, 35.1, 102.6, 106.1, 111.4, 111.7, 121.3, 126.4, 126.8, 127.5, 128.3, 128.9, 132.9, 135.0, 145.6, 150.0, 153.7, 165.5, 166.9; IR (cm^{-1}): 3067, 2987, 2924, 2305, 1612, 1423; HRMS (ESI) calculated for $C_{24}H_{20}N_3O_2$ [M – H]$^-$: 382.1561, found 382.1555.

4-(5-Bromo-2-(4-(tert-butyl)phenyl)-1H-indol-3-yl)-2,5-dioxo-2,5-dihydro-1H-pyrrole-3-carbonitrile (20ab):

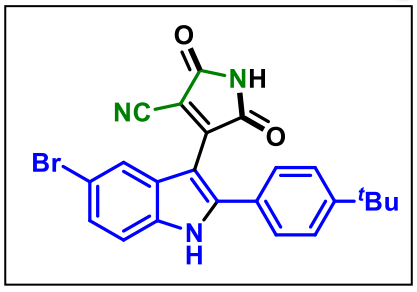

Red solid (34 mg, 51%); ^{1}H NMR (400 MHz, $CDCl_3$): δ (ppm) 1.32 (s, 9H), 7.32 (t, 2H, J = 6.8 Hz), 7.40 (d, 2H, J = 7.6 Hz), 7.46 (t, 2H, J = 8.0 Hz), 7.90 (s, 1H), 9.93 (s, 1H), 11.94 (s, 1H); ^{13}C NMR (100 MHz, $CDCl_3$ + DMSO-d_6): δ (ppm) 31.2, 34.8, 101.5, 106.1, 111.4, 113.8, 115.3, 123.5, 126.2, 126.5, 128.5, 128.67, 128.70, 136.0, 146.5, 149.5, 153.0, 167.0, 168.6; IR (cm^{-1}): 3072, 2980, 2954, 2307, 1615, 1420; HRMS (ESI) calculated for $C_{23}H_{28}BrN_3O_2$ [M - H]$^-$: 446.051, found 446.0524.

2-Phenyl-1H-indole (B):

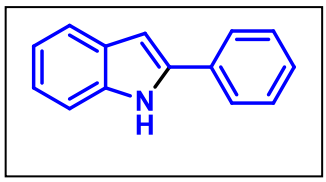

White solid ^{1}H NMR (500 MHz, $CDCl_3$): δ (ppm) 6.84 (s, 1H), 7.13 (t, 1H, J = 7.0 Hz), 7.20 (t, 1H, J = 7.5 Hz), 7.33 (t, 1H, J = 7.5 Hz), 7.41 (d, 1H, J = 8.0 Hz), 7.45 (t, 2H, J = 8.0 Hz), 7.64 (d, 1H, J = 8.0 Hz), 7.67 (dd, 2H, J_1 = 8.0 Hz, J_2 = 1.0 Hz), 8.34 (s, 1H); ^{13}C NMR (125 MHz, $CDCl_3$): δ (ppm) 100.3, 111.1, 120.5, 120.9, 122.6, 125.4, 127.9, 129.3, 129.5, 132.7, 137.1, 138.1.

2-Phenyl-1H-indole-3-carbaldehyde (G):[9]

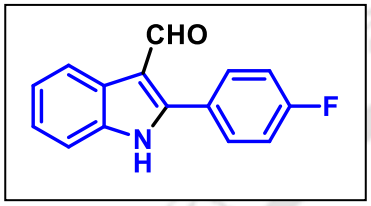

Pale yellow solid ^{1}H NMR (500 MHz, $CDCl_3$ + DMSO-d_6): δ (ppm) 7.18–7.20 (m, 1H), 7.22 (dd, 1H, J_1 = 9.0 Hz, J_2 = 2.0 Hz), 7.42 (d, 1H, J = 6.5 Hz), 7.47 (dd, 3H, J_1 = 7.0 Hz, J_2 = 2.0 Hz), 7.63 (dd, 2H, J_1 = 7.0 Hz, J_2 = 1.5 Hz), 8.27 (dd, 1H, J_1 = 8.5 Hz, J_2 = 1.5 Hz), 9.97 (s, 1H), 11.65 (s, 1H); ^{13}C NMR (125 MHz, $CDCl_3$ + DMSO-d_6): δ (ppm) 111.5, 114.1, 121.4, 122.3, 123.5, 125.9, 128.5, 129.4, 129.6, 130.1, 136.0, 149.3, 186.1.

2-((2-Phenyl-1H-indol-3-yl)methylene)malononitrile (H):[10]

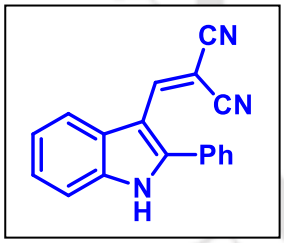

Yellow solid ^{1}H NMR (500 MHz, $CDCl_3$): δ (ppm) 7.38–7.40 (m, 2H), 7.47-7.48 (m, 1H), 7.49–7.51 (m, 2H), 7.60 (dd, 3H, J_1 = 7.0 Hz, J_2 = 3.5 Hz), 7.80 (s, 1H), 8.24 (dd, 1H, J_1 = 5.0 Hz, J_2 = 1.5 Hz), 9.12 (s, 1H); ^{13}C NMR (125 MHz, $CDCl_3$): δ (ppm) 76.1, 110.1, 112.1, 115.2, 116.3, 123.3, 123.4, 125.2, 125.3, 129.7, 129.8, 131.0, 136.6, 148.1, 154.0; IR (cm-1): 3284, 2985, 2218, 1566, 1420.

2-Methyl-1H-indole-3-carbonitrile (30b):

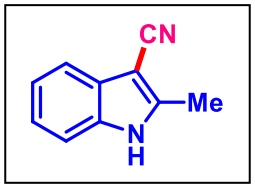

Brown solid; ^{1}H NMR (400 MHz, $CDCl_3$): δ (ppm) 2.45 (s, 3H), 7.14-7.18 (m, 2H), 7.23 (dd, 1H, J_1 = 6.0 Hz, J_2 = 1.6 Hz), 7.60 (d, 1H, J = 6.8 Hz), 8.44 (s, 1H); ^{13}C NMR (100 MHz, $CDCl_3$): δ (ppm) 12.3, 89.3, 111.4, 112.1, 118.3, 121.8, 123.2, 128.9, 135.3, 142.1; IR (cm^{-1}): 3441, 2923, 2152, 1637, 1411, 1262.

V.6. Representative NMR Spectra:

2-(5-Methyl-2-phenyl-1H-indol-3-yl)ethene-1,1,2-tricarbonitrile (2a): **^{1}H NMR (400 MHz, DMSO-d$_6$)**

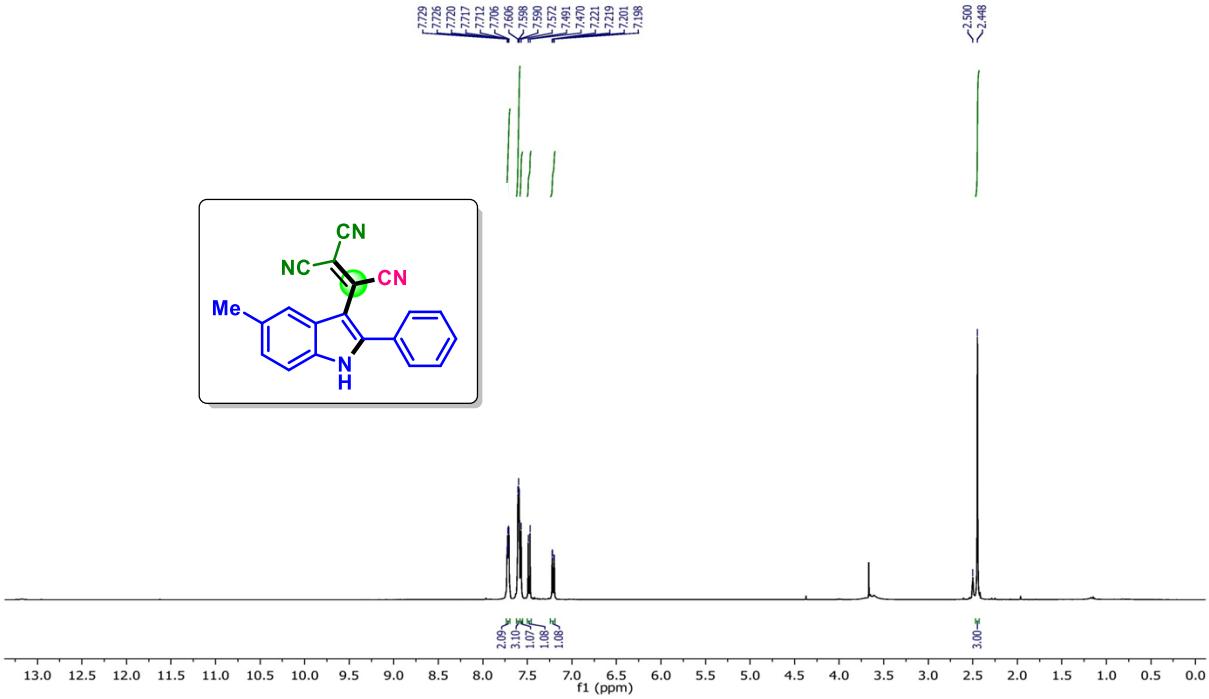

2-(5-Methyl-2-phenyl-1H-indol-3-yl)ethene-1,1,2-tricarbonitrile (2a): **^{13}C NMR (100 MHz, DMSO-d$_6$)**

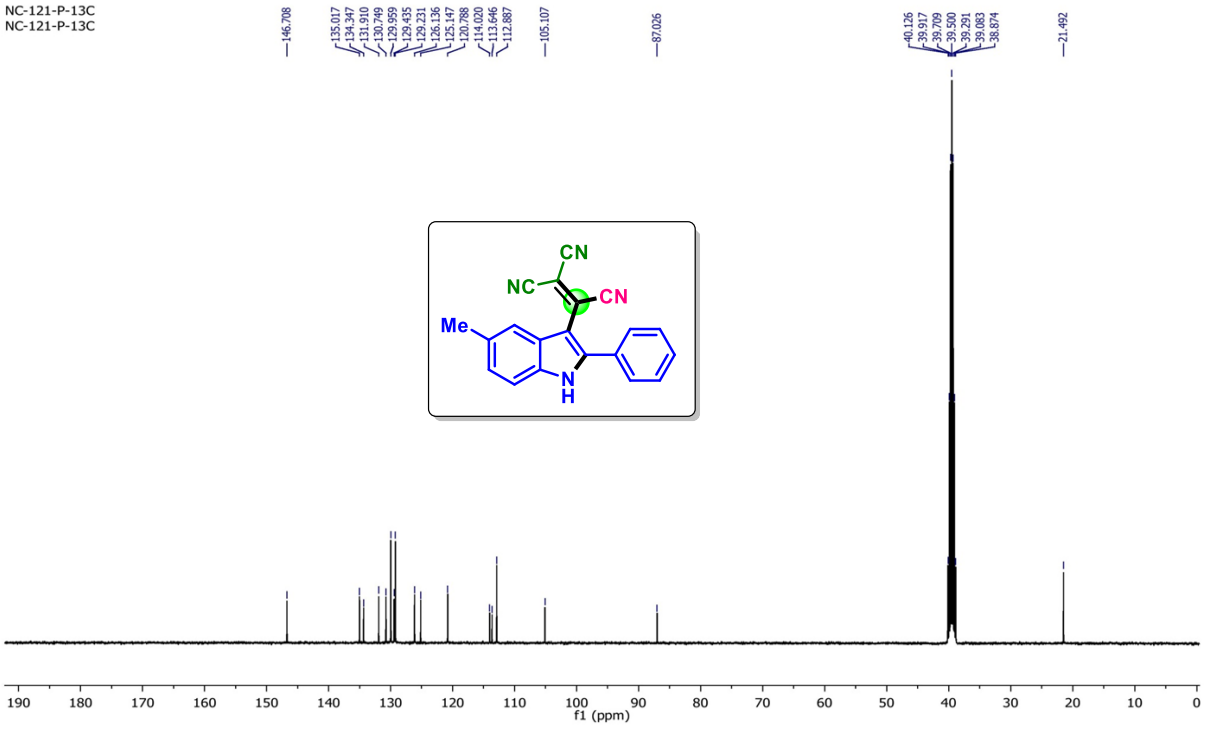

***2-(5,7-Dimethyl-2-phenyl-1H-indol-3-yl)ethene-1,1,2-tricarbonitrile (4a)*: ^{1}H NMR (400 MHz, $CDCl_3$ +DMSO-d_6)**

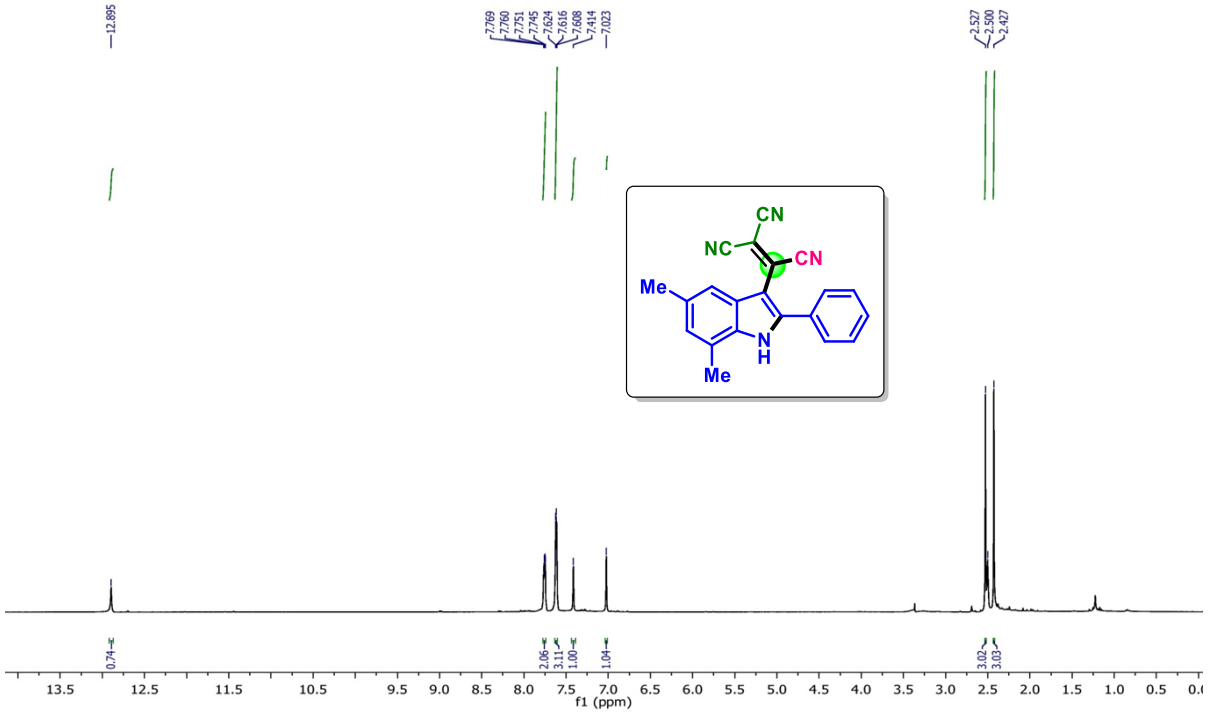

***2-(5,7-Dimethyl-2-phenyl-1H-indol-3-yl)ethene-1,1,2-tricarbonitrile (4a)*: ^{13}C NMR (100 MHz, $CDCl_3$ + DMSO-d_6)**

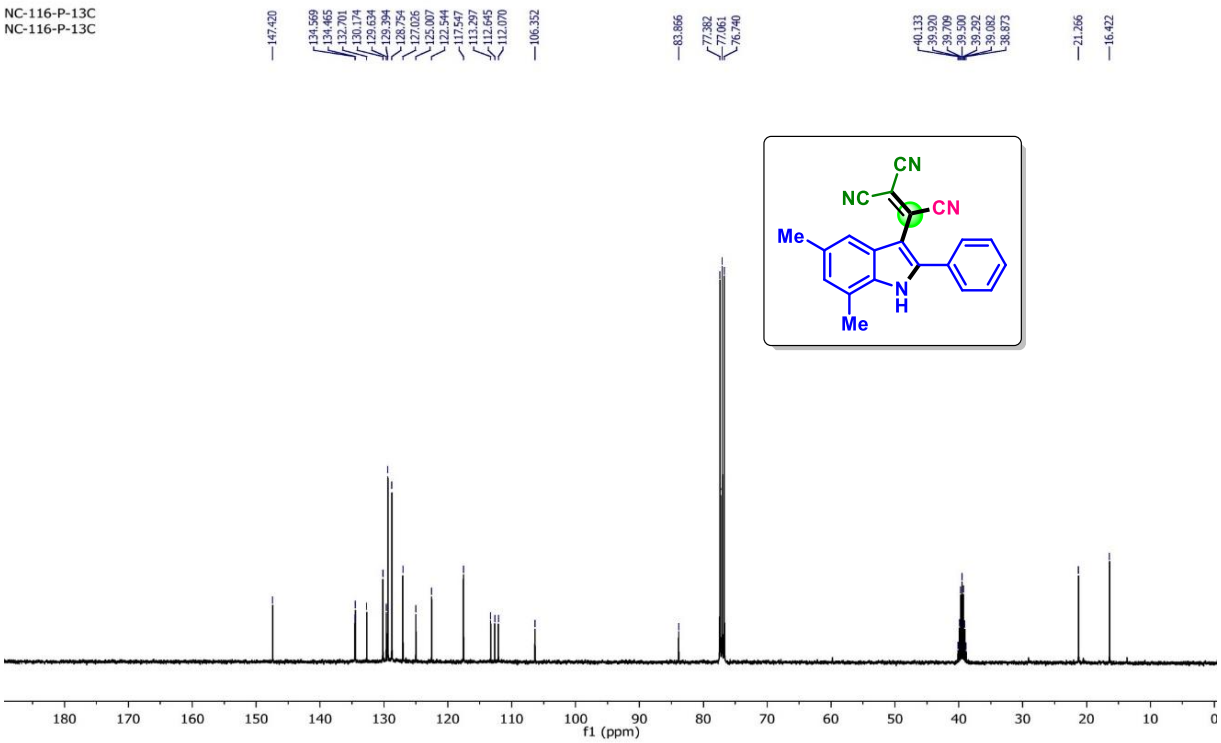

2-(2-(4-Methoxyphenyl)-1*H*-indol-3-yl)ethene-1,1,2-tricarbonitrile (11a): ^{1}H NMR (400 MHz, $CDCl_3$ + DMSO-d_6)

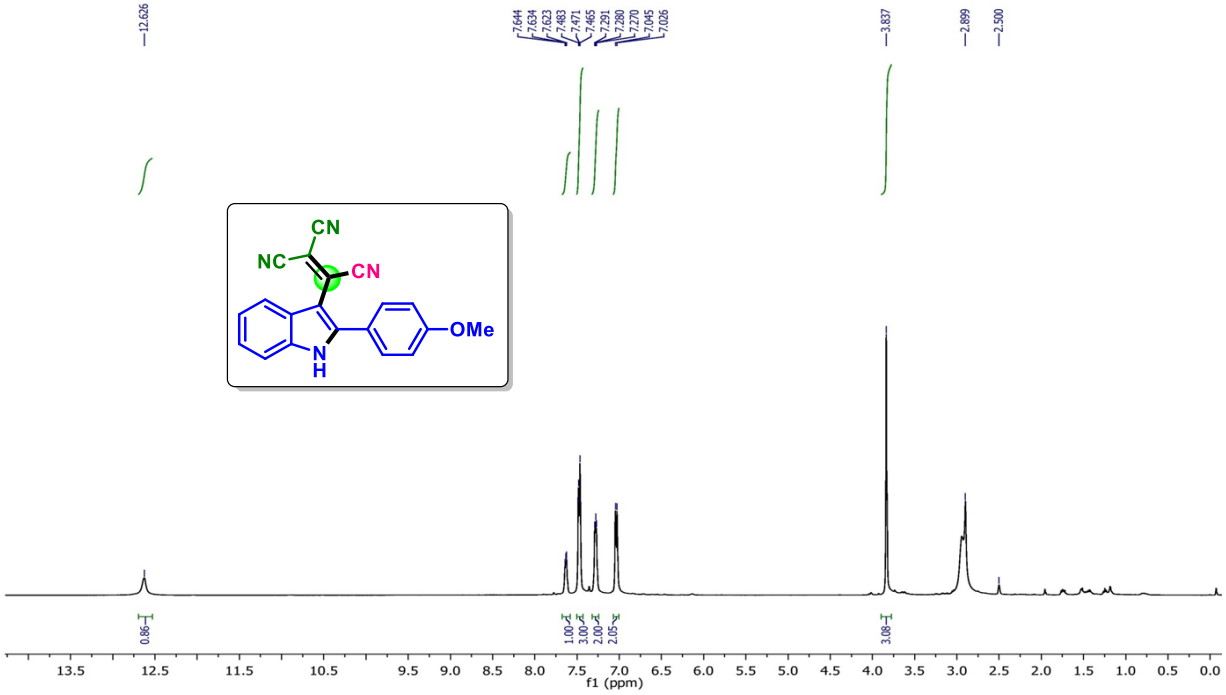

2-(2-(4-Methoxyphenyl)-1*H*-indol-3-yl)ethene-1,1,2-tricarbonitrile (11a): ^{13}C NMR (100 MHz, $CDCl_3$ + DMSO-d_6)

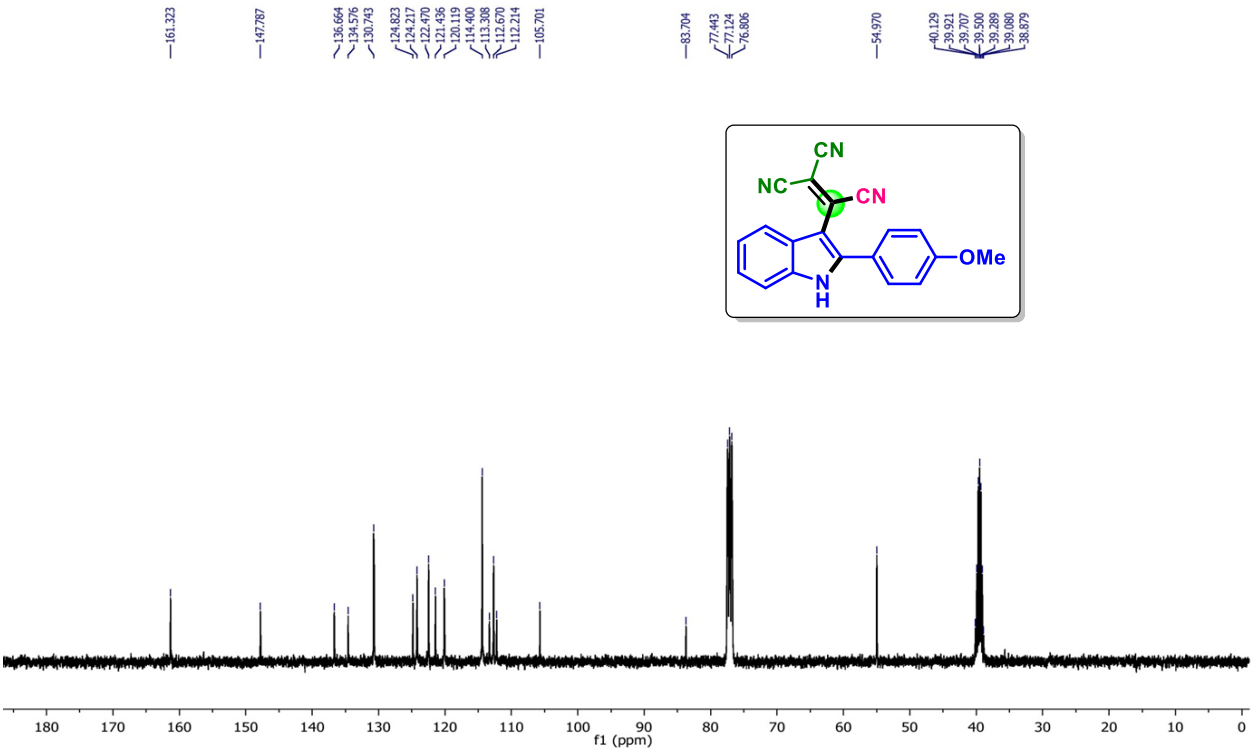

2-(5-Bromo-2-(4-(*tert*-butyl)phenyl)-1*H*-indol-3-yl)ethene-1,1,2-tricarbonitrile (20a): ^{1}H NMR (400 MHz, DMSO-d$_6$)

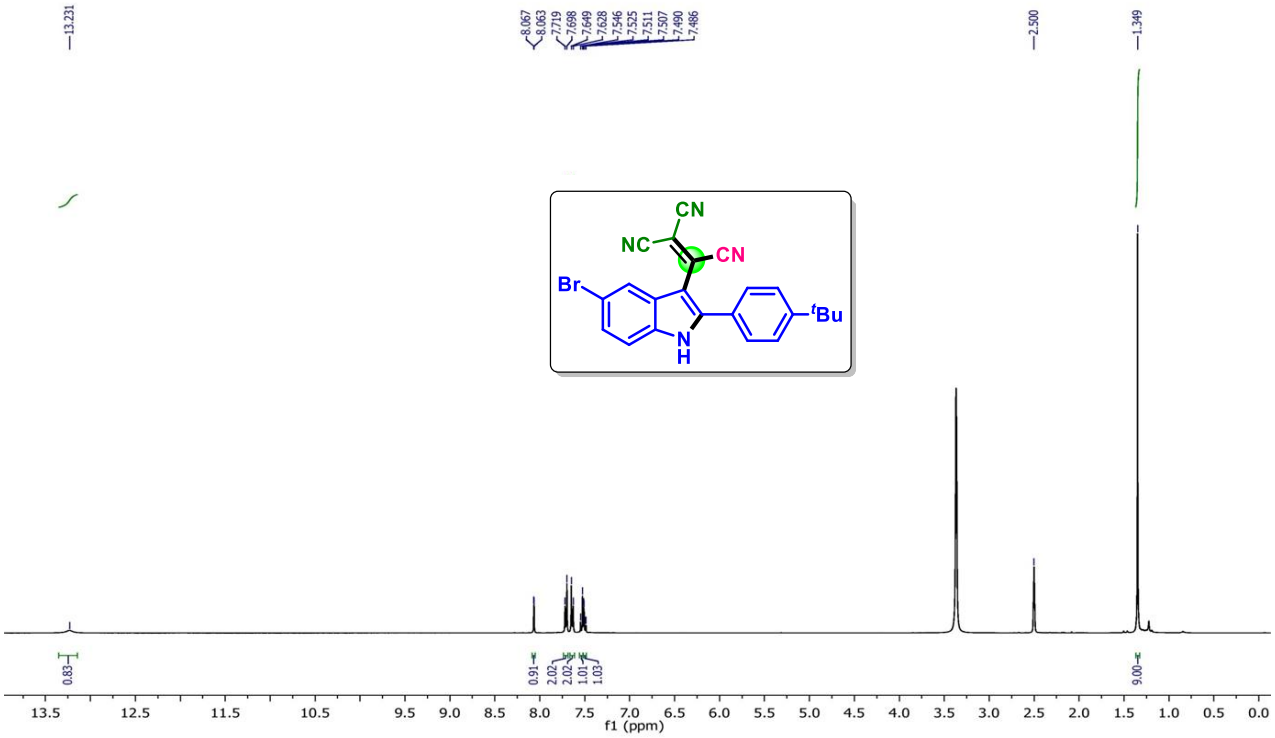

2-(5-Bromo-2-(4-(*tert*-butyl)phenyl)-1*H*-indol-3-yl)ethene-1,1,2-tricarbonitrile (20a): ^{13}C NMR (100 MHz, DMSO-d$_6$)

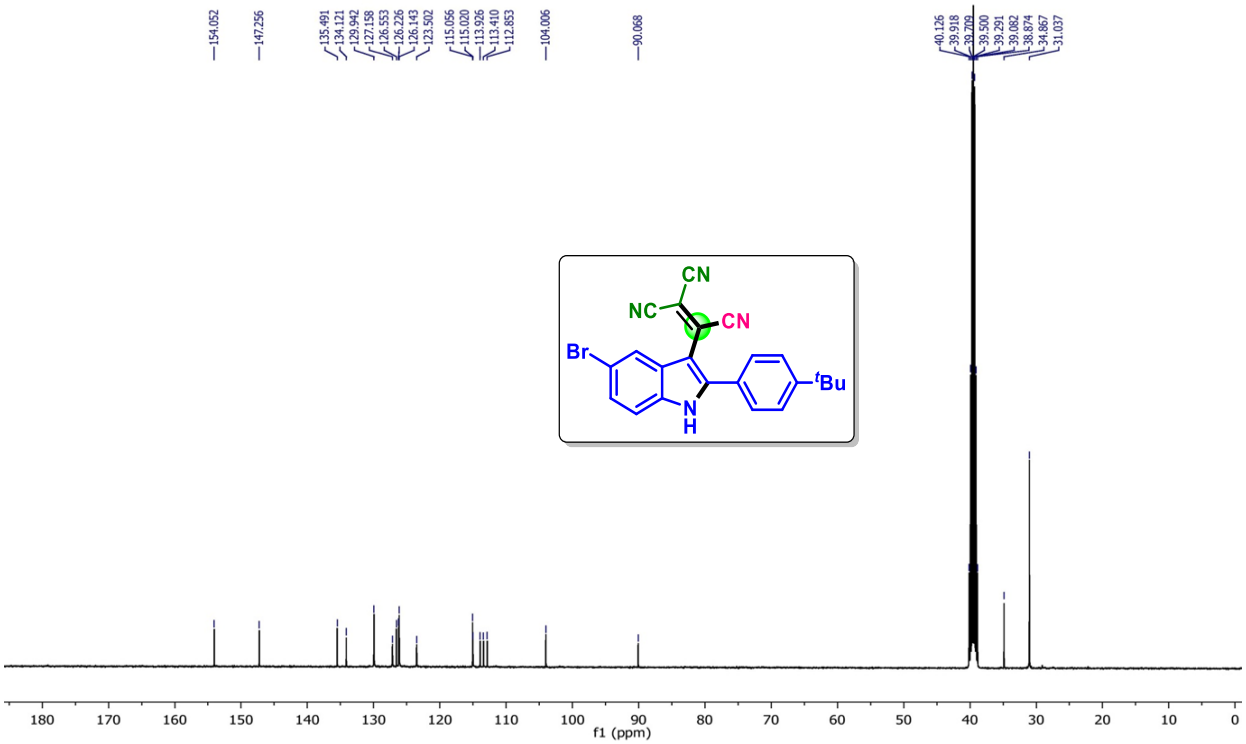

***4-(2-(4-Fluorophenyl)-1H-indol-3-yl)-2,5-dioxo-2,5-dihydro-1H-pyrrole-3-carbonitrile (12ab)*: ^{1}H NMR (400 MHz, $CDCl_3$ + DMSO-d_6)**

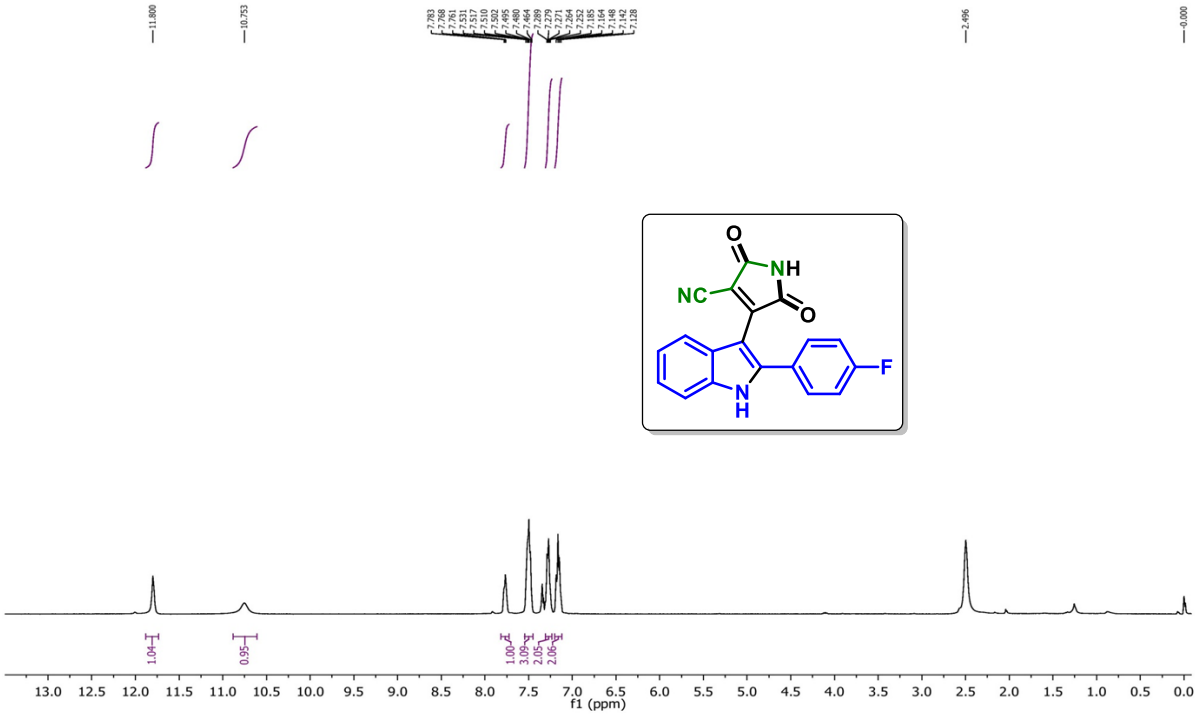

***4-(2-(4-Fluorophenyl)-1H-indol-3-yl)-2,5-dioxo-2,5-dihydro-1H-pyrrole-3-carbonitrile (12ab):* ^{13}C NMR (100 MHz, $CDCl_3$ + DMSO-d_6)**

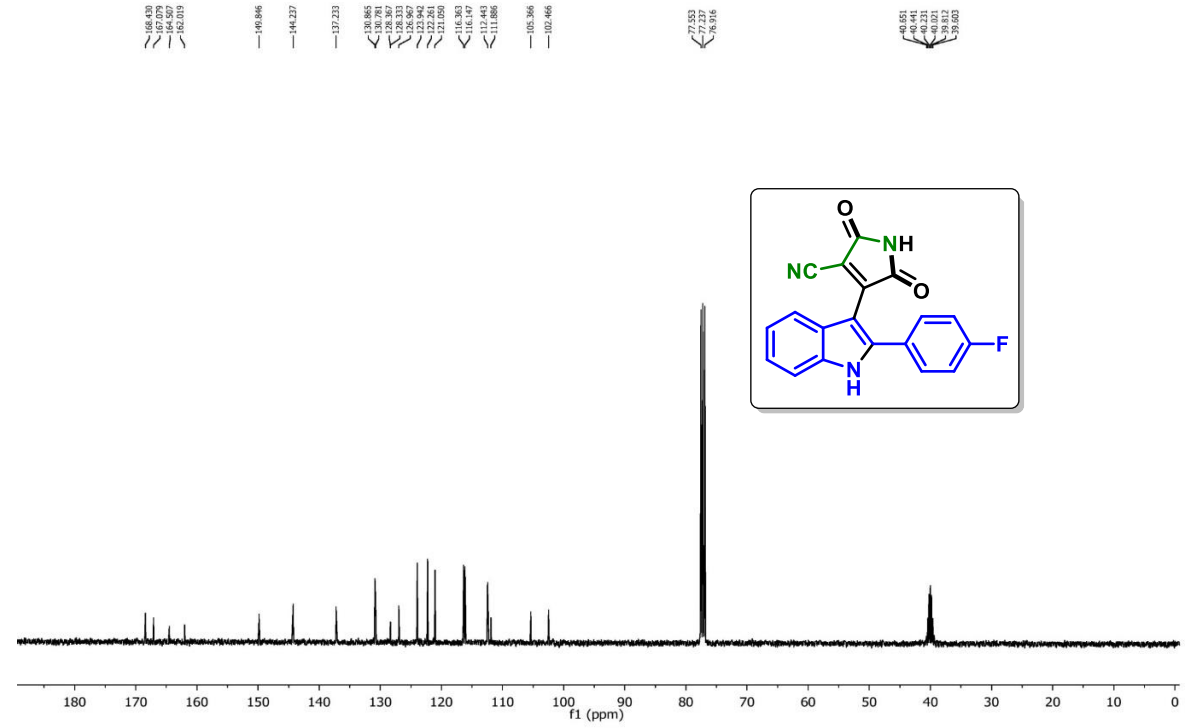

4-(2-(4-Fluorophenyl)-1H-indol-3-yl)-2,5-dioxo-2,5-dihydro-1H-pyrrole-3-carbonitrile (12ab): ^{19}F NMR (400 MHz, $CDCl_3$ + DMSO-d_6)

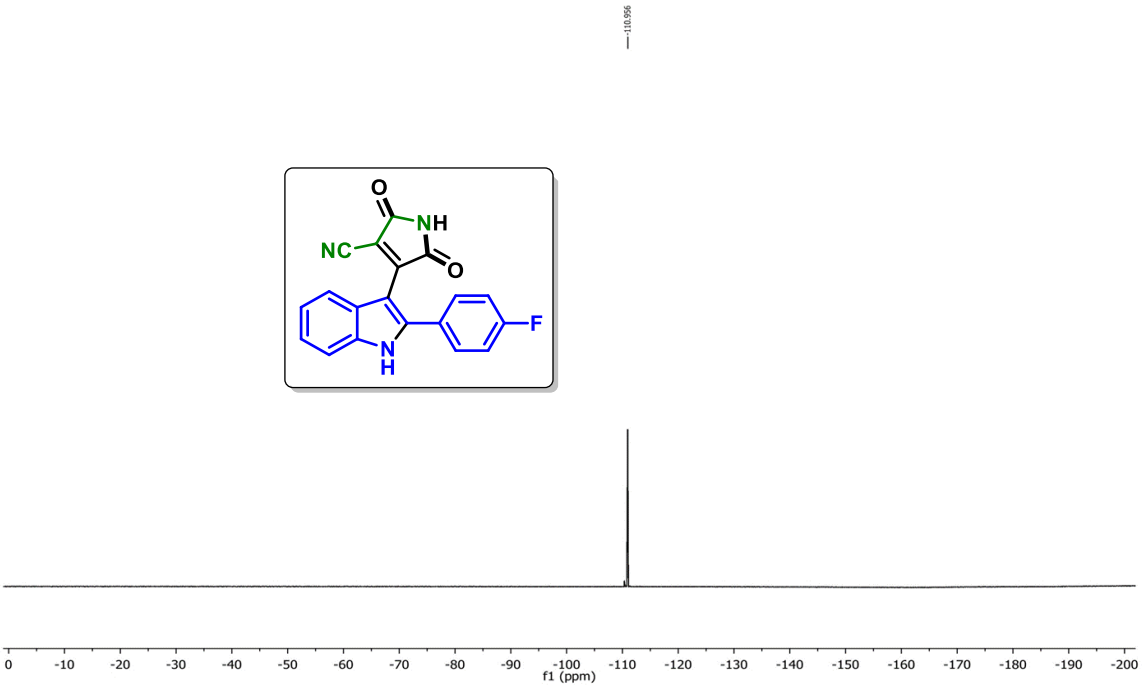

V.7. References:

(1) (a) K. C. Nicolaou and J. S. Chen, *Chem. Soc. Rev.*, 2009, **38**, 2993–3009; (b) J.-F. Vincent-Rocan, R. A. Ivanovich, C. Clavette, K. Leckett, J. Bejjani and A. M. Beauchemin, *Chem. Sci.*, 2016, **7**, 315–328; (c) M. G. Ciulla, S. Zimmermann and K. Kumar, *Org. Biomol. Chem.*, 2019, **17**, 413–431; (d) X. Zeng, *Chem. Rev.*, 2013, **113**, 6864–6900; (e) Y. Wang, H. Lu and P.-F. Xu, *Acc. Chem. Res.*, 2015, **48**, 1832–1844; (f) Shivam, G. Tiwari, M. Kumar, A. N. S. Chauhan and R. D. Erande, *Org. Biomol. Chem.*, 2022, **20**, 3653–3674.

(2) (a) X.-F. W. Wu, *Solvents as reagents in organic synthesis: Reactions and applications*, Wiley, 2017; (b) M. M. Heravi, M. Ghavidel and L. Mohammadkhani, *RSC Adv.*, 2018, **8**, 27832–27862; (c) P. Zhong, L. Zhang, N. Luo and J. Liu, *Catalysts*, 2023, **13**, 761.

(3) (a) X.-F. Wu and K. Natte, *Adv. Synth. Catal.*, 2016, **358**, 336–352; (b) Z. Tashrifi, M. M. Khanaposhtani, B. Larijani and M. Mahdavi, *Adv. Synth. Catal.*, 2020, **362**, 65–86; (c) H. Lu, Z. Tong, L. Peng, Z. Wang, S.-F. Yin, N. Kambe and R. Qiu, *Top. Curr. Chem.* 2022, **380**, DOI:10.1007/s41061-022-00411-8.

(4) P. Yang, W. Xu, R. Wang, M. Zhang, C. Xie, X. Zeng and M. Wang, *Org. Lett.*, 2019, **21**, 3658–3662.

(5) Y. Zhang, Y. Ding, R. Chen and Y. Ma, *Adv. Synth. Catal.*, 2020, **362**, 5697–5707.

(6) (a) H. Cao, S. Lei, N. Li, L. Chen, J. Liu, H. Cai, S. Qiu and J. Tan, *Chem. Commun.*, 2015, **51**, 1823–1825; (b) Z. Zhang, Q. Tian, J. Qian, Q. Liu, T. Liu, L. Shi and G. Zhang, *J. Org. Chem.*, 2014, **79**, 8182–8188; (c) S. Xiang, H. Chen and Q. Liu, *Tetrahedron Lett.*, 2016, **57**, 3870–3872; (d) J. Qian, Z. Zhang, Q. Liu, T. Liu and G. Zhang, *Adv. Synth. Catal.*, 2014, **356**, 3119–3124; (e) S. Bhattacharjee, S. Laru, P. Ghosh and A. Hajra, *J. Org. Chem.*, 2021, **86**, 10866–10873.

(7) (a) M. M. M. Raposo, A. M. R. C. Sousa, G. Kirsch, F. Ferreira, M. Belsley, E. de M. Gomes and A. M. C. Fonseca, *Tetrahedron*, 2005, **61**, 11991–11998; (b) M. M. El-Nahass, K. F. Abd-El-Rahman and A. A. A. Darwish, *Physica B Condens. Matter*, 2008, **403**, 219–223; (c) S. A. Lermontova, I. S. Grigoryev, N. Y. Shilyagina, N. N. Peskova, I. V. Balalaeva, M. V. Shirmanova and L. G. Klapshina, *Russ. J. Gen. Chem.*, 2016, **86**, 1330–1338.

(8) (a) A. K. Sanap and G. S. Shankarling, *Catal. Commun.*, 2014, **49**, 58–62; (b) Y. Shigemitsu, B.-C. Wang, Y. Nishimura and Y. Tominaga, *Dyes Pigm.*, 2012, **92**, 580–587.

(9) Y. Yuan, X. Guo, X. Zhang, B. Li and Q. Huang, *Org. Chem. Front.*, 2020, **7**, 3146–3159.

(10) K. S. Siddegowda, K. M. Zabiulla, and S. Yellappa, *Org. Commun.*, 2016, **9**, 119–124.

(11) (a) J. Wang, B. Sun, L. Zhang, T. Xu, Y. Xie and C. Jin, *Org. Chem. Front.*, 2020, **7**, 113–118; (b) A. Wagner and A. R. Ofial, *J. Org. Chem.*, 2015, **80**, 2848–2854.

(12) V. Reddy and R. Vijaya Anand, *Org. Lett.*, 2015, **17**, 3390–3393.

(13) (a) Y. Deguchi, M. Kono, Y. Koizumi, Y.-I. Izato and A. Miyake, *Org. Process Res. Dev.*, 2020, **24**, 1614–1620.

(14) (a) E. M. Schneider, M. Zeltner, N. Kränzlin, R. N. Grassa, and W. J. Stark, *Chem. Commun.*, 2015, **51**, 10695–10698; (b) Y. Ogiwara, K. Takahashi, T. Kitazawa, and N. Sakai, *J. Org. Chem.*, 2015, **80**, 3101-3110.

(15) Gaussian 16, Revision C.01, M. J. Frisch, G. W. Trucks, H. B. Schlegel, G. E. Scuseria, M. A. Robb, J. R. Cheeseman, G. Scalmani, V. Barone, G. A. Petersson, H. Nakatsuji, X. Li, M. Caricato, A. V. Marenich, J. Bloino, B. G. Janesko, R. Gomperts, B. Mennucci, H. P. Hratchian, J. V. Ortiz, A. F. Izmaylov, J. L. Sonnenberg, D. Williams-Young, F. Ding, F. Lipparini, F. Egidi, J. Goings, B. Peng, A. Petrone, T. Henderson, D. Ranasinghe, V. G. Zakrzewski, J. Gao, N. Rega, G. Zheng, W. Liang, M. Hada, M. Ehara, K. Toyota, R. Fukuda, J. Hasegawa, M. Ishida, T. Nakajima, Y. Honda, O. Kitao, H. Nakai, T. Vreven, K. Throssell, J. A. Montgomery, Jr., J. E. Peralta, F. Ogliaro, M. J. Bearpark, J. J. Heyd, E. N. Brothers, K. N. Kudin, V. N. Staroverov, T. A. Keith, R. Kobayashi, J. Normand, K. Raghavachari, A. P. Rendell, J. C. Burant, S. S. Iyengar, J. Tomasi, M. Cossi, J. M. Millam, M. Klene, C. Adamo, R. Cammi, J. W. Ochterski, R. L. Martin, K. Morokuma, O. Farkas, J. B. Foresman, and D. J. Fox, Gaussian, Inc., Wallingford CT, 2019.

(16) (a) A. Rakshit, P. Sau, S. Ghosh, and B. K. Patel, *Adv. Synth. Catal.*, 2019, **361**, 3824-3836; (b) X. Xin, D. Xiang, J. Yang, Q. Zhang, F. Zhou, and D. Dong, *J. Org. Chem.*, 2013, **78**, 11956–11961.

(17) (a) R. K. Gurram, M. Rajesh, M. K. Reddy Singam, J. B. Nanubolu and M. S. Reddy, *Org. Lett.*, 2020, **22**, 5326–5330; (b) Y.-L. An, Z.-H. Yang, H.-H. Zhang and S.-Y. Zhao, *Org.*

Lett., 2016, **18**, 152–155; (c) Z.-H. Yang, Y.-L. An, Y. Chen, Z.-Y. Shao and S.-Y. Zhao, *Adv. Synth. Catal.*, 2016, **358**, 3869–3875.

List of Publications:

Research Articles:

(1) An Expedient Route to Tricyanovinylindoles and Indolylmaleimides from *o*-Alkynylanilines Utilizing DMSO as One-Carbon Synthon. *Org. Biomol. Chem.* 2021, **19**, 6847–6857. **Nikita Chakraborty**, Anjali Dahiya, Amitava Rakshit, Anju Modi and Bhisma K. Patel.

(2) NIS-initiated photo-induced oxidative decarboxylative sulfoximidation of cinnamic acids. *Chem. Commun.* 2023, **59**, 2779–2782. **Nikita Chakraborty**, Kamal Krishna Rajbongshi, Anjali Dahiya, Bubul Das, Akshar Vaishnani, and Bhisma K. Patel.

(3) Base-Promoted Synthesis of S-Arylisothiazolones via Intramolecular Dehydrative Cyclization of α-Keto-N-acylsulfoximines. *J. Org. Chem.* 2024, **89**, 778–783. **Nikita Chakraborty**, Bubul Das, Dinabandhu Barik, Kamal Krishna Rajbongshi and Bhisma K. Patel.

(4) PIDA/I_2-Mediated Photo-Induced N-Acylation of Sulfoximines with Methylarenes. *Org. Biomol. Chem.* 2024, **22**, 2375–2379. **Nikita Chakraborty**, Kamal Krishna Rajbongshi, Amisha Gondaliya, and Bhisma K. Patel.

(5) A "Thiocarbonyl-Directed" Regiospecific C-H/S-H Annulation of Quinoline-4(1*H*)-thiones with Alkynes. *Adv. Synth. Catal.* 2019, **361**, 1368–1375. Anju Modi, Prasenjit Sau, **Nikita Chakraborty** and Bhisma K. Patel.

(6) Synthesis of Chromenopyrroles (Azacoumestans) from Functionalized Enones and Alkyl Isocyanoacetates. *Org. Lett.* 2023, **25**, 5209–5213. Bubul Das, Anjali Dahiya, **Nikita Chakraborty**, and Bhisma K. Patel.

(7) Access to Chromenopyrrole via Tandem [3 + 2] Cycloaddition and Intramolecular C–O Coupling. *J. Org. Chem.* 2024, **89**, 1331–1335. Bubul Das, **Nikita Chakraborty**, Hirendra Nath Dhara and Bhisma K. Patel

(8) Iodine Promoted Sulfoximidation of Cinnamic Acids via Oxidative C=C Bond Cleavage. Manuscript under Communication. Parbin Rohman, Nikita Chakraborty, Kamal K. Rajbongshi and Bhisma K. Patel.

Review Articles

(1) Combined Power of Organo- and Transition Metal Catalysis in Organic Synthesis. *Eur. J. Org. Chem.* 2022, e202200273. **Nikita Chakraborty**, Bubul Das, Kamal K. Rajbongshi and Bhisma K. Patel

(2) Synthetic utility of styrenes in the construction of diverse heterocycles via annulation/cycloaddition. Tetrahedron, 2023, 134, 133270. Bubul Das, **Nikita Chakraborty**, Kamal K. Rajbongshi and Bhisma K. Patel.

(3) Updates on hypervalent-iodine reagents: metal free functionalisation of alkenes, alkynes and heterocycles. *Org. Biomol. Chem*. 2022, **20**, 2005–2027. Anjali Dahiya, Ashish Kumar Sahoo, **Nikita Chakraborty**, Bubul Das, Bhisma K Patel.

Book Chapters:

(1) Counterbalancing Common Explosive Pollutants (TNT, RDX and HMX) in the Environment by Microbial Degradation. Development in Wastewater Treatment Research and Processes. Elsevier, 2022, pp. 263–310. doi: 10.1016/B978-0-323-85839-7.00012-8. **Nikita Chakraborty**, Pakiza Begum and Bhisma K. Patel*

(2) 3 Significant role of nitrogen cycle in wastewater treatment." Anaerobic Ammonium Oxidation: For Industrial Wastewater Treatment. De Gruyter 3, 2023, 31–54. Bhaskar Deka, **Nikita Chakraborty**, and Bhisma K. Patel*

(3) An important tool for wastewater treatment. Application of Nanotechnology for Resource Recovery from Wastewater. Taylor & Francis. CRC Press, Boca Raton, 2023. https://doi.org/10.1201/9781003176350 Binoyargha Dam, **Nikita Chakraborty** and Bhisma K. Patel.